UNIVERSITY OF CANTERBURY
Te Whare Wānanga o Waitaha
CHRISTCHURCH NEW ZEALAND

Performance Improvements to a Fast Internally Circulating Fluidized Bed (FICFB) Biomass Gasifier for Combined Heat and Power Plants

A thesis submitted in partial fulfilment for the Degree of Master of Engineering in Chemical and Process Engineering, University of Canterbury, New Zealand

By Doug Bull

University of Canterbury

2008

Supervised by: Mr Ian Gilmour and Dr. Chris Williamson

Dedicated to my grandfather, Norman Louis Pannell,
who shared his practical skills with me from a young age
and instilled my passion for engineering.

Executive Summary

This thesis describes the development and experimental testing of a 100 kW dual fluidized bed biomass gasifier (also called a Fast Internally Circulating Fluidized Bed (FICFB) biomass gasifier). This steam-blown gasifier is being studied for its suitability within combined heat and power plant systems for the New Zealand forest products industry. This advanced design of gasifier has the ability to generate producer gas with a lower heating value (LHV) of 11.5-13.4 MJ/Nm^3, which is two to three times higher than yielded by conventional gasification systems. This is accomplished because the gasification and combustion processes occur in two physically separated reactors.

Several modifications to the gasifier were required after it was first constructed in order to achieve stable and reliable operation. Producer gas yields were measured through the use of helium as a tracer gas. A new simultaneous producer gas and tar sampling system was developed, allowing accurate samples to be obtained in a matter of minutes.

Experimental testing included a cold testing exercise which provided valuable information on the circulation behaviour of the bed material and char within the gasifier. This helped in achieving stable and reliable operation of the plant. Producer gas yields of 14.6 Nm^3/h were recorded with a fuel (radiate pine wood pellets) feed rate of 18.9 kg_{dry}/h. The cold gas efficiency ranged from 16-40 % with limited heat recovery in place, but depended noticeably on the plant operating conditions especially gasification temperature.

The amount of polycyclic aromatic hydrocarbon (PAH) tars measured in the producer gas ranged between 0.9-4.7 g/Nm^3 with naphthalene and acenapthylene being the most abundant compounds. The moisture content of the producer gas was determined to be 0.9-1.2 $g/g_{dry\ gas}$. It was found that a steam to biomass ratio of 0.45-0.7 kg/kg_{dry} was most favourable for generating a 12-13.4 MJ/Nm^3 producer gas while limiting the amount of steam generation. Gasification temperatures above 750 °C encouraged higher producer gas yields and higher cold gas efficiencies. The catalytic bed material olivine (forsterite olivine) was found to increase the producer gas yield by approximately 20 % compared to the non-catalytic bed material greywacke. The use of olivine meant higher cold gas efficiencies were achieved for a given wood feed rate.

Acknowledgements

There are many people I would like to thank for their contribution and support during this masters' project.

Sincere thanks are extended to Mr Ian Gilmour, initially my primary supervisor, before formally taking a secondary supervision role upon partial retirement. Ian's expertise was highly appreciated and his network with overseas experts was invaluable.

Thanks also to Dr Chris Williamson who co-supervised my master's project. Dr Williamson contributed his thermodynamic experience and guided me in my other course work components.

Thanks to Dr Shusheng Pang, the overall project coordinator who is responsible for establishing this project. Shusheng has allowed many postgraduate students a unique start to their engineering careers through their attendance on the project he founded.

Thanks to Mr Rick Dobbs who brought a great deal of practical experience to the project, contributed to building the gasifier and assisted with early laboratory trials.

I wish to extend thanks to Chris Penniall and Gershom Mwandila who were colleagues of mine on the department's gasification project. Both Chris and Gershom spent many hours in the laboratory helping with experimental tests. Chris attended every gasifier trial and helped to operate the plant while I took samples and recorded data.

Thanks to Trevor Berry, the laboratory technician who assisted with tests on the gasifier and provided extensive assistance with the micro-gas-chromatograph and other laboratory analysis equipment.

Thanks also to the Leigh Richards, for his workshop fabrication support and creative ideas on construction of plant items.

Finally, my thanks go to Jock Brown who was the predecessor masters' student for building and commissioning the gasifier, before I started in June 2006.

Abbreviations

BFB	'Bubbling Fluidized Bed' located in the gasification reactor/column
BIG	Biomass Integrated Gasification
BIG/GE	Biomass Integrated Gasification/Gas Engine
BIG/GT/ST	Biomass Integrated Gasification / Gas Turbine / Steam Turbine
BIGCC	Biomass Integrated Gasification with Combined Cycle
CFB	**'**Circulating Fluidized Bed' located in the combustion reactor/column
CV	Calorific value (same as the term 'heating value' HV)
daf	Dry Ash Free basis
FICFB	*Fast Internally Circulating Fluidized Bed* also referred to as the 'Fast Internally Circulating Dual Fluidized Bed' gasifier. Note: the term 'dual fluidized bed' gasifier can also be used.
GC-FID	Gas Chromatograph-Flame Ionisation Detection
HHV	Higher Heating Value also called Higher Calorific Value 'HCV'
HRSG	Heat Recovery Steam Generator
IPA	Isopropyl alcohol
LHV	Lower Heating Value also called Lower Calorific Value 'LCV'
Micro GC	micro gas chromatography
MJ/Nm^3	Mega Joules/Normal meter cubed (measured at STP: 0 °C and 1 atm)
PAH	Poly aromatic Hydrocarbon
SNG	Synthetic Natural Gas
SPA or SPE	Solid phase adsorption or Solid Phase Extraction
STP	Standard temperature and pressure (0 °C, 1 atm)
TDH	Transport Disengaging Height
VSD	Variable Speed Drive
XRD	X-Ray Diffraction
XRF	X-Ray Fluorescence

Contents Page

1.0 Introduction

1.1 Overall Focus of the University of Canterbury Gasifier Project

The University of Canterbury, Chemical and Process Engineering Department are assessing the suitability of gasification based *Combined Heat and Power* (CHP) plants for integration into New Zealand forest industries. Part of the project has involved developing and testing a 100 kW laboratory scale biomass gasifier fuelled on wood pellets. The type of gasifier chosen for development has the potential to form the front-end of a future full scale CHP plant system consuming wood residue. The dual fluidized bed gasifier, also known as the *Fast Internally Circulating Fluidized Bed* (FICFB) gasifier, generates a combustible gas which can be used to fuel internal combustion engines (such as reciprocating engines or gas turbines) coupled to generators. The CHP plant project is based on using this innovative dual fluidized bed gasifier first developed in Austria, to convert the energy in solid wood fuels into a gaseous fuel 'producer gas'.

Gaseous fuels are advantageous over solids fuels because they are easier to utilise and have more applications, such as directly fuelling internal combustion engines. The 100 kW prototype gasifier has been constructed in a laboratory at the University of Canterbury where it can be experimentally tested. Once gas cleaning equipment has been developed and installed, a reciprocating gas engine can be integrated to demonstrate the overall CHP plant system.

In the future, a larger scale CHP plant may be constructed, where a gasifier could fuel a gas turbine and exhaust heat could be recovered to generate steam to drive a steam turbine. Both the gas turbine and the steam turbine can be coupled to generators to produce electricity. This is known as a combined cycle power plant. A portion of the steam generated can also be supplied as process heat to a local user.

This thesis work has focused on understanding and documenting the behaviour of the 100 kW (laboratory scale) FICFB gasifier, plus modifying and experimentally testing the plant. The laboratory scale power plant system proposed can be seen in Figure 1.1, and the layout of a possible larger scale combined cycle cogeneration plant to aim for is shown in Figure 1.2.

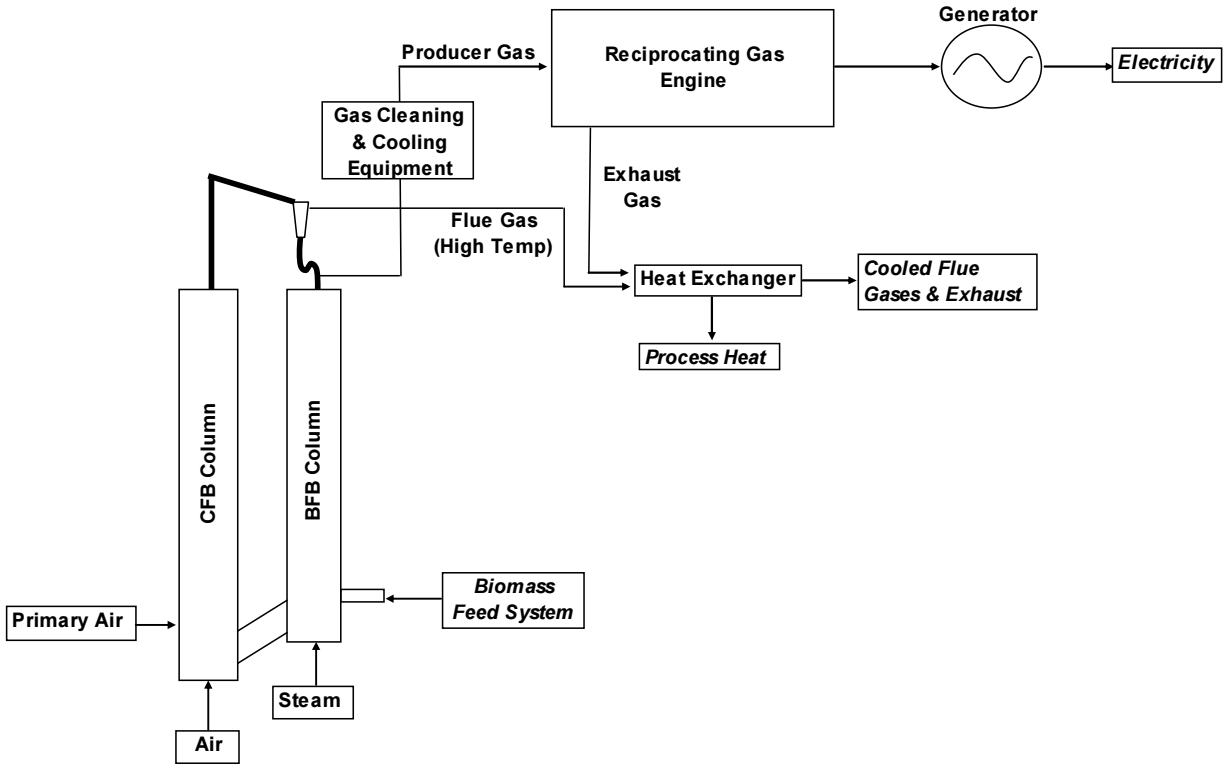

Figure 1.1: Intended laboratory scale biomass CHP plant at the University of Canterbury.

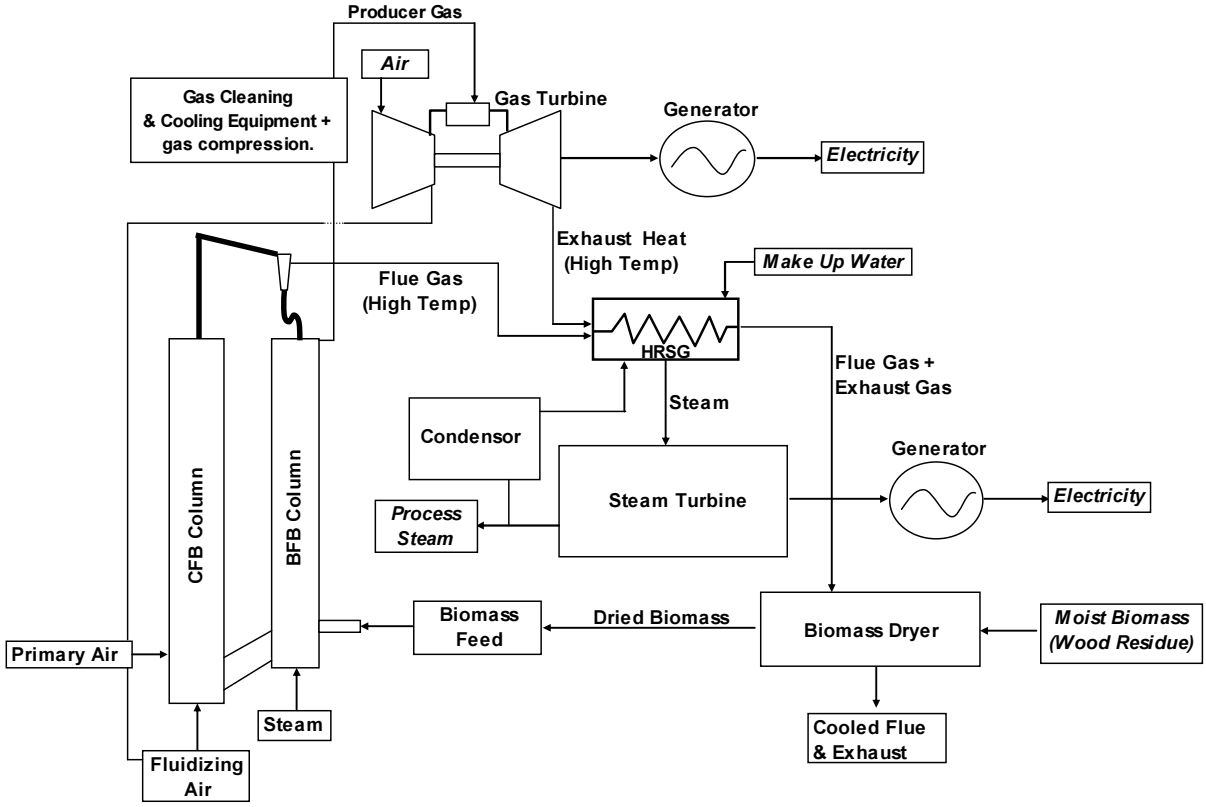

Figure 1.2: Example of a full scale biomass gasification, combined cycle power plant.

1.2 Objectives for the University of Canterbury's Biomass Gasification Project

The University of Canterbury, Chemical and Process Engineering Department, aims to assess Biomass Integrated Gasification Combined Cycle (BIGCC), CHP plants for integration into the forest products industry of New Zealand. The four specific objectives of the current program are:

Obj 1. To evaluate overseas BIGCC technologies and identify the most suitable gasification based CHP arrangements for the New Zealand forest industry.

Obj 2. To transfer the most suitable gasification technology to New Zealand and prove the performance of the technology at laboratory scale using New Zealand wood residue fuels.

Obj 3. To establish a biomass feedstock supply computer model and energy demand computer model to support the final feasibility assessment of situating gasification based CHP plants in the New Zealand forest industry.

Obj 4. To generate CHP plant system concepts and supporting economic feasibility assessments, plus a software model that other parties can use to evaluate if gasification based CHP plant technologies are suitable for a given application.

These objectives are being satisfied by a number of postgraduate students each allocated different areas and guided by supervisors specific to the different project objectives.

1.3 Overview of the Author's Research Goals and Contents of this Thesis

The author's research goals are part of objective two in studying and further developing the performance of the chosen gasification technology. These research goals are associated around four main areas:

1. To complete the construction and improve the design of the lab scale gasifier to achieve stable, reliable operation.
2. To begin establishing the most favourable operating conditions to yield a medium to high calorific value producer gas, with low levels of tars suitable for CHP applications.

3. To benchmark the performance of the FICFB gasifier in terms of the lower calorific value of the producer gas, the total producer gas output and the cold gas efficiency under different operating conditions.
4. To perform a technical assessment of the 100 kW FICFB gasifiers design to identify and recommend improvements for future gasifiers of this type.

This thesis work has been performed over two years from 1st June 2006 to 23th May 2008. It contains the *modifications* section which describes improvements to the gasifier's hardware, the *cold testing* section which explains the work performed to improve the gasifier's operational stability, and the *hot testing* section. The hot testing section begins to investigate the most favourable operating conditions of the gasifier by varying plant parameters and assessing there effect on the producer gas and the overall gasifier's performance. Lastly recommendations on the design of future FICFB gasifiers are suggested to help optimum plant performance to be achieved.

1.4 Distinguishing Features of the FICFB Gasifier

The type of gasifier chosen for this project was the 'Fast Internally Circulating dual Fluidized Bed' (FICFB) gasifier. FICFB gasifiers are unique to traditional gasifier designs because they yield a gas of two to three times the heating value that conventional gasifiers generate.

This medium calorific value gas (LHV: 11.5-13.4 MJ/Nm^3) is achieved because the gasification process and the heat generating combustion processes are physically separated in two different reactors. By using steam as a gasifying agent and separating the gasification and combustion reactions, no air is introduced into the gasification column. By preventing air entering (containing approximately 79 % N_2 and 21 % O_2), nitrogen is excluded which dilutes the producer gas. The two fundamental problems with biomass gasification around the world for CHP applications, is the production of hydrocarbon tars in the producer gas, and the poor heating value of the producer gas. Tars cause fouling of components down steam of the gasifier such as heat exchangers and engines, and a low heating value gas reduces the efficiency of CHP plants and thermal firing systems.

1.5 International Electricity Production Current and Future

Many opportunities exist for the utilisation of biomass such as wood residue for renewable electricity production in thermal power plants. The demand for renewable energy generating technologies in the electricity production sector is becoming increasingly important, driven by concerns over global climate change. Globally, coal is the dominant fuel for electricity production, combusted in thermal power plants operating on the Rankine (steam turbine) thermodynamic cycle. Approximately 40 % of the worlds electricity is generated from coal (Energy Information Administration, 2006). Climate change awareness and rising oil and natural gas prices are increasing the proportion of renewable energy plants in the electricity generation mix. The Energy Information Administration of the United States has developed predictions for future global electricity generation, as shown in Figure 1.3.

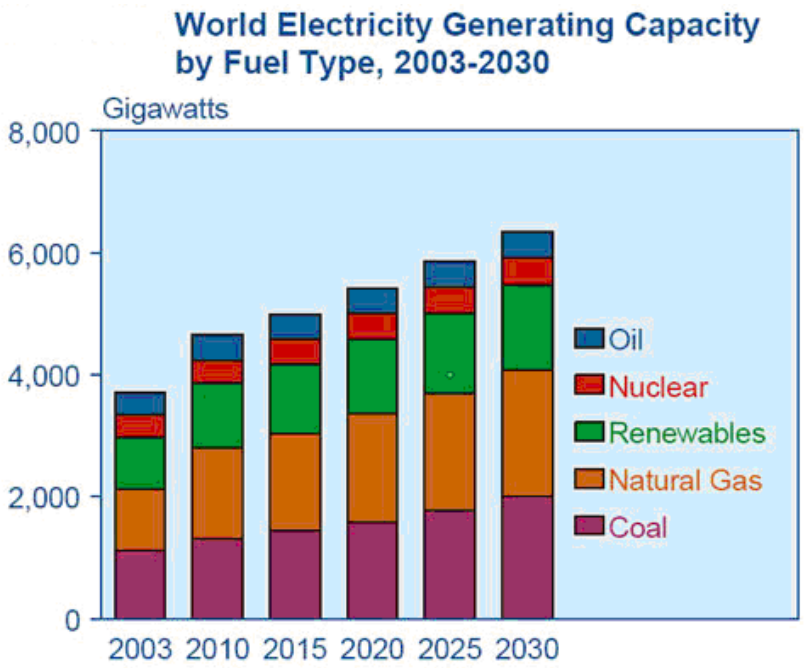

Figure 1.3: Predicted world electricity generation capacity from 2003 to 2030 by type (Energy Information Administration, 2006).

Combustion based thermal power stations fuelled by coal are a mature technology, but extensive international research is occurring to develop new thermal power stations which have higher electrical efficiencies and can operate on renewable (biomass) sources. One high volume, potential fuel source for thermal biomass power stations is wood residue.

A conventional wood fired combustion based power plant typically has a maximum electrical efficiency of only 20-30 % (depending on scale and design). This is lower than for coal fired

combustion based power plants, because biomass power plants are generally smaller in size due to local fuel sources limitations, and the higher reactivity of biomass means it has a lower combustion temperature (Breeze, 2005). However, through the use of gasification, high electrical efficiencies of up to 50 % are achievable using combined cycle systems, where a gas turbine supplies exhaust heat to generate steam for a steam turbine (Fletcher *et al.*, 2005).

1.6 The Demand for Process Heat in Industry Internationally

The demand for process heat production in industries around the world is continuing to increase strongly. Expansion of metallurgical industries such as steel making and cement production are driving the international trade of fossil fuels like coal. Renewable fuel equivalents such as wood could be used, but the lower energy density of these fuels means that larger volumes need to be consumed. Economic growth and expansion of industries in Asian countries including China and India is proliferating the demand for process heating fuels. Developing technologies which allow these industries to use renewable fuels in place of fossil fuels would significantly reduce the greenhouse gas emissions and sulphur oxide emissions generated (Energy Information Administration, 2007).

1.7 New Zealand Electricity Production and Process Heat Trends

In New Zealand 65 % of the countries total electricity production was generated from hydropower in 2004 (Cowie & Dang, 2006). Due to population expansion and economic development, approximately 320 MW_e of new generation capacity is required to be installed in New Zealand each year. This represents an increase of about 2.3 % of the total electricity generated in 2004 of 41,807GWh (Leyland, 2004). Since New Zealand has a well established forestry sector, feasible quantities of wood residue exist which could be used to generate renewable electricity and help meet the forecast 320 MW_e annual additional capacity requirement.

An estimated 40 MW_{th} of new and replacement heat plant has been installed in recent years in the New Zealand wood processing sector. This is more energy plant than is being installed on a regular basis in the electricity sector (East Harbour Management Services, 2002). This has received little recognition as the energy industry has traditionally focused on electricity generation. “A paradigm shift in thinking to encompass energy rather than electricity will allow

bioenergy to consolidate as a premier fuel for the wood processing industry" (East Harbour Management Services, 2002, p.3).

1.8 Settings for Biomass Gasification based CHP Plants

Two main scenarios exist for the placement of gasification based energy plants:

1. As *industrial* energy plants embedded within industries to co-generate electricity and process heat, with the ability to export surplus electricity to a local grid. See Figure 1.4 of a cogeneration plant in the forest industries.

Figure 1.4: Industrial cogeneration plant using wood residue (Power Plants around the World, 2007).

2. As *large centralised* energy plants near plantation areas which can either consume forest arisings, or specifically grown plantation fuel wood from trees grown on a sustainable cycle. See Figure 1.5 of the 46 MW Grayling biomass fuelled power station in the United States.

Figure 1.5: This 46 MW power station is fuelled by wood residue from local sawmills, plantation wood residue, and clean timber meant for landfills situated in Michigan, US (Jones, 2006).

1.9 Factors Encouraging the Development of Gasification Technologies for CHP Applications

There are two main factors driving the development effort and adoption of gasification based electricity and CHP plants. They are the high electrical efficiencies which can be achieved through the ability to execute a combined cycle utilising solid fuels, and the environmental benefits from improved emission control (Higman & Burgt, 2003; Kehlhofer, 1991).

The electrical efficiency of a single cycle power plant is:

$$\eta_{electrical} = \frac{\text{Electrical output (kW)}}{\text{Fuel input (kW)}}$$

The electrical efficiency of a combined cycle power plant is:

$$\eta_{electrical\ CC} = \frac{\text{Electrical output from topping cycle (kW)} + \text{electrical output from bottoming cycle (kW)}}{\text{Fuel input (kW)}}$$

Overall Efficiency of a CHP Plant (total energy utilised):

$$\eta_{CHP} = \frac{\text{Useful thermal energy (kW)} + \text{Electrical output (kW)}}{\text{Fuel input (kW)}}$$

Combined cycles are more efficient, because a single cycle heat engine can not produce 'work' between the temperature extremes of the burning fuel and the ambient environment. To overcome this limitation, two heat engines are used where one operates at a higher temperature range and its waste heat is used as the heat input to another heat engine forming the bottoming cycle. Most commonly, a gas turbine operating on the Brayton thermodynamic cycle is used for the topping cycle and a steam turbine operating on the Rankine thermodynamic cycle is used for the bottoming cycle. This is shown in Figure 1.6.

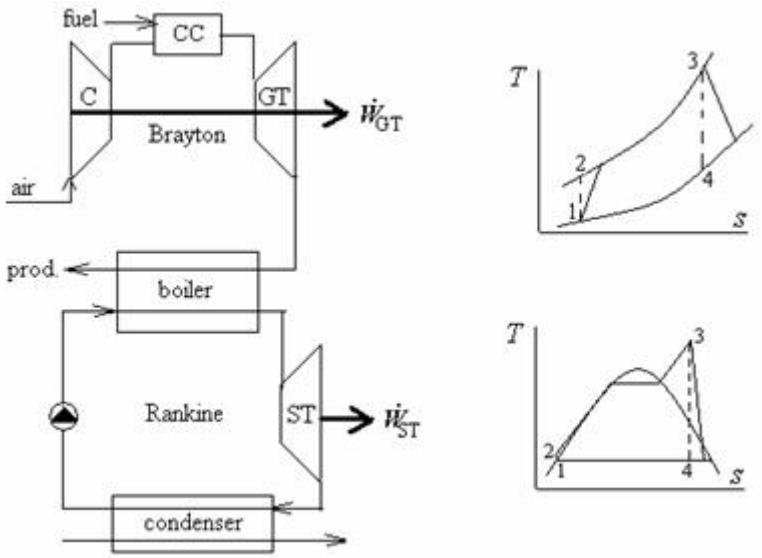

Figure 1.6: Diagrams of the major components and the T-S charts for the Brayton and Rankine thermodynamic cycles. Exhaust heat from the Brayton cycle is the input heat to the Rankine cycle. Source (Isidoro Martínez, 2007).

The environmental benefits that are achieved through gasification of solid fuels are based on the fact that it is easier to clean a *fuel* gas than a *flue* gas. This is because smaller quantities of fuel gas have to be treated than flue gas, and the fuel gas is often at lower temperatures. Consider sulphur for example. It is more practical to remove sulphur from a small stream of producer gas at temperatures from ambient to 800 °C, than it is to remove sulphur from larger volumes of flue gas after combustion in a gas turbine or boiler. Flue gas volumes are larger after combustion because all the combustion air and products of combustion are present, and the temperatures of the gas are often high. Commonly other pollutants such as heavy metals, chlorides etc can be removed in the gasification process.

For many applications where producer gas is being utilised, it often has to be cooled for downstream processes. This can mean bag filters and other conventional gas cleaning equipment that is not suitable for high temperature gases can then be used (Higman & Burgt, 2003). By operating energy plant with very high efficiencies, a greater reduction in the proportion of emissions can be achieved per unit of energy utilised (Kehlhofer *et al.*, 1999).

1.10 Existing Technologies for Energy Production in the Forest Products Industries

Many wood processing industries do have bioenergy facilities using combustion plants where process heat and less frequently electricity is generated. Electricity is normally only generated at the larger processing sites which have significant quantities of residues available. In CHP plants, process heat generation is normally the preference over electricity production, because process heat must be generated onsite or much more locally than electricity, which can be purchased at competitive prices from the national grid. Also the production of electricity is only economically feasible in most circumstances when acceptable economies of scale can be reached.

Energy efficiency is often not maximised in older style bioenergy plants which typically use combustion. Although gasification technologies exist which allow combined cycle systems to operate, these are only of interest when it is desirable to maximise electricity production, since these systems allow for a high electrical efficiency to be achieved. Combined cycles plants are especially desirable when the intention is to generate surplus electricity for export into a local grid. If process heat is the preferred form of energy and the generation of electricity is not the goal, then in most cases a combustion based energy plant is more suitable. However, gasifying does allow for a combustible gas to be generated which can be fired directly inside a kiln or furnace for specialised purposes when a solid fuel is not suitable. Studies have shown that forest residues have the potential to meet all the wood processing industries energy needs for process heat and electricity in New Zealand (East Harbour Management Services, 2002).

1.11 Differences between Biomass and Coal Gasification

The main difference between coal and biomass gasification is the proportion of volatile gases released during the pyrolysis process per unit mass of fuel. For coal, at least 50 wt% of the feedstock is converted into char, with the rest being the pyrolysis gases (assuming a dry, ash free basis). For biomass, a much higher pyrolysis gas yield occurs in the vicinity of 80-85 wt%, with the remaining 15-20 wt% being char (for a dry ash free basis) (Logdberg, 2007). This is because the composition of biomass such as wood contains 70-90% volatile matter compared to 30-45 % for common coals. Hence a larger fraction of biomass can devolatilise to gaseous products than for coal. Additionally, the cellulose and hemicellulose components of biomass have higher reactivates than the carbonaceous materials in coal (Klass, 1998).

Since coal char is much less reactive than biomass char, it requires considerably higher gasification temperatures to achieve satisfactory char-gas reaction rates (Klass, 1998). For coal, gasification reaction temperatures of 1200 °C plus are employed, compared to 800-850 °C for biomass. One disadvantage of lower gasification temperatures, is that higher levels of hydrocarbon tars are generated in the producer gas. Additionally, higher levels of methane are also present with lower temperature gasification, which is desirable for thermal firing and engine applications, but not for fuels and chemicals production (Klass, 1998; Logdberg, 2007).

An advantage of biomass gasification being performed at lower temperatures than coal, is that the energy yield (energy content in the producer gas / energy content of the feedstock) is higher. This is because less thermal energy has to be generated from the feedstock to create the required gasification temperatures, and heat loss rates are less at lower reactor temperatures (Logdberg, 2007).

1.12 Co-firing Existing and Future Thermal Power Plants

As environmental concerns grow and governments set higher requirements for power generation from renewable resources, co-firing of biomass in existing thermal power plants consuming coal is becoming increasingly common. This is often seen as the easiest way for a power generation company to meet the required legislation, rather than building new biomass fuelled power plants. It also incurs less capital investment and a lower level of risk provided an abundant fuel supply is locally available.

Biomass is a slower response fuel than coal so co-firing in biomass power plants can be used to permit better fine tuning of the heat supply and a faster response to changing energy demands in some power plants (depending on the original fuel type and plant design). Natural gas is often a secondary fuel which can be used.

In the case of combined cycle energy plants, secondary fuelling could occur in both the gas engine and the heat recovery steam generator. However, it is most advantageous to supply extra fuel to the topping cycle so that both the topping and bottoming cycles can benefit from the increased heat input (Kehlhofer, 1991).

1.13 Other Biomass Processing Routes for Energy Production

Many technologies exist for utilizing biomass and in particular wood residue, other than in gasification plant. Figure 1.7 shows the common processing routes for biomass feedstocks and the products that result. The two main process paths for biomass are *thermal* and *biological* conversion. The general factor that distinguishes which processing route is followed is the moisture content of the biomass resource. High moisture content biomass is better suited to a biological processing path because micro organisms prefer very damp conditions. Thermal conversion methods such as combustion, gasification and pyrolysis are most feasible with low moisture content feedstocks where large quantities of moisture do not have to be removed for the process to be achievable (Sims, 2002).

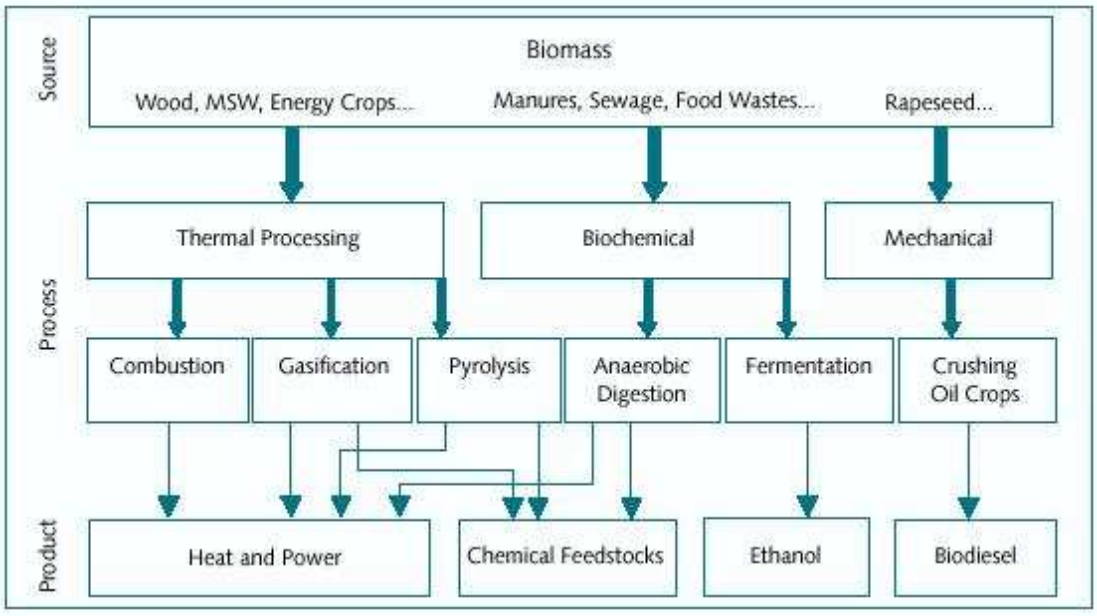

Figure 1.7: Diagram of the three general process paths form biomass source to end products (Schuck, 2007).

1.14 The Carbon Imbalance

The world's forests and forest soils are an integral part of the global carbon cycle. The carbon cycle has been substantially altered by human activity, population growth and urbanisation, including the burning of fossil fuels and deforestation. This anthropogenic activity is now accepted as contributing to global warming. Provided biomass fuels are used in a sustainable manner, where what is consumed gets replanted; the total balance of biomass derived carbon in the biosphere remains in equilibrium (Robinson, 2006). It is principally the burning of fossil fuels, where the carbon contained within the fuels chemical structure is released, which causes

the imbalance in our atmosphere and induces global warming. If these fossil fuels had remained unutilized in their natural underground reservoirs, the carbon levels in our atmosphere would have largely remained at there natural levels (Sims, 2002).

It is evident that to combat global climate change, humans need to change their practices to live more sustainably within the planets ecosystems. For example, renewable energy sources need to be prioritised over fossil energy sources. Construction materials such as aluminium, cement and plastics products require large energy inputs, often from fossil fuels during manufacture. The production of wood products typically requires less energy than competing materials (Robinson, 2006). Changes in people's mindsets and demands need to occur to redirect ourselves from our current poor practices.

1.15 Environmental Aspects

Wood is a renewable resource which has many advantages over burning other solid fuels like coal. Wood has a lower sulphur content than coal, which minimizes the potential of forming sulphur oxides. It is also largely a carbon neutral fuel source provided the biomass is sustainably managed and minimal fossil fuel inputs occur during the management and harvesting phases of the plantations. Trees absorb carbon dioxide from the atmosphere during growth, and the carbon gets incorporated into the plant's cell structure. When combusted or gasified the carbon is re-released to the atmosphere so the net levels of carbon in the biosphere remain in equilibrium. The fate of industrial residues such as wood is important in terms of there greenhouse impact. If residues are burnt to waste or land filled, the carbon is emitted back into the atmosphere without any benefits. However, if the sawdust is combusted or gasified to generate electricity or process heat, the energy generated typically displaces the use of fossil fuels. If residues are used for energy generation, they are usually displacing the use of fossil fuels, permanently eliminating atmospheric emissions that would otherwise have resulted (Robinson, 2006).

As discussed in Section 1.9, gasification has advantages over combustion processes when it comes to emission control. This is because it is far easier to control emissions by cleaning a fuel gas than it is by cleaning flue gases after combustion has occurred (Kehlhofer, 1991). Additionally, biomass gasification provides the possibility to use renewable solid fuels such as wood and agricultural residues in place of conventional technologies many of which consume fossil fuels in a range of occurrences. The development and deployment of gasification

equipment will help to displace the use of fossil fuels in many applications over time. These opportunities are further highlighted in the following section.

1.16 Competing Applications and Future Opportunities for Biomass Gasification

Biomass has a complex composition and comes in so many differing forms, that it can undergo a great range of conversion processes into different end products. The four main energy related uses of biomass derived producer gas are:

1. Electricity generation.
2. The production of synthetic liquid fuels from purified producer gas (syngas).
3. Industrial, process and domestic heating from combustion of producer gas.
4. Hydrogen production after separation of the other gaseous components.

1.16.1 Electricity Generation and CHP Plants

There is a good potential for biomass gasification based electricity generation in the future in areas where a low cost biomass resource is abundant. This is particularly the case for embedded energy plants in industries where the by-products from an industrial process can be consumed to generate electricity and process heat for a factory. Industrial energy plants can have the notable economic advantage of off-setting disposal costs of a waste stream, which significantly helps their financial viability. In some cases there may be the potential to export surplus electricity into a local grid, providing another revenue stream for the company.

Gasification based CHP plants have considerable potential in industries/factories such as: forestry industries, sugar mills, rice mills, cotton factories, cereal factories and sewage treatment plants, where large volume waste streams suitable for thermochemical processing exist. Because a range of other renewable electricity generation technologies normally exist in most countries, often electricity can be generated cheaper by other methods that do not consume biomass, commonly wind, hydro, and geothermal. It often makes sense to focus primarily on the thermal markets within factories, and off set their consumption of electricity purchased from the national grid when feasible. This is because thermal energy in most cases has to be generated on-site and can not be transported over large distances like electricity and readily purchased from a grid network.

1.16.2 Production of Synthetic Liquid Fuels from Biomass

It is possible to produce a range of liquid transport fuels from biomass via a gasification processing route. The two most applicable potential transport fuels are Fischer-Tropsch fuels and biomethanol. With increasing prices of petroleum based transport fuels, this is becoming increasingly investigated throughout the world. The production of synthetic liquid fuels has traditionally been from coal gasification, with the Sasol plant in South Africa being a large scale example of how a country can produce their own transport fuels.

To manufacture a hydrocarbon liquid fuel similar to petroleum fuels from biomass, the producer gas is converted into syngas, and the syngas is further reacted to yield the hydrocarbon products. Since gasification does not generate pure syngas which is a mixture of only hydrogen and carbon monoxide, the additional components in producer gas such as carbon dioxide, methane, light hydrocarbons and tars have to be removed or further reacted to break them down into CO and H_2. Normally gasification reactions do not yield hydrogen and carbon monoxide close to the required proportions, so additional processing to obtain the necessary H_2/CO ratio is often required to maximise the production of the desired fuel product (Probstein & Hicks, 2006; Supp, 1990).

1.16.3 Generation of Gaseous Heating Fuels

The easiest application to integrate a gasification process to is normally a direct thermal application such as firing a boiler or kiln. This is because thermal firing applications like kilns and boilers have the lowest producer gas quality requirements, especially with respect to there acceptance of tars. Additionally, these systems are often simpler and less capital intensive than the other applications for producer gas being discussed in Section 1.16. Producer gas can also be upgraded and used as a replacement for natural gas (SNG: 'Synthetic Natural Gas'). A methanation step can be applied to increase the methane content and hence the heating value of the gas, so that it can be introduced into existing gas pipeline networks to supplement fossil based natural gas (Knoef, 2005).

1.16.4 Hydrogen Production from Biomass

Steam injected gasification processes can be developed to yield a high proportion of hydrogen in the producer gas. This can be as high as 35-45 vol% as occurs in the 8 MW biomass gasifier in Güssing, Austria. Hydrogen has many diverse applications and is used extensively in oil

refineries to upgrade heavy oil fractions into lighter products. It is also used throughout other industries including the food, silicon wafer and in optic fibre production (Hydrogen Now, 2001).

Traditionally hydrogen production has been mainly performed through steam reforming of natural gas and gasification of heavy oil residues, but methanol cracking, ammonia cracking and electrolysis of water is also commercially available (Knoef, 2005). The demand for hydrogen production from renewable resources is likely to increase in the future as the deployment of fuel cells becomes more wide spread and it may one day be widely used in the transportation sector (Billings, 2000).

2.0 Background Theory and Review of Literature

2.1 Explanation of Gasification

2.1.1 What is Gasification?

Gasification is a thermo-chemical conversion process for transforming solid & liquid carbonaceous fuels into a combustible gaseous fuel 'producer gas'. Producer gas is an energy carrier commonly comprised of hydrogen, carbon monoxide, methane, carbon dioxide, nitrogen and some higher hydrocarbons. Gasification occurs when sub-stoichiometric levels of oxygen are present with heat, during an oxidation process. A gasifier is the chemical reactor system used to carry out the gasification process within. The percentage of thermal energy in the original fuel which becomes available in the producer gas is generally between 75-88 % (Higman & Burgt, 2003).

Gasification is performed because it allows *wider utilisation* of solid & low grade liquid fuels (such as black liquor), by converting these fuels into a mixture of combustible gases. Since biomass is converted into producer gas, its versatility is increased because a greater range of technologies exist which can operate with gaseous fuels. Hence gasification is an up-grading process for solid and liquid carbonaceous fuels into gaseous fuels.

For example, wood and coal are largely restricted to being combusted in a boiler or fireplace to generate heat, but they can not be directly used to fuel internal combustion engines (gas turbines, reciprocating engines), unless they are first converted into a gaseous or liquid state. In combined heat and power applications, performing a gasification step allows combined cycle arrangements to be performed from solid fuels. This means that a topping cycle such as the Brayton cycle can reject its waste heat into the Rankine cycle, to further generate more electricity in a highly efficient manner. Gasification also allows the possibility for the energy in solid fuels to be used in fuel cells and in the manufacture of liquid transport fuels and chemicals.

The ratio of oxygen available to the amount of oxygen that would be required for complete combustion is called the *equivalence ratio*. For equivalence ratios between 0 and 0.1 the process is called *pyrolysis*. The main products of pyrolysis include char and oily residues, with some gaseous fractions yielded. If the equivalence ratio is between 0.2 and 0.5, the process is called

gasification. In an oxidation process where close to the stoichiometric quantities of oxygen are present, the process is called *combustion* (Sorensen, 2004). This is shown in Figure 2.1. Processes occurring at equivalence ratios between the boundaries of two generalised groups create mixed processes, such as mixed pyrolysis and gasification (Reed & Desrosiers). Gasification with steam instead of air or oxygen is similar to gasification at a low equivalence ratio in the mixed pyrolysis-gasification region.

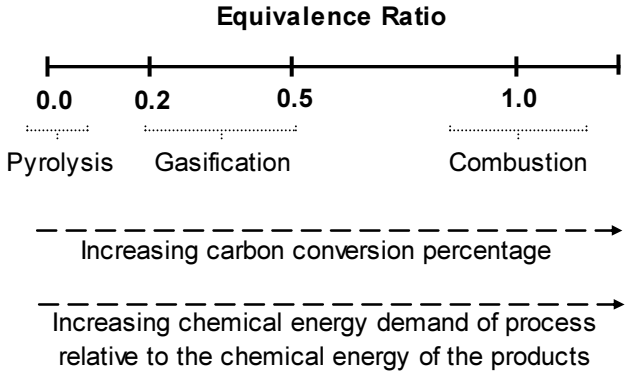

Figure 2.1: Continuum of the equivalence ratios representing the amount of oxidant present in thermochemical reactions relative to the stoichiometric requirement for complete oxidation. Derived from: (Arena & Mastellone, 2005; Wergelandsveien, 2008).

Specifically the equivalence ratio Φ for any process is the division of the actual oxygen-fuel ratio present, by the oxygen-fuel ratio required for complete combustion. Because the gasification reactions take place with such low levels of oxygen, the overall gasification process is endothermic, requiring a heat source to drive the process (Brown, 2003).

$$\textit{Equivalence ratio } \Phi = \frac{\text{Actual oxygen/fuel ratio}}{\text{Stoichiometric oxygen/fuel ratio for complete combustion}}$$

At an equivalence ratio of about 0.25, all the char is converted into gas giving the highest energy densities in the gas (for air blown gasification systems). This is the region where maximum energy transfer to the gaseous state occurs (Knoef, 2005). Figure 2.2 shows how producer gas production peaks at an equivalence ratio of 0.25 as the char is consumed for a wood feedstock having an enthalpy of 22 MJ/kg. The enthalpy of the gaseous products rise until a limit at around Φ = 0.25 is reached, after this point the fuel gas components begin to get consumed and the

process tends more towards combustion. At higher equivalence ratios the chemical conversion efficiency is low as more flue gas is yielded. Since a fuel gas is desired with gasification, the process is operated under conditions where maximum chemical-fuel energy in the gas is obtained, unlike combustion which maximises the sensible energy of the gaseous product (flue gas). With pyrolysis more solids are generated so this technology is usually employed where the solid product is largely favoured.

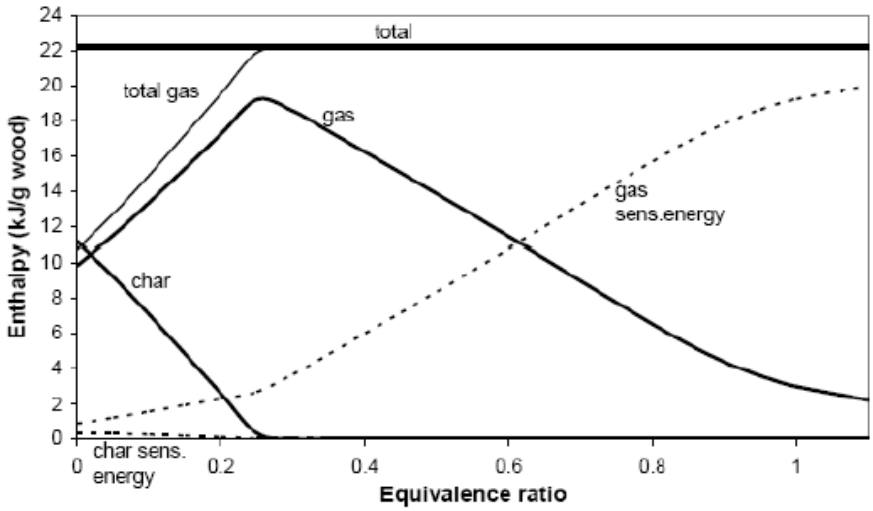

Figure 2.2: Graph showing the changes in product states yielded at different equivalence ratios for wood. Peak producer gas production occurs at $\Phi = 0.25$. Source: (Wergelandsveien, 2008).

As the equivalence ratio changes, the group of thermochemical reactions are influenced and different proportions of gaseous products are evolved. This is shown in Figure 2.3 from computer generated data on air blown gasification (Kaupp & Goss, 1981; Knoef, 2005).

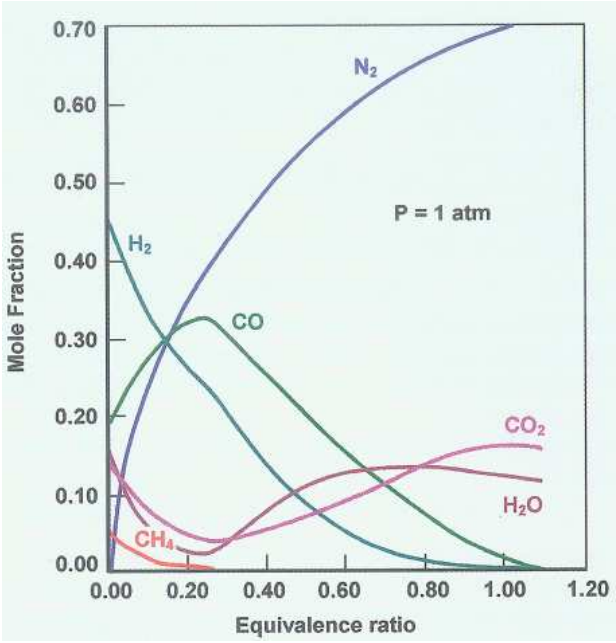

Figure 2.3: Computed gas composition as a function of equivalence ratio. Kaupp (as cited in Knoef, 2005).

2.1.2 Optimal Composition of Producer Gas

There are three general classes of producer gas that can be generated, distinguished in terms of which heating value range the gas falls within. The groups are: low, medium and high heating value producer gas. The boundaries of the groups are not fixed but are commonly classed as follows (Klass, 1998):

- Low energy value gases 3-12 MJ/Nm^3
- Medium energy value gases 12-27 MJ/Nm^3
- High energy value gases 27-40+ MJ/Nm^3

Low energy producer gas is normally generated when there is direct contact of biomass and air in the reactor. The air introduces large quantities of nitrogen which dilutes the producer gas. Medium energy gases are obtained from autothermal biomass gasifiers where oxygen is used and allothermal gasifiers where indirect heating occurs because combustion and gasification are physically separated. High energy producer gas is generated when the gasification conditions promote the formation of methane and other light hydrocarbons, or when subsequent processing and shift reactions are carried out (Klass, 1998).

For heat and power applications, a high heating value gas is the aim, so the gasification process should be optimised to maximise the production of methane and other light hydrocarbon gases. This is because the lower heating value of methane and light hydrocarbons is much greater than that of hydrogen and carbon monoxide as shown in Table 2.1 (Klass, 1998).

Table 2.1: Lower heating values of the combustible gases commonly formed in gasification processes.

Combustible Gas	Lower heating value (MJ/Nm^3)
Methane	32.8
Ethane	58.4
Ethene / Ethylene	49.8
Hydrogen	9.9
Carbon monoxide	11.6

Increasing pressures tend to lower the equilibrium concentrations of hydrogen and carbon monoxide and increase the concentrations of methane and carbon dioxide. Methane and carbon dioxide formation are also favoured by lower reaction temperatures, which is opposite to increase the level of hydrogen and carbon monoxide generated. Gasification carried out in environments with elevated levels of hydrogen, appear to also favour methane production (Klass, 1998).

For combined heat and power applications where a heat engine is to be fuelled or where the producer gas will be used for process heating, the highest calorific value gas composition is most favourable. This is not the case for syngas production to manufacture liquid fuels and chemicals where instead only hydrogen and carbon monoxide is desired and in proportions specific to the chemical product being manufactured. Synthesis gas has a theoretical limit of 10.5-12.5 MJ/Nm^3 on its heating value if methane and other hydrocarbons are minimised (Olofsson *et al.*, 2005).

The maximum LHV of synthesis gas with air as an oxidising agent is about 7 MJ/Nm^3 when methane and other hydrocarbon formation is minimised. This is due to the high levels of nitrogen present. If pure oxygen is used as the oxidant the LHV is limited to about 12 MJ/Nm^3, and for steam gasification the upper limit on the LHV is about 11.5 MJ/Nm^3 for gas mixtures of predominantly hydrogen and carbon monoxide (Olofsson *et al.*, 2005).

2.1.3 Description of the Thermochemical Processes of Biomass Gasification

In a gasifier a range of thermochemical reactions occur which can be collected into four general groups. These are the *heating-drying*, *pyrolysis* (or devolatilisation) reactions, *char-gas* reactions and *gas-phase* reactions (Brown, 2003). These are loosely termed gasification reactions because they take place at an equivalence ratio within the gasification range. The reaction path is shown in Figure 2.4. Note that different parallel reaction sets occur once the pyrolysis products have been formed.

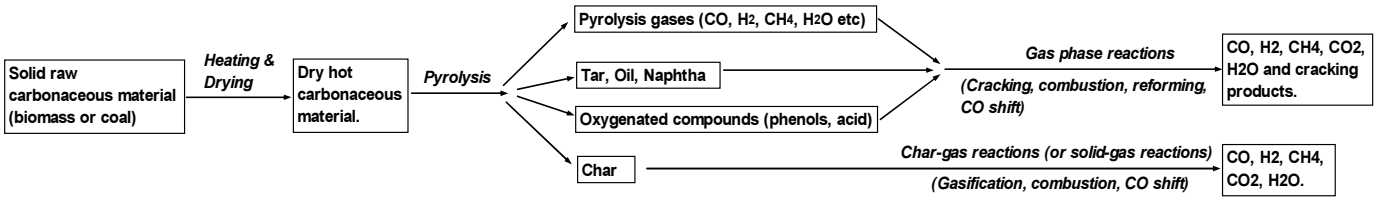

Figure 2.4: The reaction paths for carbonaceous material at an equivalence ratio of 0.25 corresponding to gasification. Source: (Higman & Burgt, 2003).

Heating and Drying

The heating and drying process for a fuel particle is normally not accompanied by any chemical reaction. As the thermal front advances into the interior of the particle water vapour is driven out. This concept is shown in Figure 2.5. As long as water remains in the particle, the temperature can not rise high enough to initiate pyrolysis (Brown, 2003). The drying process for wood occurs up to a temperature of around 200 °C after which pyrolysis reactions begin to occur (Grassi & Bridgewater, 1991).

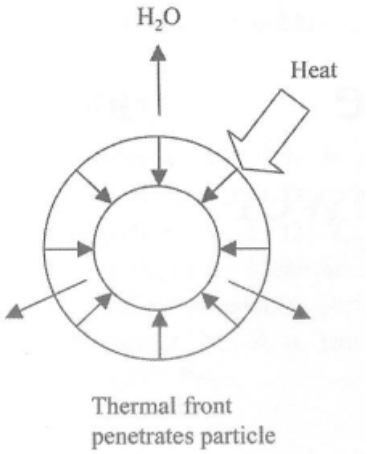

Figure 2.5: The physical drying of a fuel particle in a hot environment. Source: (Brown, 2003).

Pyrolysis (Devolatilisation) Reactions

Pyrolysis (or devolatilisation) is the thermal decomposition of a fuel to yield gaseous and solid products. The pyrolysis process is highly complex and moves through different phases depending on the temperature. As wood is heated from about 200 °C to 280 °C, the less thermally stable hemicellulose breaks down. Xylans give off water, acetic acid, formic acid and furfural plus carbon monoxide, carbon dioxide and methanol (Grassi & Bridgewater, 1991). The breakdown of lignin is also initiated but at a slightly higher temperature than for hemicellulose (commonly between 250-500 °C). Oxygen is excluded from the pyrolysis zone by the large gaseous outflow of pyrolysis products evolving from the surface of the particle (Brown, 2003). At 280 °C a distinct exothermic reaction occurs where the temperature rises rapidly to 350 °C with no external energy input. Lighter hydrocarbons and tars begin to be generated (Grassi & Bridgewater, 1991).

At temperatures above 350 °C an external heat source is required to maintain the process. Cellulose breaks down producing water, CO_2, and charcoal via an intermediate substance levoglucosan. Lignin also degrades to phenol compounds and methanol, with heavier tars appearing (Grassi & Bridgewater, 1991). Throughout the devolatilisation process, the release of volatile compounds creates pores that penetrate into the fuel particle forming the carbonaceous residue known as char (Brown, 2003). This is represented in Figure 2.6. Although the pyrolysis process needs a certain level of heat to initiate, the sensible heating process of the fuel particles continues as the pyrolysis process advances. The rate of heating of the fuel particles influences the way the pyrolysis process occurs (Higman & Burgt, 2003). The rate of heating depends on the size of the particles and the reaction temperatures. Larger particles have slower heating rates and require longer residence times in the gasification reactor (Brown, 2003).

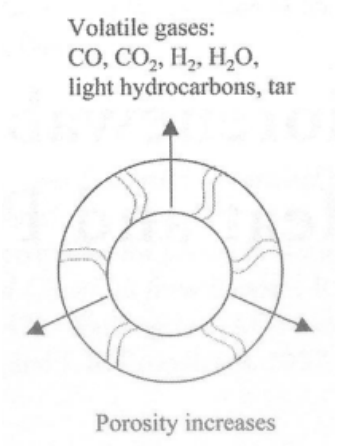

Figure 2.6: The increasing porosity of a fuel particle as volatile gases are released. Source: (Brown, 2003).

The products of pyrolysis are: char, gases (mainly CO, CO_2, H_2 and light hydrocarbons) plus condensable vapours (including water, methanol, acetic acid, acetone and heavy hydrocarbons) (Brown, 2003). Hydrocarbons which have a molecular weight higher than benzene are collectively classed as tars and are most unfavourable to have in the producer gas (Devi *et al.*, 2002). Tars have significant detrimental effects on downstream processes and equipment and can render catalysts inactive and adhere to any internal surfaces where they condense. The distribution of these products depends on the chemical composition of the fuel, the heating rate and the conditions in the reactor (especially temperature). "The fuel's volatile matter roughly corresponds to the pyrolysis yield, while the combination of fixed carbon and ash content can be used to estimate the char yield" (Brown, 2003, p. 146).

The interplay between pyrolysis and the gasification reactions (both gas phase and char-gas reactions) under different heating conditions affect the quantity of tars yielded in the producer gas. If the heat up rate is slow then the endothermic pyrolysis reactions set in at about 350 °C and the gasification reactions of steam and char follow, but are very slow at this temperature. With a slow heating rate the concentration of volatiles outside the fuel particle grows rapidly producing a smoky gas and the gasification reactions only set in after pyrolysis is complete (Higman & Burgt, 2003). Figure 2.7 shows how slow and fast heating rates cause different process paths to be taken.

If the heating rate is high, then the pyrolysis and char-gasification reactions occur more simultaneously and a high concentration of volatiles is not allowed to build up around the outside of the fuel particles (Higman & Burgt, 2003). The slower the heating rate of the fuel particles, the higher is the chance of tars forming, which are mainly generated during the pyrolysis stage. This tar laden gas can leave the reactor with the producer gas un-reacted. So it is advantageous to feed the biomass directly into the bed of the gasification reactor where the heat up rate will be fastest. Feeding the biomass directly into the gasifier bed material also improves contacting with any catalytic bed material (Hofbauer,Rauch *et al.,*2000). The product distribution from the devolatilisation process varies significantly with changes in the pyrolysis temperature and the speed of heating up of the particles (Higman & Burgt, 2003). Higher moisture contents tend to slow the rate at which pyrolysis occurs and is likely to influence the interplay between gasification and pyrolysis (de Diego *et al.*, 2001).

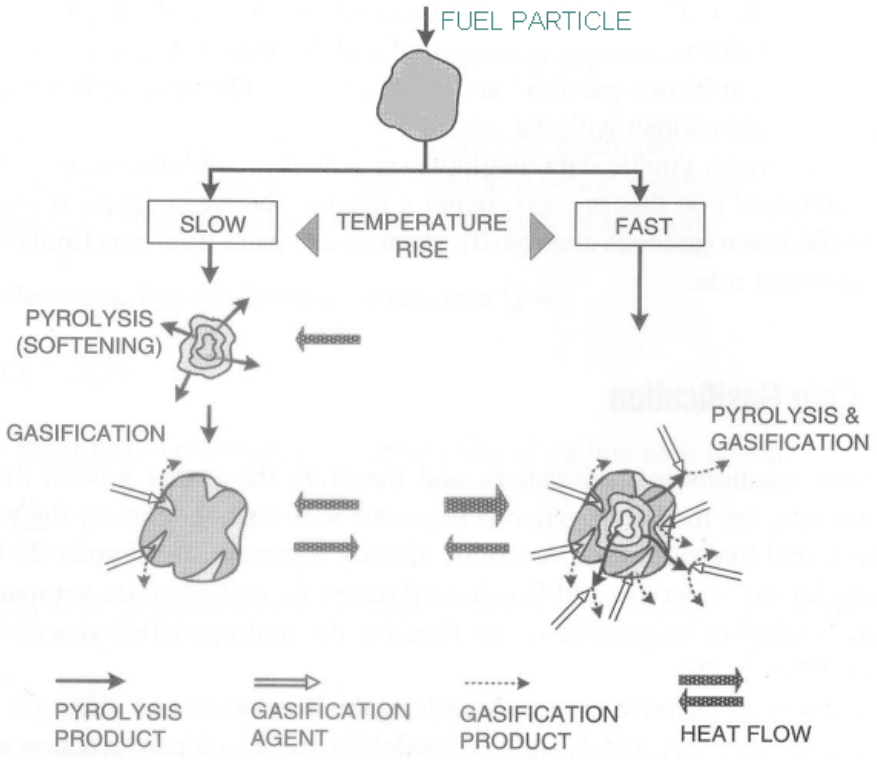

Figure 2.7: The thermochemical reaction paths taken for slow and fast heating rates of fuel particles. These are not mutually exclusive so an intermediate heating rate shares characteristics of both the slow and the fast path. Source: (Higman & Burgt, 2003).

Studies carried out in Spain concluded that the surrounding gases in the pyrolysis environment have minimal influence on the amount of volatiles yielded during pyrolysis (de Diego *et al.*, 2001). If methane is produced along with undesirable carbon dioxide, the process becomes progressively more exothermic. Oxidation reactions are exothermic except at low oxygen levels. The types of products from pyrolysis and their proportions determine the degree of endothermicity and exothermicity of the process. As the formation of methane and carbon dioxide increases, and the formation of carbon monoxide decreases, the trend is towards a more exothermic process (Klass, 1998).

Char-Gas Reactions (Solid-Gas Reactions)

After initiation of pyrolysis, char begins to be formed. The char undergoes a set of reactions generally termed the char-gasification reactions. Char is primarily carbon with a small amount of mineral matter interspersed. Depending on the porosity and the reactivity of the char plus the reaction temperatures, the oxidising agent may react with char at the surface of the particle or, it may penetrate into the pores within the char particle. If the oxidising agent reacts at the surface

of the fuel particle, a steadily shrinking core of char results. If the oxidising agent penetrates into the pores of the char particle, a constant diameter particle of increasing porosity occurs (Brown, 2003). Much higher temperatures are required for the char gasification reactions than is required for the pyrolysis reactions (Antal, 1983).

The gas-solid reactions are slow compared to the gas phase reactions and often limit the overall rate of the gasification process and the carbon conversion efficiency (Knoef, 2005). The reactivity of different solid fuels such as charcoal and coal depend on many factors particularly (Higman & Burgt, 2003):

- The porosity of the substrate (inner structure, surface and active sites)
- The crystal structure of the fixed carbon in the material
- The catalytic effects of ash components present

Materials which have a large specific surface area have a high reactivity. Reactivity can also be enhanced by the presence of alkalis such as potassium (Higman & Burgt, 2003).

Gas Phase Reactions

The concluding set of thermochemical reactions are the gas-phase reactions which determine the final mix of gaseous products because they also involve the gases released from the char-gas reactions (Brown, 2003). Gas-phase reactions of the liberated pyrolysis gases often occur simultaneously with the char-gas reactions of the porous charcoal particles as shown in Figure 2.6. However the gas phase reactions of the pyrolysis products are much more rapid than the char-gas reactions. The volatile matter yielded from the pyrolysis process begins to take part in the gas-phase reactions when temperatures exceed about 600 °C (Antal, 1983). The pyrolysis reactions produce a variety of species including tars, hydrocarbon liquids and gases. The volatile gases react with any oxidant surrounding the fuel particle and the extent to which the oxidant is completely or partially depleted depends on the quantity of volatiles produced during the pyrolysis stage. In a combustion environment there is enough excess oxygen to drive the combustion process to completion, but under gasification conditions this is not the case especially with biomass which has a high volatile matter content.

The gasification conditions such as reaction temperatures, steam to biomass ratio, equivalence ratio and residence times all effect the final gas composition. When long residence times prevail the thermochemical reactions can reach equilibrium with the main producer gas products being:

CO, CO_2, H_2, CH_4 and nitrogen if air is present. The production of high levels of methane in the producer gas is favoured by low temperatures and high pressures and increased residence times. In contrast the formation of H_2 and CO is encouraged by high temperatures and low pressures. The gas-phase reactions are considered to dominate the gasification chemistry (Antal, 1983). Commonly residence times in gasifiers are not long enough and temperatures are too low for chemical equilibrium to be obtained and various amounts of light hydrocarbons such as C_2H_2 and C_2H_4 plus heavy hydrocarbon tars are formed (Brown, 2003).

2.1.4 Description of the Thermochemical Reactions for Biomass Gasification

The specific paths taken by chemical species and full set of reactions for thermochemical process such as gasification are not fully understood. This is particularly the case for the pyrolysis reactions which are renowned for their complexity. The subheadings below present the most common reactions associated with the different stages of the gasification process. The standard heats of formation and heats of reaction have been included so that the reader gets a feeling for the magnitude of heat liberation and consumption, but it must be remembered that these are different for the temperatures occurring in a gasifier. Where a definitive heat of reaction can not be specified the endothermicity or exothermicity of the reactions has been indicated. Reactants and products are in the gaseous state unless otherwise indicated.

Heating and Drying

The heating and drying process is a physical evaporation and heating process, which technically does not involve any chemical reactions but has been presented here for completeness.

Wet biomass $\Leftrightarrow$ Dry biomass + Water vapour +ve ΔH (Rutherford, 2006)

($CH_{1.44}O_{0.66\,(s)} + H_2O_{(L)}$) $\Leftrightarrow$ $CH_{1.44}O_{0.66\,(s)} + H_2O_{(g)}$ +ve ΔH (Rutherford, 2006)

Pyrolysis (Devolatilisation)

These reactions are very complex and poorly understood. Many intermediate products are formed which then proceed through secondary reactions (Grassi & Bridgewater, 1991). The overall process is endothermic and the end products of the pyrolysis process are: CO, H_2, CH_4, H_2O, tar, oil, naphtha plus oxygenated compounds such as phenols, acids etc (Higman & Burgt, 2003).

Biomass: $C_{4.8}H_{5.8}O_{2.8\,(s)} \Rightarrow n_{tar}\, CH_aO_b + n_{char}\, CH_cO_{d\,(s)} + n_{H2}\, H_2 + n_{CH4}\, CH_4 +$

$N_{CO}\, CO + n_{CO2}\, CO_2 + n_{C2H4}\, C_2H_4 + n_{C2H2}\, C_2H_2$ +ve ΔH (Rutherford, 2006)

Solid-Gas Reactions (Char-Gas Reactions)

These reactions are far better understood than the pyrolysis reactions. They are all solid-gas reactions consuming carbon in the solid state to form CO, H_2 and CH_4. They occur much more slowly than the gas phase reactions and are often the limiting factor for the gasification process reaching thermodynamic equilibrium (Higman & Burgt, 2003).

The endothermic *carbon-water reaction* (primary) where carbon in the char reacts with steam to yield H_2 and CO is favoured by higher gasification temperatures and is shown below. Some researchers report another carbon-water reaction known as the *secondary carbon-water reaction.* For this reaction carbon and two moles of steam react to yield CO_2 and two moles of H_2 (Franco *et al.*, 2002). (These reactions are also called the primary and secondary 'water gas' reactions but must not be confused with the 'water gas *shift*' reaction. For ease of understanding the name carbon-water reaction will be used in this thesis). These reactions can be controlled by changing the steam to biomass ratio of the gasification process and are both favoured by higher reaction temperatures.

Primary: $C_{(s)} + H_2O_{(g)} \Leftrightarrow CO + H_2$ $\Delta H = 131.3$ kJ/mol

Secondary: $C_{(s)} + 2H_2O_{(g)} \Leftrightarrow CO_2 + 2H_2$ $\Delta H = 90.1$ kJ/mol

The *hydrogenation reaction* involves the exothermic conversion of carbon in a hydrogen rich environment to methane. This is one of the important reactions for CHP applications as it leads to a medium to high calorific value producer gas being generated (Klass, 1998).

$C_{(s)} + 2H_2 \Leftrightarrow CH_4$ $\Delta H = -74.5$ kJ/mol

The *Boudouard reaction* is an endothermic reaction of solid carbon with CO_2 to form CO. Since CO_2 has no energy value, this reaction also wants to be driven in the forward direction to maximise the production of the fuel gas CO.

$C_{(s)} + CO_2 \Leftrightarrow 2CO$ $\Delta H = 172.5$ kJ/mol

Gas Phase Reactions

The gas phase reactions are more rapid than the solid-gas reactions. They occur throughout the reactor vessel, even above the particle/fuel bed. They often determine the final mix of gaseous products in the producer gas (Probstein & Hicks, 2006).

The *steam methane reforming reaction* is a highly endothermic reaction which converts methane and water vapour to carbon monoxide and hydrogen:

$$CH_4 + H_2O_{(g)} \Leftrightarrow CO + 3H_2 \qquad \Delta H = 205.8 \text{ kJ/mol}$$

The exothermic *water-gas shift reaction* involves the conversion of carbon monoxide and water vapour into carbon dioxide and hydrogen.

$$CO + H_2O_{(g)} \Leftrightarrow CO_2 + H_2 \qquad \Delta H = -41.2 \text{ kJ/mol}$$

The water gas shift reaction is considered one of the most dominant reactions for setting the final gas composition in the steam gasification temperature range of 730-830 °C. At temperatures above 830 °C the carbon-water reactions and the Boudouard reaction become increasingly dominant with most wood feedstocks (Franco *et al.*, 2002).

Partial and Complete Combustion Reactions

During the pyrolysis and char gasification processes, any available oxygen undergoes localised combustion in the gasification column (Higman & Burgt, 2003). Oxygen is introduced from the injected steam and any oxygen in the fuel. The induction of air into the gasification reactor also introduces oxygen. These reactions should not be thought of as a separate process because they can occur at all stages in the conversion of wood to producer gas. These reactions are all exothermic. Note: in air blown gasification, partial and complete oxidation reactions are more abundant and mainly partial oxidation reactions have been displayed below.

$$C_{(s)} + {}^1/_2\, O_2 = CO \qquad \Delta H = -101.5 \text{ kJ/mol}$$

$$CO + {}^1/_2\, O_2 = CO_2 \qquad \Delta H = -393.5 \text{ kJ/mol}$$

$$H_2 + {}^1/_2\, O_2 = H_2O_{(g)} \qquad \Delta H = -241.8 \text{ kJ/mol}$$

$$CH_4 + {}^3/_2\, O_2 = CO + 2H_2O_{(g)} \qquad \Delta H = -519.6 \text{ kJ/mol}$$

2.1.5 Oxidising Agents

Three common oxidising agents are used in gasification. They are: air, oxygen and steam. An *oxidising agent* (or *blast* or *gasification agent*) is any substance which causes oxidation by increasing the oxidation state of the substance. For the gasification process, this has the effect of increasing the equivalence ratio of a thermochemical reaction to a level higher than occurs for pure pyrolysis. The oxidising agent can either provide free oxygen or bound oxygen such as in

steam. Air is the most practical oxidising agent as it is readily available but has the major disadvantage of containing about 79 % nitrogen. Hence if air enters the gasification reactor it significantly lowers the calorific value of the producer gas due to the high levels of nitrogen it introduces. Oxygen is a good oxidant and produces a higher calorific value gas than air blown gasifiers, but its major disadvantage is it introduces the need for an oxygen plant. This adds significant cost and complexity to a gasification system and often the gasification temperatures are high enough to enter the slagging mode of operation when oxygen is being used (Higman & Burgt, 2003). To counteract this, steam is sometimes injected as a moderator to lower the gasification temperatures. Since there is almost no steam in oxygen blown gasifiers to promote the water-gas shift reaction, the producer gas is rich in carbon monoxide (Knoef, 2005). Other moderators such as nitrogen and carbon dioxide can be used but they lower the calorific value of the producer gas.

Steam is the third type of oxidising agent used and has two unique properties not shared by air. Steam does not introduce nitrogen into the producer gas, and it contains two hydrogen atoms for every atom of oxygen. Steam takes part in the equilibrium reactions inside the gasifier at the elevated temperatures and any unreacted oxygen from the steam, partly or fully oxidises carbon and hydrogen to CO, CO_2 and H_2O. The remaining hydrogen introduced from the steam then takes part in the gas-phase and solid-gas reactions. Hence, the introduction of steam significantly raises the hydrogen content of the producer gas (Rauch, 2004). As shown later in Table 2.4, wood commonly contains about 6 % hydrogen on a dry mass basis, so the majority of hydrogen in producer gas is generated from the injection of steam and not from the feedstock. The equation for the steam to biomass ratio (also known as the steam to fuel ratio) is (Hofbauer & Rauch, 2000):

$$\textit{Steam to biomass ratio} = \frac{\text{mass flowrate}_{\text{steam in}} + \text{mass flowrate}_{\text{fuel moiture in}}}{\text{flowrate}_{\text{dry fuel in}}} \qquad (\text{kg/kg}_{\text{dry}})$$

In a fluidized bed gasifier the oxidising agent is often used to serve the second purpose of fluidizing the particle bed to obtain isothermal bed temperatures. Hence in fluidized bed gasifiers the term oxidising agent and fluidizing agent represent different things, but often the one fluid serves both purposes.

Some researchers use a term called the gasifying ratio. This is shown below and is a ratio of the mass flow rate of steam plus oxygen being introduced into the reactor divided by the feed rate of the fuel on a dry-ash-free ($_{daf}$) basis. This term is normally only applied when combinations of steam and air or steam and oxygen are used as the oxidant. The relative proportions of steam and oxygen are not distinguished between.

$$\textit{Gasifying Ratio (GR)} = \frac{\text{Steam (kg/h)} + \text{Oxygen (kg/h)}}{\text{Biomass (kg}_{daf}\text{/h)}} \qquad (\text{kg/kg}_{daf})$$

2.1.6 Measures of Gasification Efficiency and Performance

The efficiency of a gasification process can be expressed in two ways: the cold gas efficiency and the hot gas efficiency. The *cold gas efficiency* is the combustion energy of the producer gas divided by the energy content of the feedstock (biomass) entering the reactor plus any supplementary fuel. The *hot gas efficiency* is the combustion plus sensible heat of the producer gas divided by the energy content of the feedstock plus any supplementary fuel. It should always be stated whether the heating values are on a LHV or a HHV basis. "In well insulated reactors the hot gas efficiency can be close to 100 %" (Knoef, 2005, p.18). In FICFB gasifiers, the cold gas efficiency is commonly low, around 60-70 % (Devi *et al.*, 2002).

$$\textit{Cold Gas Efficiency (\%)} = \frac{\text{Combustion energy of producer gas}}{\text{Total Energy to Gasifier (biomass + external energy used)}} \text{ x } 100$$

$$\textit{Hot Gas Efficiency (\%)} = \frac{\text{Combustion energy + sensible heat of the producer gas}}{\text{Total Energy to Gasifier (biomass + supplimentary fuel)}} \text{x } 100$$

Another measure of a gasifier's performance is how well it converts carbon from the feedstock into carbon containing gases in the producer gas. This is known as the carbon conversion and is defined as (Higman & Burgt, 2003):

$$\textit{Carbon Conversion (\%)} = \left[1 - \frac{\text{Carbon in gasification residue (kmol/h)}}{\text{Carbon in feedstock (kmol/h)}}\right] \text{ x } 100$$

The water conversion of a gasifier is a measure of the amount of water vapour which is consumed in the gasification reactions. The equation for this is (Hofbauer & Rauch, 2000):

$$\textit{Water Conversion (\%)} = \frac{\text{sum water input}_{\text{fluidizing steam + fuel}}\ (\text{kg/h}) - \text{sum water output}_{\text{in producer gas}}\ (\text{kg/h})}{\text{sum water input}_{\text{fluidizing steam + fuel}}\ (\text{kg/h})} \times 100$$

At high steam to biomass ratios, much steam leaves a gasifier unreacted so an optimum between the required gas quality and the efficiency loss due to heating unreacted steam has to be found. Water conversion increases with increasing temperature and increasing amounts of catalyst .

2.1.7 Slagging and Non-slagging Gasification

Fluidized bed and entrained flow gasifiers can operate in slagging and non-slagging modes, referring to either molten ash or dry ash production respectively. Slagging gasification is less practical for biomass due to the lower ash fusion temperatures compared with coal. Some minerals found in biomass melt at very high temperatures which are not desirable to achieve (Knoef, 2005).

In a slagging gasifier the molten slag condenses on the reactor wall to form a protective solid layer. On this solid layer molten liquid slag flows down and is removed at the bottom of the gasifier. In order to generate a liquid slag with the right viscosity at the chosen temperature, generally a fluxing material such as limestone is added. For slagging gasifiers expensive membrane walls have to be used, while non-slagging reactors are refractory lined. In non-slagging gasification the fuel should contain only small amounts of minerals and ash (less than 1 %) otherwise the ash may melt and fuse creating blockages and fouling on the reactor walls (Knoef, 2005).

It is the aim of most non-slagging gasifiers to keep temperatures below approximately 850-900 °C which is a common fusion temperature of fly ash (Knoef, 2005). At temperatures above the ash softening point, the ash becomes sticky and will agglomerate. Once temperatures are above the slagging temperature, the ash is in a molten form and can be removed. No gasifiers are designed to operate in this intermediate region between approximately 900-1200 °C (depending on the feedstock) because of the difficulties with the ash behaviour (Higman & Burgt, 2003).

Normally oxygen blown gasifiers operate in the slagging mode because there is no, or very limited injection of steam which lowers gasification reaction temperatures due to the high specific heat requirement to raise the steam up to the reactor temperatures. Slagging oxygen

blown gasifiers are restricted to large scale applications where the significant cost of an oxygen plant is more justifiable (Knoef, 2005).

2.2 Parameters that Effect the Composition of Producer Gas

The composition of the producer gas is highly important, and determines what types of applications gasification can be used with. The specifications for producer gas are very different for fuel and chemical applications than they are for thermal and engine applications. Currently the lab scale FICFB gasifier at the University of Canterbury is being developed to yield a medium to high calorific value producer gas for CHP applications.

2.2.1 Effect of Temperature on Gasification Reactions

Many literature sources conclude that raising *gasification temperatures* favours the formation of hydrogen and usually carbon monoxide (but CO trends can differ). The increase in the hydrogen content is more distinct with increasing temperatures. Hydrocarbon contents often decrease with increasing reactor temperatures. The formation of methane and to a lesser extent CO_2 is favoured by lower reaction temperatures (Franco *et al.*, 2002; Higman & Burgt, 2003).

Research at the Institute of Chemical Engineering in Vienna found that increasing gasification temperatures from 790-900 °C caused the following trends with their 100 kW_{th} FICFB gasifier (Hofbauer & Rauch, 2000):

- H_2 contents increased
- CO concentration increased (but to a lesser extent)
- CO_2 and CH_4 levels decreased.

These trends were reported to occur because the reaction rates are faster at higher gasification temperatures and a gas composition nearer to equilibrium results. Figure 2.8 shows a plot of the data obtained for this experiment.

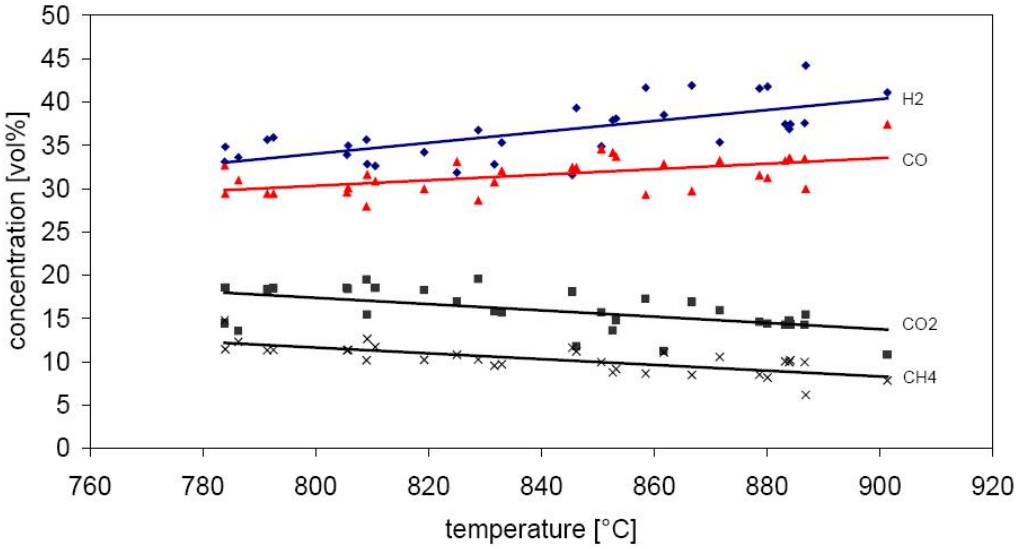

Figure 2.8: Dependency of gas composition with temperature for the 100 kW_{th} FICFB gasifier in Austria. Nitrogen is reported as being below 5 % and is not shown. Source: (Hofbauer & Rauch, 2000).

At higher temperatures, total gas yields are generally higher but the heating value of the producer gas decreases, because less methane and light hydrocarbons are formed with more hydrogen instead. Although the heating value of the gas is reduced, the quantity yielded increases with increasing temperatures. Correspondingly the quantities of char and liquids formed are reduced. This is believed to be due to the further cracking of liquids and enhanced char reaction with the oxidising agent. Other factors which may increase gas yields at higher temperatures include: a higher production of pyrolysis gases, greater gas production from char at higher endothermic reaction temperatures, and an increase in gas yield due to steam reforming and cracking of heavier hydrocarbons (Franco *et al.*, 2002; Higman & Burgt, 2003).

Literature also states that gas composition yields for different wood species becomes less varied as the gasification temperatures are increased. The increased variation in gas composition is believed to be linked to the different reactivity of chars produced during the pyrolysis step. The char reactivity is thought to vary considerably with different cellulose and lignin contents (Franco *et al.*, 2002).

It was found in the 8 MW FICFB gasifier in Güssing, Austria, that higher gasification temperatures lowered the heating value of the producer gas which caused the electrical efficiency of the whole CHP plant to decrease. In addition to this, more energy had to be

expended in circulating bed material to achieve the higher gasification temperatures. Güssing use gasification temperatures of about 850-900 °C in there 8 MW demonstration scale plant (Rauch, 2004).

2.2.2 Effect of Pressure on Gasification Reactions

Elevated *pressures* increase the concentration of methane and carbon dioxide yielded, while the concentrations of hydrogen and carbon monoxide decrease (Higman & Burgt, 2003; Klass, 1998). Many gasifiers operate at elevated pressures. The reason for operating at elevated pressures is the compression energy requirements are less and equipment can be smaller, improving economic viability. The pressure in a gasifier is generally selected in accordance with the requirements of the process or downstream equipment. When elevated pressures are required, compression of the reactants is energetically superior to compression of the producer gas evolved (Higman & Burgt, 2003).

2.2.3 Steam to Biomass Ratio

Steam to biomass ratio tests have been performed on the 100 kW FICFB gasifier in Vienna, Austria. Two temperature groups were investigated 800-850 °C and 850-900 °C with the steam to biomass ratios ranging from approximately 0.2-0.6 kg/kg and 0.2-0.8 kg/kg respectively (see Figure 2.9). The same trends were found for both temperature ranges as steam to biomass ratio was increased (Hofbauer & Rauch, 2000):

- H_2 increased, especially at higher temperatures
- CO_2 increased
- CO decreased
- CH_4 remained unchanged between 800-850 °C, but decreased slightly between 850-900 °C.

With increasing steam to fuel ratio, hydrogen increases and methane levels decrease (Rauch *et al.*, 2002).

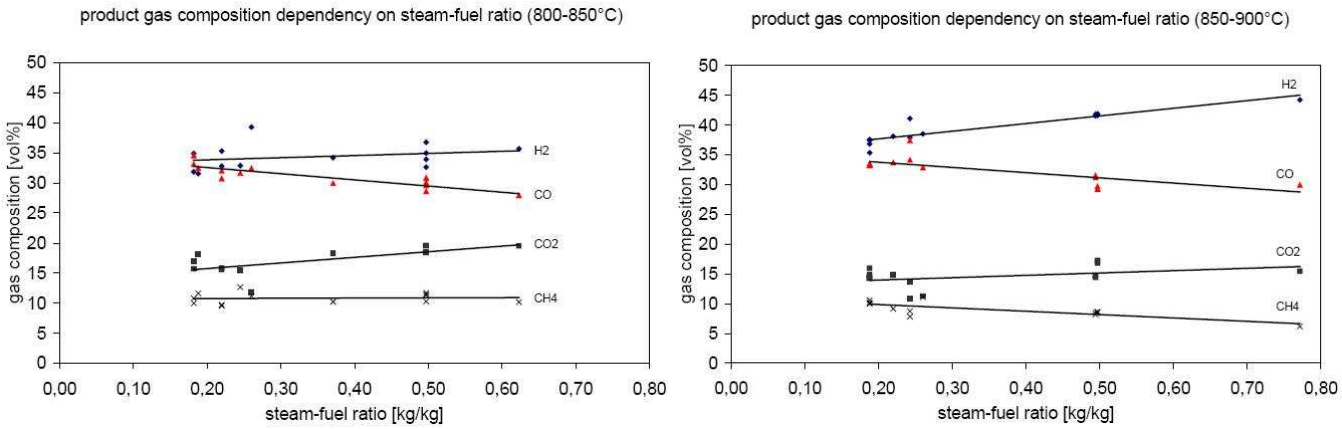

Figure 2.9: Changes to the producer gas composition in the 100 kW_{th} FICFB gasifier in Austria at two different temperature ranges (800-850 °C & 850-900 °C). Source: (Hofbauer & Rauch, 2000).

A parameter which needs to be considered when investigating the steam to biomass ratio is the ***water consumption***. The steam content in the producer gas increases with increasing steam to biomass ratio (Hofbauer & Rauch, 2000). This relationship does not appear to have a linear dependency and is shown in Figure 2.10. Adding excessive amounts of steam can cause too much thermal energy to be consumed in raising the steam to the temperatures found in the gasification reactor. However, excess steam can be desirable to minimise the levels of tar (see Figure 2.15).

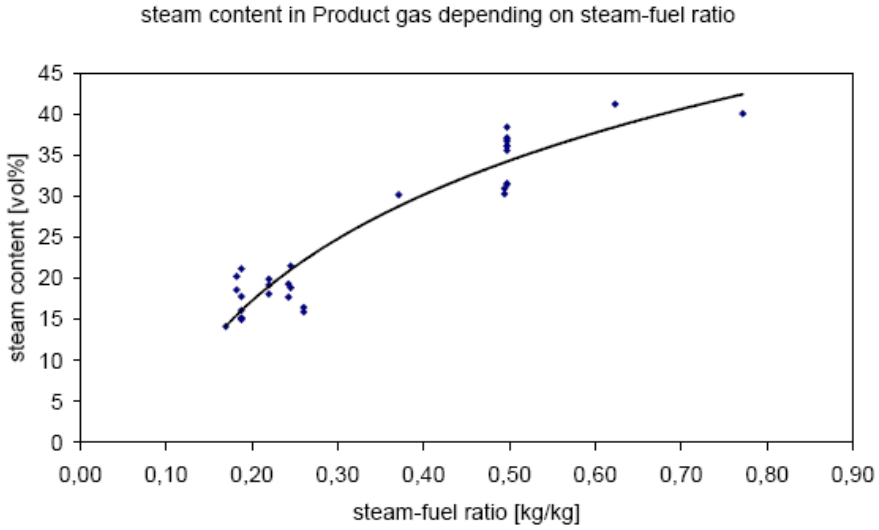

Figure 2.10: Change in the quantity of steam contained in the producer gas with different steam to biomass ratios between 0.15-0.8. Source (Hofbauer & Rauch, 2000).

The ***water conversion*** in the steam gasification process is important as it reflects the amount of water consumed by the gasification reactions. It can be seen that water conversion decreases with increasing steam to fuel ratio in Figure 2.11. The water conversion also increases with increasing temperature. The optimal steam to fuel ratio was considered to be below 0.5 kg/kg_{daf} fuel. It was

considered that above a steam to biomass ratio of 0.5 kg/kg, that water conversion does not vary much and more steam only causes the steam content in the producer gas to increase without shifting reactions (Hofbauer & Rauch, 2000). Güssing use steam-fuel ratios of 0.5-0.68 kg/kg in their 8 MW FICFB gasifier (Rauch, 2004).

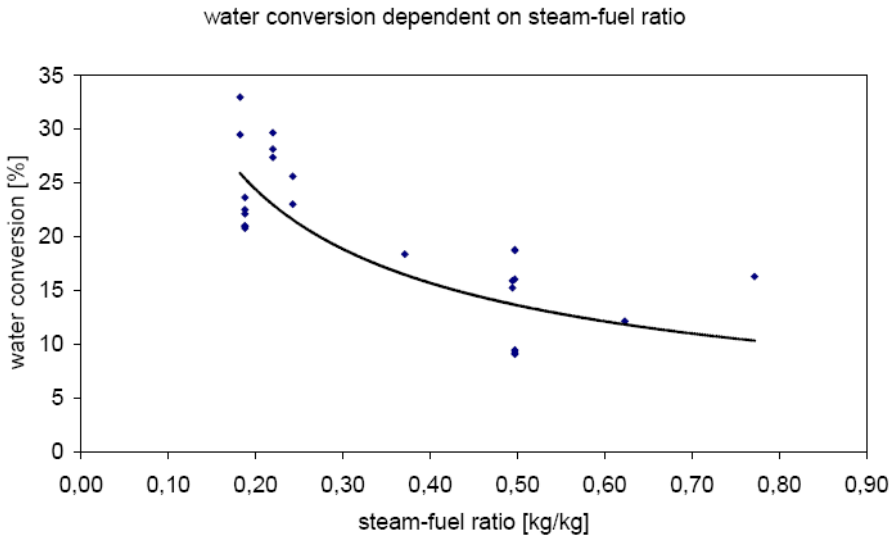

Figure 2.11: The water conversion dependency with different steam to biomass ratios between 0.2-0.8 kg/kg. Source (Hofbauer & Rauch, 2000).

The influence of the steam to biomass ratio on the dry gas yield was investigated at Vienna University of Technology, Austria. The trend found was: as the steam to biomass ratio is increased from 0.5-1 kg/kg_{daf} , the total gas volume yielded increased slightly and the total level of tars was reduced. This is shown in Figure 2.12:

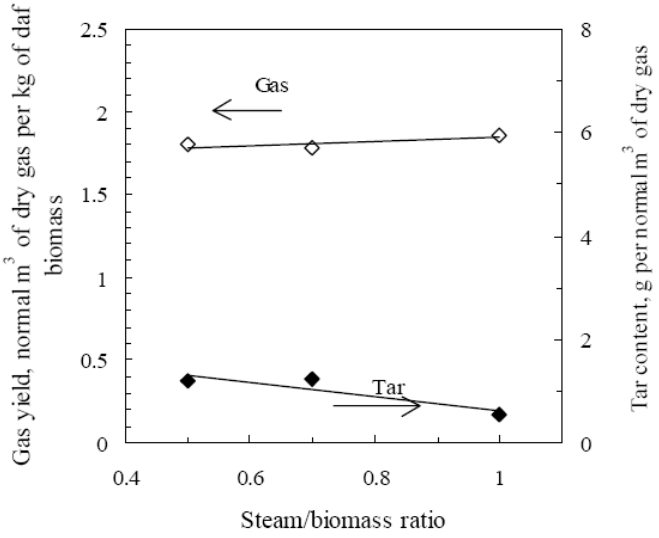

Figure 2.12: The influence of the steam to biomass ratio on producer gas yield and tar levels in the 100 kW_{th} FICFB gasifier in Austria. Source: (Hofbauer, Rauch *et al.*, 2000).

2.2.4 Equivalence Ratio

Equivalence ratio is critical because its higher value decreases the heating value of the producer gas due to the following (Devi *et al.*, 2002):

- Decrease in the concentrations of H_2 and CO (plus CH_4).
- Increase in the CO_2 content in the producer gas.

In steam blown gasification this term is not applied since introduction of air is not intended. However small amounts of air do enter the gasification column of FICFB gasifiers by tracking up the chute from the combustion column. This was found to also occur in the University of Canterbury's FICFB gasifier. Figures 2.2 and 2.3 show how equivalence ratio affects the gas composition.

2.2.5 Gasifying Ratio

In gasifiers where combinations of steam plus air or steam plus oxygen are used for the oxidising agents, the following trends apply as *gasifying ratio* increases from 0.6-1.7 (Devi *et al.*, 2002):

- Decrease in H_2 and CO
- Small decrease in CH_4
- Increase in CO_2
- Increase in C_2 hydrocarbons

2.2.6 Residence Time

Residence time of the thermochemical reactions influences the gas composition and determines how closely the process proceeds to equilibrium. It is well known that the gas phase reactions occur faster than the char-gas reactions after the pyrolysis process. The char-gas reactions are often the rate limiting step for the gasification process to reach equilibrium (Higman & Burgt, 2003). The size of the wood feedstock is important as this effects the residence time needed for the reactions. This in turn effects the producer gas composition due to the different heating rates and the interplay between the pyrolysis and char gasification reactions as discussed in Section 2.1.3. Despite the importance of residence time, limited information sources were found, most likely because this variable is difficult to change in a gasifier without modifying its design.

2.2.7 Catalytic Bed Materials

Catalytic bed materials are primarily used to promote the decomposition of tars, but they also influence the composition of the producer gas. Nickel based catalysts are known to increase the volumetric levels of H_2 and CO contents but can considerably decrease methane and carbon dioxide levels .

Some generalised conclusions can be drawn from the use of in-bed catalysts in biomass gasifiers (Devi *et al.*, 2002):

- Product gas distribution is influenced.
- Hydrogen levels increase.
- A slight decrease in the amount of CO
- Increase in the amount of CO_2.
- Tar levels decrease but the extent of this is influenced by gasification conditions (temperature, steam to biomass ratio etc).

Generally as the amount of in-bed catalyst proportion is increased, gas yields increase and the lower heating value of the gas mix decreases as more hydrogen is generated at the expense of methane.

2.2.8 Composition of the Fuel

The elemental analysis of the fuel has a significant effect on the composition of the producer gas. The C, H and O contents are most influential. Fuels with a high carbon content and a low oxygen content lead to a hydrogen rich producer gas (Fercher *et al.*, 1998). Section 2.1.3 discusses the thermal gasification process and indicates how the amount of volatiles and fixed carbon in the fuel source affects the relative proportions of pyrolysis gas and char-derived gas that is evolved. The compositional data of wood pellets used in the 100 kW gasifier is presented in Appendix A.

2.3 Contaminants in the Producer Gas

Many contaminants can be present in producer gas and the levels of each are specific to the type of gasifier, the fuel and the operating parameters. Contaminants are one of the main factors that govern whether a particular type of gasifier is suited to a certain application. So the end use appliance determines the requirements for gas quality. Kilns, boilers and co-fired systems have the lowest gas clean up requirements where gas engines and gas turbines have higher requirements. Synthetic fuels and chemicals production have the strictest gas quality requirements (Knoef, 2005). Table 2.2 outlines common contaminants in producer gas and the problems caused.

Table 2.2: Common contaminants in producer gas and their associated problems. Source: (Ciferno & Marano, 2002).

Contaminants	Examples	Potential Problems
Particles	Ash, char, bed material	Erosion of equipment
Alkali metals	Sodium & potassium compounds	Hot corrosion, catalyst poisoning
Nitrogen compounds	NH_3 and HCN	Emissions
Tars	Refractive aromatics	Clogging of filters & valves in engines.
Sulphur, Chlorine	H_2S and HCl	Corrosion, emissions, catalyst poisoning.

Indicative specifications for producer gas quality requirements are presented in Table 2.3. These are generalised because specifications differ between different manufacturers (Knoef, 2005). Note they are milligrams per normal meter cubed, not g/Nm^3 which is often reported for contaminant levels from many gasifiers.

Table 2.3: Indicative specifications for producer gas quality requirements. Source: (Knoef, 2005).

Application	Tar (mg/Nm^3)	Particles (mg/Nm^3)	Alkalis (mg/Nm^3)	Ammonia (mg/Nm^3)	Chloride (mg/Nm^3)	Sulphur (H_2S & COS) (mg/Nm^3)
Gas engine	<50	<50	<1	<50	<10	<100
Gas turbine		<30	<0.25			
Syngas/methanol	<0.1	<0.02	$<1ppm_V$	$<1ppm_V$	$<1ppm_V$	$<1ppm_V$
Fuel cell	<0.1	$<1ppm_V$	$<1ppm_V$	$<1ppm_V$	$<1ppm_V$	$<1ppm_V$

Gas turbines are rather tolerant to tars because the gas is usually feed hot, and no tars are allowed to condense out onto surfaces. This is not the case with reciprocating gas engines where the gas

needs to be cooled to approximately 30-50 °C so that the engines have a reasonable volumetric efficiency. The specifications for boilers are much lower and emission limits rather than tar levels are often the determining factor (Knoef, 2005).

2.3.1 Overview of Tar Control Methods

Tars are defined as mixtures of condensable hydrocarbons with a molecular weight larger than benzene (Devi *et al.*, 2002). Tars can condense on surfaces within an engine (particularly reciprocating gas engines) clogging the gas supply lines, the gas-air mixer and can accumulate on intake valves and valve stems. Build-up of tar on intake valves is particularly a problem when the engine is shutdown and the tars solidify on cooling, preventing correct valve travel (Quaak *et al.*, 1999).

The presence of tars in producer gas is one of the most widespread drawbacks of producer gas utilisation which is trying to be overcome internationally (Higman & Burgt, 2003; Klass, 1998). A gasifier should be operated under conditions where minimum levels of tars are produced without adversely affecting the producer gas composition required for a given application.

Some researchers separate tars generated in gasifiers into different classes. These groupings differ significantly in their designation. In general there are two groups of tars, water soluble and water insoluble tars.

Primary method*s* of tar elimination involve techniques executed inside the gasifier. These can be either formation prevention methods or post-formation treatments performed inside the gasification reactor vessel. *Secondary* tar control methods occur outside the gasifier in downstream equipment (Devi *et al.*, 2002).

Primary methods of tar reduction include:

- Using catalytic bed materials
- Optimising gasification conditions (temperatures, steam to biomass ratio, equivalence ratio, gasifying ratio, oxidising agents and residence times).
- Optimising reactor design (secondary air injection & multi-stage gasification)
- Fuel assessment (e.g.: moisture content, fuel type selection).

The two basic ways of performing *secondary* tar removal are (Knoef, 2005):

1. *Physical* removal of the tar (through removing condensed or dissolved tar particles).
2. *Thermal* cracking of the tar (with or without a catalyst).

Physical tar removal methods include (Knoef, 2005):

- Wet scrubbers
- Wet electrostatic precipitators
- Rotating particle separators
- Other methods such as barrier filters and cyclones can be used but are not widely practised.

The degree of tar removal required is dependant on the end use application of the producer gas (Devi *et al.*, 2002). The classical way to remove tars is to cool the gas causing the tars to condense out. Hence, the condensation temperature is very important as the heavier molecular weight tars condense at higher temperatures than the lower molecular weight tars (Quaak *et al.*, 1999). Although downstream gas cleaning can be very effective, it is not always economically viable, so primary methods of tar elimination are important (Devi *et al.*, 2002).

Secondary *thermal* tar destruction methods are used where the producer gas stream is subjected to elevated temperatures with or without a catalyst being present. The cracking temperature required is dependant on the type of tars present, but 900-1300 °C is common. At temperatures above 1300 °C soot can form and a reduction in the heating value of the producer gas can occur due to secondary reactions (Brandt & Henriksen, 2000).

Secondary *catalytic* tar cracking can occur without additional heating by exposing the producer gas to a catalyst. Non-metallic catalysts such as dolomite, zeolites and calcite's can be used. Metallic catalysts are less common but can aid in destroying ammonia. A drawback is they can be poisoned if excessive H_2S is present (Knoef, 2005). Experimentation of secondary tar control methods is outside the scope of this Masters' thesis and will not be further discussed.

A typical range of tar compounds generate during biomass gasification is shown in the chromatogram of Figure 2.13. This is based on research performed at Eindhoven University of Technology, The Netherlands.

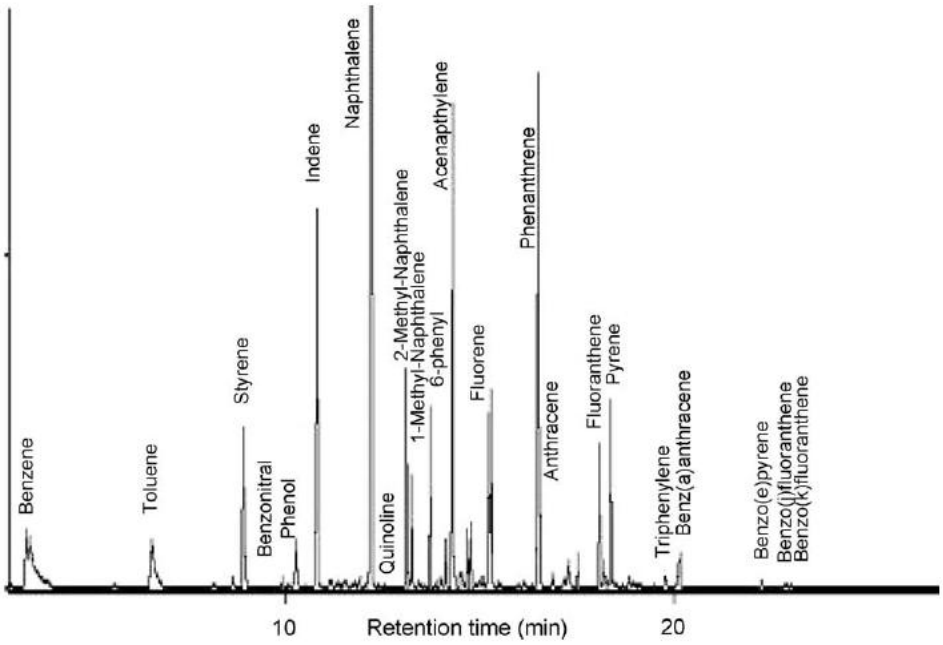

Figure 2.13: A GC/MS analysis showing tar composition from an air-blown biomass gasifier. Source (Devi *et al.*, 2004).

A typical tar composition found by Vienna University of Technology for dual FICFB gasifiers at 850 °C, with a steam to biomass ratio of 0.6 kg/kg and 10 wt% catalyst (3.7 wt% Ni on olivine after calcination at 1100 °C) is (Pfeifer *et al.*, 2004):

64 wt%	naphthalene
16 wt%	acenaphthylene
8 wt%	fluorene
6 wt%	phenanthrene
5 wt%	acenaphthene
1 wt%	indene

Compared to air-blown gasification, steam gasification generates lower quantities of tar, because of steam reforming of the tars. Air-blown gasifiers commonly have tar levels of 1-30 g/Nm^3, but is highly dependant on reactor type. Downdraft gasifiers typically have much lower tar levels than updraft gasifiers (Knoef, 2005).

2.3.2 Removal of Particles from Producer Gas

The main reason for the removal of particles from the producer gas stream for engine applications is to reduce erosion. Particle removal methods chosen are dependant on the temperature of the gas and include (Knoef, 2005):

- Cyclone filters
- Barrier filters (porous candle filters, bag filters, packed bed filters).
- Electrostatic filters
- Wet scrubbers

Reactor design is critical for reducing the degree of particle removal systems required in producer gas. One key design feature is to have an adequate freeboard region above the beds, especially in the case of fluidized bed reactors. This zone serves as a region for particles to drop out under gravity. Adequate freeboard is most important on fluidized beds gasifiers because they have higher levels of particle entrainment compared to moving bed gasifiers. Increasing column height and diameter in the freeboard region helps to reduce the superficial velocities and encourage particles to drop out. This is explained more in Section 2.6.

Common particle contents in the producer gas measured in the 100 kW_{th} biomass gasifier at the Institute of Chemical Engineering, Fuel and Environmental Technology in Vienna, was 20 g/Nm^3. This quantity was reduced to 3 g/Nm^3 after the producer gas passed through a cyclone (Fercher *et al.*, 1998).

2.3.3 Removal of Alkaline Contaminants

Alkalis are removed to reduce corrosion and prevent the poisoning of catalysts. In engine applications the focus is on corrosion prevention, especially when alkali salts can vaporise at the combustion temperatures found in engines. Most conventional methods of control involve cooling the producer gas to below 600 °C to condense solid alkali particles out. Wet scrubbers, electrostatic filters, barrier filters or cyclones can remove the particles once condensed. Often alkali salts are removed with the ash from gasifiers and with the tar removal system (Knoef, 2005).

2.4 Primary Methods of Tar Elimination

Tars found in producer gas are considered to be one of the greatest hurdles to the widespread application of gasifiers. The presence of tars in producer gas have different effects depending on the gases end use, but in the case of CHP plants, tars are notorious for building up on cooler surfaces, and are particularly a problem in engines which are routinely turned off and allowed to cool down. Hence tar reduction by formation prevention is most favourable, but in almost all cases some downstream tar removal is necessary.

2.4.1 The Effect of Gasification Conditions on Tar Yield

Limited research has been carried out on the influence of different biomass gasification conditions on the types of tars and the total quantity of tars generated in biomass gasifiers. Most research has been directed at secondary tar removal methods and primary methods such as catalytic bed materials. Many variables effect the gasification reactions which influence tar generation. Information is presented below on how different operating parameters have been found to influence tar levels.

Gasification Temperature

Temperature affects both the amount of tar formed, and the composition of the tar. A 40 % reduction in tar yield can occur when temperatures are increased from 700 °C to 900 °C (Devi *et al.*, 2002). The upper limit of gasification temperatures are set by the fusion temperatures of the ash and inert components found in the bed material and feedstock (Higman & Burgt, 2003).

Oxygen containing tar compounds such as phenol, cresol and benzofuran only exist in significant quantities below 800 °C. Destruction of aromatic hydrocarbon tars (benzene, naphthalene, phenanthrene etc) occurs only at temperatures above 850 °C (Devi *et al.*, 2002).

The effect of gasification temperature on tar levels was investigated at the University of Vienna on their 100 kW FICFB gasifier. This investigation was performed with varying temperatures at two different steam to biomass ratios (0.25 kg/kg and 0.5 kg/kg) as shown in Figure 2.14.

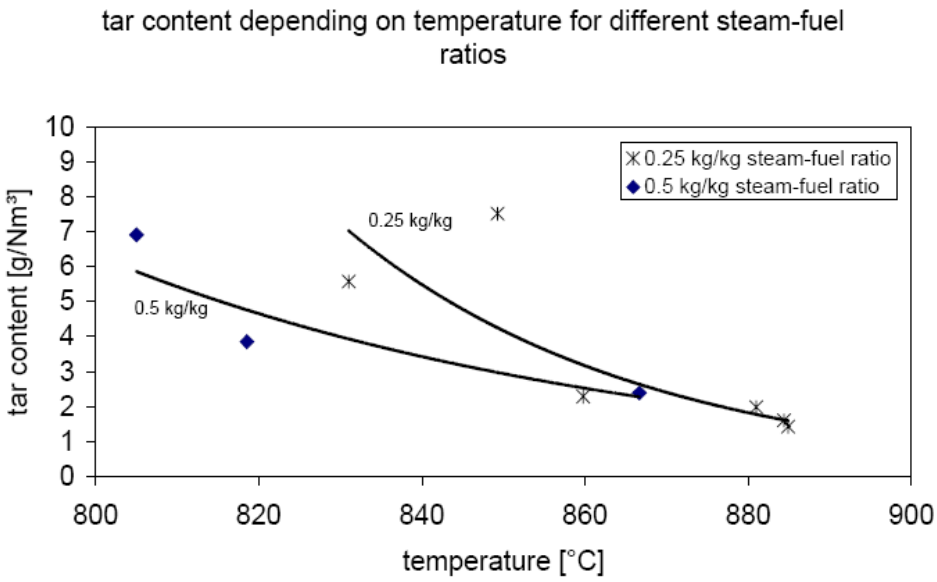

Figure 2.14: The change in tar levels with temperature at steam to biomass ratios of 0.25 kg/kg and 0.5 kg/kg. Source: (Hofbauer & Rauch, 2000).

It can be seen from Figure 2.14 that the reduction in tar levels with increasing gasification temperature is more prevalent at low steam to biomass ratios. Researchers at the Institute of Chemical Engineering, Fuel and Environmental Technology in Austria concluded that the optimal steam to fuel ratio for a low tar content is higher than 0.5 kg of steam per kilogram of dry fuel. The optimal temperature for a low tar content was reported as being higher than 850 °C (Hofbauer & Rauch, 2000). Note high steam to biomass ratios lower tar levels, but it also increases the steam content in the producer gas, consumes more thermal energy, and steam conversion levels for the gasification reactions are poorer.

Steam to biomass ratio

Increasing the steam to biomass ratio causes the tar content to decrease . Excess water in the gasification zone is reported as lowering tar levels (Fercher *et al.*, 1998). It was discovered on the 100 kW plant in Austria that increasing the steam to biomass ratio at 850 °C, caused the tar content to decrease from 7.5 g/Nm^3 at steam to biomass ratio of 0.2 kg/kg, to about 3 g/Nm^3 at steam to biomass ratio of 0.5 kg/kg (Hofbauer & Rauch, 2000). Figure 2.15 shows this trend.

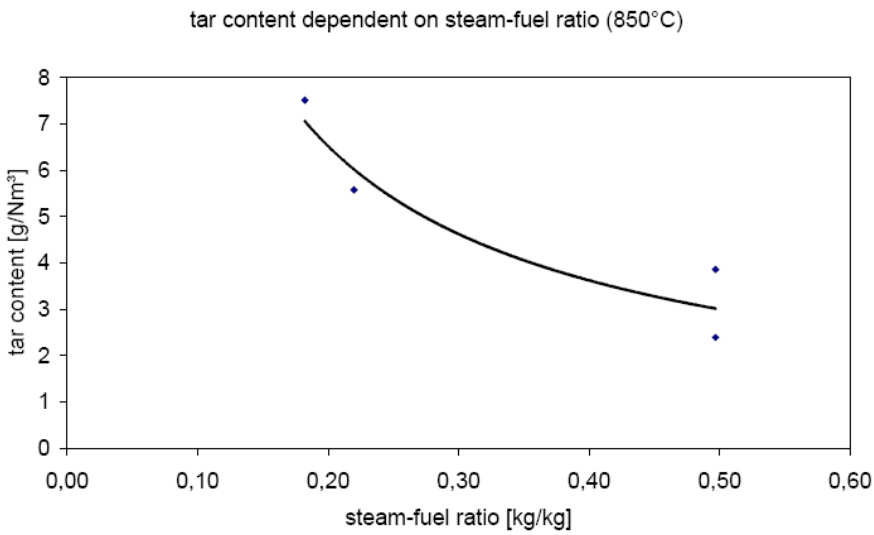

Figure 2.15: Change in tar levels of FICFB gasifiers at different steam to biomass ratios between 0.18-0.5. Source: (Hofbauer & Rauch, 2000).

Research at Vienna University indicated that the moisture content of the fuel has almost no influence on tar levels when gasifying with steam (Fercher *et al.*, 1998). This is likely to be because the quantity of water introduced with moist fuel would be negligible compared to the quantities of steam being injected.

Equivalence ratio

If air or oxygen is used as the oxidising agent the equivalence ratio is important. Equivalence ratio strongly influences the type of gasification products. Tar yield and tar concentration decreases as the equivalence ratio is increased because more oxygen is available to react with volatiles. This also increases the percentage of CO_2 in the producer gas. The effect of equivalence ratio is more noticeable at higher temperatures (Devi *et al.*, 2002).

Gasifying ratio

Tar content in the producer gas sharply decreases with increasing gasifying ratio. A good gasifying ratio is about 0.8-1.2. Basic research reported in literature indicates that more tars are formed with pure steam than with steam-oxygen mixes and even less with air as an oxidant (Devi *et al.*, 2002).

Residence time

Residence time has been found by Kinoshita et al. (Kinoshia *et al.*, 1994) to have minimal influence on total tar yield but can significantly influence tar composition. Yields of one and two ring tar compounds (except benzene and naphthalene) decrease, and three and four ring

hydrocarbon tars increase in the total tar fraction when the residence time is increased. The amounts of oxygen containing compounds tend to decrease as residence time increases (Devi *et al.*, 2002).

The effect of residence time on tars was also studied at the Technical University of Eindhoven in the Netherlands. This research confirmed that raising gasification temperatures and lengthening the residence time that the producer gas remains hot, lowers the total tar levels in the gas. Residence times were studied by passing a stream of producer gas through an externally heated tubular reactor. Residence times of 1-12 seconds were studied at four different temperatures. This is shown in Figure 2.16. Although this was performed in a downstream reactor, the same principles should be transferable to inside a gasification reactor. Total tar levels were found from the summation of all tar components using the SPE method to collect the tar samples. Initial tar levels from the gasifier were around 8 g/Nm^3 (Houben & Geldrop, 2004).

Increasing the residence time at successively higher temperatures distinctly reduced the tar concentration. This was only significant at temperatures above 900 °C. In the producer gas sample used, oxygen-rich tars were found to be abundant and the easiest to break down with higher temperatures.

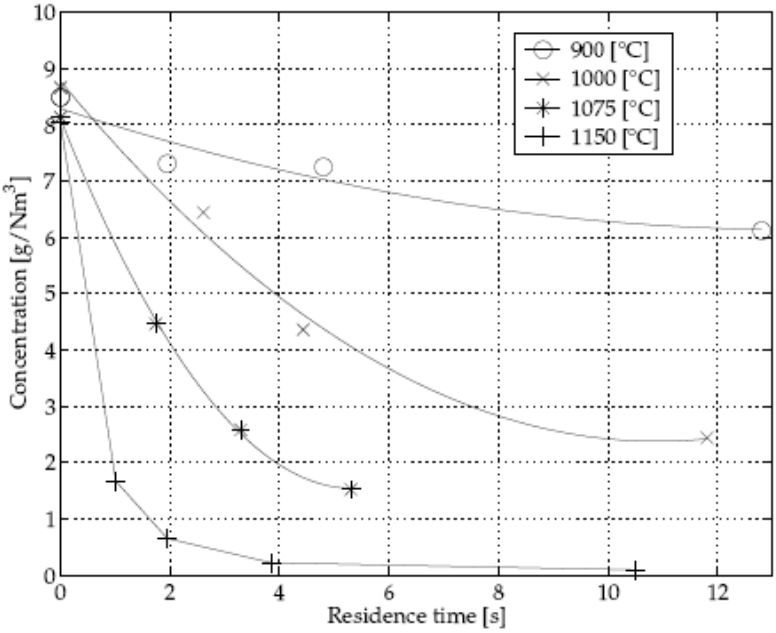

Figure 2.16: The effect of residence time on total tar levels in a gasifier at four different temperatures. Source: Figure 5.2 of (Houben & Geldrop, 2004).

At the highest temperature shown in Figure 2.16 of 1150 °C, a residence time of four seconds reduced the tar quantity down to 0.2 g/Nm^3 from 8 g/Nm^3. This is a common level of tars that is considered suitable for use in gas engines. Further experiments at the Technical University of Eindhoven confirmed that the gas composition can change in downstream tar crackers at elevated temperatures. This often has the same results as increasing the gasification temperature where more hydrogen and carbon monoxide is generated at the expense of methane and carbon dioxide. For power and thermal applications this would be unfavourable as the calorific value of the producer gas is reduced. Instead designing a gasifier for longer residence times at the selected gasification temperature is favourable over secondary cracking (Houben & Geldrop, 2004).

When the concentration of the tar compounds were grouped and analysed, it was found increasing the residence time has the most noticeable effect at reducing the levels of one and two-ring tar components. Progressively as the residence time that the producer gas was exposed to increased (at T=1075 °C), the quantity of most tar fractions noticeably decreased. This is shown in Figure 2.17 (Houben & Geldrop, 2004).

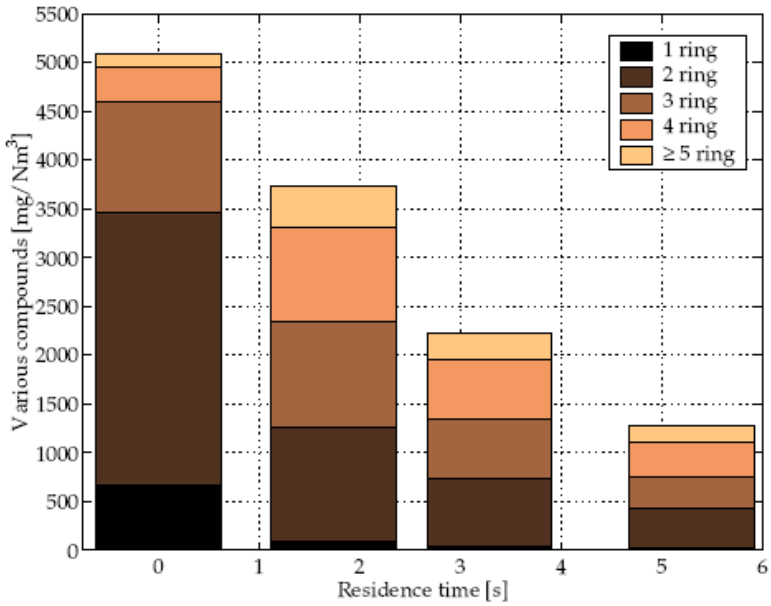

Figure 2.17: The change in the types of tars and their quantities with different residence times at 1075 °C. Source Figure 5.4 of (Houben & Geldrop, 2004).

2.4.2 Selection of Bed Materials

The types of bed materials used in fluidized bed gasifiers effects both there gas composition and there tar yield (Devi *et al.*, 2002). The use of catalysts allows tar cracking to occur at much lower temperatures (600-800 °C) than would otherwise be possible (1000 °C plus) (Brown, 2003). Catalysis can be located downstream of the gasifier or put directly into the reactor to form the bed material. During testing of different bed materials at Güssing Austria, toluene was selected as a reference tar to assess the catalytic properties of different bed materials against (Rauch, 2004). Other research groups select naphthalene as a reference tar which has been reported as being the most abundant tar in FICFB biomass gasifiers (Pfeifer *et al.*, 2004).

Bed materials tested in the past and reported in literature include (Rauch, 2004) :

- Nickel based bed materials
- Olivine (Mg, Fe oxides and silica).
- Dolomites (naturally occurring and calcined)
- Limestone
- Magnesites and magnetites
- Zeolites
- Iron ore
- Calcite
- Quartz
- Ash
- Mixes of many of the above with silica sand.

Nickel based catalysts have been widely tested in gasifiers (Sutton *et al.*, 2001). These catalysts can become severely deactivated due to carbon deposition and can be poisoned in the presence of H_2S. In FICFB gasifiers, deposited carbon can be burnt off catalysts to regenerate them since the bed material circulates through a combustion zone. Nickel based catalysts can increase gas yields at the expense of tar and char conversion. They can also be effective at reducing ammonia levels (Devi *et al.*, 2002).

Much past research into catalysed steam gasification of wood has focused on the use of nickel and alumina. Nickel precipitated on silica alumina, mixtures of silica alumina, and nickel on alumina have all been tested. The function of the silica alumina was to crack hydrocarbon intermediates,

while the nickel was to promote methane reforming and hydrogenolysis of higher molecular weight hydrocarbons (Klass, 1998). The use of nickel promoting the reformation of methane is advantageous when liquid fuels are being manufactured but is detrimental to obtaining a high calorific value producer gas.

Olivine has been tested in some biomass gasifiers and has shown encouraging results. Olivine is a name for a series between fayalite and forsterite. Fayalite is the Fe-rich olivine with pure formula Fe_2SiO_4. Forsterite is the Mg-rich olivine with a pure formula Mg_2SiO_4 . Olivine has good attrition resistance with good tar reduction performance and a similar level of activity as dolomite. Olivine catalysts are good at steam reforming methane and tars (Devi *et al.*, 2002). However, reducing the methane content lowers the producer gases calorific value!

Olivine is popular in Austrian FICFB gasifiers because of its attrition resistance and catalytic activity in hydrocarbon and tar reforming. Olivine can be activated by heating it for more than 100 hours above 900 °C. It was discovered that natural olivine was most superior at converting toluene followed by activated olivine, iron ore, dolomite, magnetite, silica sand and lastly ash during testing of different bed materials in Austria. Toluene was selected as the reference tar to assess the catalytic properties of different bed materials against (Rauch, 2004). This is shown in Figure 2.18. The tar contents in the producer gas all decreased with temperature when different bed materials were used (Fercher *et al.*, 1998).

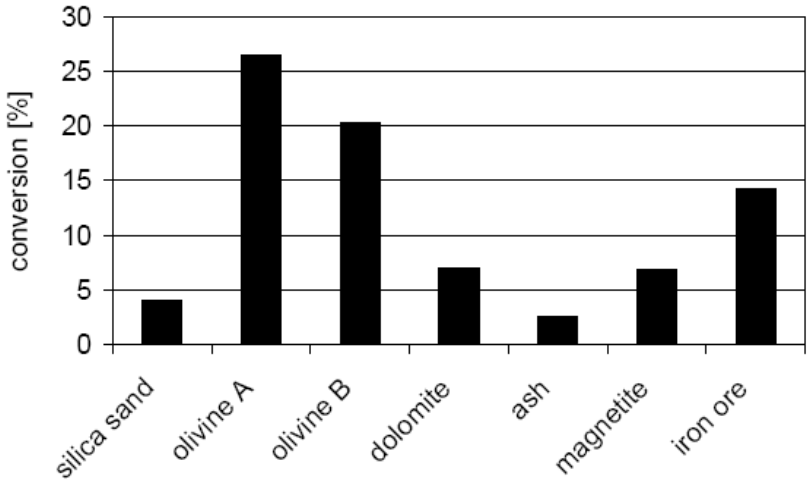

Figure 2.18: Conversion of toluene used as a reference tar in tests performed at Güssing, Austria. Source: (Rauch, 2004).

Different mixtures of olivine and other bed materials have been tested at Vienna University of Technology. Ratios of naturally occurring olivine and nickel enriched olivine have been analysed at levels from 0-45 % nickel enriched olivine. As the proportion of olivine in the bed material increases, the tar levels decrease linearly . Olivine is more reactive at higher temperatures. Gasification temperatures should be 800-900 °C to obtain high tar conversion rates .

Dolomite is a magnesium ore with the general formula $MgCO_3 - CaCO_3$. It generally contains about 30 wt% CaO, 21 wt% MgO and 45 wt% CO_2 (Sutton *et al.*, 2001)**.** Dolomite has been widely tested in gasification systems as a catalytic bed material but has poor attrition resistance. It gets eroded more easily than other bed materials like silica sand. It has proven to significantly reduce tar levels. Experiments have found that a 77-95 % reduction in tars is possible in producer gas when dolomite is used in downstream catalytic reactors. The catalyst is most active if calcined and placed downstream of the gasifier in a fluidised bed at temperatures above 800 °C. The high activity of dolomite is related to its pore sizes and distribution (Sutton *et al.*, 2001).

Many bed materials can be used that do not have catalytic tar reduction properties. ***Quartz*** bed materials have been tested. This was the original type of bed material investigated in FICFB gasifiers in Austria. Quartz was replaced with other bed materials that had catalytic properties which improved the tar and hydrocarbon levels (Rauch *et al.,* 2002). ***Silica*** sand is a very common bed material but has no catalytic properties. It is widely available and has good attrition resistance.

The *proportion of catalytic bed material amongst total bed material* has been studied with a number of catalysts in the Austrian 100 kW FICFB gasifier at Vienna University. It was concluded that increasing the proportion of catalytic bed material to total bed material successively reduced tar levels. A reduction in tar levels of more than 75 % was achieved when 43 % of the bed material was catalytic using an artificial Ni-catalyst (Rauch *et al.,* 2002). Figure 2.19 shows these results for a steam to biomass ratio of 0.5 kg/kg_{daf} and a gasification temperature of 850 °C. This trend is common with other catalytic bed material experiments.

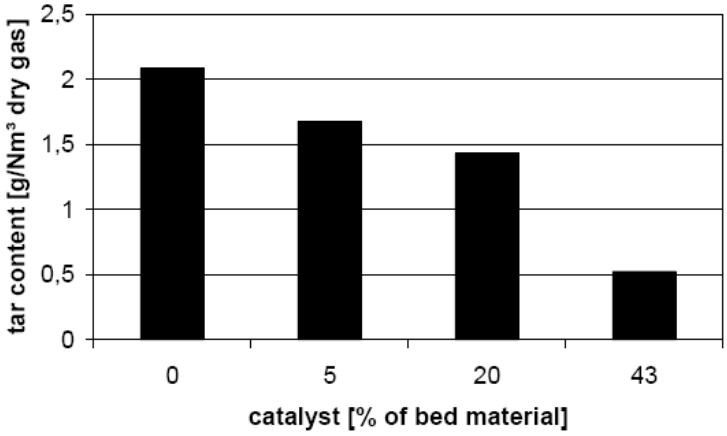

Figure 2.19: The change in tar content of the 100 kW_{th} FICFB gasifier in Austria, as the proportion of Ni-catalyst in the plant is increased. Source: (Rauch *et al.,* 2002).

The criterion for catalytic bed materials is that they should be economically available, attrition resistant, active and selective to only reduce tar levels. Past experience with gasifiers has revealed that adding limestone (e.g. 25 %) with silica sand (75 %) as bed material, can prevent agglomeration problems (Devi *et al.*, 2002). Having high iron levels present in all the bed materials discussed is advantageous at reducing tar levels (Sutton *et al.*, 2001). Attrition of bed material in a fluidized bed is directly proportional to gas and particle velocities (Devi *et al.*, 2002).

2.4.3 Reactor Design

Secondary air introduction into the gasification reactor results in significant tar reduction because higher temperatures can be obtained. Separating the pyrolysis zone and reduction zone is also effective. This is known as two stage gasifying. Tars formed during the first pyrolysis stage are decomposed in the secondary reduction zone of the gasifier (Devi *et al.*, 2002). Many new reactor designs that seek to use a two stage gasification process are being investigated in different parts of the world. One of the driving factors for this design concept is increasing residence times so that gasification reactions can get closer to equilibrium and tars can further breakdown.

2.4.4 Summary of Tar Control Parameters

1. Gasification temperatures should be high (preferably 800 °C plus).
2. Choice of oxidising agent should reflect desired gas composition for the application.
3. The equivalence ratio should be at an optimum level where a suitable gas composition is produced for the application.
4. Residence time should be adequate.

5. Increasing pressure appears to reduce tar levels but this needs further research.
6. Catalytic bed materials and downstream catalysts can be used.
7. High steam to biomass ratios are helpful but excessive steam content in the producer gas is energy intensive.

2.5 Common Types of Gasifier Designs

2.5.1 Classification of Gasifiers

Several different types of gasification reactor designs exist. Different variations and combinations are still being developed but the most common designs will be outlined in Section 2.5. Most reactor types fall into one of three categories: moving-bed gasifiers, fluid-bed gasifiers, and entrained-flow gasifiers. Each of these types of gasifiers share certain characteristics that differentiate them from the other types (Higman & Burgt, 2003). The reactor design of a gasifier is important because it has a significant influence on the producer gas quality, governing the application of the gasifier.

Moving-bed gasifiers (also called fixed bed gasifiers) are characterized by a bed of particles which slowly move downward under gravity as the thermochemical reactions occur. *Fluidized-bed gasifiers* have a bed of particles which are partially suspended by an upward flowing fluid. This allows for extremely good mixing between the feedstock and the oxidising agent, promoting good heat and mass transfer. *Entrained-flow gasifiers* operate with the feedstock and the blast in a co-current flow arrangement. Residence times are short in entrained flow reactors and the feedstock has to be ground to a small particle size so reactions occur quickly and to ensure correct entrainment of the feedstock. High temperatures are usually required to ensure good conversion efficiency and most entrained-flow gasifiers operate in the slagging range (Higman & Burgt, 2003).

Gasifiers can be classified in many ways including (Knoef, 2005):

According to the reactor type:

- Moving-bed gasifiers
- Fluidized bed gasifiers
- Circulating fluidized bed gasifier
- Entrained flow gasifiers

According to the number of reactors used:

- Single bed reactors
- Twin bed reactors
- Multi bed reactors

According to the oxidising agent/moderator used:

- Air blown gasifiers
- Oxygen blown gasifiers
- Steam blown gasifiers

According to the heat supply criterion:

- *Autothermal* gasifiers (or direct gasifiers) where the heat is supplied by practically combusting some of the feedstock inside the gasification reactor.
- *Allothermal* gasifiers (or indirect gasifiers) where heat is supplied from outside the actual gasification reactor itself.

According to the pressure in the gasifier:

- Atmospheric pressure gasification
- Pressurised gasification

According to the ash fusion characteristics:

- Slagging
- Non-slagging

2.5.2 **Moving Bed Gasifiers**

Three main types of moving bed (or fixed bed) gasifiers exist. They are updraft, downdraft and crossdraft. Additionally a twin-fired gasifier exists which is a combination of a down-draft and an updraft. In all cases the feedstock material moves downwards under gravity in a piled/stacked state. Thermal energy is exchanged between different levels in the feedstock and many endothermic and exothermic processes occur simultaneously in different localised regions inside the reactor.

In *updraft moving bed gasifiers* the feedstock is fed into the top of the reactor and moves downwards evolving gases and being converted into ash. The air intake is at the base and the producer gas moves upwards and leaves at the top. The feedstock travels counter-currently to the gas flow and passes through the drying zone, the pyrolysis zone, the reduction zone and the oxidation zone. The advantage with this type of gasifier is its simplicity, high charcoal burnout and good internal heat exchange as it passes through the drying zone yielding lower temperature producer gas. Another advantage is that fuels with high moisture content can be used as the producer gas performs the drying process as it leaves the bed. The main disadvantage of this type of gasifier is the high amounts of tars and pyrolysis gases that occur (Knoef, 2005). Figure 2.20 shows an updraft moving bed gasifier.

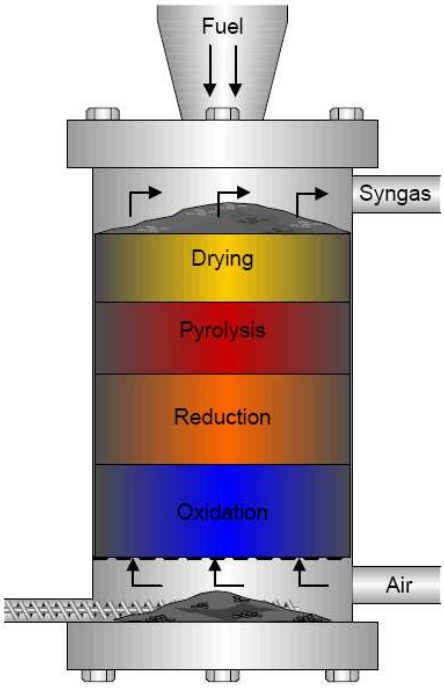

Figure 2.20: Diagram of an updraft moving bed gasifier (Olofsson *et al.*, 2005).

In *downdraft moving bed gasifier's* the feedstock is fed into the top of the reactor with the oxidising agent and moves downwards with the bed material. Producer gas is removed out the base as is the ash. Hence the feedstock and the gases move in a co-current arrangement. The main advantage of a downdraft moving bed gasifier is the low tar content in the producer gas. Downdraft gasifiers produce the lowest tar levels and are well suited to engine applications (provided the calorific value of the gas is suitable). The main disadvantage of downdraft gasifiers is the high ash level in the producer gas. The ash gets entrained in the producer gas as it moves through the final reduction section of the reactor bed. Downdraft gasifiers require lower moisture content fuels, typically less than 25 % (Knoef, 2005). Figure 2.21 shows a typical downdraft moving bed gasifier configuration.

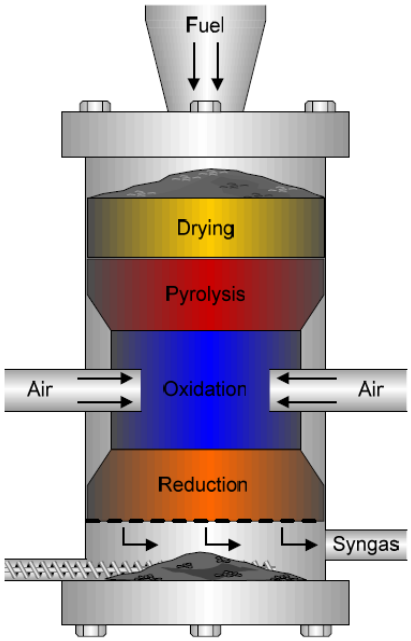

Figure 2.21: Typical downdraft moving bed gasifier (Olofsson *et al.*, 2005).

Crossdraft moving bed gasifiers introduce the oxidising agent into one side of the reactor and remove the producer gas on the other side. Instead of the different processes occurring at different horizontal levels in the gasifier, the different processes occur concentrically around each other radiating outwards from the hearth. An advantage of crossdraft gasifiers is the very small scale at which they can be operated. Commonly the tar levels are quite high and either high carbon feedstocks have to be used or more extensive gas clean up equipment (Knoef, 2005). Figure 2.22 shows the design of a crossdraft gasifier.

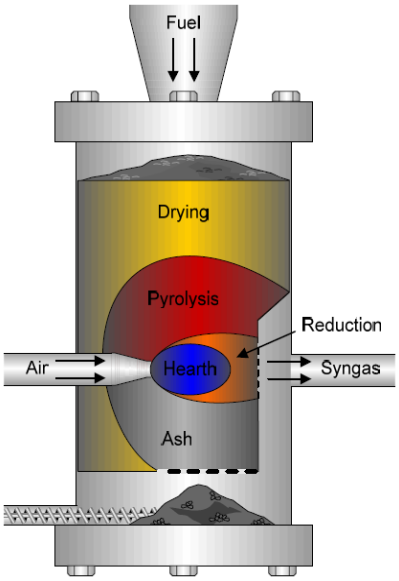

Figure 2.22: A Crossdraft gasifier with the concentrically arranged process stages (Olofsson *et al.*, 2005).

2.5.3 **Fluid Bed Gasifiers**

Three common types of fluidized bed gasifiers exist. They are the more common *bubbling fluidized bed* gasifier, the *single circulating fluidized bed* gasifier and the *dual circulating fluidized bed* gasifier. Fluidized bed gasifiers have many advantages over the moving bed type. One of the most important characteristics is that the particle beds have much more uniform temperature distributions because of the ready mixing of the particles in the bed. The solid to gas contacting is also improved with fluidization (Knoef, 2005).

In *bubbling fluidized bed* gasifiers, a distinct interface between the freeboard and the dense phase of the particle bed exists. The bubbling fluidized bed exhibits liquid-like behaviour as bubbles of gas percolate upwards through the bed like a pot of boiling water. Due to the intense mixing, separate drying, pyrolysis, oxidation and reduction zones cannot be distinguished like in moving bed gasifiers (Knoef, 2005). An example of a single reactor fluidized bed gasifier is shown in Figure 2.23.

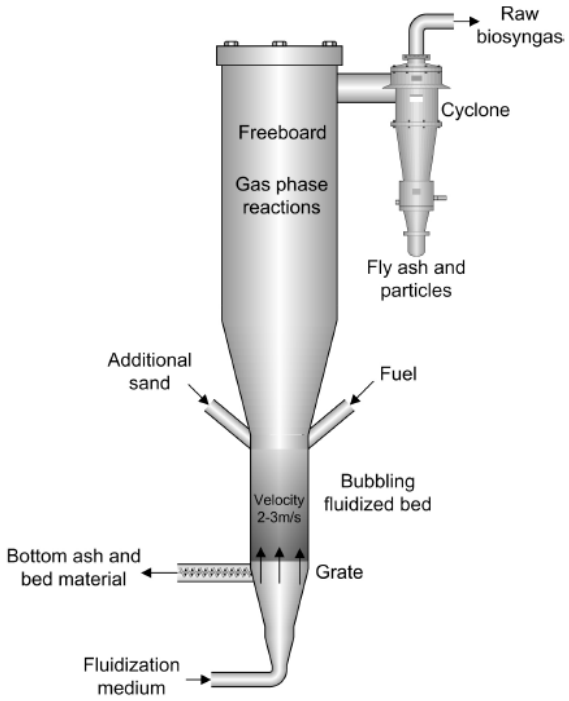

Figure 2.23: Single reactor bubbling fluidized bed gasifier (Olofsson *et al.*, 2005).

Single circulating fluidized bed gasifiers are similar to standard fluidized bed gasifiers but some of the particulate material is circulated internally around a circuit outside the gasification reactor. Usually a portion of the particulate matter (bed material, biomass and ash) is withdrawn from the top of the reactor and enters a cyclone. The cyclone separates the heavier particles and returns them to the lower region of the gasifier via a downcomer (Knoef, 2005). Such a gasifier is shown in Figure 2.24.

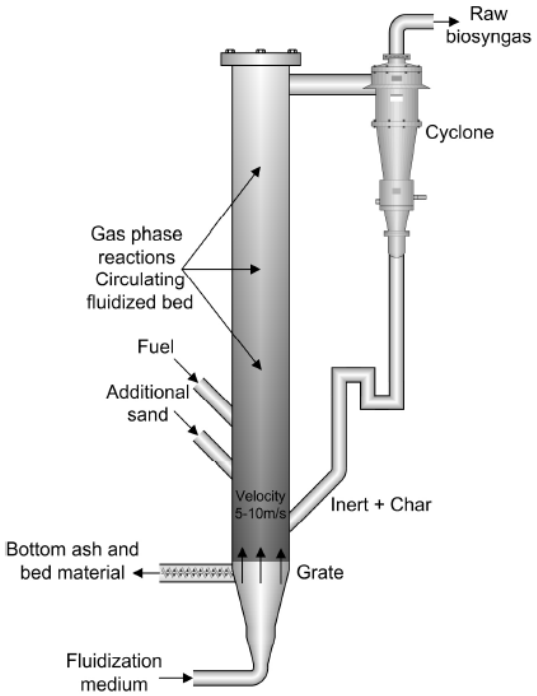

Figure 2.24: Circulating fluidized bed gasifier (Olofsson *et al.*, 2005).

Dual circulating fluidized bed gasifiers are a variation of the standard circulating fluidized bed gasifier where a section of the return circuit (downcomer) has instead been made into another reactor. (See Figure 2.25). This creates a major advantage because it allows the gasification and heat generating combustion reactions to be separated and occur in two separate reactors. This is an example of an allothermal gasifier. The result is producer gas can be generated with a heating value three times higher than conventional gasifiers because very little nitrogen is allowed to enter the gasification reactor where the producer gas is generated. Hence the producer gas can have a calorific value of 13-15 MJ/Nm^3 compared to the usual 4-6 MJ/Nm^3 (Knoef, 2005). This is the type of gasifier being studied at the University of Canterbury. More details of the operation of circulating dual fluidized bed gasifier are presented in Sections 2.7 and 2.8.

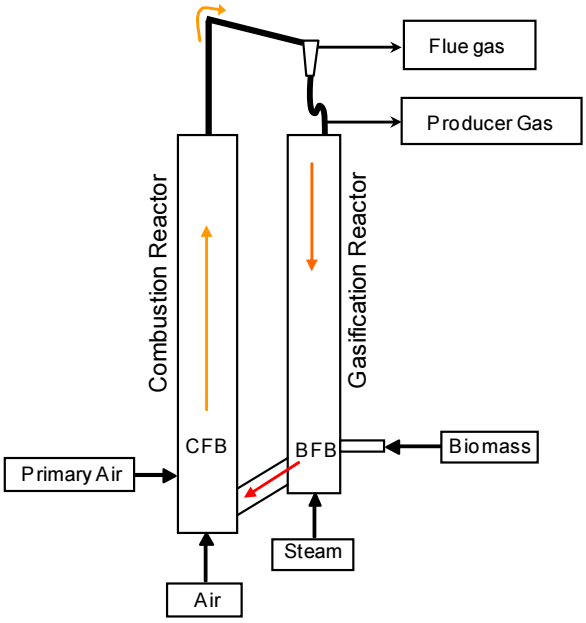

Figure 2.25: Circulating dual fluidized bed gasifier which is the design used in this project.

2.5.4 Entrained Flow Gasifiers

Entrained flow gasification is where the feedstock and the oxidising agent flow co-currently through the reactor vessel. The solids residence time inside the reactors is very short, commonly a few seconds, compared to minutes or hours in fluidised and moving bed gasifiers respectively. High temperatures over 1200 °C and small particle sizes are required to ensure satisfactory conversion to producer gas occurs. Because of the high temperatures required in entrained flow gasifiers they commonly operate in the slagging mode and at elevated pressures (Knoef, 2005). An example of an entrained flow gasifier is shown in Figure 2.26.

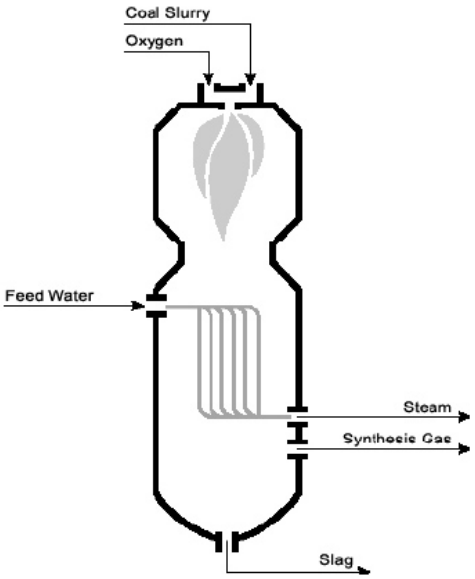

Figure 2.26: An entrained flow gasifier reactor (Olofsson *et al.*, 2005).

2.6 Fundamentals of Fluidization

The science of fluidization is important to the design of gasifiers, especially FICFB gasifiers because this is the method by which isothermal reaction temperatures are maintained, and explains the theory behind how the bed material transfers heat between the reactors. Residence times for the reactions and gas composition are all influenced by the fluidization regimes employed.

The science of fluidization has been extensively written up in this thesis because it was so relevant to improving the reliable operation of the gasifier. It is also explained in great detail so that future researchers on the FICFB gasifier at the University of Canterbury have a quick reference specific to FICFB gasifier characteristics.

2.6.1 Fluidization Regimes

Fluidization is the method by which solid particles are transformed into a fluid-like state through contacting with an upward flowing gas or liquid. Six modes of fluidization are generally recognised. These are shown in Figures 2.27a and b.

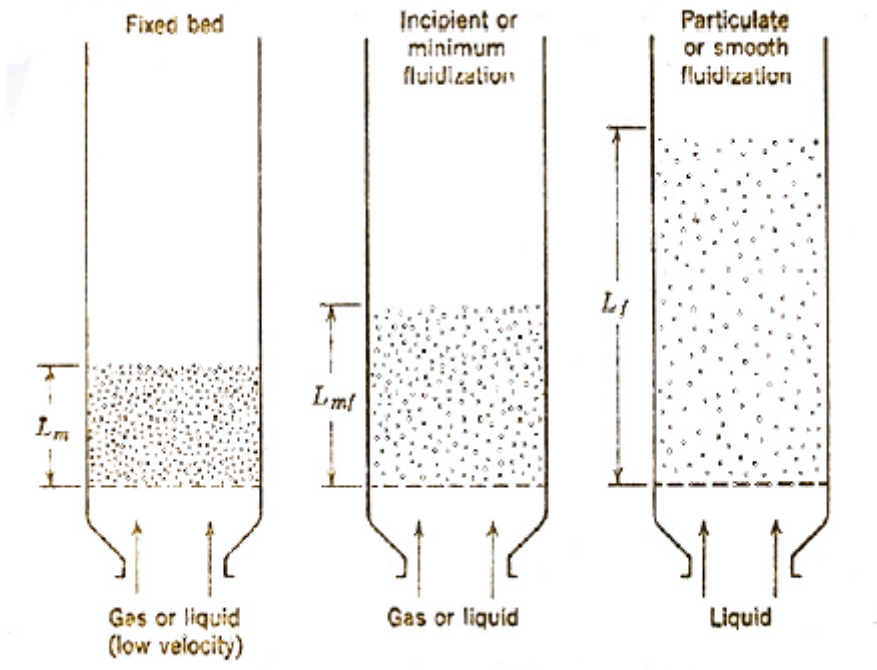

Figure 2.27a: The first three common modes of fluidization for particles (Chase, n.d.).

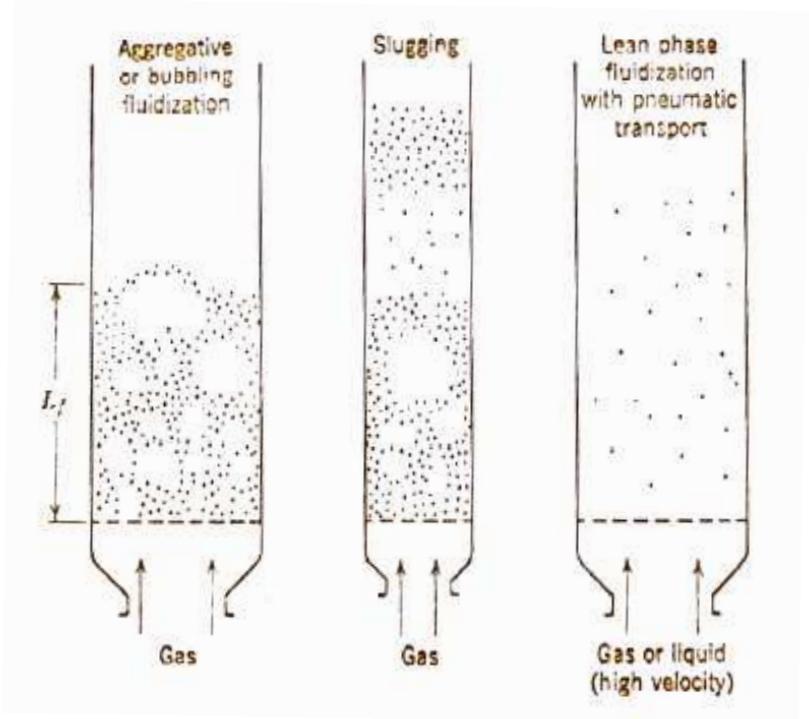

Figure 2.27b: The latter three common modes of fluidization for particles (Chase, n.d.).

The fluidizing agent (gas or liquid) percolates through the void spaces between the stationary particles when at low flow rates. This is known as a *fixed bed* and the particles remain in a packed state. As the flow rate of the fluidizing agent increases, particles move apart more in localised regions of the bed. This is known as an *expanded bed*. As the velocity further increases, a point is reached when the particles are all just suspended in the upward flowing gas or liquid. The frictional (drag) force between a particle and the upward flowing fluid counterbalances the force of weight of the particle and it becomes suspended (see Figure 2.28). This is known as minimum fluidization (or an *incipiently fluidized bed*). The vertical component of any compressive forces from the bed of particles sitting on top of other particles disappears when minimum fluidization conditions are reached. Hence, the pressure drop through any section of the bed is equal to the force of weight of the fluid and particles in that section (Kunii & Levenspiel, 1969).

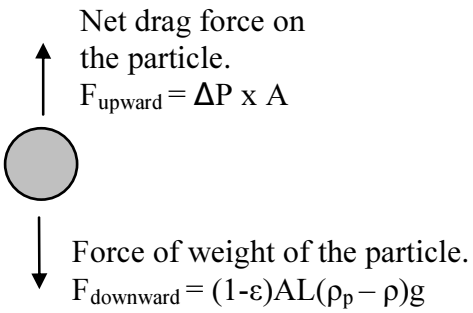

Figure 2.28: The balance of forces on individual particles in a fluidized bed (Abrahamson, 2007).

As the flow rate of the fluidizing agent increases beyond minimum fluidization, bubbling and channelling of the gas occurs. The bubbling becomes more aggressive as the flow rate increases and high levels of bed mixing take place. Once at this point, the bed does not expand much beyond its volume at minimum fluidization. This is called a *bubbling fluidized bed (BFB)* or an *aggregative fluidized bed*. Further increase in the gas flow rate can cause slugging to occur. This is where the bubbles coalesce and grow to such a diameter that they take up the full diameter of the fluidized bed column. This occurs most readily in long narrow columns and is often unfavourable as the bed is continually lifted up with the bubble and then collapses. This is known as a *slugging* (Kunii & Levenspiel, 1969).

If the terminal velocity of the particles in the bed is exceeded, the upper surface layer of the bed gets entrained off with the fluidizing agent. This is known as a *lean phase fluidized bed* or an *entrained flow bed.* The superficial velocity has to be considerably in excess of the terminal velocity of a closely sized group of particles for them to become entrained. Once entrainment occurs, it increases strongly with an increase in superficial velocity, roughly by a factor of 100 for a doubling of gas velocity (Kunii & Levenspiel, 1969).

2.6.2 Characteristics of Fluidized Beds

The properties of the solid particles and the fluid determine whether smooth or bubbling fluidization occurs. However many other factors influence: the rate of solids mixing, the size of bubbles and the extent of heterogeneity in the bed. These factors include (Kunii & Levenspiel, 1969):

- bed geometry
- gas flow rate
- design of gas distributor and,
- presence of vessel internals such as screens, baffles and heat exchangers.

A fluidization vessel usually consists of two zones, a *dense bubbling phase* having a distinct upper surface, and a *lean* or *dispersed phase*. The section of the vessel between the surface of the dense phase and the exiting gas stream is the lean phase section with a corresponding *freeboard height* (see Figure 2.29). As long as a recognisable upper surface exists for the bed of particles a dense-phase fluidized bed is present (Kunii & Levenspiel, 1969).

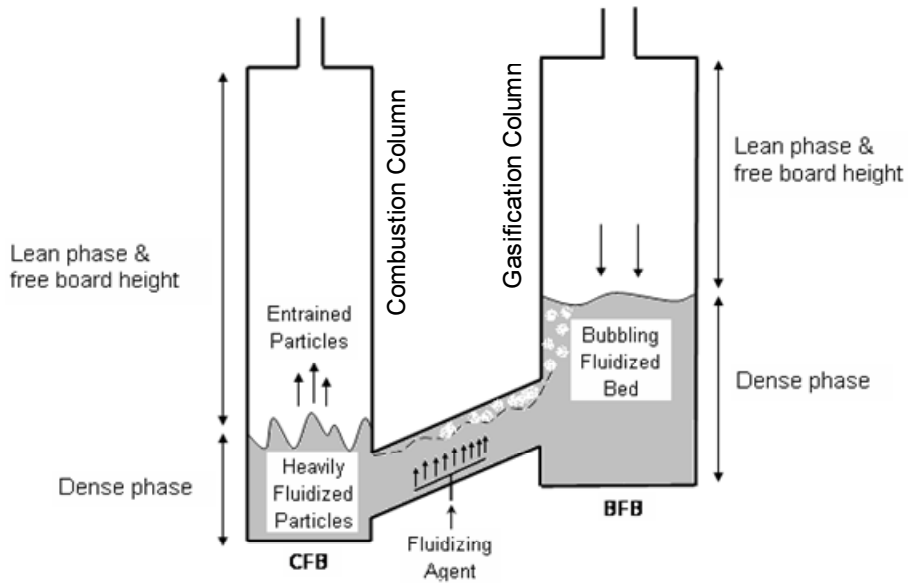

Figure 2.29: The dense and lean phases of a dual circulating fluidized bed showing the freeboard heights in the reactor columns.

Fluidized beds have a number of advantages to other contacting methods which makes fluidized bed gasifier designs favourable. These include (Kunii & Levenspiel, 1969):

1. The rapid mixing of solids creates nearly isothermal conditions throughout the bed with uniform fuel concentrations.
2. Liquid-like behaviour which is easy to control and automate.
3. The circulation of solids between reactors allows controllable amounts of heat to be interchanged.
4. Large quantities of heat are stored in granular bed material, so fluctuations in feed rate, feedstock composition and water content are better tolerated than other particle bed systems (Jeffers *et al.*, n.d.).
5. Heat and mass transfer rates are high, so surface areas of heat exchangers can be small.
6. Fluidized beds contain no moving parts in the hot regions, so minimal maintenance and a high availability factor is achieved.
7. Fluidized beds can be used on a wide range of scales (Arena & Mastellone, 2005).

Gases have poor heat transfer characteristics and very low heat capacities compared to heats of reaction, so it is difficult to obtain isothermal bed temperatures in a fixed bed gasifier. Control of bed temperatures is much easier in fluidized bed gasifiers because the rapid motion of solids

efficiently distributes the heat and keeps bed temperatures uniform. It is common in fluidized beds, particularly circulating fluidized beds to have aggregate particles present amongst the biomass to aid heat transfer because sand has a higher heat capacity than the biomass substrate (Kunii & Levenspiel, 1969).

Some gasifiers designed for coal feedstocks circulate coal char between reactors with no aggregate bed materials present (Probstein & Hicks, 2006). This not done in circulating fluidized bed biomass gasifiers because of the lower heat capacity of the biomass and the irregular morphology of the biomass means that it is difficult to create good gas seals between the reactors. The presence of aggregate amongst the biomass significantly aids its flow characteristics and reduces its porosity. One of the disadvantages with fluidized beds is that the rapid mixing of solids in the bed leads to non-uniform residence times occurring for some solid particles. Erosion of reactor walls and break up of the particles is also common (Kunii & Levenspiel, 1969).

How easily particles become fluidized, depends on factors such as the vessel geometry, fluidizing gas inlet temperature, and whether the solids are free flowing or tend to agglomerate. One of the most important factors is the size and size distribution of the particles. A bed of particles with a wide size distribution remains fluidized over wider variations in the gas flow rates. However, beds of large uniformly sized particles tend to fluidize poorly and over a narrow range with spouting and slugging more likely. The quality of fluidization can often be dramatically improved by having a small amount of fines present which reduce the occurrence of voids in the bed (Kunii & Levenspiel, 1969).

The quality of bubbling fluidization is strongly influenced by the design of the gas distributor below the bed. If the gas distributor has many fine holes the gas is distributed more evenly and the bubbling regime is more uniform throughout the bed. If only a few holes are present to pass the gas into the bed via, slugging is more likely as this encourages larger bubbles to be generated which coalesce more readily (Kunii & Levenspiel, 1969).

2.6.3 Entrainment in Fluidized Beds

Entrainment is the removal of solids from a fluidized bed by the drag forces of the fluidizing gas lifting the particles against gravity and pneumatically conveying a portion of them out of the dense phase of the bed. The purpose of the freeboard is to allow solids to separate from the gas stream under gravity, and as the freeboard height is increased, entrainment reduces. Eventually a height is

reached above which entrainment becomes constant and this is called the *transport disengaging height* (TDH) (Kunii & Levenspiel, 1969).

Both the total quantity of particles and the size distribution of the particles change as you move up a column from the dense phase of a fluidized bed to the TDH elevation. Entrainment rate decreases with height until the saturation carrying capacity of the fluidizing medium is reached. When a gas exits above the TDH, the size distribution and entrainment rate are constant as shown in Figure 2.30 (Kunii & Levenspiel, 1969).

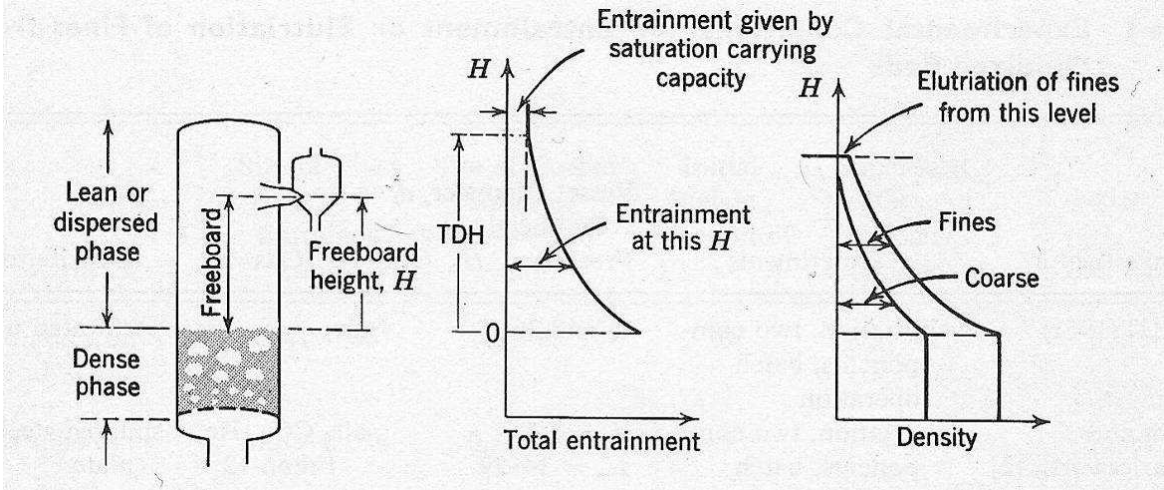

Figure 2.30: Diagrams showing the changes in particle dynamics. Source (Kunii & Levenspiel, 1969)

If the freeboard is extended, the density of the dispersed phase decreases for any given height. Increasing the freeboard height actually increases the particle density for any given height up the column until the TDH is reached. When the freeboard length extends above the TDH, then the density of particles at any given height is maximised (Kunii & Levenspiel, 1969). This is shown in Figure 2.31.

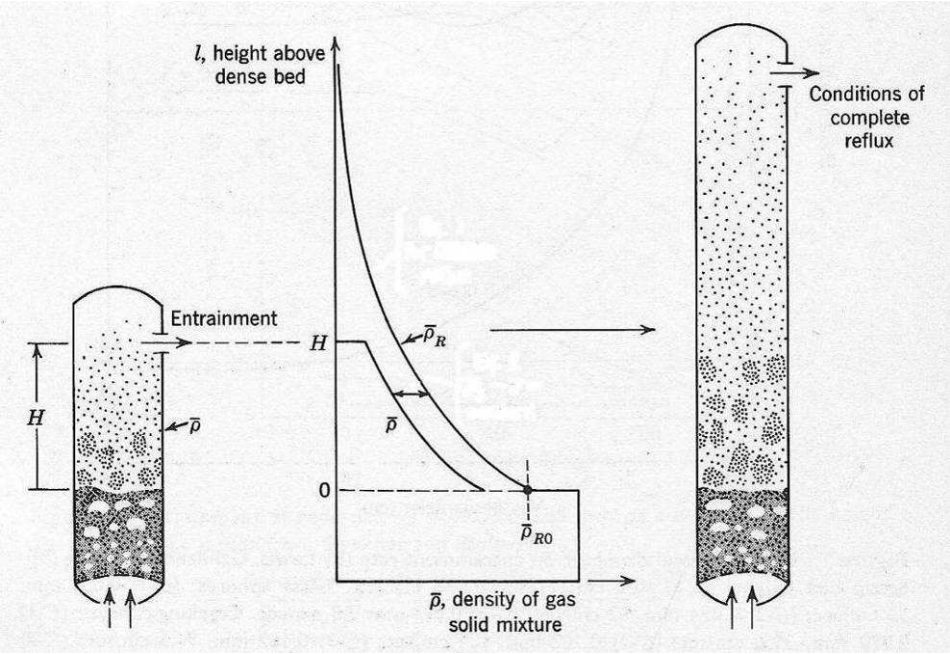

Figure 2.31: Changes in particle density in the freeboard region with height. Modified from: (Kunii & Levenspiel, 1969).

Elutriation is common in fluidized beds, where the finer particles are separated and drawn off from the mixture of particles in the bed leaving the coarser particles. Especially in combustion reactions, bubbles of gas can rise through the dense phase of the bed and erupt at the surface projecting particles into the freeboard region. This intermittent bursting action can cause sharp velocity fluctuations which dissipate with height as the gas velocity smoothes out. In low temperature environments, stirrers can be used to break up gas bubbles, to minimise the violence of the bursting gas bubbles and lower the entrainment rate. Grids can also be installed in the freeboard region of the fluidized bed to smooth out velocity fluctuations. However this also reduces the entrainment rate and lowers the TDH (Kunii & Levenspiel, 1969).

2.6.4 Pressure Drop Characteristics of Particle Beds

A minimum velocity is needed to fluidize a granular bed (V_{om}). If the velocity is too small the bed stays fixed and behaves as a packed bed. Initially if the bed is densely packed, the pressure drop overshoots the fluidization pressure until the particles separate and become fluidized. The pressure related characteristics of a particle bed can be seen in Figure 2.32. The bed can operate at quite high velocities with little or no loss of solids as long as the superficial velocity remains lower than the terminal velocity of the individual particles (Abrahamson, 2007; Chase, n.d.).

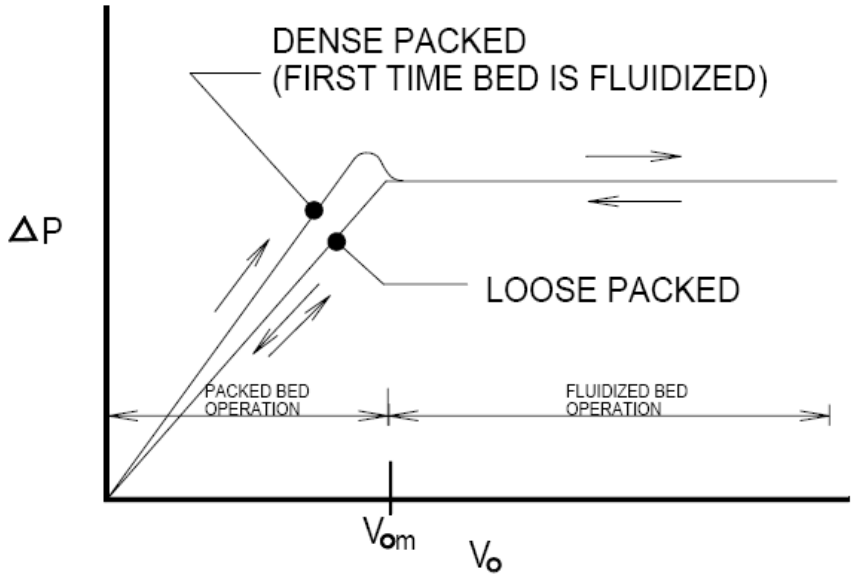

Figure 2.32: Pressure drop (ΔP) versus gas velocity (V_o) for a bed of uniformly sized sand particles. V_{om} represents the minimum fluidization velocity (Chase).

2.7 Operational Description of the Fast Internally Circulating Fluidized Bed Gasifier.

An early photo of the fast internally circulating, (dual) fluidized bed gasifier constructed at the University of Canterbury is shown in Figure 2.33. This photo was taken before any insulation was installed and used here since it is easier to see the different plant components. The distinction between this gasifier and most others around the world is that the generated producer gas has a higher calorific value of 11.5-13.4 MJ/Nm^3. This is due to the gas composition being nearly free of nitrogen with methane levels of 12-15 vol%. By using steam as a fluidizing agent in the gasification column, no air is introduced where nitrogen would dilute the producer gas.

The conventional set of thermochemical gasification reactions are divided to take place in two separate reactors. Wood is fed via an auger into the gasification reactor where it is fluidized with steam amongst granular bed material. Bed material is used because it has a high heat capacity, higher than the biomass itself. The endothermic pyrolysis and char gasification reactions take place here in the oxygen free environment. After a period of time the wood is converted into charcoal (commonly called char) and passes into the combustion reactor via the chute. The combustion reactor is fluidized with air and combusts the char to generate heat for the entire process. The exothermic reactions in the combustion column heat the bed material (which can have catalytic properties). By pneumatically circulating the hot bed material, thermal energy is transferred from the combustion column (CFB) to the gasification column (BFB).

The hot entrained bed material from the combustion column gets separated out in a cyclone and descends through a siphon (or dip-leg) into the top of the gasification column. The siphon allows bed material to be metered through, but creates a barrier to the exchange of gases between the flue gas line and the top of the gasification reactor. The chute which is a packed inclined channel between the bases of both reactors, allows solids to meter through but very little gas to exchange between the reactors. Hence, the siphon and the chute translate the bed material around the internal circuit but prevent the exchange of gases between the reactors. A simplified schematic is shown in Figure 2.34. In the current set up any producer gas which gets generated is analysed for volume composition and tar levels before being combusted in an afterburner for safety reasons. In the future an engine would be fuelled with the producer gas before any remaining producer gas would be directed to the afterburner for safe handling.

The Fast Internally Circulating Dual Fluidized Bed Biomass Gasifier

Figure 2.33: Early photo of the FICFB gasifier during the construction phase.

2.8 Particle Dynamics of Internally Circulating Dual Fluidized Bed Gasifiers

Optimisation of the particle-dynamic behaviour of circulating dual fluidized bed reactors is crucial to maintain stable operation and optimal heat transfer between the reactor columns. The circulation rate of bed material throughout the gasification system must remain in equilibrium to prevent the build up or run out of bed material at any regions in the plant. Failure to do so often results in very poor plant performance, requiring shut down of the gasifier to rectify the problem.

'Cold testing' is a technique used to allow investigation into the particle-dynamic behaviour at ambient temperatures. Often this involves placing transparent components on the gasifier and additional view ports to observe the bed material circulation behaviour. Cold tests are not fully representative of hot operating conditions, but are easier to perform and reduce the risks to operators in understanding the circulating behaviour of the plant. Under cold conditions equipment can more easily be pulled apart and interchanged without having to wait for plant components to cool down. An overall diagram of the FICFB gasifier is shown in Figure 2.34. It can be seen that the circulation of the bed material is clockwise when viewing the plant from the front. Lighter coloured arrows indicate the hottest regions of bed material (in the combustion reactor and siphon).

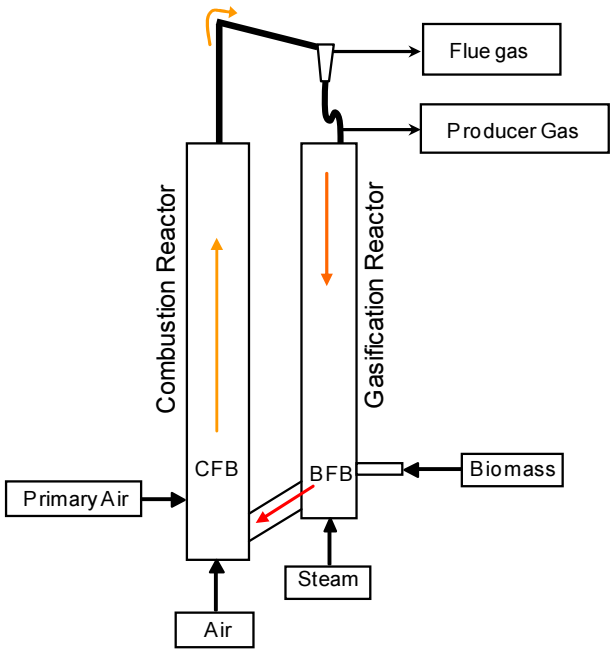

Figure 2.34: Bed material circulation through the FICFB gasifier.

2.8.1 Design Aspects of the Circulating Dual Fluidized Beds

Air is injected into the base of the combustion reactor to fluidize the bed material in the bottom of the combustion column and provide some air for combustion of the char. Additional air injection is supplied through the primary air jets to entrain the bed material against gravity up the combustion column. This extra air also oxidises char and any additional fuel that is introduced. The amount of fluidizing air must be controlled to limit the flow of air up the chute into the gasification zone. Too much air, too lower down, means unacceptable amounts of air track up the chute into the gasification column (Loffler *et al*., 2003).

Some combustion columns have a diffuser section in, above the primary air jets to keep the gas velocity in the desired range. A diffuser strongly enhances particle reflux by increasing the thickness of the wall layer of the down-flowing solids (annulus) (Loffler *et al*., 2003). The vertical positioning of the diffuser is important in relation to the fluidization regime. Figure 2.35 shows a diffuser and its circulation characteristics.

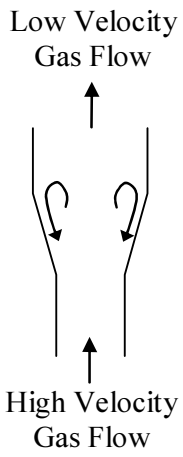

Figure 2.35: A diffuser which can be placed in the riser of a combustion column to increase the particle reflux for lengthening residence times in fluidized bed reactors.

Many factors affect the solids circulation rate throughout the FICFB gasifier. This is important because the circulation rate determines the amount of thermal energy which is conveyed form the combustion column to the gasification column. This affects the temperature of the gasification reactions which is a significant parameter influencing the producer gas composition and the tar levels in the gas. Speeding up the circulation rate will

reduce the temperature difference between the exothermic combustion reactions and the endothermic gasification reactions. However, circulation rate also incurs secondary influences as residence times and fluidization regimes change. Optimising the gasification temperatures is an important parameter to drive the equilibrium gasification reactions in the most favourable directions. It is also important that the residence times are long enough in the different stages of the processes occurring within the gasifier so that optimal performance occurs (Kunii & Levenspiel, 1969).

Increasing the particle diameter or the particle density decreases the solids circulation rate and the solids preferentially remain in the lower parts of the fluidized bed. The solids circulation rate can be increased by increasing the total pressure differential across the bed by having a greater bed material loading in the gasifier. At high gas velocities in the combustion column, the solids circulation rate is limited by the bed height in the BFB. The lower the bed height in the BFB, the lower the head of sand developed to push bed material through the chute and into the combustion column. The combustion column does have an upper limit on the maximum amount of solids-carrying capacity it has for a given gas velocity as discussed in Section 2.6.3 (Grace, 1997).

Gas volume flow rate is the most significant factor effecting circulation rate. However, solids circulation rate is also strongly increased if the entraining gases are introduced lower down in the combustion column. Thus, the bottom air flow has the most pronounced effect on the solids circulation rate. Increasing the height of the primary air jets significantly decreases entrainment and the solids circulation rate (Loffler *et al*., 2003).

An increase in the freeboard height of the combustion column increases the TDH and significantly reduces solids entrainment, reducing the circulation rate. Changes in the geometry of the combustion column, besides the cross-sectional area and the total height, have no significant effect compared to the operating parameters (gas flow rates and amounts of air introduced at different levels) (Loffler *et al*., 2003).

An important criterion for operating a dual fluidized bed system is the stability of solids circulation with variations in the outlet pressures of the two reactors (flue gas and producer gas outlets). These variations can be caused during normal operation by downstream fabric

filters and power plants malfunctions (Loffler *et al*., 2003). The stability of the solids circulation rate is mainly determined by the design of the siphon.

Restricting the flue gas exit from the gasifier, increases the counter-pressure of the flue gas and reduces the solids circulation rate because the entraining gas velocities up the combustion column are reduced. The same effect occurs for high pressure drops in the flue gas cyclone. A high counter-pressure at the outlet of the flue gas line causes the bed height in the standpipe to decrease as the flue gas exerts more pressure on material passing through the siphon. Eventually blow-through of the siphon occurs and the gas seal is lost. See Figure 2.36 for a view of the bed material flow downwards through the siphon.

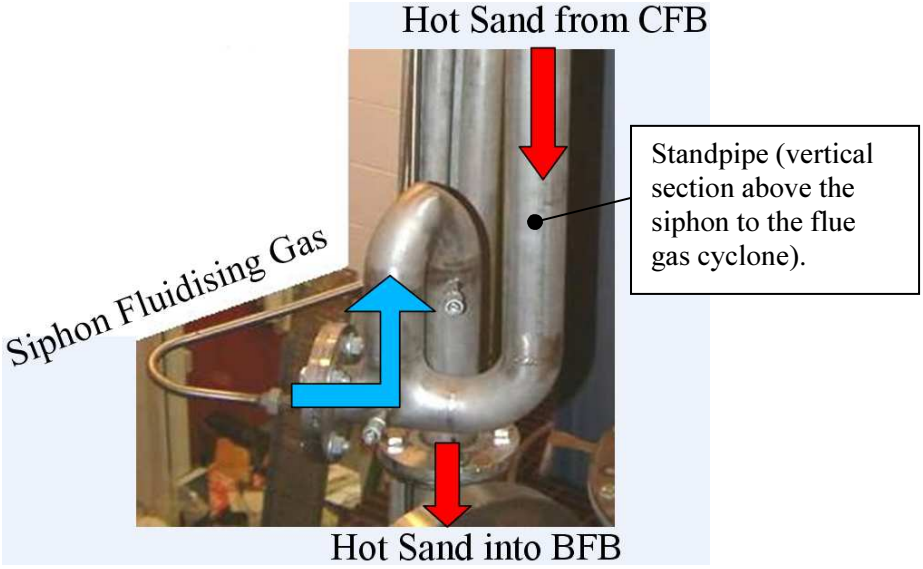

Figure 2.36: View of the siphon used to create a barrier to the exchange of gases between the reactor circuits but still allow bed material to be metered through.

An increase in pressure in the producer gas outlet line causes an increase in the solids circulation rate because more bed material is pushed into the combustion column via the chute. An increase in counter-pressure in the producer gas line increases the bed material height in the standpipe and some producer gas may also be lost up the siphon and out with the flue gas. When the backpressure is too high, filling-up of the standpipe can occur causing increased pressure in the combustion column (Loffler *et al*., 2003).

In summary:

1. Increasing the counter-pressure at the exit of the CFB, decreases solids circulation rate and decreases the bed height in the siphon and standpipe.
2. Increasing the counter-pressure at the BFB outlet, increases solids circulation rate and increases bed height in the siphon and standpipe.

2.8.2 Characteristics of Chute Return Systems on Gasifiers

The chute is used to supply char and bed material to the combustion column from the gasification column. This fuels the combustion column and prevents the need to continually replace the heat carrier. Chutes are a key functional device in the steady operation of FICFB gasifiers. Both the chute and the siphon are metering devices and require a method of flow control through them. These need to be responsive to changes in bed material levels and circulation rates, fast enough that no operator intervention is required. Figure 2.37 shows the location of the chute on the gasifier.

Two factors drive bed material through the chute: the force of weight of the bed material in the chute, and the pressure differential exerted across the chute. The pressure differential arises from the dynamic pressure exerted on bed material at the entrance of the chute relative to the pressure arising from gases and solids at the base of the chute.

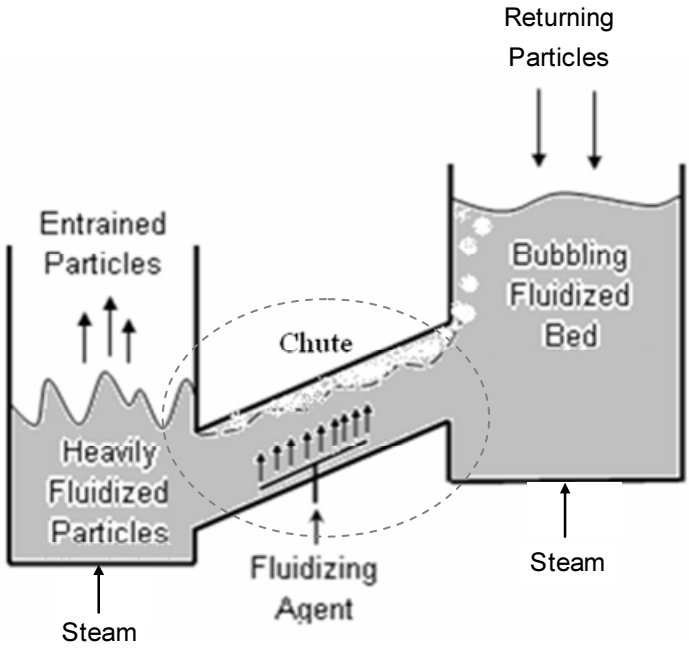

Figure 2.37: Location of the chute with the fluidizing agent rising from the sparger and flowing along the upper chute surface into the BFB.

Gases and solids separate in the chute and flow in opposite directions. Gas bubbles flow upwards along the top of the chute while solids flow down the bottom. Both the fluidizing medium and gases originating from the base of the combustion column can flow along the upper surface of the chute and into the BFB. This is generally unfavourable as the chute is designed to create a plug to prevent the exchange of gases between the two columns as any air supplies nitrogen, reducing the heating value of the producer gas.

To control the flow rate of bed material through the chute, different quantities of fluidizing gas are supplied through a sparger. This can be via either a roof-mounted sparger or a base-mounted sparger and Figure 2.38 shows both variations. It is common for a sparger to bend upwards in hot environments and normally a clamp is used to fix it in place (Grace, 1997).

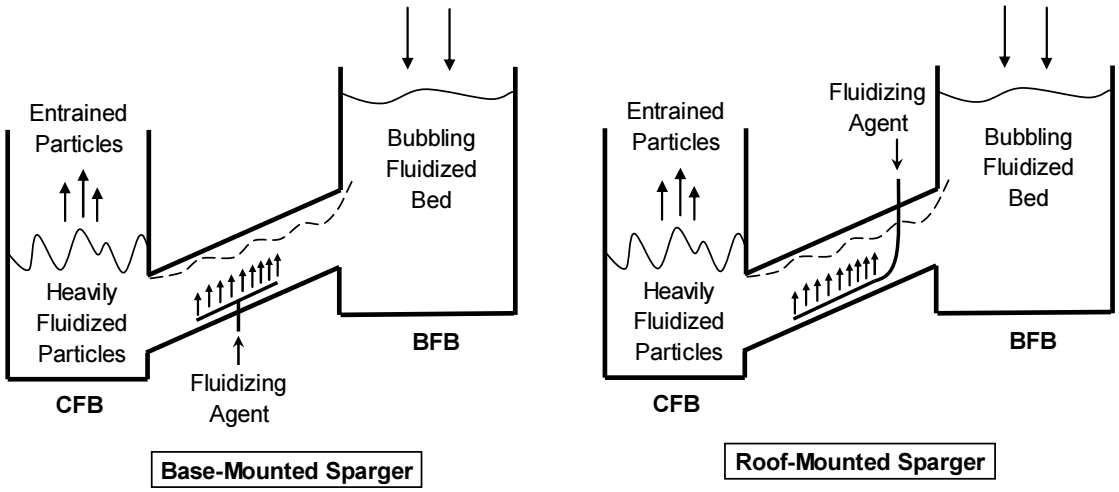

Figure 2.38: The two common mounting arrangements for spargers used to fluidize material in an inclined chute.

When the amount of bed material increases, the solids flow rate into the combustion column increases because of the higher head of sand in the BFB. A higher head of sand in the BFB creates a larger pressure differential across the chute causing more sand to move through. Provided that the maximum carrying capacity of the entraining gases in the combustion column are not exceeded, the circulation rate will increase with increasing BFB bed heights (Grace, 1997).

To increase the residence time of solids in the CFB, the inventory of bed material entering can be increased relative to the rate of entrainment out of the reactor. This is possible because

the combustion column gases can only entrain a certain amount of bed material for a given superficial velocity up the reactor.

Some circulating fluidized beds use a valve (such as a knife gate valve) to control the cross sectional area of the chute. This means the circulation rate can be easily controlled but material selection is very important at these temperatures. The University of Canterbury's FICFB gasifier achieves flow control through the extent of fluidization used in the chute, introduced via a base mounted sparger. The sparger runs along the chute base for most of its length. By changing the extent of fluidization in the inclined chute, a flow control range can be achieved. A higher mass flow occurs through a chute if the reservoir before the chute (in this case the BFB) is also fluidized.

In summary the mass flow rate of material through the chute is proportional to:

- Bed material heights (effects pressure differential across the chute)
- Cross sectional area of the chute
- Angle of inclination of the chute
- Particle density (effects the force of weight exerted)
- Particle size (effects the resistance to flow)
- Particle shape (effects the resistance to flow)

When a chute or siphon is operating in the bubbling regime, it will require a longer length to seal the same pressure differential compared a regime where the solids are just above minimum fluidization conditions. Long angled chutes have a limited solids circulation rate relative to vertical chutes (Grace, 1997).

2.8.3 Characteristics of Siphon Flow Control Systems

The siphon is the device used to prevent producer gas from rising out the top of the gasification reactor as hot bed material is introduced. It is essential that the bed material level in the siphon standpipe remains between an acceptable height range to ensure a producer gas is not lost out the flue gas line and that a constant supply of bed material enters the gasification column. If the sand level in the standpipe builds up too high, it fills up into the base of the cyclone and sand passes out with the flue gas. However, if the sand level in the

standpipe gets too low, blow-through can occur and the gas exchange barrier between the two reactor systems is lost.

The standpipe has many of the same characteristics as have been previously discussed in Sections 2.6 and throughout Section 2.8. As the bed material height increases in the standpipe, a greater pressure is exerted on the particles in the lower region of the standpipe and more bed material is forced through the siphon. An equilibrium point is established where the force of weight of the particles in the standpipe and pressure differential across it balances the frictional forces, and a self-regulating bed material level is achieved. This level is highly susceptible to changes in system pressures and is a traditional challenge with maintaining stable operation of FICFB gasifier at the University of Canterbury. Figure 2.39 shows a diagram of a siphon with balloons explaining its operation.

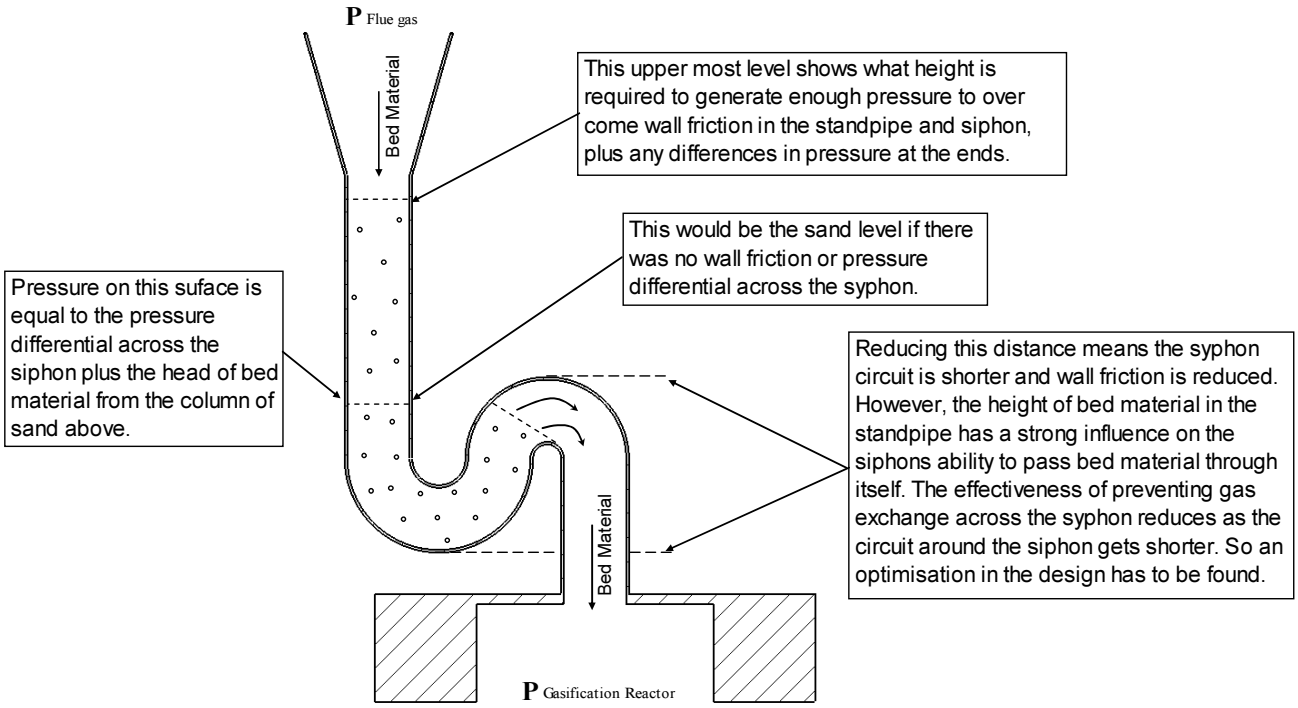

Figure 2.39: Diagram of a siphon used to pass hot bed material into the gasification column while preventing the exchange of gases between both reactor systems.

The solids flow rate through a siphon is mainly controlled by the amount of fluidizing gas introduced. Figure 2.40 shows where fluidizing air is introduced into the siphon used in this FICFB gasifier.

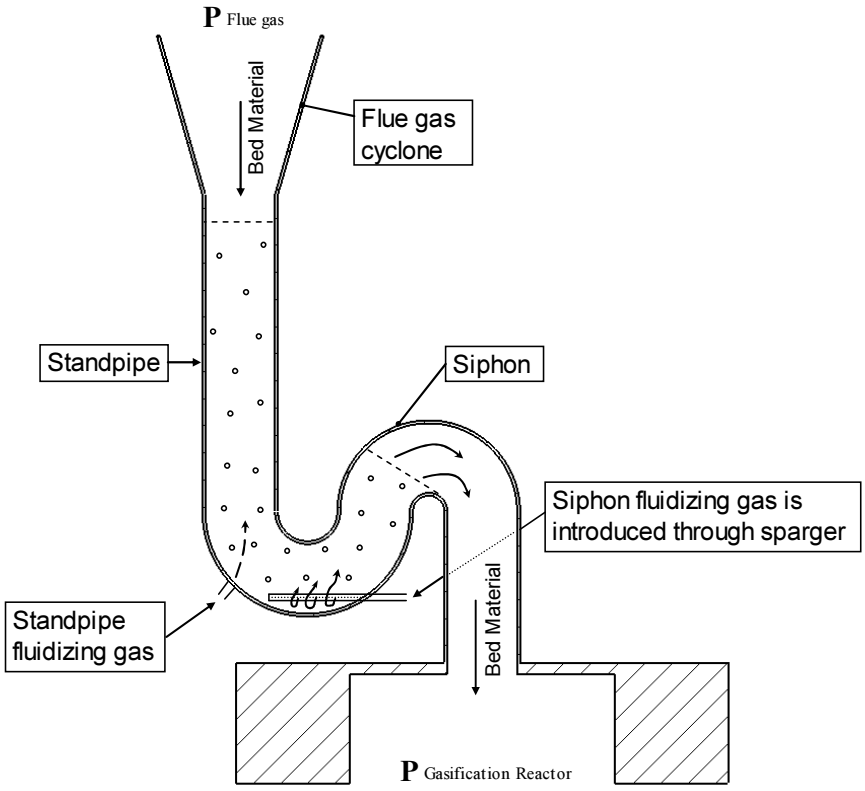

Figure 2.40: Diagram of a siphon showing the two entry points for fluidizing gas and the paths taken by each gas stream. The two entry points for fluidizing gas are in the bottom curve of the siphon and at the base of the standpipe (vertical section above the siphon).

The force driving the particles around the siphon is generated from the drag forces of the gases on the particle's surfaces, plus the head generated from bed material in the standpipe. The drag forces on the particles exert a pressure on the sands surface. When the drag forces exert a great enough pressure that the frictional forces of the particles on the siphon wall are exceeded, the bed material begins to flow through. Solids do not begin to flow immediately. The initial fluidization gas has to overcome a threshold quantity to initiate flow (Grace, 1997).

Siphons work best with particles in the size range of 100-5000 microns. Above 2000 microns (2 mm) substantial amounts of gas are required to generate large enough drag forces to move the solids around the bend. This is because larger solids have less surface area to volume available for the generation of drag forces. Small particles mixed in with the larger particles help fill the voids and increase the drag forces on the entire solids mass (Grace, 1997).

There is a maximum pressure drop per unit length (ΔP/L) that a moving packed bed standpipe can develop. Further increases in the solids flow rate can occur up until the ΔP/L in the moving bed standpipe reaches the limiting maximum value. A short standpipe reaches its maximum ΔP/L limit at a lower solids flow rate compared to a longer standpipe. This is because a short standpipe has a less obstructive path for gases and hence a reduced capacity to absorb pressure drops than a long standpipe. So the maximum solids flow rate through a siphon depends upon the length of the standpipe above it (Grace, 1997).

To determine the diameter of a siphon, it is necessary to select the linear solids velocity desired. Nearly all siphons operate with velocities between 0 to 0.3m/s. Velocities greater than about 0.3m/s can result in stick-slip flow (Grace, 1997).

It is desirable to add aeration air as low as possible in a standpipe and siphon bend. This results in maximising standpipe length and minimising a siphon's pressure drop. Both help to increase solids flow rate through the siphon. At high temperatures less aeration gas is required because the viscosity of the gas decreases at higher temperatures (Grace, 1997).

Literature sources state that it is generally recommended for fluidization gas to be supplied to the base of the downward flowing portion of a standpipe. The additional gas supplies should be separate so they can be varied independently (Grace, 1997). Figure 2.40 shows this.

Using a standpipe too small in diameter above the siphon causes the fluidizing air to be drawn around the siphon with the bed material, rather than rising up the standpipe and out with the flue gas. If excessive air is feed to the siphon, too much air flows around the siphon with the bed material (Grace, 1997).

The effects of changing various parameters on the siphons performance are shown below:

- Increasing the standpipe diameter means more aeration gas is required.
- Increasing particle size and density means more aeration gas is required.
- Increasing particle density and decreasing cross sectional diameters, increases pressure drops.
- Increasing pressure drop across the standpipe increases solids flow rate (same applies to an inclined chute).

2.9 Wood Residue Fuels

2.9.1 Wood Residue Classification and Composition

Wood residue is the material remaining after forestry and forest industry operations such as logging, sawmilling, and timber product manufacturing which is not produced intentionally. One of the challenges with wood residue is that it has a range of sizes, shapes, chemical properties and moisture contents. Some wood residue also contains unfavourable materials like dirt, stones and tramp metal.

Wood is a composite of three polymers: cellulose, hemicellulose and lignin. These polymers are chemical combinations of carbon, hydrogen and oxygen. Wood also contains extractives such as resins and tannins, minerals and moisture. The relative proportions of carbon and hydrogen to oxygen influences the heating value of wood. Wood species are generally characterised into softwoods and hardwoods (Baines, 1993). Table 2.4 gives the typical composition of oven dry softwoods and hardwoods.

Table 2.4: The typical composition of oven dry softwoods and hardwoods. Source: (Baines, 1993).

Format of Analysis	Softwoods (wt%)	Hardwoods (wt%)
Chemical composition (dry basis)		
Cellulose	43	43
Hemicellulose	28	35
Lignin	29	22
Ultimate analysis (dry basis)		
Hydrogen	6.1	6.2
Carbon	53.0	51.0
Oxygen	38.8	39.9
Sulphur	-	-
Ash	1.7	2.5
Proximate analysis		
Volatiles	40.6	52.4
Fixed carbon	12.4	12.9
Ash	1.0	2.7
Moisture	46.0	32.0

Wood is generally designated into one of three categories: *green wood*, *air dried wood* and *oven dried wood*. Green wood is freshly cut wood, air dried wood has been exposed to the air and its moisture content has been reduced. Oven dried wood has had all its moisture removed. On a macro scale, a fresh log contains about 55 % water, with about 50 % of the remaining quantity being carbon (New Zealand Forest Industry, 2006). This is shown graphically in Figure 2.41.

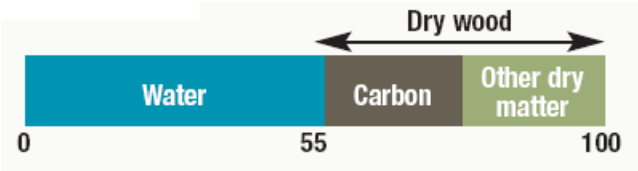

Figure 2.41: Basic composition of wood. Source (New Zealand Forest Industry, 2006).

The high volatile content of biomass (70-90 wt%) compared to coal (30-40 wt%), and the high reactivity of the char makes biomass a good gasification fuel (Brown, 2003). An ideal biomass feedstock for any gasification or combustion process is one that contains low levels of elements such as nitrogen, sulphur, and chlorine which can form undesirable pollutants and acids that cause corrosion. The presence of mineral elements that can form inorganic ash and particles are undesirable. Alkali metals such as potassium and sodium can lead to fouling and erosion problems. Wood has a lower ash content than coal, produces less particulate emissions and almost no sulphur oxides. From an emission point of view, wood is a very good fuel source compared to coal (Klass, 1998).

2.9.2 Moisture Content of Wood

The amount of energy wood residue liberates when it is combusted or gasified, is largely dependant on its moisture content. Energy yield is usually expressed as a materials net calorific value, which will increase as the wood moisture content is reduced. Figure 2.42 shows this concept. The moisture content of biomass is measured as a percentage of the materials weight on either a dry or wet basis (Knoef, 2005). The wet basis moisture content directly reflects the fuel value of the material. The moisture content of wood measured on a wet basis is the weight of water in the wood sample divided by the total weight of the sample:

$$\textit{Moisture content (wet basis) \%} = \frac{\text{mass of water (kg)}}{[\text{mass of dry wood} + \text{mass of wet wood}]\,(\text{kg})} \text{ x } 100\%$$

The moisture content of a material on a dry basis is the weight of water in the sample divided by the dried weight of the material:

$$\textit{Moisture content (dry basis)}\ \% = \frac{\text{mass of water (kg)}}{\text{mass of dry wood (kg)}} \text{ x } 100\%$$

Often timber in saw mills is sawn in a green state, so the moisture content of the wood limits its immediate energy yield (Energy Information Administration, 2006). Lower moisture contents in gasification feedstocks are desirable because it prevents the need to supply additional latent heat to vaporise water in the feedstock and raise the steam to the temperatures found in the reactor. But unlike combustion reactions, the steam can take part in the gasification reactions. Despite this it is more favourable to use steam specifically generated from waste heat rather than to use wet feedstocks and vaporise the inherent moisture drawing thermal energy from within the reactor.

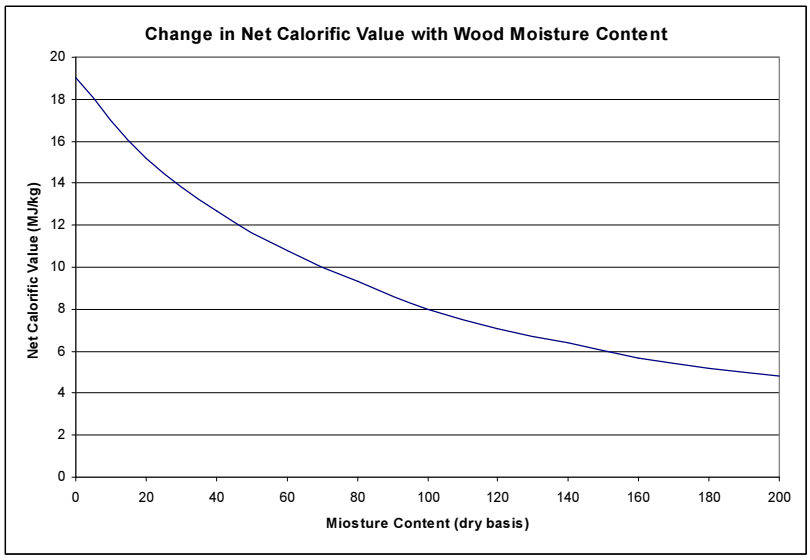

Figure 2.42: Change in net calorific value of wood with moisture content. Drawn from (Fordyce & Ensor, 1982).

Energy balance calculations applied to FICFB gasifiers in Austria have shown that water content in the fuel is very important. With increasing water content the chemical efficiency decreases and the flue gas temperature increases. Compared to air-blown gasifiers, fuel moisture content in steam blown FICFB gasifiers does not seem to noticeably effect the gas composition (Fercher *et al.*, 1998). It has also been identified in the 8 MW FICFB gasification plant in Güssing, Austria, that water content in the biomass has the greatest influence on the electrical efficiency of the overall CHP plant process (Rauch, 2004).

2.9.3 Ash Content of Woody Biomass

Ash is the inorganic or mineral content of the biomass which remains after complete combustion. The amount of ash found in different types of feedstocks varies widely from 0.1 % in wood up to 15 % for some agricultural residues. The presence of ash in the feedstock for gasifiers influences the design of the reactor vessel and the capabilities of the ash removal system. The chemical composition of the ash is important because it effects the melting behaviour and whether slagging is likely to occur (Knoef, 2005). The most troublesome components of ash are usually SiO_2, and alkalis such as Na_2O and K_2O (Goss & Kaupp, 1984). Alkali salts, especially sodium and potassium chlorides melt at the normal operating temperatures of fluidized bed reactors. NaCl and KCl have melting points of 787 °C and 762 °C respectively (Jeffers *et al.*, n.d.). In general ash that is high in silica and/or alumina has a high melting point but this is reduced by the presence of iron and calcium (Higman & Burgt, 2003).

Because of the diversity of biomass materials, not all feedstocks can be gasified under the same conditions. For example woody biomass has lower ash contents than coal, and some of the lowest sulphur levels of all biomass materials. Grasses and straws have a higher ash content than wood and can cause fouling problems (Klass, 1998). For all gasifiers the ash softening and ash melting (or fusion) temperatures are important variables. In fluidized bed gasifiers these ash properties govern the upper operating temperature at which agglomeration of ash is initiated (Higman & Burgt, 2003). Hence temperatures in a fluidized bed should be kept below the ash softening temperature which is commonly around 850 °C for biomass (Knoef, 2005).

2.9.4 Volatile Matter Content

The amount of volatiles in the fuel for the gasifier has a noticeable impact on the tar production levels found in the producer gas. Depending on the design of the gasifier, the volatiles may reach high enough temperatures to be thermally cracked into smaller hydrocarbon components. The percentage of volatiles is an indication of the quantities of pyrolysis gas that can be generated. For biomass materials the volatile matter content commonly varies between 50-80 %! (Knoef, 2005)

2.9.5 **Dimensional Variations in Wood Residue**

The dimensional variability of woody biomass is a significant problem for the design of bioenergy plant. The fuel handling and feed systems of bioenergy plants are often one of the most challenging areas for engineers of woody biomass energy plant (Joesph, 2006). The size and shape of the wood residue has significant implications on auger feeding systems, flow through hoppers and general interlocking of material.

FICFB gasifiers are unique to other gasifier designs because the bed material and fuel particles are translated between two reactors (the combustion reactor and the gasification reactor). Due to this operating characteristic, correct circulation and metering of the wood residue around the internal gasifier circuit is important. The gasifier must be designed so that a wide range of fuel sizes and shapes can be accepted without adversely effecting plant performance. For example, light flat shavings may be rapidly entrained out of the combustion column causing them to have a shorter residence time compared to clumped biomass particles that may not be able to be entrained out of the combustion column until they combust to a smaller size. Irregularly shaped pieces of wood residue may also interlock and cause blockages in the narrow parts of the gasifier circuit, particularly in the siphon. Hence, gasifiers need to be made as ‘fuel flexible’ as possible for maximum reliability! This will allow the greatest varieties of wood residue to be utilized so economies of scale can be best achieved for any given location.

3.0 Modifications to the 100kW FICFB Gasifier

The University of Canterbury's FICFB gasifier was built and commissioned by Jock Brown and Rick Dobbs from 2004 to mid 2006. Many operational problems existed during early test runs which have been addressed through several of the modifications discussed in this section. These modifications were necessary to get the gasifier running in a stable manner and to increase the ease of operation of the plant. Only the more significant modifications have been included here. It is outside the scope of this thesis to include the numerous design calculations and CAD drawings used for the fabrication of the components.

3.1 Completed Modifications

3.1.1 Design of Clear Standpipe for Cold Testing

Early gasifier trials were very temperamental with major problems surrounding the flow of bed material through the siphon. Often the siphon was either in an over-filled state or blew-through preventing any gas sealing between the gasification reactor and flue gas passage. It was realised that the gasifier's particle dynamics needed to be studied to better understand how the bed material flows around the gasifier circuit. The main area of study surrounded the siphon. Both installing multiple view ports and completely replacing some sections of the gasifier with transparent sections was considered. To aid operators in understanding the behaviour of the siphon, a transparent standpipe section was installed to enable cold testing trials to be performed. This can be seen in Figure 3.1.

Figure 3.1: Transparent standpipe section used during the cold testing phase to study the flow of bed material through the siphon.

Installing the transparent standpipe section was invaluable to understanding the siphons operation. Extensive cold testing was performed on the gasifier and much progress was gained through increasing the operator's understanding of this critical component. It became realised that being able to observe the flow of bed material through the standpipe was so important, that a permanent view port was installed on the steel standpipe section used under hot conditions.

3.1.2 **Installation of View Ports**

Operators needed a method to make visual observations around different regions of the gasifier. After the successful period of cold testing was completed to better understand the bed material flow characteristics in the gasifier, two additional view ports were installed as shown in Figure 3.2.

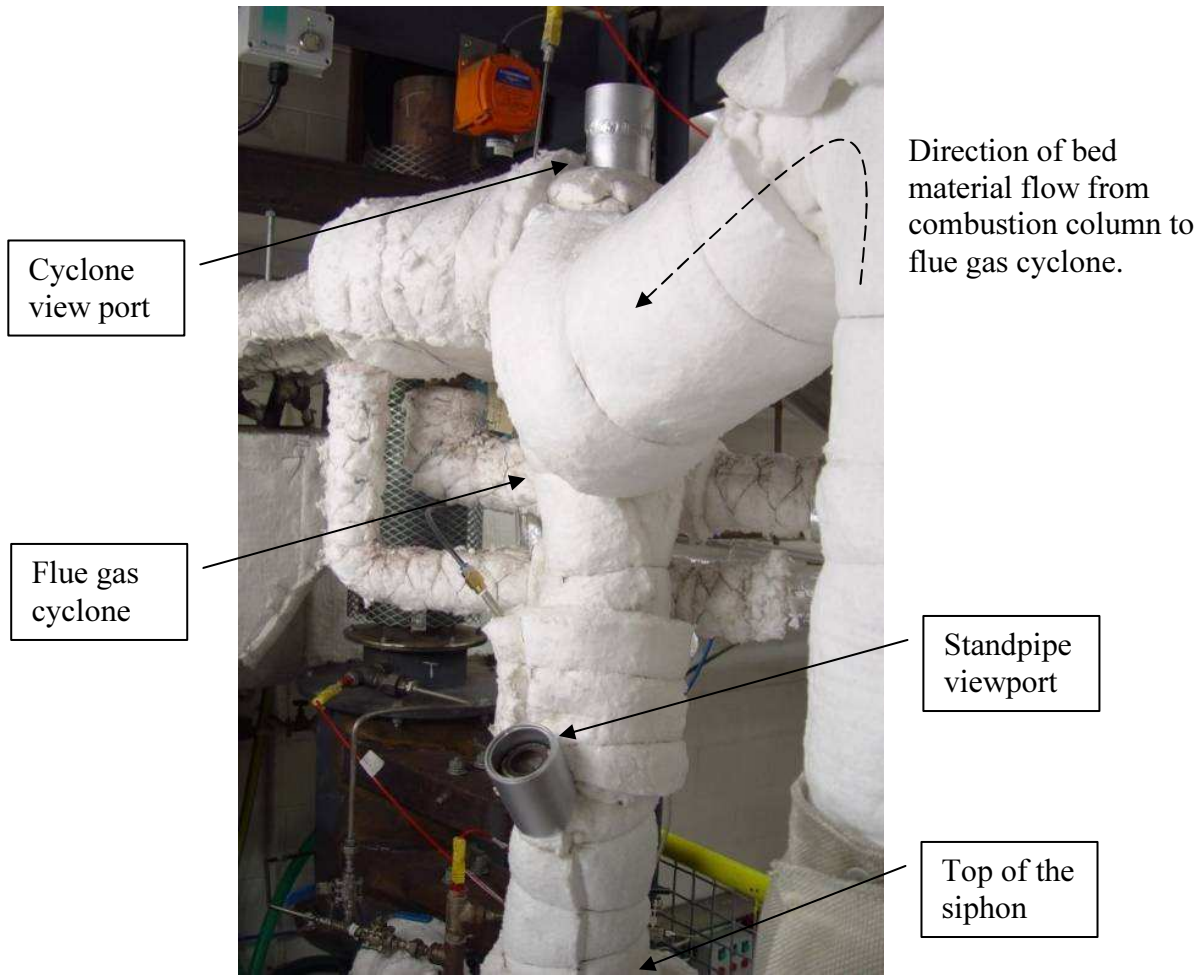

Figure 3.2: The flue gas cyclone, the standpipe and the top of the siphon with view ports extruding from the kaowool insulation.

The view ports were installed either vertically or at a steep incline downwards so they were self clearing and did not fill up with bed material. High temperature, double glazed quartz glass was used with tesnit gaskets. The reason for double glazing was to minimise condensation forming on the underside of the glass. Heat shields were placed around the view ports so that no hot surfaces were exposed to people moving around the plant. These consisted of a concentric steel tube loosely fitted around the eye glass holder so that minimum amounts of heat were transferred to the outer sleeve. On any other FICFB gasifiers

developed, it is encouraged that view ports are installed wherever possible to enable operators to make visual observations.

3.1.3 Conversion of the Siphon to Air Fluidization

During early operation of the gasifier in 2006, extensive problems existed with the erratic circulation of bed material between the reactors. This was a significant problem as the plant could not be operated reliably and there was a minimum of understanding by the operators about the circulation behaviour of the bed material in the gasifier. The details of the siphon's operation are now well understood and have been outlined in Sections 2.6 and 2.8.

One of the main operating problems was achieving consistent flow of bed material though the siphon. During the start up phase of gasifier operation, blockages would occur in the siphon causing the bed material to back-fill up in the standpipe and into the flue gas cyclone. This resulted in bed material passing out with the flue gas, instead of being retained and circulated within the gasifier loop. In the early stages of the heat up phase of the gasifier, the fluidizing steam would condense and wet the bed material. This caused the bed material to clump together and its ability to flow smoothly was reduced. It was also discovered that the bed material sometimes remained wet in the siphon from a previous test run as a result of the steam condensate collecting in the siphon.

To rectify this problem, the siphon fluidizing agent was changed from steam to air which passed through a heat exchanger in the flue gas line to preheat it to approximately 250 °C. This significantly helped prevent blockages especially during start up when the bed material was at ambient temperature. The small amount of air that this introduces into the gasification column reacts with the producer gas behaving much like an air-blown gasifier and introduces some nitrogen.

After extended testing of the gasifier under hot conditions in 2008, it was realised that steam was preferable to fluidize the siphon during the gasification phase. The main reason for this was that the siphon temperatures were getting too high (840 °C plus) which is undesirable in the stainless steel siphon and increases the risk of fusing the bed material. Instead air should be used as the fluidizing medium during the heat up and cool down stages, and steam fluidization used during gasification. This is the same procedure as occurs with fluidizing the

chute and base of the gasification reactor, where air fluidization is converted over to steam before wood is conveyed into the gasification reactor. The additional benefit with steam fluidization of the siphon during gasification, is that the producer gas would have an even lower nitrogen content than is currently achieved.

3.1.4 Adding Fluidization to the base of the Standpipe

During the early stages of cold testing on the gasifier the flow of bed material through the siphon continued to be problematic with the bed material regularly filling up into the base of the flue gas cyclone. There was too much resistance to the flow of the bed material through this part of the circuit. The fluidizing gas in the siphon was constrained to only part of the standpipe-siphon circuit, limiting its effectiveness. So additional air fluidization was installed at the bottom of the standpipe where the first bend of the siphon began. See Figure 2.40 and Figure 3.3.

Discovering that introducing a small stream of fluidizing air into the base of the standpipe radically improved the flow characteristics of the bed material through the siphon was a major step forward. This was later clarified in literature as commonly being required (see Section 2.8.3). Fluidizing the base of the standpipe also allowed much lower levels of siphon fluidizing air to be used. On evaluation, the siphon became more effectively fluidized with a lower total flow rate of gas being required. Cold tests showed that almost all the standpipe fluidizing air vented out through the producer gas line.

These changes to the siphon and standpipe fluidization meant that a gently self-regulating bed material level could be maintained in the standpipe and thereafter blockages ceased. The upper surface of the bed material in the standpipe now fluctuated within a much narrower range, almost holding a constant level. Significant improvements were noticed in the siphon's ability to maintain a barrier to gas exchange between the two reactor systems. The siphon no longer blew-through as happened in the past. Experimental testing performed, revealed that changing the level of fluidizing air in the siphon and standpipe has minimal effect on the producer gas composition. This is most likely because the flow rates are rather low in comparison to the amount of producer gas generated.

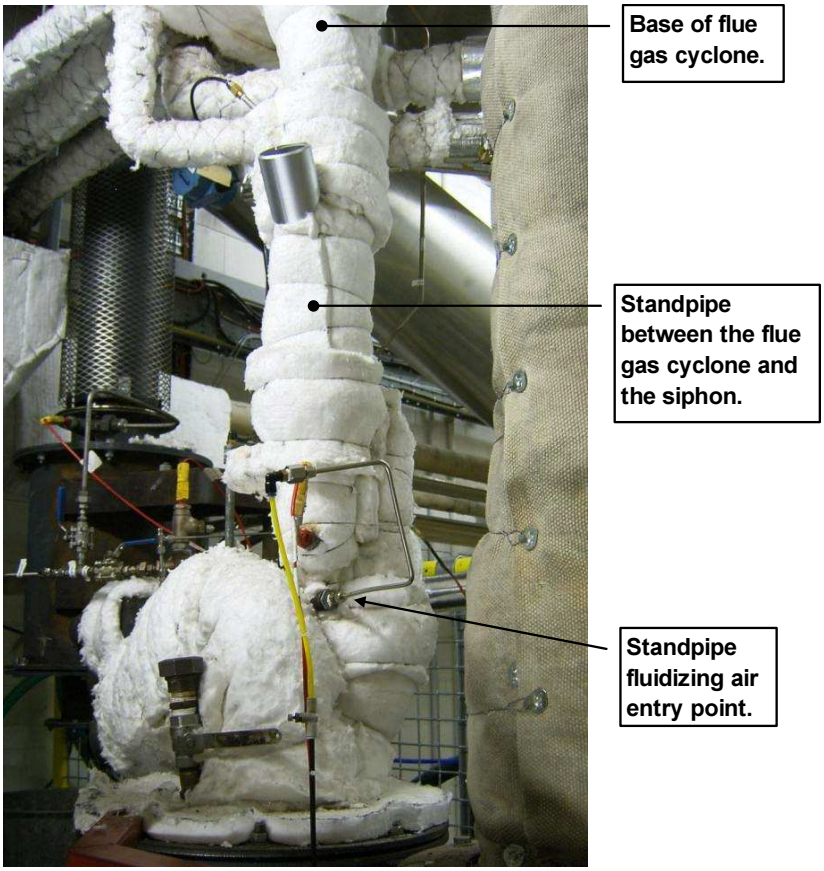

Figure 3.3: Location of the standpipe air entry point. The small air flow rate of 4-5 L/min allows the standpipe to be sufficiently fluidized so that a self-regulating bed level is maintained within it.

3.1.5 Installation of Siphon and Standpipe Warning System

As the gasifier development progressed, more control and warning systems were installed for the operators. Cold testing of the plant with manometers revealed that the pressure differential across the siphon could be adequately measured. This opportunity was used to install a DP (differential pressure) cell which sounds an alarm if the standpipe begins to overfill. This system proved to be effective but the pressure differential across the siphon under cold conditions and hot conditions differ, so the alarm thresholds have to be adjusted during operation. Figure 3.4 shows the two locations that the pressure measurements are taken across.

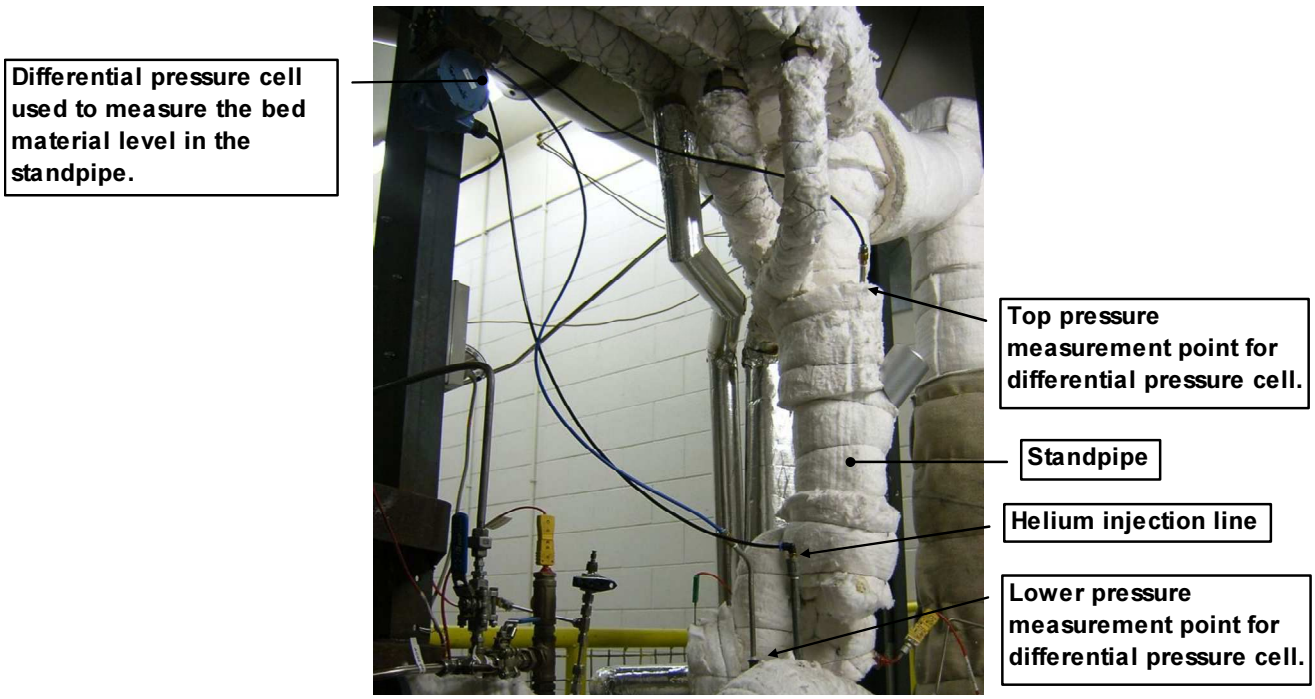

Figure 3.4: The differential pressure (DP) cell and the two locations the pressure readings a measured across.

3.1.6 Conversion of the Chute to Fluidization with Steam instead of Air

During early gasifier trials in 2006 the chute was also causing running problems. This was largely related to a lack of understanding of the chute's operation and the required amount of fluidization necessary. The final destination of the chute's fluidizing gas was also unknown.

Cold testing with nitrogen revealed that the majority of gas which enters the chute, flows up the inclined chute into the gasification column in a counter-current arrangement to the flow of bed material. This characteristic is shown in Figure 2.37 and explained in Section 2.8.2. This meant that the chute's fluidizing air was introducing unfavourable quantities of nitrogen into the gasification reactor and hence the producer gas composition was affected.

Since the level of chute fluidization is a method to control the circulation rate in the gasifier, maintaining a fluidizing gas was necessary, even though the chute had enough incline to allow some bed material to gravitate naturally into the combustion reactor. Air and steam are the most practical fluidizing agents which can be used on all scales of plant, so the chute fluidization gas was changed to superheated steam for gasification. During the heat-up and cool-down phases, preheated air is supplied by passing it through a flue gas heat exchanger.

By preventing steam entering the chute when the gasifier temperatures are low, the risk of steam condensate causing blockages was eliminated.

The change to steam fluidization when gasifying proved successful and it became apparent that the chute acts as an extension of the BFB. Steam gasification reactions continue to occur in the chute and the producer gas which evolves passes into the gasification reactor contributing to the total producer gas output. Figure 3.5 shows where the fluidizing gases enter the chute.

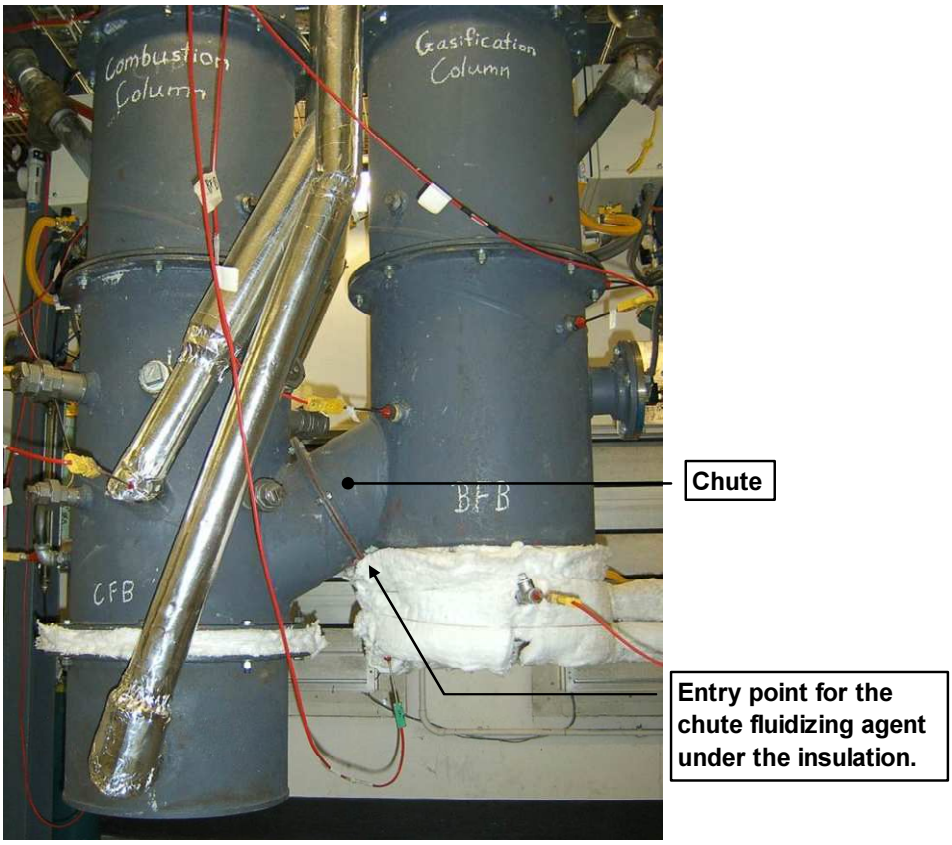

Figure 3.5: The chute with the fluidizing gas entry point indicated.

3.1.7 Conversion to an Independent Steam Supply

Gasifier tests performed by Jock Brown (the previous gasifier operator before mid 2006) found that the original steam generation system introduced problems. There was too much interplay between the production of steam from combusted producer gas in the afterburner, and the generation of the producer gas itself. This had negative feedback connotations because the quantity and quality of steam introduced into the gasification column affected the producer gas yield, thus effecting steam production.

While other parts of the gasifier were being modified, the original steam generator situated above the afterburner was removed and a chimney was installed in its place. Following this conversion, steam is supplied by the departmental boiler which is independent of the gasifier. This also simplified the set up of the gasifier and improved its operational flexibility. Steam could now be used at any stage during operation of the gasifier without having to wait for enough producer gas to be generated to generate the steam. Additional superheating of the steam was provided by installing electrical trace heating on the final section of the steam lines to the gasification reactor and chute. The new instrumentation to control the flow rate of steam introduced into the chute and gasification reactor is shown in Figure 3.6.

In a larger scale plant it would make thermodynamic sense to use waste heat to generate steam to run the process. However, supplementary firing of an independent fuel such as bottled LPG would be advisable so that steam could be generated on demand during start-up, so the need to rely on producer gas production is eliminated. By providing enough redundancy in the steam generator and having a feedback system to supply supplementary fuel for steam generation when required, the majority of the plant's steam demand could be met from waste heat reliably.

Figure 3.6: Photo of the steam lines (with silver and black insulation) and the air lines (yellow and blue hoses) that supply fluidizing gas to the gasification reactor and chute.

3.1.8 **Chimney Modification**

After the removal of the original steam generation system mounted above the afterburner, a mild steel chimney was installed. Preliminary hot tests during mid 2007 revealed that the chimney needed redesigning. The chimney was getting too hot without any refractory lining, and for safety to operators, insulation was wrapped around its outside to eliminate hot surfaces. This caused the steel to get too hot introducing a secondary risk of chimney collapse.

Two options were available to reduce the heat radiation to operators, either place insulation inside the chimney or redesign the chimney with a concentric shield allowing for an air current to pass up between the two layers. The second option was chosen with a similar principle to a cooling tower where an upward flowing draft is induced. An additional mesh guard was installed around the outside as protection against accidental contact. The final construction of the chimney is shown in Figure 3.7.

Figure 3.7: The final version of the chimney with a stainless steel inner tube, mild steel outer tube and mesh guard around the outside.

A constraint on the chimney design was the desire to maintain a sufficient inner diameter to minimise the velocity of the combusted producer gas impinging on the extraction hood above the afterburner in the laboratory. This was accomplished by selecting a 160mm diameter stainless steel inner tube which can tolerate higher temperatures than the original mild steel chimney. A shield was also installed on the extraction hood so that the combusted producer gas did not impinge directly onto the skin of the extraction hood in the laboratory. The twin tube concentric chimney design performed well with enough air current being generated up between the two steel tubes so that the surface temperatures posed no risk to personnel.

3.1.9 Biomass Lock Hopper Addition

This change was required because the existing floor mounted hopper had insufficient capacity, meaning it had to be refilled regularly during operation of the gasifier. The main concern driving this change was to prevent the possibility of operators being exposed to any back flowing producer gas via the auger feed system when refilling the hopper. When the hopper lid was removed the positive pressure supplied by the nitrogen purge was lost, increasing the possibility that producer gas could be vented.

Four options were identified which included: operators wearing personal safety gear during filling, highly ventilating the laboratory during filling, increasing the capacity of the main floor mounted hopper so it only needed to be filled at the start of the day before gasifier operation, and mounting a second hopper above the main hopper with a gas tight seal in between. This last concept was chosen because it was most practical and would not restrict the length of operation of the gasifier in the future. This final feedstock storage system with main hopper and lock hopper is shown in Figure 3.8.

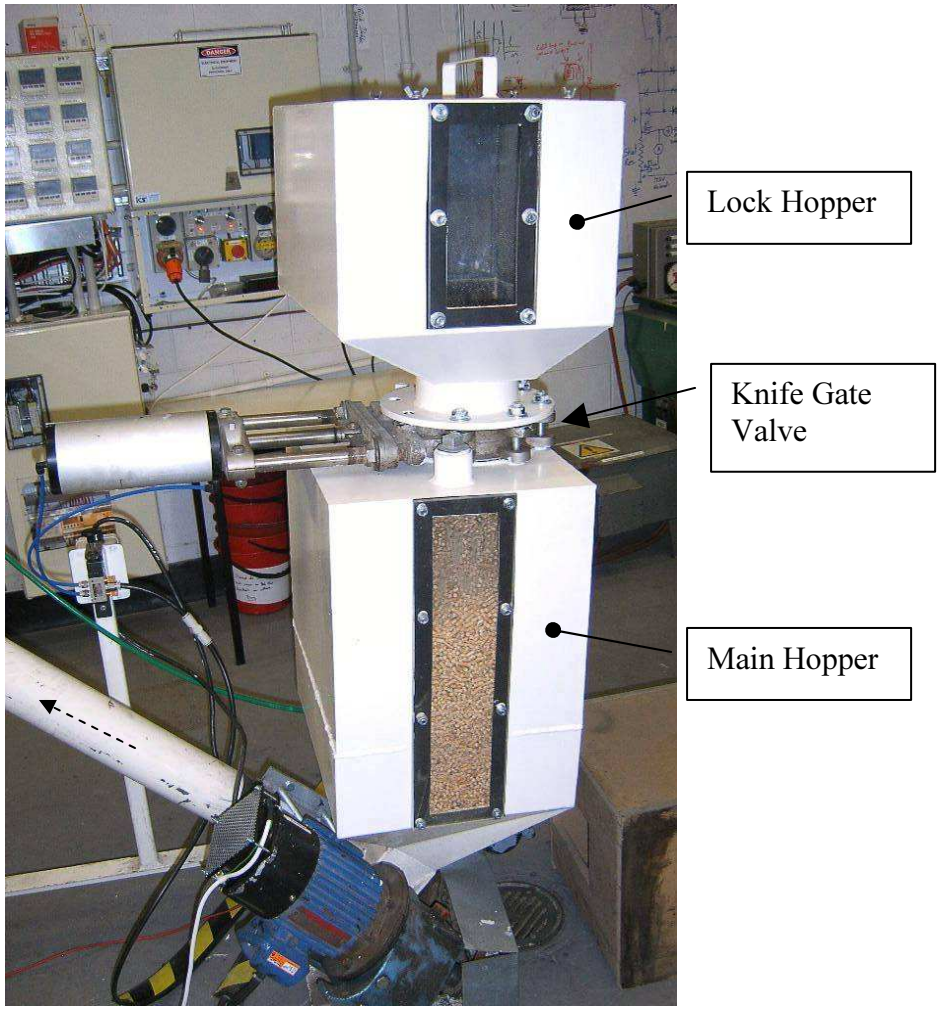

Figure 3.8: The final hopper set up for the 100 kW gasifier with top lock hopper, knife gate valve and clear sides installed on both hoppers.

Improvements were made to the existing ground mounted hopper (main hopper) also. This included the installation of a polycarbonate window so that the fuel level could be easily observed from the adjacent control room. This served a secondary purpose of providing an access point to empty the hoppers and inspect the auger flighting when empty.

The hoppers were constructed from mild steel to minimise materials costs. The top lock hopper was designed to contain a 20 kg bag of wood pellets with the angle of repose taken into account during filling pellets into the hopper. All hoppers were designed with sloping bases so that material flowed down them with minimal hold-up. This increased the height of the hoppers which had to be considered with respect to the ability of plant operators to pour fresh pellets into the feed system.

For ease of operation, the lock hopper was designed with no tools being required to routinely fill hoppers. This was achieved through using wing-nuts to fasten components which were routinely removed and providing handles on components. To create a seal between the main hopper and the top lock hopper, a knife gate valve was selected. This was chosen amongst a range of other types of valves because it created an adequate seal, could be automated, and had the ability of cut through pellets if the main hopper was overfilled. It also had a compact flat shape preventing the lock hopper from being mounted too high. The knife gate valve was installed with the larger diameter opening facing downwards, so there was no ledge for material to build up on which would hamper the valve closing. All operation with the gasifier to date has confirmed that the fuel storage system works outstandingly. This style of set up would be encouraged for other plants in the future.

3.1.10 Flue Gas Particle Trap Redesign

During preliminary gasifier hot tests in 2006, extensive running problems were occurring with the plant. A particle trap had been fitted to the gasifier to catch particles entrained in the flue gas line that were not removed and re-circulated by the flue gas cyclone. The original particle trap was not effective at catching the majority of the particles entering, which were routinely at temperatures as high as 800 °C. The flue gas was discharged downwards into an open rectangular box, but much of the material that entered into the particle trap during periods of siphon blockages, bounced back out into the laboratory with the high air currents. Because of the safety concerns with the possibility of hot sand and char particles spraying into the laboratory, this component was redesigned.

The space constraints limited changing the flue gas exit location so a specially shaped particle trap was designed as a replacement. The amount of space the particle trap occupied on the upper platform around the gasifier was minimised by keeping the particle trap dimensions minimised. The design of the particle trap is shown in Figure 3.9.

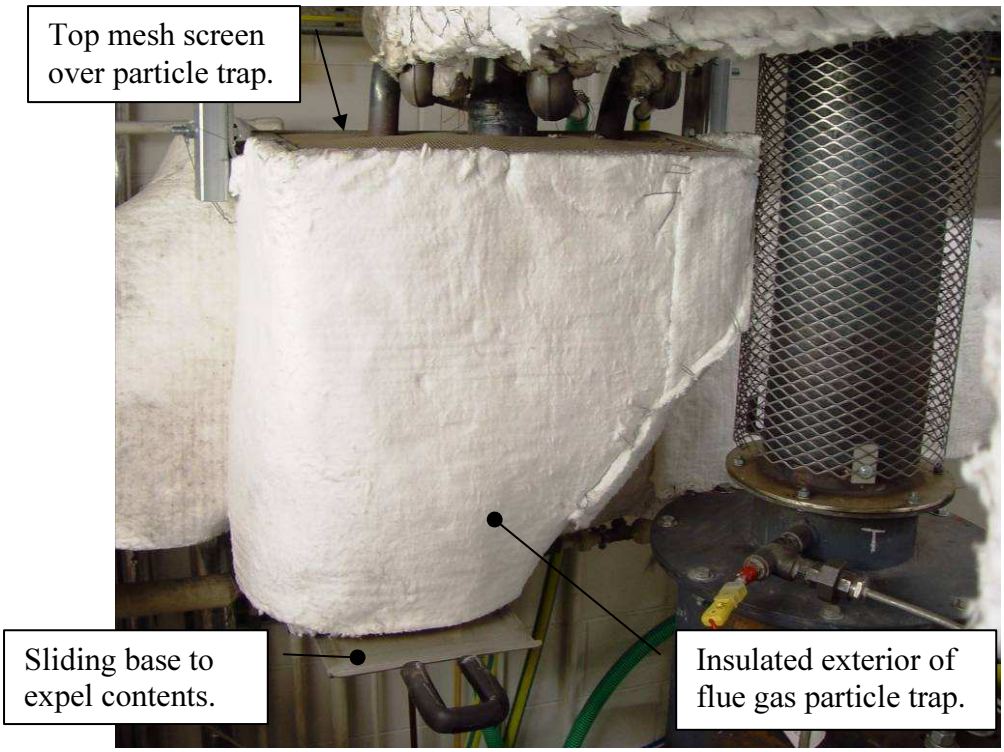

Figure 3.9: The flue gas particle trap fitted to the gasifier. The heat exchanger tubes which are directed downward through the top mesh introduce flue gas into the unit.

Firstly the depth and cross sectional area of the particle trap was increased to reduce the superficial velocity of gas rising out of the unit. Both the cross sectional area and the depth of the new particle trap were made approximately twice the dimensions of the original box. To dissipate the channels of flue gas exiting from the three outlets of the heat exchanger tubes, an internal baffle was installed, constructed from stainless steel mesh. A similar mesh screen was also fitted over the top of the particle trap so that the gas vented into a mesh envelope preventing the possibility of any hot glowing char particles bouncing out.

The flue gas particle trap was constructed from stainless steel because of its lower emissivity reducing the amount of radiant heat that the unit could transfer to the surrounding equipment. Both the rear of the unit and one side were inclined to clear the steam pipes fitted to the lab wall and the afterburner respectively. The inclined sides helped to direct any particles to collect at the discharge point at the base. A sliding plate was designed into the base of the particle trap which was made narrow enough so that the bed material could flow into a standard sized metal bucket. A sliding tray at the base of the particle trap was selected over the original hinged flap style of base because the latter did not create a good seal as learned from the previous unit.

Once fitted, the particle trap was insulated with kaowool glass fibre. This design is not likely to suit a larger scale plant in the future as the arrangement of equipment in the lab was the driving factor for its atypical design.

3.1.11 Design of a new Auger Feed System for the Gasifier

Current Feed System Set up

The FICFB gasifier was originally designed and built with an inclined feed port mounted about half way up the gasification reactor. Biomass travelled up the main auger from the ground mounted hopper and fell under gravity down the inclined feed pipe onto the surface of the BFB. This can be seen in Figure 3.10.

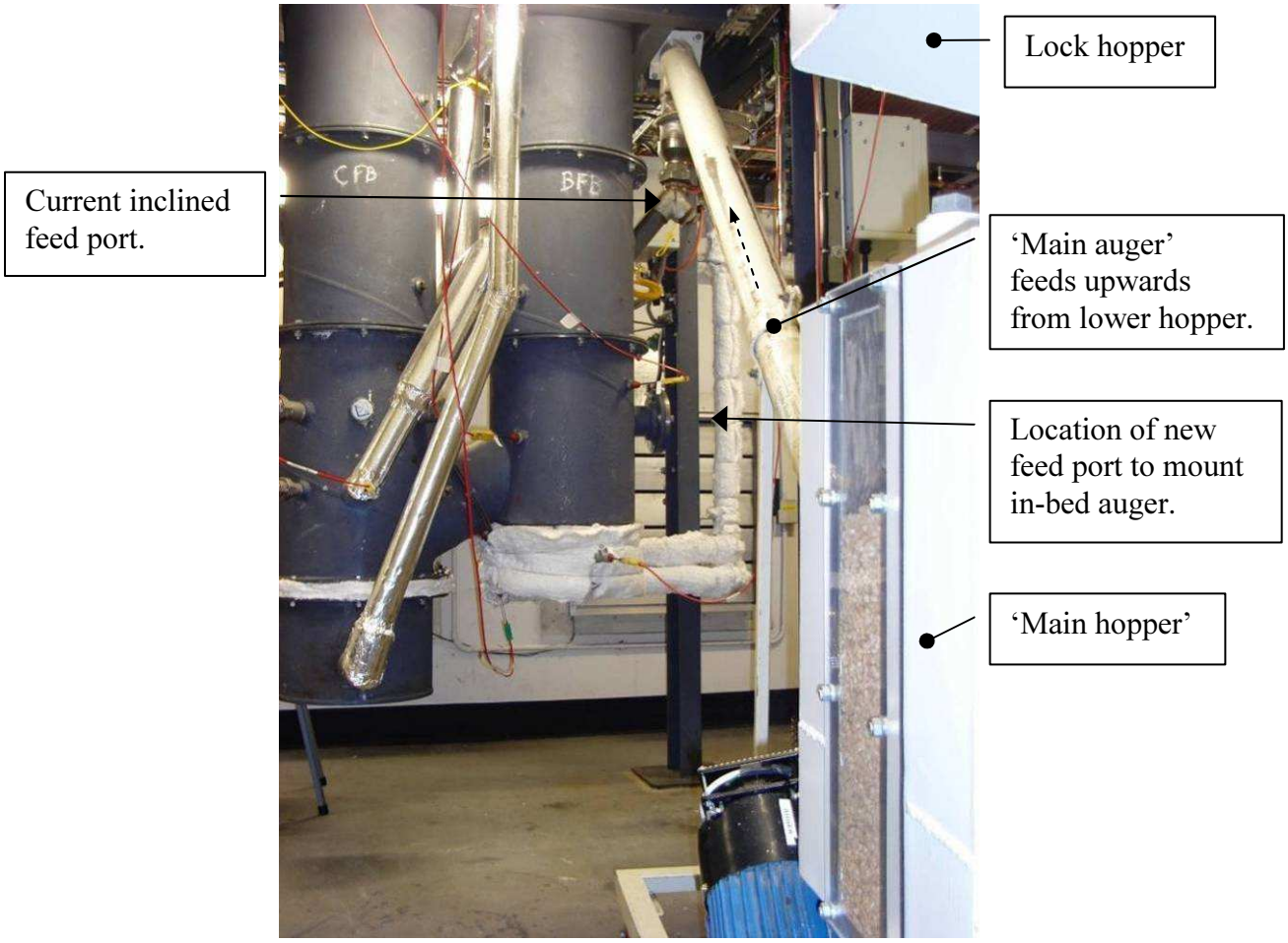

Figure 3.10: The original feed system set up for the laboratory scale FICFB gasifier at the University of Canterbury.

During the latter stage of building the gasifier, it was realised that the adopted feed system arrangement was not common place with other biomass gasifiers. Normally the biomass is

fed directly into the fluidised bed, not passed into the freeboard region of the reactor. The reasons for feeding biomass directly into the fluidized bed material is to rapidly heat the fuel particles so that the pyrolysis and char-gasification reactions occur more simultaneously inside the fuel particle pores, rather than the pyrolysis gases creating a halo around the outside of the fuel particle. This is explained in Section 2.1.3 and shown in Figure 2.7. A faster heating rate reduces the quantity of tars generated (Brown, 2003). Feeding directly into the hot bed material of the BFB, is likely to increase the residence time for the pyrolysis gas and tars generated, which should further improve the gas composition.

New Fuel Feed System Concept

During the latter stages of the gasifier's construction in 2006, design of a new feed system began. Space constraints were a major issue influencing the layout of the new system. The concept chosen was to use two augers with an intermediate hopper all operated in series. The original inclined 'main auger' would be repositioned to feed fuel into the 'intermediate hopper' mounted above the 'in-bed auger'. The in-bed auger was designed to insert into an existing 80 mm diameter port on the side of the gasification reactor. This limited the internal size of the auger flighting. The new feed system concept can be seen in Figure 3.11 and 3.12.

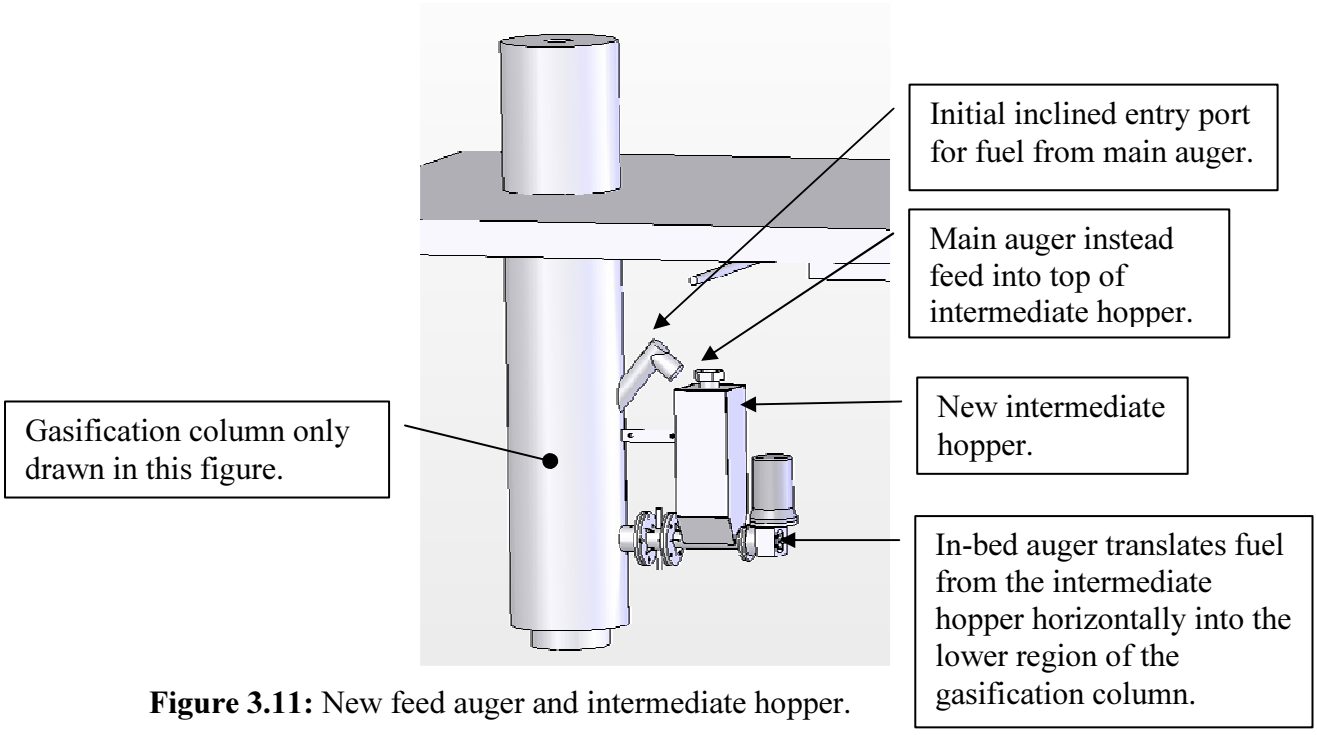

Figure 3.11: New feed auger and intermediate hopper.

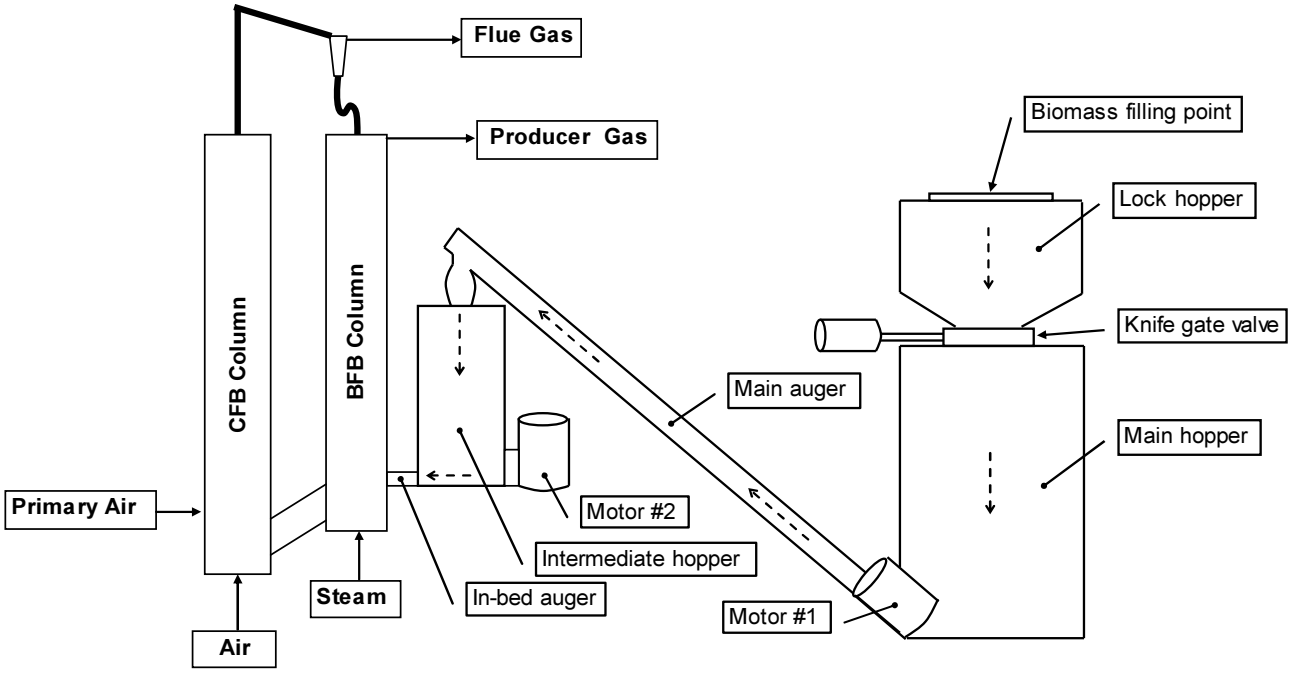

Figure 3.12: The layout of the new biomass feed system with three hoppers and two augers.

Intended Mode of Operation

The gasifier feed system needed to be designed for feed rates of 15-25 kg/h of wood pellets having a bulk density range of 500-670 kg/m^3. The system needed to be flexible so that other feedstocks such as wood chips could be conveyed. The worst case scenario was identified as the gasifier consuming coarse wood chips with a bulk density of 110 kg/m^3, sourced from a local sawmill. Hence, the in-bed auger needed to be capable of different rotational speeds so that a range of feedstock types and different fuelling rates could be conveyed. A variable speed drive was installed, and a motor size and gearbox ratio were identified for the necessary torque levels and speed ranges. This is shown in Appendix B.

The proposed operation of the feed system is as follows (refer to Figure 3.12). Fuel is poured into the lock hopper with the knife gate valve closed to prevent the loss of positive pressure supplied by the nitrogen purge gas into the main hopper. Once the lock hopper is loaded, the top lid is replaced and the lock hopper contents are expelled through the knife gate valve into the main hopper. Fuel is fed up the main auger and falls into the intermediate hopper. The main auger is operated intermittently to ensure the intermediate hopper always contains adequate fuel. This is achieved by regularly running the main auger on a set time period. A vibrating fork type sensor is mounted in the upper region of the intermediate hopper to act as a cut out switch for the main auger when the intermediate hopper is full.

The in-bed auger is controlled by the plant operator where the speed can be varied through a second variable speed drive (VSD). The main auger's role is to simply maintain fuel in the intermediate hopper. Fuel from the intermediate hopper is translated horizontally via the in-bed auger into the base of the gasification reactor. (Note: this system has been constructed but is still to be installed and trialled).

Detailed Design of the In-bed Auger

Stainless steel was the material used to construct the in-bed auger and the intermediate hopper. Stainless steel was chosen because of its corrosion resistance, especially in the aggressive environment in the gasification reactor, and because it has a lower thermal conductivity than mild steel. Stainless steel has an approximate thermal conductivity of 19 W/mK, compared to mild steel at 47 W/mK both at a reference temperature of 225 °C (The Engineering Toolbox).

The generation of tars in the auger was a concern because they could encourage fuel binding in the auger flighting. Another concern was the wood pellets expanding in the auger from the moist, high temperature environment. To allow for this, a water jacket was designed into the outer housing of the auger to remove excess heat. By controlling the water flow the heat transferring through the auger casing can be controlled. The last 30 mm section of the auger was designed with an outwardly tapered inner housing so that as the wood pellets expand in the hot, humid environment near the end of the auger they were less likely to jam. The in-bed auger is shown in Figure 3.13 with two concentric tubes forming the water jacket at the end that inserts into the gasifier.

So that steam used in the gasifier does not expand the wood pellets while the plant sits idle, wood feed should always occur before the steam is injected during start-up. The steam should also be turned off before the wood feed is stopped during shut-down.

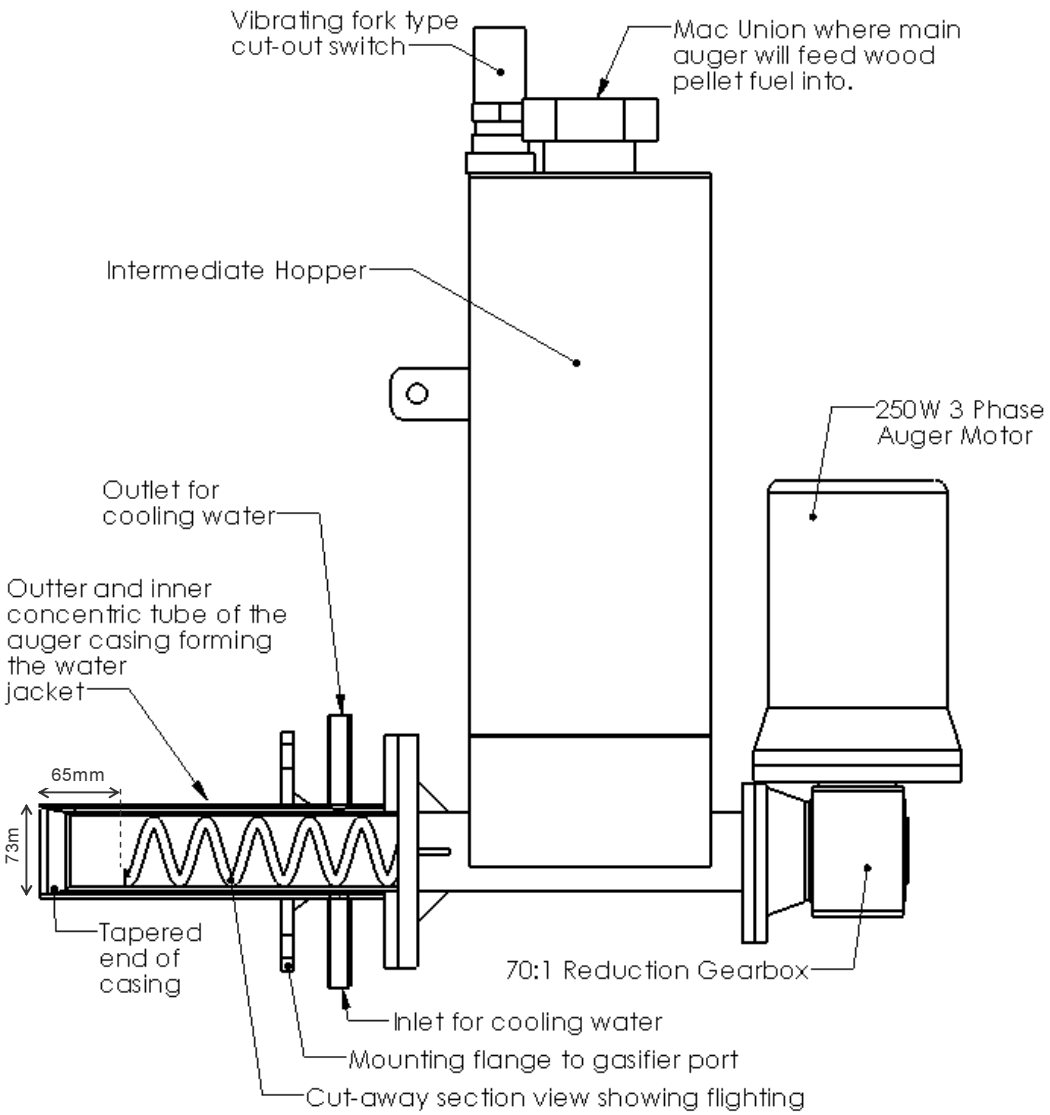

Figure 3.13: The in-bed auger with cut-away final section showing flighting and water jacket.

Some other gasifiers, especially in Denmark are designed for the pyrolysis reactions to occur in the fuel feed auger so that the char-gasification reactions and the gas-phase reactions are partly or fully separated from the pyrolysis reactions. This means that tars are generated early and their residence time in the hot environment of the reactor is increased. However, this may cause more total tars to be generated due to slower heating rates being present and lower overall pyrolysis temperatures, so requires further analysis. This mode of operation could also be trialled in the gasifier at the University of Canterbury where the cooling water can be turned off. Future experiments on the gasifier need to investigate this pre-pyrolysis option when this new auger is put into service.

A centre-less flighting was selected over a centre-shaft flighting to maximise the volume for the fuel amongst the auger flighting, since it had to fit within the 80 mm diameter port on the gasification reactor. Since the auger flighting is operating in a push-type arrangement with the motor at the opposite end to the direction of feed, there is the risk that a jam could cause the flighting to unwind and jam even tighter in the housing. An aluminium key is fitted to the auger flighting but additionally a torque cut-out device could be installed on the auger motor. If deformation of the flighting occurs, it may be necessary to weld a centre-shaft onto the flighting to provide it more rigidity and tolerate any constraint on fuel size that can be conveyed.

Preventing the backflow of producer gas and heat along the auger into the intermediate hopper was a concern. To prevent the backflow of producer gas, a nitrogen purge currently set at 12 L/min on the existing feed system would be maintained. This provides positive pressure throughout the feed system so that the net flow of gas is into the gasifier with the fuel. Hence any pyrolysis gases that are generated in the auger pass into the gasifier.

Other factors used to prevent the backflow of producer gas included having a long feed system with many stages of hopper. The auger was also designed with a high degree of packing of the wood pellets amongst the flighting. The auger flighting extends along the full width of the intermediate hopper's base, which has inclined sides to channel wood pellets into the flighting. Tapering the auger casing and flighting, in addition to varying the pitch of the flighting were all considered, but this added complexity and increased the likelihood of jams occurring. After the auger was constructed it was tested on the laboratory bench. The packing factor of wood pellets amongst the auger flighting, created by the void spaces amongst the pellets was determined to be about 65 %, as estimated in the design.

In addition to cooling the outside of the auger casing to stop the wood pellets pyrolysing, the auger flighting was stopped 65 mm short of the end of the outer casing. This is indicated in Figure 3.13. It was hoped a plug/billet of wood fuel would form at the end of the auger to minimise heat transfer back along the unit. Trials showed that a plug/billet did form when there was some resistance to the medium the auger fed into. It is unclear if the fluidised bed environment will create enough resistance for this billet to form as intended.

Motor and Gearbox Selection

A 250W three phase 240V induction motor was installed and wired into a variable speed drive. A three phase motor was chosen because of its ability to deliver more torque than a single phase motor for a given size. A 70:1 reduction gearbox was fitted between the motor and auger flighting so that the motor could be operated in the range of 20-75 Hz. The gearbox was specifically chosen because this ratio allowed the highest bulk density fuel, (wood pellets) to be fed at a motor speed of 22Hz, while the lowest bulk density wood chips likely to be used required a motor speed of 83Hz. This was within the optimum frequency range of the motor for the fuel types envisaged. Running the motor below 20Hz was avoided because of its likelihood to overheat at low speeds.

Sizing the Intermediate Hopper

The intention was to size the intermediate hopper to hold five minutes of the least dense fuel likely to be used. This was coarse wood chips with a bulk density of 113 kg/m^3. The surrounding equipment placed height restraints on the hopper so the final dimensions chosen were a breadth of 180 mm, width of 200 mm wide and height of 430 mm. This gave a total storage volume of 0.015 m^3. For wood pellets these dimensions mean that there is about 30 minutes of fuel supply when 20 kg/h are conveyed. However the main auger will be set to operate on a four minute cycle to keep an adequate amount of fuel in the intermediate hopper despite what bulk density fuel is used.

3.1.12 Absorption Spray Column Design

Another postgraduate (Gershom Mwandila) on the gasifier project is studying secondary gas cleaning systems and hoping to integrate an absorber-stripper system to the gasifier. Gershom outlined the concept for an absorption column that he wanted to construct and the detailed design work and CAD drawings were carried out on his behalf. This apparatus is likely to use a slip-stream of the producer gas so the effectiveness of tar removal can be studied as part of his PhD work.

The final unit can be seen in Figure 3.14. The column was constructed from stainless steel to resist corrosion. View ports were placed in the lower region and one on the top plate so that the solvent level and the spray pattern could be observed. The column was designed for maximum operating flexibility with two different modes possible. The first mode was for tar-

carrying gas to enter at the bottom of the column where the producer gas bubbles through the solvent and then rises up the column against a counter-flowing mist of solvent. Alternatively, the liquid level in the base of the column could be lowered below the gas entry point so that tar was solely removed by the counter-flowing mist of solvent.

Figure 3.14: The absorption column designed to investigate secondary gas cleaning methods for tar removal from producer gas.

3.1.13 Producer Gas Flow Rate Measurement

The gasifier required a method to measure the output rate of the producer gas. Most equipment to measure the flow rate of gases was unsuitable because of the high temperature environment and the presence of condensable tars in the gas. The main instruments considered included: venturies, pitot tubes, rotameters and orifice plates. An orifice plate appeared best but had the limitation that it requires a straight section of pipe so that it receives laminar gas flow. This was not possible due to the arrangement and spatial constraints around the plant. Additionally an orifice plate could cause excessive back pressure in the gasification reactor encouraging producer gas to pass into the combustion column via the chute, or through the siphon and out with the flue gas.

The method chosen to determine the flue gas flow rate was suggested by Dr. Bram van der Drift of the Energy research Centre of the Netherlands (ECN), where a measured amount of tracer gas (helium) is injected into the producer gas stream and its concentration is measured further down the gas path with the existing producer gas sampling equipment. The helium acts as a tie component since it remains unreacted amongst the producer gas. This is displayed in Figure 3.15 where the gas sample is obtained after the producer gas cyclone to ensure adequate mixing of the gases has occurred. A helium mass balance was performed to determine the total mass flow rate of producer gas. These calculations are shown in Appendix C.

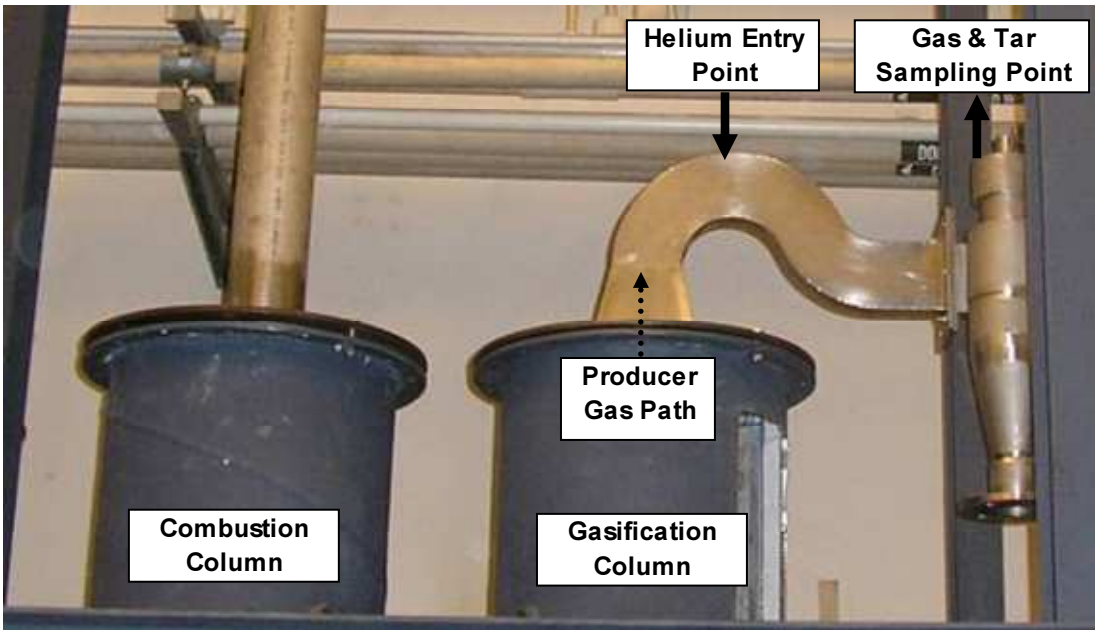

Figure 3.15: Photo of the reactors showing the helium entry and sampling points.

3.1.14 Modifications to the Gas and Tar Sampling System

Approximately 12 hot runs had occurred with the gasifier in 2007. None of these hot runs provided good gas and tar data because the sample collection techniques and measuring equipment were very problematic. Operation of the gasifier during 2007 continued to identify further improvements that were necessary just to get the plant operating in a stable manner. Finally by late 2007, reliability of the gasifier was satisfactory, but the gas and tar sampling equipment remained troublesome.

The original producer gas sampling set up is shown in Figure 3.16. This method was used because it aligned with the IEA tar sampling protocol for biomass gasification systems. It works by passing a slip stream of producer gas through a number of flasks containing a solvent such as isopropyl alcohol (IPA). Tars collect in the IPA while the cleaned producer gas continues through a pump to a micro gas chromatograph (micro GC) for analysis. Tars are evaporated from within the solvent in a fume cupboard and usually analysed by GC-FID (Gas Chromatograph-Flame Ionisation Detection).

When the sampling system was first set up a tee was installed to draw a slip stream of producer gas through solid phase extraction (SPE) columns. This method is easier to perform because the tars are collected on an intermediate solid phase eliminating the hassles of handling solvent trains. The original intention was to set up both methods and compare their results. However, the solvent train method was too problematic and time consuming to contend with, and blockages regularly occurred due to tar condensing out in the sampling lines. Hence representative samples were not being collected.

After many changes to the numbers and orders of wash bottles, it became obvious that the sampling set up was not suitable for the intended research regime planned. The impinger trains took too long to set up, were temperamental to operate and took too long to clean up. The gasifier at the University of Canterbury was still at small scale and only operated intermittently, and the IEA tar sampling method was unsuitable for the rapid successive sampling that was required.

Since the effect of changing operating parameters was going to be studied, a fast reliable method of sampling both tars and producer gas was required. The need for a fast reading was critical because each gasifier hot run usually took ten to eleven hours from heat up to shut down. Warming the plant up to 750 °C took five to six hours because of the high thermal mass of the refractory and other components. The plant needed to be cooled down to about 500 °C before it was considered safe for operators to leave the laboratory for the night. So there was only about a three hour window to carry out all the gasification tests for that day. The IEA tar sampling method appeared to be more aimed at demonstration scale plants that operated in a continuous manner where a single sample was taken over many hours.

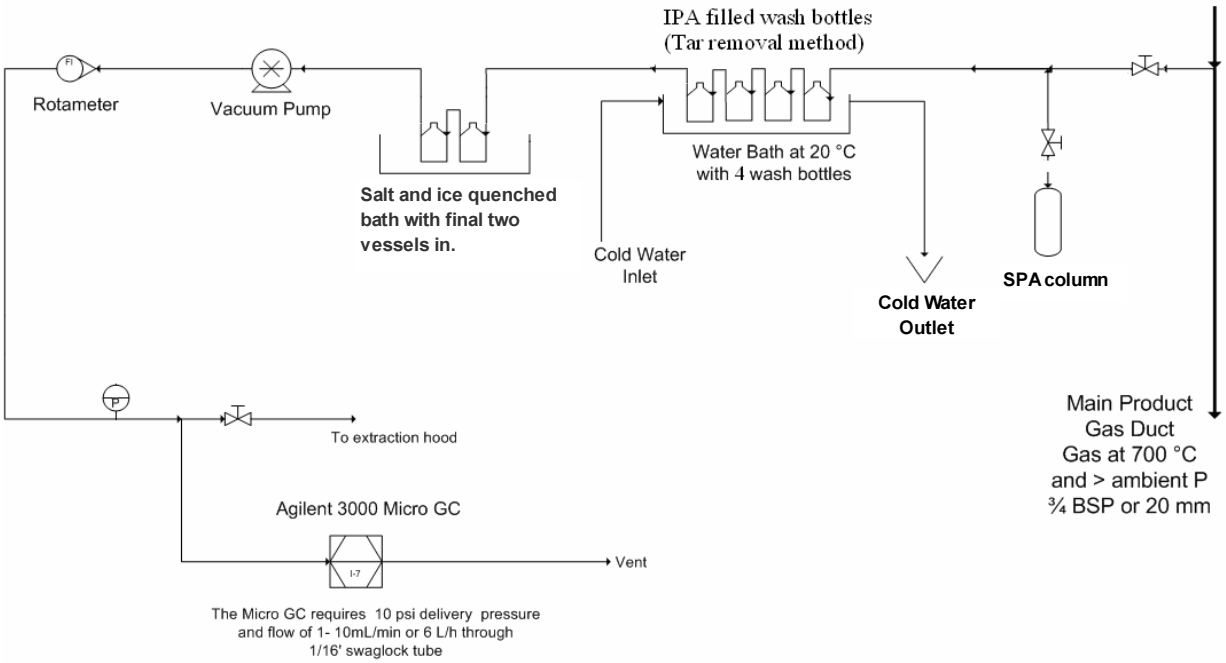

Figure 3.16: Original gas and tar sampling set up with IPA wash bottles and SPE column junction in the sampling line.

The original tar and gas sampling system with wash bottles, took over one hour just to displace the air out of the redundant space in the flasks, before the producer gas sample even reached the microGC! So the time delays were unacceptable and did not allow the operating conditions of the plant to closely correspond with the samples being taken.

In late 2007, the SPE column tar sampling system was further developed and adopted in place of the wash bottle system. A new sampling port is installed directly into the outlet of the producer gas cyclone to minimise the presence of particles. This sampling point is kept short so that temperatures in the sampling line are well above 100 °C, preventing moisture condensing. The temperature of the gas stream being drawn from the cyclone into the sampling equipment is initially 650 °C, but cools down to ambient temperature as it passes through the SPE column and moisture trap. The sampling valve with SPE column connected is shown in Figure 3.17.

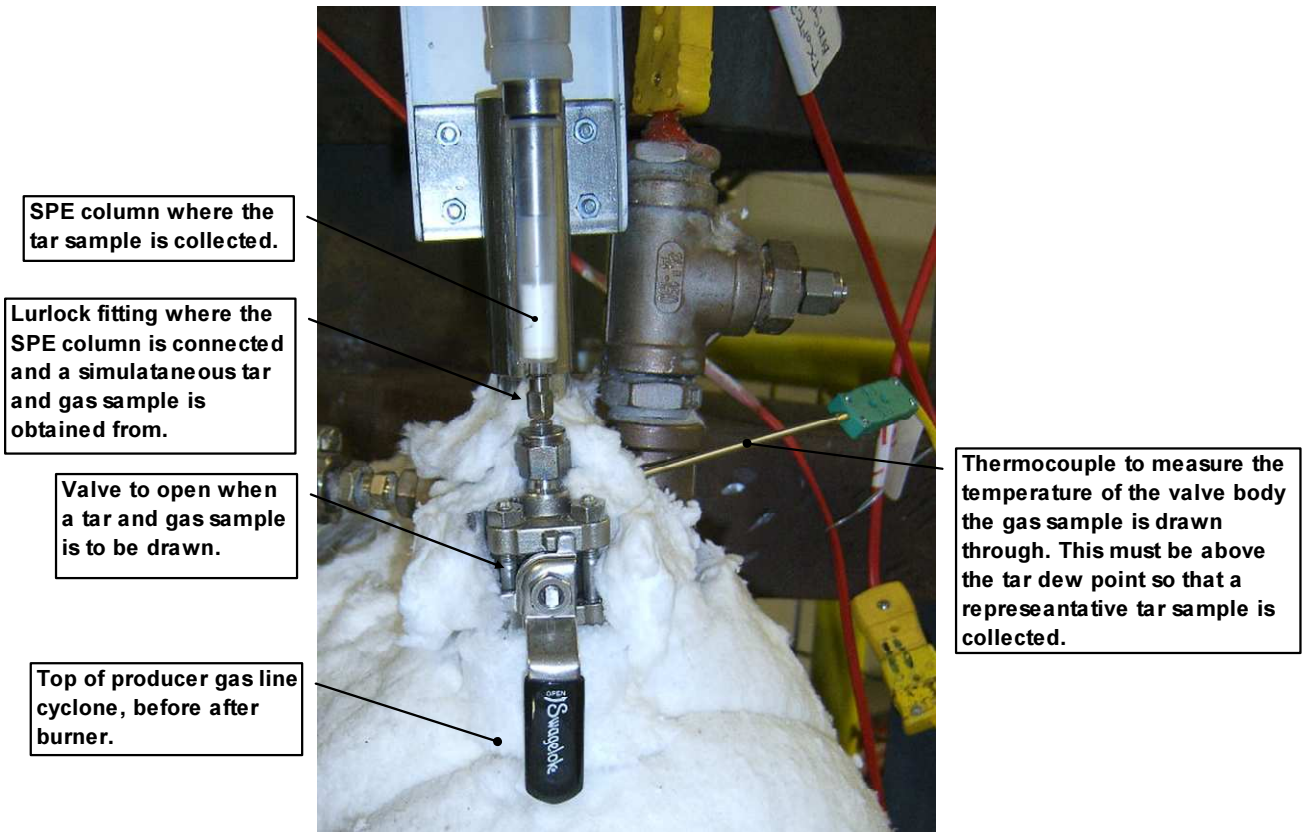

Figure 3.17: New tar and gas sampling point with sampling syringe apparatus fitted.

So that good quality graphs could be plotted, 8-10 data points were aimed at being obtained for each variable being studied during the hot testing regime planned. This meant only 18-23 minutes was available to change the plant settings, wait for steady state conditions to be reached, and take measurements. In addition to this, the two plant operators had to continually monitor the gasifier, record data and intervene with other settings when required to maintain stable operation.

To achieve these sampling requirements a new system was also developed where a simultaneous tar and producer gas sample could be rapidly obtained. A 100 ml volume of producer gas was drawn into a glass syringe, first through an SPE column and then through a moisture trap containing silica gel. The tar sample is collected in the SPE column which is capped to prevent evaporation of any tar components. The gas sample is passed out of the glass syringe and into a plastic syringe which gets connected up to a micro GC to determine the producer gas composition. Injecting the producer gas sample into one of many plastic syringes, means that the glass sampling syringe is available to draw another sample, irrespective of how long the microGC needs to complete its analysis. This sampling

technique meant that simultaneous producer gas and tar samples could be successively obtained only minutes apart.

The in-line moisture trap was used to prevent water vapour being present in the syringes which would fill the pores on the molecular sieve column in the microGC. The new sampling system is shown in Figure 3.18.

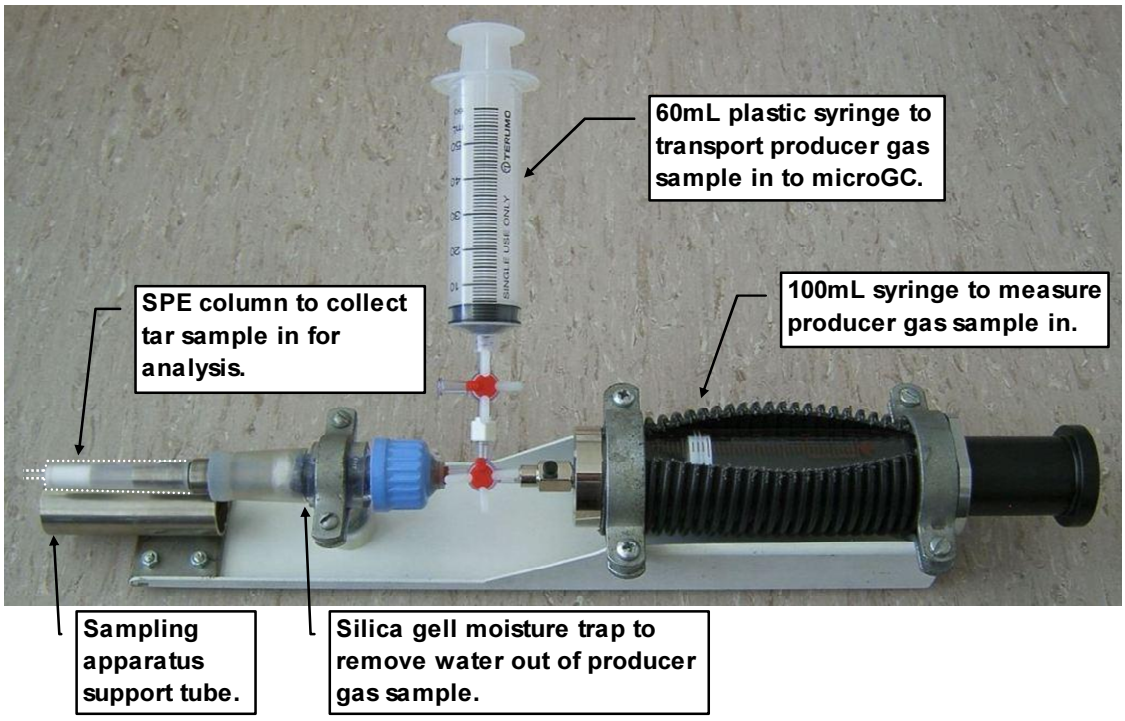

Figure 3.18: Set up of tar and gas sampling hand piece containing: an SPE column to collect tars, a moisture trap to remove water, a 100ml syringe to collect a dry producer gas sample in, and a 60ml plastic syringe to transport a producer gas sample in to the microGC.

3.2 Future Modifications to Consider for the 100 kW Gasifier

3.2.1 Moisture Measurement in the Producer Gas

The 100 kW gasifier at the University of Canterbury requires a direct method to determine the moisture content of the producer gas. This was one of the important parameters needing to be regularly measured, but it is difficult to perform because the producer gas is at high temperatures, commonly 650-700 °C. Since plant operating parameters are often varied regularly during a test, the method to determine the water content should be easy and fast to perform, as many different operating conditions commonly have to be assessed in a three hour period.

Changing parameters such as the steam to biomass ratio have a large influence on the moisture content of the producer gas as explained in Section 2.2.3. Many methods to measure the moisture content were investigated but the high temperatures and presence of tars in the producer gas prohibits the use of standard instrumentation. After extensive searching the MAC 125 high temperature moisture analyser is believed to be suitable. The moisture content is calculated from the ratio of the partial and total pressures of the water vapour in the hot gas stream.

3.2.2 Separation of the Siphon Exit and Producer Gas Line

To further reduce bed material losses out of the gasifier, the siphon exit and entrance of the producer gas line need to be separated by a greater distance. Particles are being entrained out with the producer gas. The first way to accomplish this is by removing the 90° bend fitted below the siphon exit so that the sand drops vertically into the gasification reactor. Currently the bed material is directed horizontally into the reactor wall near the entrance to the producer gas line. This configuration reduces the freeboard height between the siphon exit and the producer gas line entrance to about 200 mm. The plant was originally designed like this because it was hoped that the 90° bend would direct the hot incoming bed material over the freshly introduced wood pellets conveyed into the reactor. However the sand tends to bounce back off the reactor wall so does not work as planned. This ricocheting nature of the particles increases their likelihood of getting entrained out of the out of the reactor, especially during the heating up period when pulses of high velocity gas rising up the column are frequent.

The second advantage with directing the sand vertically is that it might allow for the sand entering the gasification reactor to be viewed through the eye glass installed on the gasification column. This would provide operators of the plant another method to visually check whether the gasifier is circulating adequately, in addition to the eye glass on the standpipe.

In any future FICFB gasifier being designed, the siphon should discharge lower down into the gasification reactor than occurs in the 100 kW plant at the University of Canterbury. A suitable freeboard height needs to exist above the entry point of any particles, to allow particles to efficiently drop out of the rising producer gas stream. It appears better to design a FICFB gasifier so that bed material from the siphon enters part way down the side of the gasification reactor rather than being introduced into the top of the reactor near the gas outlet.

3.2.3 Alternative Air and Steam Fluidization in the Siphon

This is a design change that has been identified from the hot testing performed on the gasifier during 2008. The siphon fluidizing set up needs to be modified so that air fluidization can be used during the heat-up and cool down stages of operation, with steam fluidization during the gasification process. As explained in Section 3.1.3, the siphon was converted over to air fluidization in place of steam fluidization for the three stages of plant operation (heat-up, gasification and cool down). Steam was originally used but condensed and caused the bed material to clump, creating blockages in the siphon at low bed material temperatures. The current problem is that siphon temperatures are getting too high. This is due to the high temperature bed material passing through the siphon from the combustion column, plus the additional heat generated from combustion of char in the siphon itself, due to the fluidizing air introduced. This is a problem because the fusion risk is increased and it creates excessive temperatures (840 °C plus) in the stainless steel siphon.

A new steam flow meter and piping have been ordered so that improved siphon fluidizing apparatus can be installed. The new set up will allow air to be used during the heat-up and cool down stages of plant operation, but steam will be used during the gasification process. This will help to moderate siphon temperatures, reduce the heat generated from combusting char in the siphon, and will reduce the amount of nitrogen entering the gasification reactor. A small amount of combustion will still occur in the siphon, because the standpipe air (shown in

Figure 3.3), will be maintained for practical reasons. This flow rate is so small (4-5 L/min) that the combustion heat and any introduced nitrogen should be tolerable.

3.2.4 Increasing CFB Bed Depth to Increase Residence Time

A problem with the gasifier at the University of Canterbury is that it does not generate enough heat in the combustion reactor to maintain gasification temperatures above about 700 °C without supplementary firing of LPG. Heat losses occur during circulation of the bed material and further heat losses occur with the large quantities of entraining air and flue gas exiting the combustion column. As a result more heat needs to be generated in the combustion column so that gasification temperatures can be increased. This problem can be addressed in one of two ways assuming heat losses are minimised and heat recovery is maximised:

1. Greater quantities of hot bed material could be circulated at the same temperature, or
2. Hotter bed material could be circulated at the original rate.

Circulating greater quantities of bed material requires more blower energy and may reduce the residence times for the pyrolysis reactions in the gasification column, likely affecting the gas yield. The cyclones also have limitations on the gas flow rates they can handle, especially the flue gas cyclone which is relied upon to separate and pass hot bed material back into the siphon. However, hotter bed material could instead be circulated by generating more heat in the combustion reactor relative to the thermal energy requirements of the gasification reactions. This could be accomplished in a number of ways assuming heat losses have been minimised and heat recovery maximised.

More fuel could be combusted by installing a second auger to feed wood directly into the combustion column. The supplementary firing in the combustion column could be increased using LPG or natural gas, but this is not desirable if the intention is to only consume renewable fuels. The reflux rate of bed material and char could be increased in the combustion column by designing a diffusing taper into the combustion chamber as described in Section 2.8.1, but this requires major reconstruction work and may reduce the entrainment efficiency.

The most practical method appears to be improving the heat generation in the combustion reactor by increasing char residence times in the CFB. It is believed that this can be achieved by raising the elevation at which the primary air is introduced into the combustion reactor. This should allow a deeper fluidized bed to exist in the base of the combustion reactor in the hope that more char will be present per unit time generating heat. Increasing the bed depth in the lower part of the CFB is a relatively easy task as spare jets are already fitted 190 mm higher up on the combustion column, and the primary air can be re-directed into these jets.

3.2.5 Producer Gas Cyclone Particle Trap Modification

A better method of containing and discharging the particles from the producer gas cyclone is required. The producer gas cyclone particle trap is mounted at the base of the BFB cyclone part way along the producer gas line. See Figure D1 of Appendix D. This unit needs to be modified so that it is easier to empty, and can be emptied during hot operation. The current system is a cylindrical chamber with a flat top and base, and a narrow neck. Material does not flow out of it easily when unbolted and inverted. Often the ash binds to the chamber walls and the high temperature surfaces mean it cannot be emptied on the run. The particle trap is emptied and its contents weighed after every period of hot operation, so procedure needs to be easy to perform. Due to the fixed volume of the particle trap, the gasifier should not be operated longer than approximately 12-14hours or the particle trap may overfill.

The best concept identified for the 100 kW plant is to collect the ash in a large diameter metal tube which can run down a pillar below the cyclone. Two valves could be placed along the tube such that ash collects in the top chamber above the first valve, and periodically this charge of ash could be dropped into the intermediate space between the upper and lower valves. When the top valve is closed off, the bottom valve could be opened to discharge the slug of ash into a metal bin. This way no open passage is ever created for the producer gas to exit via, and emptying ash during hot operation of the gasifier would be possible.

3.2.6 Diffuser Redesign

The current problem with the fluidizing diffusers fitted to the base of both reactor columns is that sand drains through the nozzles and accumulates inside the distributor requiring regular dismantling and emptying. It is predicted that much of the sand flows into the diffuser when

the plant is shut down or being filled with bed material as there is no counter-flowing gas back through them.

The diffusers were designed by Mr Rick Dobbs who drew on his past experience with designing fluidized bed reactors. Rick has learned that LPG and air needs to be premixed before entering a fluidized bed reactor because poor gas mixing occurs amongst the bed material, which is required for heating up the reactors. However, the premixing of air and LPG must occur close to the point of injection into the fluidized beds and not premixed in bulk beforehand, because the high reactor temperatures can cause the LPG and air charge to self-ignite inside a distributor. This is why the current distributors were designed with the air and LPG mixing in the nozzle tubes immediately before the charge is passed into the fluidized beds. This design works well, other than the problem with sand collecting inside the distributor chamber. This can be as much as 0.8 kg for an 11 hour period of plant operation.

In future FICFB gasifiers being built, the design of the distributors need close attention to prevent the backflow and accumulation of sand. Ideally, the distributors need to be designed so that they are self-clearing, where any back flowing bed material can be discharged back into the reactor with the flow of gas passing through.

3.2.7 Method to Drain Bed Material after Testing

Researchers routinely drain the bed material from the gasifier after each test run, measure the quantity of sand remaining, then replacing it plus additional bed material to make up for sand losses during the pervious operation. This ensures that the same quantity of bed material (normally 12 kg) is used each test run. The task of emptying the sand is very laborious, taking three to four hours to complete. With the additional tasks necessary between runs on the gasifier, one whole day of replenishment work is required, plus half a day of setting up the plant for each period of operation. Project progress would be much faster if the preparation time and replenishment time was reduced. Future FICFB gasifiers being built in research environments should be designed with a discharge system in the base of the reactor columns, or allowance should be made for rapid removal and replacement of the distributors, to reduce plant maintenance time.

3.2.8 Bed Material Lock Hopper for Adding Sand

During operation of the gasifier a significant amount of bed material is lost out the flue gas and the producer gas lines. Despite efforts to minimise this, a method to add bed material into the gasifier is required. This can not currently be done unless the plant is shut down and sand is poured in manually. The ability to change the bed loadings in the gasifier would allow this variable to be studied and residence times may be able to be improved. This concept is based on the principle that it takes each individual fuel particle longer on average to meter its way through a deeper fluidized bed.

Additional bed material could be introduced with the wood fuel feed, but a more direct method such as batch discharging the contents of a lock hopper would be more reliable. It would be most practical to discharge the fresh bed material into the gasification reactor rather than the combustion reactor, as it is at lower temperature and hot flue gas and entrained sand would not be directed up into the inclined discharge tube of the lock hopper. If the new auger feed system is installed and adopted, the existing inclined fuel feed port would serve as a good entry line for the lock hoppers contents. An inert purge gas could be introduced when the lock hopper is emptied to displace any flammable producer gas through a vent line for safety reasons.

3.2.9 Producer Gas Take-off Line for Engine

At some time in the future a take-off point will need to be installed on the gasifier to supply producer gas to secondary gas cleaning equipment and to fuel an engine. It is recommended that the afterburner be left in place and that this remains the most direct passage for the producer gas. The afterburner should be the default producer gas path and any engine and gas cleaning equipment installed should draw the necessary quantity of producer gas from this default path. Provided the engine is scaled so that it never tries to draw more gas than is generated, sufficient engine fuelling will occur. The suggested set up is shown in Figure 3.19.

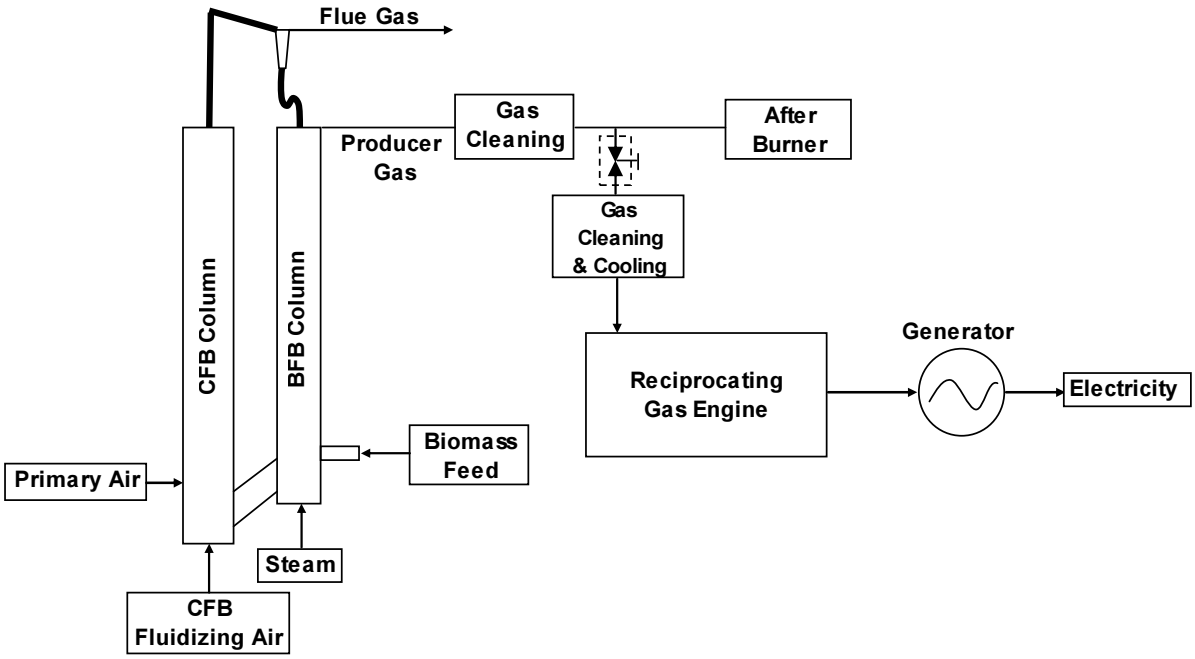

Figure 3.19: Suggested set up for the installation of secondary gas cleaning equipment and engine.

3.2.10 Chute Flow Modifications

During early operation of the gasifier when operators had limited knowledge of the particle dynamics of the bed material, the reliability of the chutes operation was questioned. Extensive cold testing proved that the chute was operating satisfactorily but improvements could be made. A sparger is used to fluidize the bed material in the chute to vary its flow rate. The current sparger is mounted too high along the base of the chute and has bent upwards due to thermal stresses. Literature sources identified this as a known problem and suggest installing a clamp to prevent a sparger from bending.

Ideally the sparger should be mounted as low as possible along the base of the chute so that the entire volume of sand above the sparger can be fluidized. The design of the sparger could also be improved to make it less obstructive to the flow of material through the chute. It could probably be integrated into the refractory base of the chute and a shorter chute could be used with a steeper incline to minimise the level of fluidizing gas required. (The current chute is inclined at 30°, is 500 mm long, with a cross-section 77 mm wide and 50 mm high). Some chute systems in similar applications control the flow rate of by having a gate valve or similar in the line to vary the cross sectional area. This could be considered in other gasifiers, but no change is necessary on the current 100 kW gasifier.

4.0 Experimental Procedure

4.1 Experimental Procedure followed for Cold Testing

4.1.1 Effect of Varying Parameters on the Bed Material Circulation Rate

The same procedure was used for all cold tests performed on the gasifier to study the circulation behaviour of the bed material. The aim of this study was for operators to gain an understanding of what effect different flow rates of gas supplied to various regions of the gasifier had on its circulation behaviour. The different variables tested are shown in Figure 4.1.

For the circulation-based cold tests, all the steam inputs used under hot conditions were changed over to air. This was to prevent the sand getting wet from condensing steam. Numerous manometers were fitted to measure the pressure at various regions in the gasifier.

To perform the cold tests, all the gas flow rates were set to the readings shown in Table 5.1, and then each of the test parameters was varied throughout a range. After each measurement, the variable being analysed was set back to its datum value shown in Table 5.1 before being adjusted to the next value. This was done to reduce experimental error and ensure that the plant operation was not being progressively influenced. Once steady state conditions were achieved (determined by many instruments all over the gasifier), a full set of experimental data was taken and recorded directly into a spreadsheet.

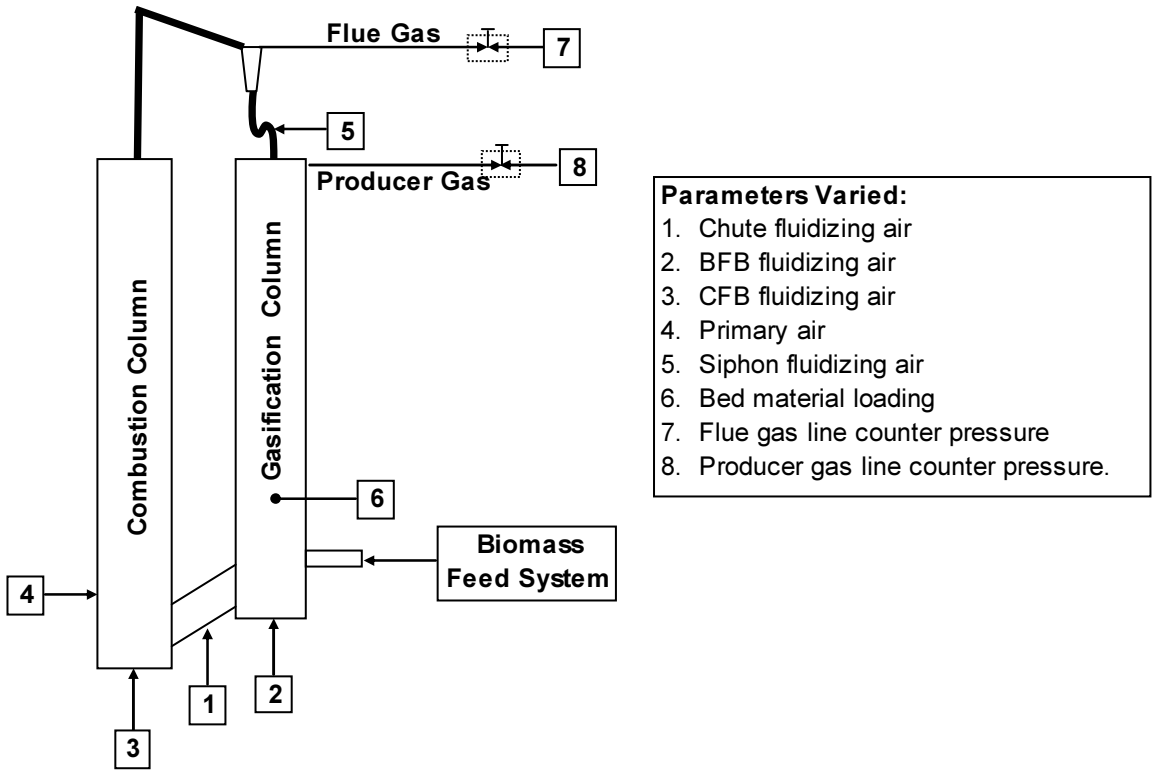

Figure 4.1: Eight different parameters including five different gas flow rates into the gasifier were studied in relation to their influence upon bed material circulation.

Circulation rate was measured by timing how long it took bed material to fill up the transparent standpipe section (see Figure 3.1) of known internal volume when the flow from the base of the standpipe was temporarily stopped. The flow was stopped by turning off the 4-5 L/min of fluidizing air passed into the base of the standpipe. Throughout this batch of tests, regularly shutting off the standpipe air was considered to have negligible influence on the rest of the gasifier since this flow rate was so low and in an isolated part of the circuit not associated with other plant operations.

After each cold test the distributors at the base of both reactors were removed and the sand loadings were measured and recorded. Additional view ports were installed to make several visual observations during the cold tests. The rest level of the surface of the fluidized beds was measured by lowering a plumb-bob down into both reactor columns, and measuring the length of the string. These measurements were approximations only as often the top of the fluidized beds did not settle horizontally.

4.1.2 Influx of air into the Gasification Column during Cold Testing

A mass balance around oxygen was performed to study the influx of air into the gasification column during cold testing. Through the induction and measurement of the flow rates of nitrogen, which were introduced in place of air at various points on the gasifier, data were collected for three different scenarios which allowed an iterative mass balance around oxygen to be solved. Figure 4.1 shows the injection points of the nitrogen/air with the control volume for the analysis being the rectangular gasification reactor. The mass balance spreadsheet can be seen in Appendix E.

The three scenarios are shown below:

1. Nitrogen in place of steam/air in the chute as the chute fluidizing gas. Nitrogen in place of air as the siphon fluidizing gas and nitrogen in place of steam/air to fluidized the BFB.
2. Nitrogen in place of steam/air in the chute and BFB distributor, with air used as the siphon fluidizing gas.
3. Nitrogen in place of air in to fluidize the BFB. Air used to fluidize the chute and siphon.

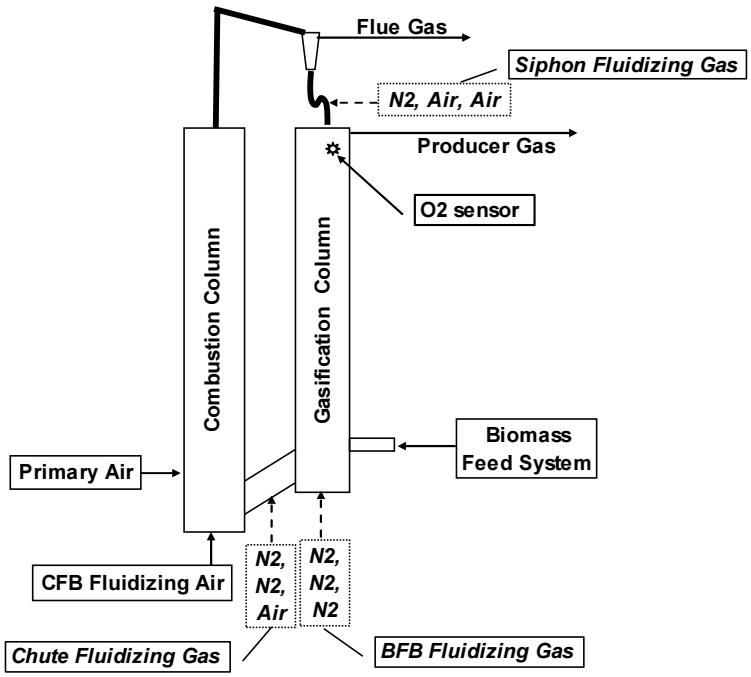

Figure 4.1: Diagram of the set up for the nitrogen testing with the different gas injection points and gases used shown. The different gases used are shown in order from left to right, and downwards in the dotted text boxes. For example the first test scenario had nitrogen in the siphon, chute and in the BFB distributor.

The method of analysis was to record the flow rates of nitrogen and air at all points into the gasifier system and use Microsoft Excel to iteratively solve the solution set using Solver. The individual flow rates of oxygen and nitrogen were set out in a spreadsheet and summed together for each of the three scenarios to give a total flow rate of gas entering and exiting the gasification column. Solver was then used to change the initial flow rate of air coming from the combustion column through the chute, to match the modelled oxygen concentration with the measured oxygen concentration. The solution converged upon did depend on the assumptions that were made, however these were later validated and the solution is as accurate as possible with the variables that were measured.

The assumptions made are presented below with their validations:

1. It was assumed that the air flow rate from the combustion column through the chute into the gasification column was the same amount for all three tests, since similar conditions were maintained. (However on one occasion a lower level of primary air was used).
2. It was assumed that no oxygen flowed back up the producer gas line to the oxygen sensor during steady state conditions, and that there was no leakage of flue gas through the siphon and into the gasification reactor. So the oxygen detected in the first scenario in the gasification reactor was believed to originate from the combustion column and migrate up the chute.
3. It was assumed all chute fluidizing gas went up the chute into the gasification column. This agrees with other researchers' findings and is discussed in Section 2.8. It was also proven with the spreadsheet mass balance that air does enter the gasification column from the combustion column, as gases do not flow in two directions in the chute in a counter-flow manner.
4. It was estimated that about 60-70 % of the siphon fluidizing gas went through the siphon and entered the gasification reactor. This value of 60-70 % was derived from testing different amounts of CFB leakage air in the spreadsheet.
5. It was assumed that the entire standpipe fluidizing air went out with the flue gas and did not push through the siphon. (This flow rate is very small, approximately 4-5 L/min and considered negligible).

4.2 Experimental Procedure followed for Investigative Hot Testing

Hot testing on the FICFB gasifier at the University of Canterbury followed the general heating-up and shutdown procedures presented in Appendix F. Only during the three to four hour period of gathering experimental data did any variations in procedures occur, specific to each test parameter being assessed. Section 6.2 explains the normal operating characteristics learned about the 100 kW gasifier and should be read along with the experimental procedures being discussed below.

All readings were recorded in a spreadsheet as the experiment was performed. It was common practice to record all plant data for a particular operating condition immediately before taking a producer gas and tar sample, so that any incorrect plant settings could be adjusted before the sample was drawn. Producer gas samples were analysed in an Agilent 3000A microGC with two columns. The first column has a molecular sieve packing using argon as a carrier gas and operating at 85 °C. The second column has a plot-Q (porous polymer) packing using helium as a carrier gas at a temperature of 60 °C. The molecular sieve column detects helium, hydrogen, oxygen, nitrogen, methane and carbon monoxide. The plot-Q column detects carbon dioxide, ethene and ethane. The experimental error with the microGC was considered negligible compared to the natural fluctuations in plant operation.

Tar samples were collected in SPE columns and stored in a refrigerator for analysis at a later date. The SPE columns were capped off to minimise loss of the lighter tar components by evaporation. Steady state conditions were determined by studying the live temperature plots on the monitoring laboratory computer and watching the digital temperature readings on the gasifier control panel instruments stabilise. The experimental errors for the tar quantities in g/m^3 were under represented. This is because the method of analysis by the commercial laboratory contracted to analyse the samples did not disclose their procedure. So only the errors incurred by drawing 100ml of producer gas through the SPE columns could be calculated.

Fuel Feed Rate Test

This test was performed first because it was the easiest parameter to vary on the gasifier. The variable speed drive (VSD) controlling the main auger was set at six different fuel feed rates

from 11.2-24.8 kg_{dry}/h. The gasification reactor was heated up to 779 °C but cooled down to 726 °C during the transition phase. Simultaneous producer gas and tar samples were taken once steady state conditions were established at each fuel feed rate. (The second producer gas composition was contaminated by an air leak which occurred during sampling and was not displayed in the results section).

Gasification Steam Test

For this test the amount of fluidizing steam being passed into the gasification reactor was varied from 3-11.2 kg/h in nine increments. The amount of steam fluidizing the chute was maintained at its usual setting of 4 kg/h, so the total quantity of steam entering the gasification reactor was the summation of the chute steam and the steam passing directly into the base of the reactor.

Gasifier Trial with Increased Bed Material

The standard operating procedures of Appendix F were followed, except 20 kg of greywacke bed material were used instead of the normal 12 kg. The gasifier was heated up to around 750 °C before gasification of wood pellets was initiated. The gasification reactor temperature reached steady state at about 720 °C. Gas and tar samples were taken regularly for a range of wood pellet feed rates from 10.5-25.6 kg_{dry}/h. This was achieved by altering the VSD controlling the main auger.

Gasification Temperature Test

The gasifier was heated up on LPG until a gasification temperature of 670 °C were reached. Once steady state conditions had been achieved a set of plant readings were recorded before a gas and tar sample was taken. After each set of samples the steam fluidization on the gasification column was converted back to air (as occurs during the normal heat-up stage), and the additional LPG firing on the combustion column was stepped back up. This was the technique used to heat the gasifier up to a higher temperature before steam was once again supplied into the gasification reactor along with reducing the supplementary LPG firing. Steam fluidization in the chute was maintained to minimise variations in the circulation behaviour of the plant. Each time the plant was converted from the heat-up phase to steam gasification of wood, a temperature decrease of approximately 30-40 °C occurred before steady state conditions were again achieved.

Steady State Operation Assessment of the Gasifier

This test was performed to study the gasifier's operation when plant settings remained unaltered to see how consistent its performance was. The standard operating procedures of Appendix F were followed while regular producer gas and tar samples were obtained. Before shutting down the plant at the end of this test, an additional assessment was performed where the supplementary firing was turned off on the combustion reactor. This was to determine if char alone could generate enough heat to fuel the gasifier alone.

Olivine Bed Material Test with Varying Fuel Feed Rates

For this test 12 kg of olivine bed material was used in place of the usual 12 kg of greywacke bed material. The olivine was sieved so that the majority of the particle sizes were in the range of 200 μm to 500 μm (see Figure 4.2). This was done to replicate as closely as possible the size distribution of the greywacke bed material and to account for the slightly higher bulk density of the olivine at 1731 kg/m^3 compared to the greywacke at 1567 kg/m^3. The same operating procedures were followed as for other hot tests while the feed rate of the wood pellets was varied through the VSD controlling the main auger.

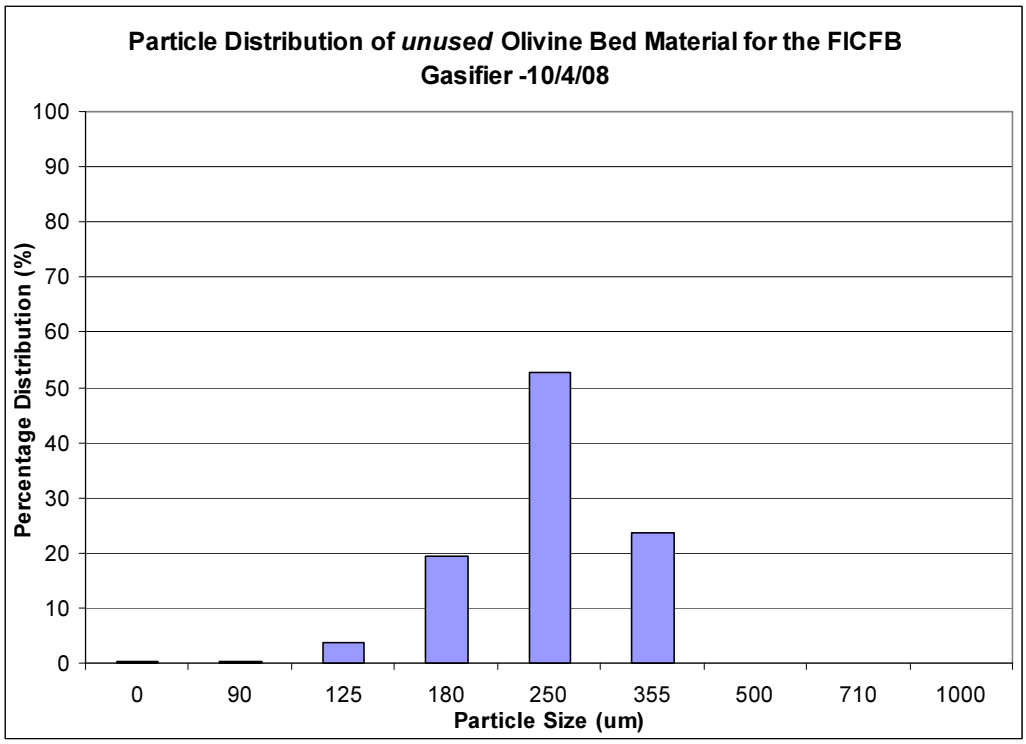

Figure 4.2: Particle size distribution of the olivine bed material used in the gasifier.

5.0 Results and Discussion of Cold Testing on the 100kW FICFB Gasifier

5.1 Effect of Varying Settings on the Bed Material Circulation Rate

The aim of the cold testing work was to allow operators of the gasifier to gain a better understanding of what effect different flow rates of gas supplied to various regions of the gasifier had on its circulation behaviour, and to better understand the particle dynamics associated with various components. This is important because heat is transferred between the reactors by the circulating bed material and the accumulation of bed material in certain regions of the gasifier is the method by which seals are created between the reactors. All cold tests were performed with the parameters initially set at the values presented in Table 5.1. To test the influence of different parameters on the circulation behaviour of the bed material in the gasifier, each parameter was varied over a range of settings while all other settings were maintained at the values displayed in Table 5.1.

Table 5.1: List of the input settings used during cold testing of the gasifier.

Control Input to the Gasifier	Range of values the setting was maintained between.
CFB fluidizing air flow rate	175-179 L/min
CFB primary air flow rate	1778-1847 L/min
Chute air flow rate	46-47 L/min
Siphon air flow rate	19-20 L/min
BFB fluidizing air flow rate	114-115 L/min
Standpipe fluidizing air	Varied to control the material level in the standpipe
Volume of bed material used	11 L
Bulk density of bed material	1703 kg/m^3 or g/L
Blower speed setting	17.5-24 Hz (changed when required)

The factor of greatest interest during the cold testing was to understand how each control input to the gasifier affected the circulation rate of the bed material around the internal circuit. The circulation rate of bed material was determined by placing a beaker in the circulating sand flow and timing how long it took to fill before weighing its contents. During

some tests, the circulation rates became so great that the testing crew had to consistently time within one second or the quality of the data deteriorated.

Experimental errors were determined to be 3 % for the circulation rate measurements. The errors for the flow rates were dependant on the graduations on the rotameter tube scales, but they ranged between 0.5 L/min for the small rotameters to 20 L/min for the primary air rotameter.

5.1.1 Analysis of the Level of Fluidizing Air used in the Chute

Fluidizing gas is supplied to the chute to control the flow of bed material passing out the gasification column and entering the combustion reactor. This also allows the relative mass loadings of the fluidized beds and the residence times of the particles in each fluid bed to be influenced. Figure 5.1 shows the chute and the path followed by the chute fluidizing agent. The sparger distributes the fluidizing agent along the base of the chute.

Originally the gasifier was designed with air being used to fluidize the chute, but this was later changed to steam fluidization as discussed in Section 3.1.6. The same particle dynamic trends should apply when steam fluidization is used in the chute as occurs with air during cold testing. Section 2.8.2 explains the chute's operating principles.

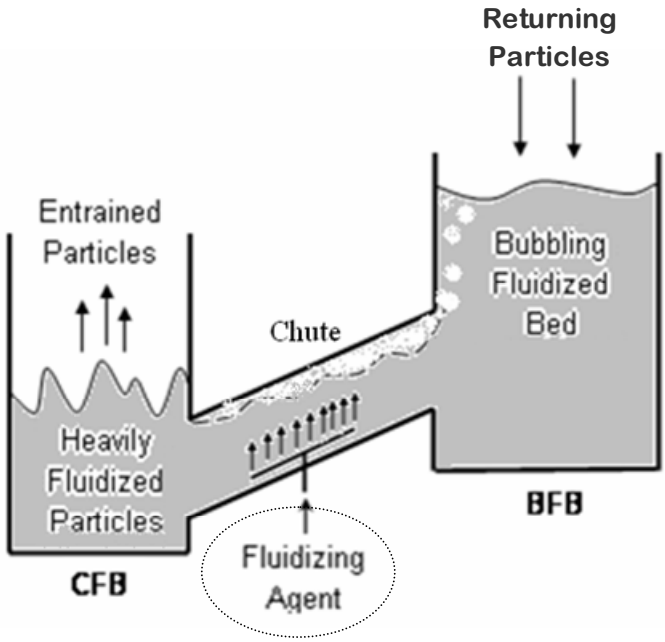

Figure 5.1: Diagram of the chute situated between the reactor bases.

Initially operators of the gasifier did not know how much fluidizing gas was needed, and what the effects of different amounts of fluidizing gas would be on the systems characteristics. From carrying out cold tests using a range of fluidizing gas flow rates in the chute, it was found that increasing the level of chute fluidizing air, increased the circulation rate in the gasifier. This can be seen in Figure 5.2.

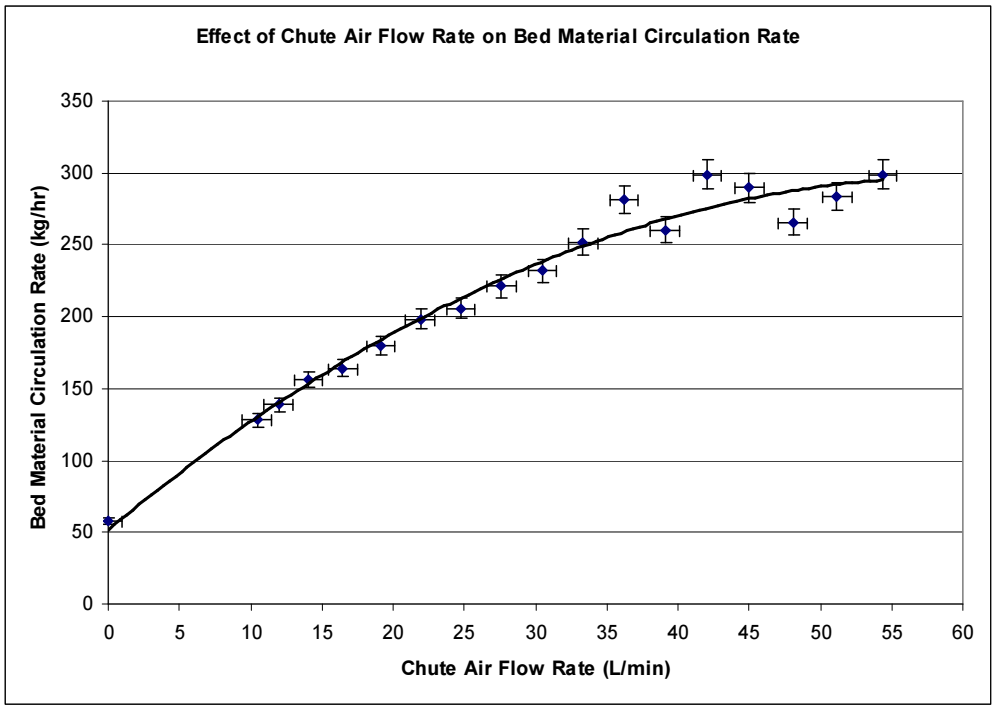

Figure 5.2: The effect of changing the level of fluidization gas flow rate in the inclined chute on the gasifier.

The circulation rate of bed material varied between 58-300 kg/h with changing the amount of chute air from zero to 54.4 L/min. This meant the circulation rate could be varied by 242 kg/h. The gasifier continued to circulate at 58 kg/h when no fluidizing air was introduced because the chute had enough incline to allow bed material to flow through unaided into the combustion column. Once in the combustion column the bed material is entrained and circulated around to the gasification reactor. These values are only representative when the other settings in Table 5.1 are used. The circulation rate range may be greater or smaller with other input settings.

The circulation rate trend became more erratic at the higher chute air settings because the blower supplying the air to the gasifier was set at too low a speed (17.6 Hz). This speed level was too slow to supply enough air for any higher chute air flow rate measurements to be

tested. Once this was realised the blower speed was set at a higher level for following cold tests.

Limitations exist on the amount of chute fluidization gas which should be supplied. High levels of chute fluidizing gas can cause a concentrated channel of gas to travel along the chute ceiling reducing its quality of seal between the reactor bases and disrupting the fluidization regime in the BFB. The majority of chute fluidizing gas moves up the top of the inclined surface of the chute and enters the BFB. (See Figure 5.1 for a pictorial representation). Excessive levels of chute gas could also reduce the amount of bed material passing down the chute. This risk is more likely if the sparger delivering the fluidizing gas is poorly designed with too large outlet orifices, and too much gas is forced in.

The amount of chute fluidization is not an independent operating parameter to control the rate of circulation in the FICFB gasifier. The chute fluidizing agent influences the gasification reactions occurring in the BFB by varying either the amount of steam or air present. Additionally it was discovered that if the CFB was fluidized, bed material passes more readily through the chute.

The rest level of the fluidized beds changed noticeably as the level of chute fluidization varied. The BFB upper surface level lowered by approximately 35 mm when changing the level of chute fluidizing air from 0 to 54.4 L/min. Obtaining an accurate measure of the bed heights was difficult, as the surface of the bed did not often settle horizontally and there were limited entry points on the gasifier through which to take measurements. It is likely that an error of 5-10 mm occurred with each reading of bed height.

The rest level of the CFB increased by 80 mm as the level of chute fluidizing air increased from zero to 54.4 L/min. A greater height increase occurred in the CFB than the BFB because the CFB internal reactor diameter is smaller, so an equivalent volume occupies a greater height in the column. The reason for the CFB rest height increasing is because the gasification reactor distributor is situated 145 mm higher than the combustion reactor distributor so that the chute is inclined, and sand preferentially flows down the chute with higher levels of fluidization air passed through the chute sparger.

The pressure drops across both fluidized beds changed with the changing bed heights as measured with manometers. The BFB reactor pressure changed from 6.6 mmH_2O when no fluidizing air was used in the chute, to 6.2 mmH_2O when 54.4 L/min of air was blown through the chute sparger. The CFB showed the opposite trend, the pressure drop across the CFB increases from 1.2-2.2 mmH_2O over the same range. This proved that bed pressure drops were a good method for assessing bed heights.

5.1.2 Analysis of the Level of Fluidizing Air used in the Gasification Column Base

Under hot testing conditions steam is used to fluidize the BFB, but during cold testing air was used in place of steam for practical purposes. A fluidizing agent is supplied to the BFB so that a fluidized bed regime is created rather than a fixed bed regime for the reasons discussed in Section 2.5.3 and 2.6. The BFB fluidizing agent is introduced through a distributor at the base of the gasification reactor as indicated in Figure 5.3.

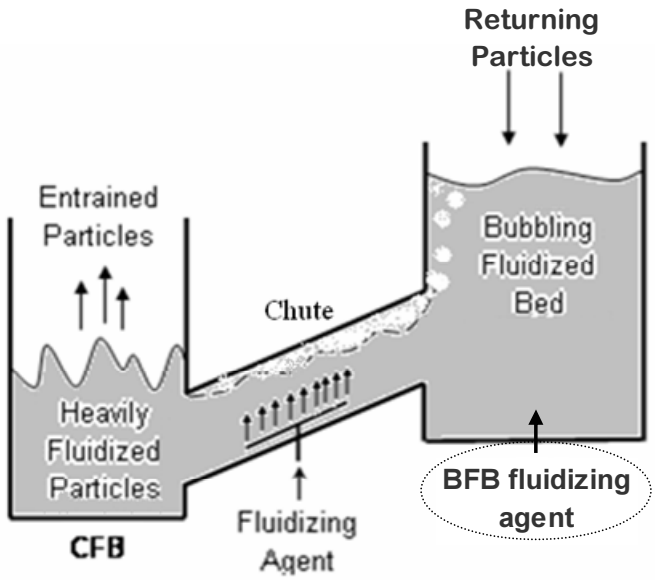

Figure 5.3: Base of the FICFB gasifier showing the location of the BFB fluidizing agent.

Fluidizing the BFB had an intriguing effect on the circulation rate of bed material in the gasifier. This can be seen in Figure 5.4. As the BFB air flow rate was increased above zero, the circulation rate rapidly increased before levelling off. The transition point from increasing circulation rate to the plateau occurred when the BFB airflow was about 50-65 L/min. This transition occurred between the off-position and the zero scale marking on the chute flow rate

rotameter. Because of the scale stopping on the rotameter tube, no lower measurements could be tested with this set up. (Note: zero on the rotameter does not mean zero air flow; it is just the start of the rotameter scale).

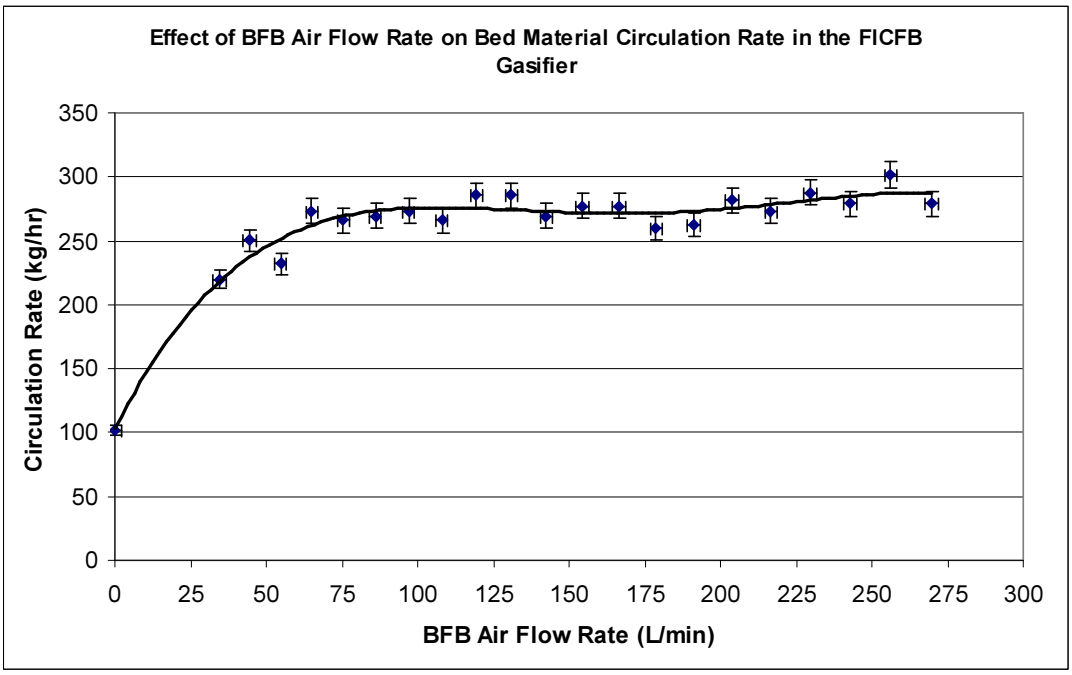

Figure 5.4: Change in the rate of bed material circulation with different levels of BFB fluidizing air during cold testing.

During a preliminary assessment, the gasifier stopped circulating when no fluidizing gas entered the BFB. This was unexpected and did not occur during the official test run displayed in Figure 5.4. A low rate of circulation was expected when no fluidizing air was used in the BFB, because provided a head of sand is available above the entrance to the chute, bed material should pass through the chute and be circulated around the loop. This will occur provided the head of sand in the BFB and chute can overcome the frictional resistance and pressure differential between the two reactors. It is important that the base of the CFB is maintained fluidized, otherwise the bed material backs up in the chute and does not pass through effectively into the CFB.

Additionally, for entrainment and circulation of bed material to be sustained around the plant, the CFB fluidizing air must be set high enough to project particles above the primary air jets. It was likely that the level of fluidization in the CFB during the initial circulation test with no BFB air was too low and responsible for the circulation ceasing as mentioned above.

The reason for the increase in the bed material circulation rate, followed by the plateau of the circulation rate in Figure 5.4, is believed to be due to the force interaction of the particles and the characteristics of the gas flow around the particles in the BFB. As the amount of gas percolating through a particle bed increases, the horizontal shear forces exerted on a vertical plane through the bed increase, as the bed becomes fluidized behaving more like a liquid. This occurs because the between the particles is reduced, causing the viscosity of the particle bed to decrease. The higher shear forces exerted on a vertical plane across the chutes' entrance, changes the pressure differential across the chute and forces more bed material through. Once the BFB has become fluidized, circulation rate remains relatively constant because a constant shear force is exerted from the fixed head of sand in the BFB. Additionally, the fluidizing air being forced through the void spaces amongst the particles in the BFB would increase until the bed becomes fluidized and maintains a constant pressure drop as shown in Figure 2.32.

No distinct trend appeared in the rest height of the CFB or the BFB surfaces, with changing the level of fluidizing air entering the BFB. The data obtained was very erratic due to the bed surfaces settling differently. From intuition and studying the poor quality data, increasing the level of BFB fluidizing air, lowered the BFB rest height initially before it remained relatively constant once fluidized. The CFB rest height showed opposite characteristics by starting low and increasing as BFB fluidizing air rates increased.

5.1.3 Analysis of the Level of Fluidizing Air used in the Combustion Column Base

The fluidizing air in the combustion column base serves two roles. It supplies some of the oxygen required for the combustion of char and LPG, and fluidizes the base of the CFB projecting particles above the primary air jets for entrainment and circulation to occur. The quantity of fluidizing air used in the CFB should be minimised to prevent excessive amounts flowing up the chute into the gasification reactor and increasing the nitrogen content of the producer gas. This is shown in Figure 5.5.

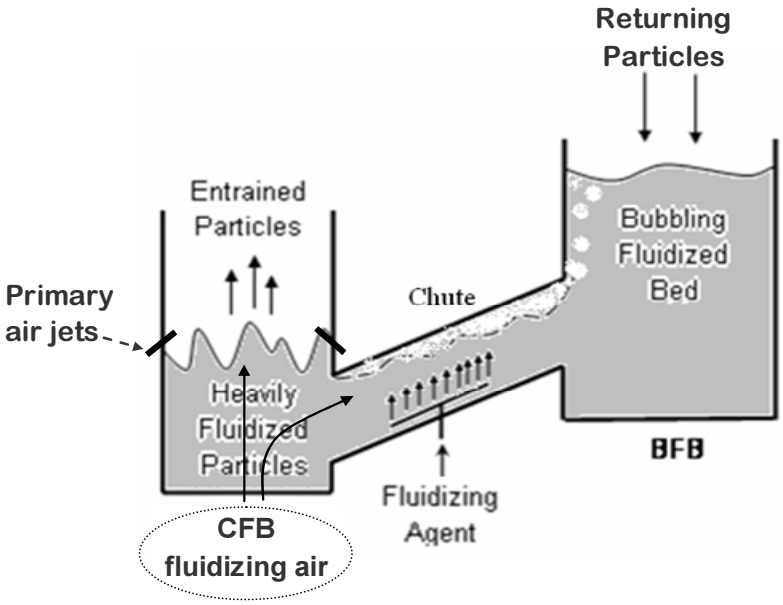

Figure 5.5: CFB fluidizing air is passed into the base of the combustion column to fluidize the base of the CFB and supply some of the combustion air. Some CFB fluidizing air tracks up the chute into the gasification reactor.

As the level of CFB fluidizing air was increased, the bed material circulation rate increased. This agrees with information presented in (Kunii & Levenspiel, 1969). The trend occurred only once the quantity of fluidizing air was above 30-35 L/min as displayed in Figure 5.6.

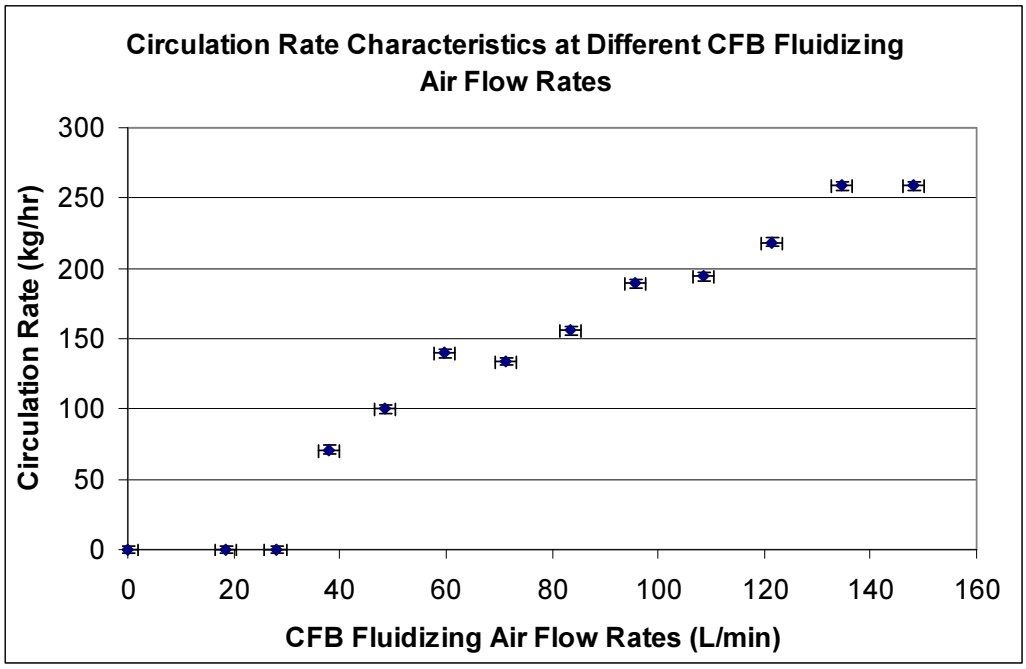

Figure 5.6: Circulation rate characteristics of the FICFB gasifier at different CFB fluidizing air flow rates.

No circulation occurred when the CFB fluidizing air was below about 35 L/min because bed material was not projected above the upwardly directed primary air jets in the combustion column. The orientation of the primary air jets is shown on the combustion column in Figure 5.5. Thus, the quantity of bed material in the gasifier also affects the bed heights and the entrainment rate of particles up the combustion column. Hence the spacing of the combustion column distributor and the primary air jets is a carefully chosen design parameter coupled with the quantity of bed material used in the gasifier. The primary air jets can not be placed too low down in the combustion column because this encourages too much air to pass through the chute into the gasification column. By introducing the majority of the combustion and entraining air above the outlet of the chute, this reduces the quantity of air which can track up the chute.

The circulation rate of bed material in the gasifier, increased from zero to 260 kg/h at a fluidizing air flow rate of zero to 148 L/min respectively as shown in Figure 5.6. The reason for the increase in circulation rate with escalating the level of fluidizing air is due to the increased number of particles being projected above the primary air jets and the greater total mass flow of air rising up the combustion column. The fluidizing air flow rate in the gasifier at the University of Canterbury is not large enough to entrain bed material by itself, so it only contributes to the total flux of air up the combustion column.

The rest level of both fluidized beds was affected by the level of fluidizing air supplied to the CFB. The bed height measurements were difficult to take accurately and the quality of the data was poor because the bed surfaces did not always settle horizontal. However, it was clear from visual observations during the testing period that once the CFB fluidizing air level increased enough to achieve a fluidized regime in the CFB, then the bed material flowed more readily through the chute. This is due to the fluidizing of the CFB reducing the frictional forces amongst the bed material so that bed material being introduced via the chutes is more readily accepted.

5.1.4 Analysis of the Level of Primary Air used in the Combustion Column

The role of the primary air introduced into the combustion column is to entrain hot bed material to circulate it around the internal loop through both reactors, plus supply most of the

oxygen required for combustion of char and any supplementary fuel. The primary air jets are located 240 mm above the combustion column distributor as shown in Figure 5.7.

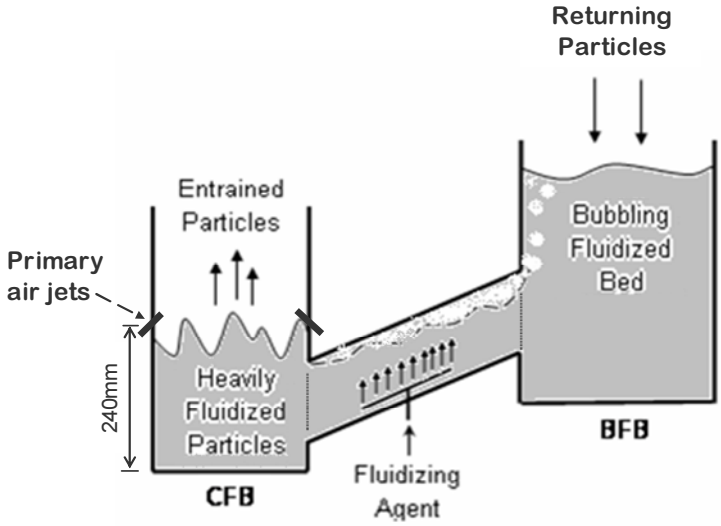

Figure 5.7: The base of the FICFB gasifier showing the elevation of the primary air jets.

The primary air supply to the gasifier is the largest gas flow input and hence the most dominant input variable. The effect of increasing the level of primary air supplied to the combustion column can be seen in Figure 5.8. A maximum circulation rate of 300 kg/h was observed at a primary air flow rate of 2265 L/min. After this point the circulation rate progressively decreased resembling a bell curve.

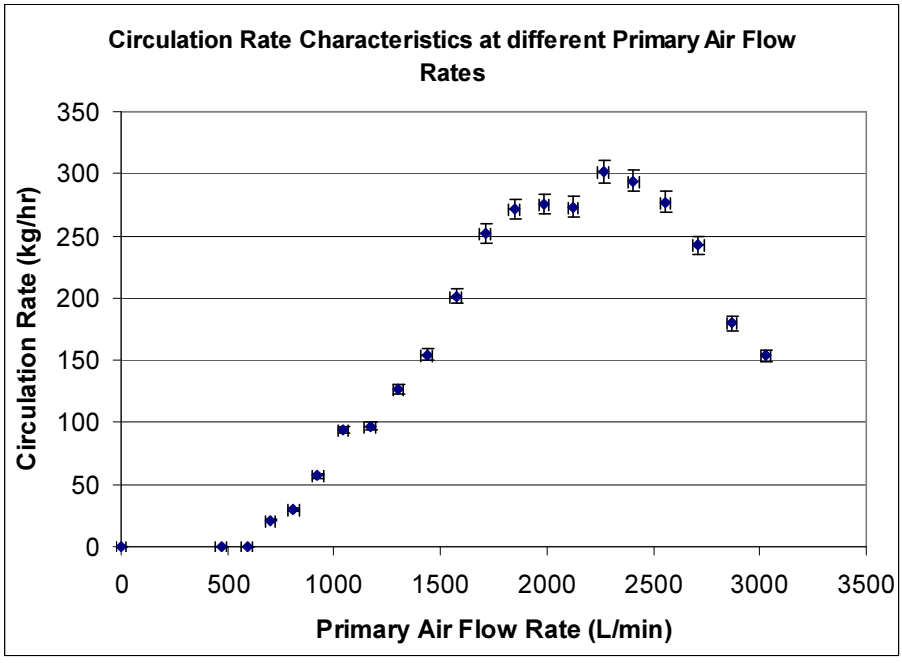

Figure 5.8: Effect of changing the level of primary air flow to the combustion column relative to the circulation rate of bed material.

Initially no bed material circulation occurred until the primary air level exceeded 590 L/min. This represents the lower threshold flow rate required to entrain bed material under ambient conditions with the other settings used from Table 5.1. The circulation rate then progressively increased to about 300 kg/h before rounding off and decreasing. The circulation rate increased initially (between 590 L/min to about 2200 L/min), because the superficial gas velocity up the combustion column entrained increasing quantities of bed material as the primary air flow rate increased. Once the primary air flow rate exceeded about 2200 L/min, the systems characteristics began to change and the circulation rate decreased.

The rounding-off and downward decline of the curve in Figure 5.8 is thought to be due to increasing quantities of air taking an additional path to the flue gas line out of the combustion column. The principle of the conservation of mass flow implies that if you increase the flow rate of a fluid into a control volume, that either the velocity of the flow exiting must also increase, or another exit path must also be taken. There are only two routes for gases passed into the gasifier to exit via: the flue gas line and the producer gas line, joined by the chute and the siphon.

As more primary air is introduced into the combustion column, the path of least resistance around the circuit appears to be shared with the passage up the chute. This occurs because the flue gas line has a rather restricted path and as the total air flow entering the combustion column is increased, the pressure in the combustion column also progressively increases forcing air out via the chute. This change in the combustion column pressure is shown in Figure 5.9.

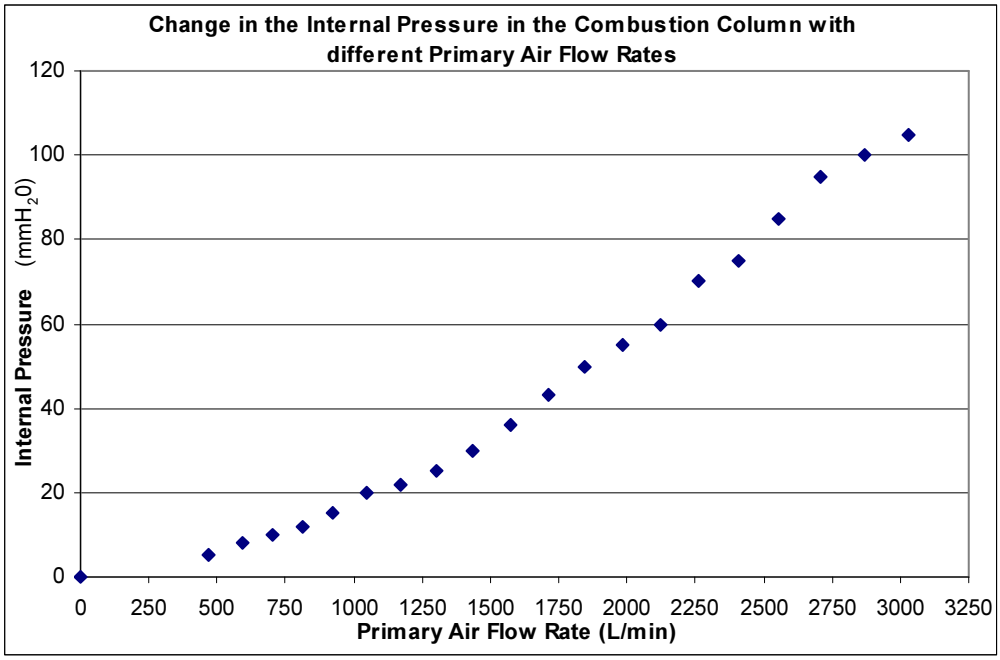

Figure 5.9: Change in the internal pressure of the combustion column at different primary air flow rates during cold testing.

The increase in the internal pressure of the combustion column is significantly greater than the increase in internal pressure in the gasification column and supports the conclusion that some air passes between the reactors. The pressure inside the gasification column increased by 14 mmH_2O at 3030 L/min, indicating that either some primary air passed through the chute, or was forced down through the siphon into the gasification column. The change in the internal pressure in the gasification column is shown in Figure 5.10.

Since the circulation rate of bed material is adversely affected by continually increasing primary air levels above 2200 L/min, this indicates that the supply of bed material to the combustion reactor is reduced. Excess air passing in a co-current manner through the siphon would act to increase the circulation rate rather than decrease it. This is the opposite for the chute where bed material and air would flow in a counter-current manner, reducing the supply of bed material to the combustion reactor. An increase in pressure of 14 mmH_2O in the gasification reactor is considerable because the producer gas line is of a large diameter with minimal restrictions, so a small pressure increase could correspond with large air flow rates entering the gasification column.

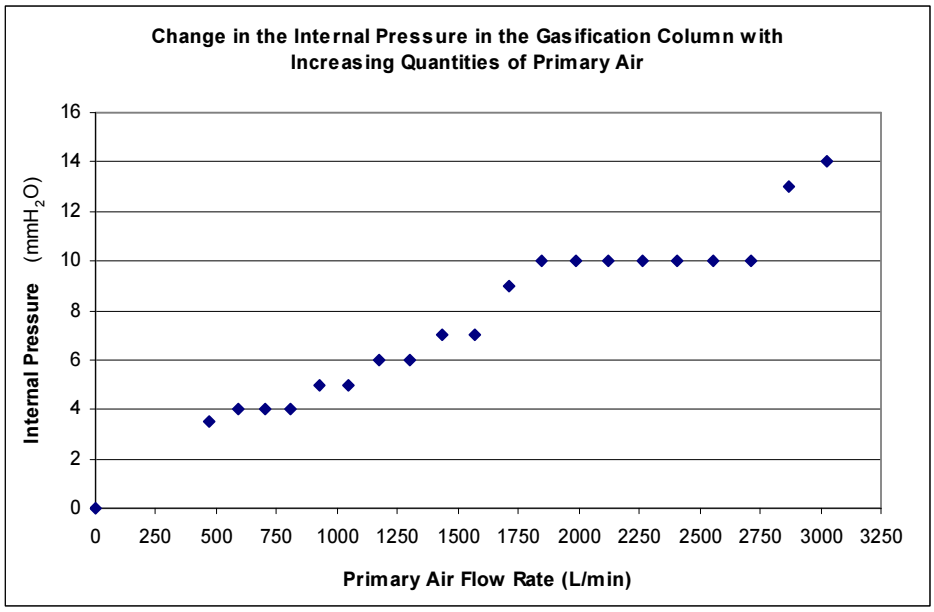

Figure 5.10: Change in the internal pressure in the gasification reactor measured at the chute entrance in the gasification column as the primary air flow rate varies.

The chute tends to have a region along its top inner surface which provides a relatively free path for gas to travel along between both reactors. (See Section 2.8.2 for details on the particle dynamics of FICFB gasifiers and chutes). As the amount of primary air increases, it is likely that this flux of air travelling up the chute due to the changing pressure differential between the reactors impedes the counter-flow of bed material down the chute.

During cold testing, the maximum shown in Figure 5.8 became realised during the experimental testing. Operators were not certain during the test if all the primary air being introduced was causing more bed material to be entrained than could be delivered through the chute. To see if the chute was creating a bottle-neck effect and supplying too little bed material to the combustion column for entrainment, the level of fluidization in the chute was temporarily more than doubled from 46.5-100 L/min. The circulation rate increased marginally from 301-327 kg/h. This small increase in circulation rate seems valid because additional fluidizing air should only have a minor influence on increasing the circulation rate when so much primary air is passing in a counter-current direction up the chute against the flow of bed material.

The rest level of the BFB got progressively higher as the level of primary air increased. This was another indication that the flow of bed material through the chute was reduced by the

increasingly larger flux of counter-flowing air back up the chute. The BFB rest level increased by 100 mm as the primary air flow rate was increased from zero to 3030 L/min. Correspondingly the CFB rest bed level decreased by 150 mm as primary air level was raised. Note the internal diameter of the gasification column is larger than the combustion column at 200 mm (with a tapered base) and 100 mm respectively.

Another assessment was performed during this primary air test to see what affect the level of siphon fluidization had on where the primary air travelled within the gasifier. The back pressure in the producer gas line could be reduced by increasing the siphon fluidizing air so that the barrier to gas exchange was reduced with the more heavily fluidized bed material in the siphon. A noticeable increase in circulation rate suddenly occurred raising the circulation by 18 kg/h. This supports the author's notion that the flue gas cyclone exit before the heat exchanger manifold is the most restrictive part of the flue gas path on the University of Canterbury gasifier.

5.1.5 Analysis of the level of Siphon Fluidizing Air used in the Gasifier

The role of the siphon fluidizing air is to reduce the frictional resistance of the bed material so it can flow through the siphon more readily but still act as a barrier to the exchange of gases between the flue gas cyclone and the top of the gasification reactor. See Figure 5.11 below.

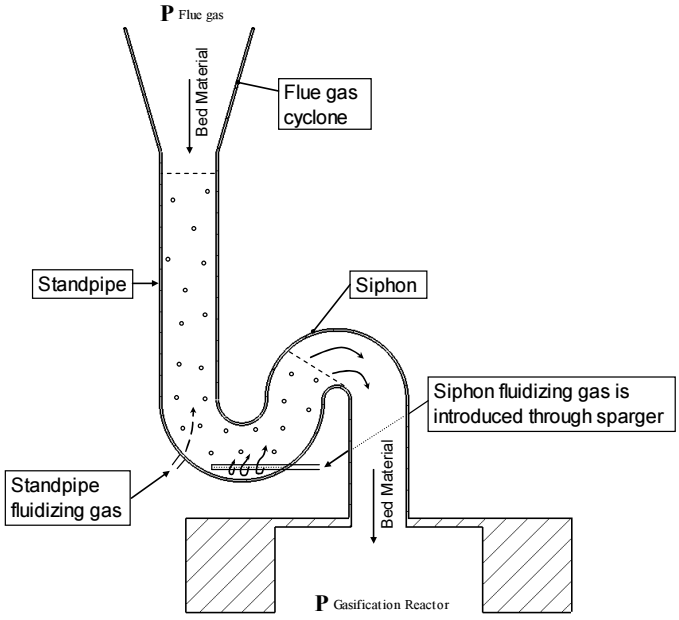

Figure 5.11: Diagram of the siphon and standpipe showing the locations where fluidizing air is passed into the siphon and the paths followed.

If no siphon fluidizing air is used, the siphon and standpipe backfill with bed material up into the flue gas cyclone causing sand to pass out with the flue gas. Fluidizing with air in the siphon is not a way to vary the circulation rate because there is no storage capacity for bed material immediately before the siphon. So whatever bed material approaches the siphon, must be passed through it to circulate around the gasifier. This is confirmed in the circulation rate plot of Figure 5.12.

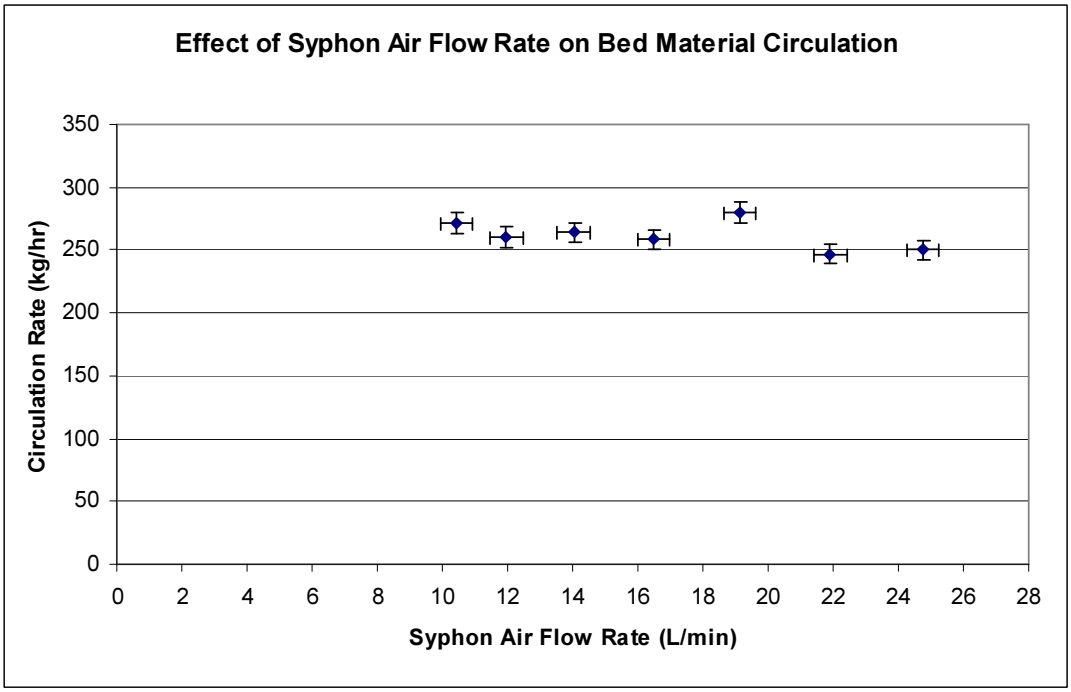

Figure 5.12: The effect of varying the siphon air flow rate with respect to circulation rate.

As the quantity of siphon air increases, the fluidization regime in the siphon tends towards a turbulent bubbling system. This affects to what extent the siphon acts as an impervious barrier to the exchange of flue gas and producer gas. The deterioration in the siphon's gas plugging ability can be expressed as the reduction in the pressure drop across the standpipe and siphon system. This is shown in Figure 5.13. The pressure differential decreased from 425-150 mmH_2O when the siphon air flow rate was increased from 10-25 L/min respectively. During this experiment, air was also introduced into the base of the standpipe to help the flow of bed material around the first bend at the base of the standpipe. Ideally a light smooth fluidization regime is desirable in the siphon to sufficiently reduce frictional resistance and still create an effective seal to the exchange of gases between both reactor systems.

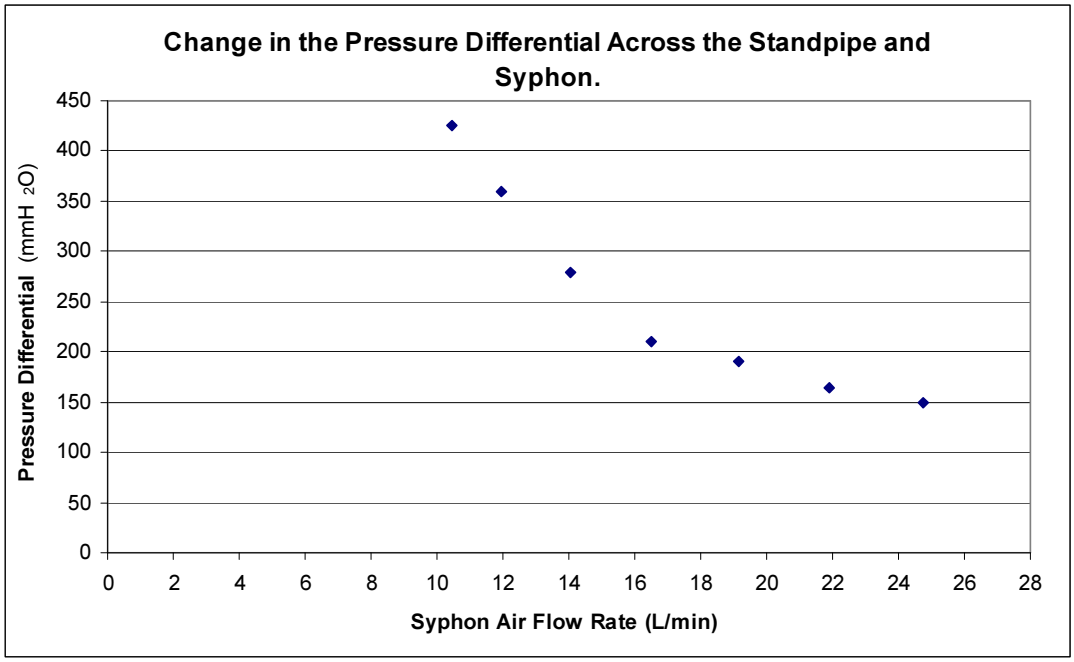

Figure 5.13: Change in the pressure differential across the standpipe and siphon which is used to create a barrier to the exchange of gases between the upper regions of both reactors.

5.1.6 Analysis of the Quantity of Bed Material used in the Gasifier

The bed material serves the primary purpose of transferring the heat generated in the combustion column around to the gasification column where the thermochemical gasification reactions occur yielding producer gas. A minimum quantity of bed material must be present inside the gasifier to accomplish circulation and ensure the chute and siphon have sufficient bed material to operate as a barrier to the exchange of gases. Before the mass loading of bed material in the gasifier was studied, it was not known what the effect of different quantities of bed material had on characteristics such as circulation rate.

Sand was added in 500ml loads. The bulk density of the existing greywacke bed material in the gasifier was 1630 kg/m^3 and the fresh bed material being added had a bulk density of 1703 kg/m^3, because it contained fines (below 200 μm) which slowly get removed out of the flue gas cyclone during operation. The new bed material being added to the gasifier had the same composition as the original but just needed some circulation time for the bulk density to decrease to 1630 kg/m^3. Experiments showed that the circulation rate increases exponentially from 235-420 kg/h as the total bed material quantity increases from 18-28.5 kg (11 L to 17.5 L) of sand. See Figure 5.14.

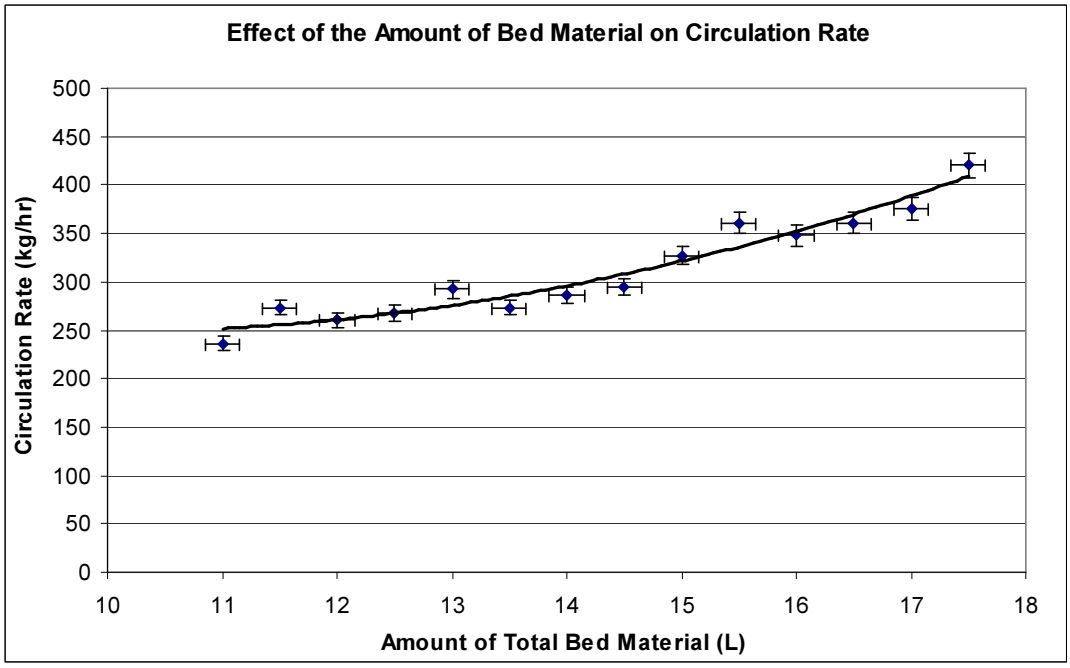

Figure 5.14: The affect of increasing the bed material loading in the FICFB gasifier on the circulation rate of the bed material.

Circulation rate increased in the gasifier when more sand was present because a higher head of sand existed at the entrance of the chute to force bed material into the combustion column. When more sand is passed into the combustion column, a greater mass of sand per unit time gets fluidized and projected above the primary air jets. This causes a larger quantity of the sand to be entrained and circulated.

The quantity of bed material in a FICFB gasifier is a factor to optimise relative to the specific design of the reactors. Too much bed material reduces the freeboard height in the reactor columns and particle loss can occur. Excessive bed material loadings may also cause bubbles in the gasifier to coalesce creating slugging. Additionally higher bed material loadings require more energy when heating up the gasifier. So bed material loadings influence both the circulation behaviour and operational characteristics of the plant.

A possible advantage to operating the gasifier with high bed material loadings is that it could increase the residence time of biomass in both the gasification and combustion columns. This may cause the plant to operate in more of a single pass mode. Currently char particles can circulate multiple times, estimated to normally involve five cycles around the internal circulation loop. A biomass particle should have a greater volume of bed material to mix

within and pass through before leaving either the BFB or CFB. This phenomenon can be seen in Figure 5.15.

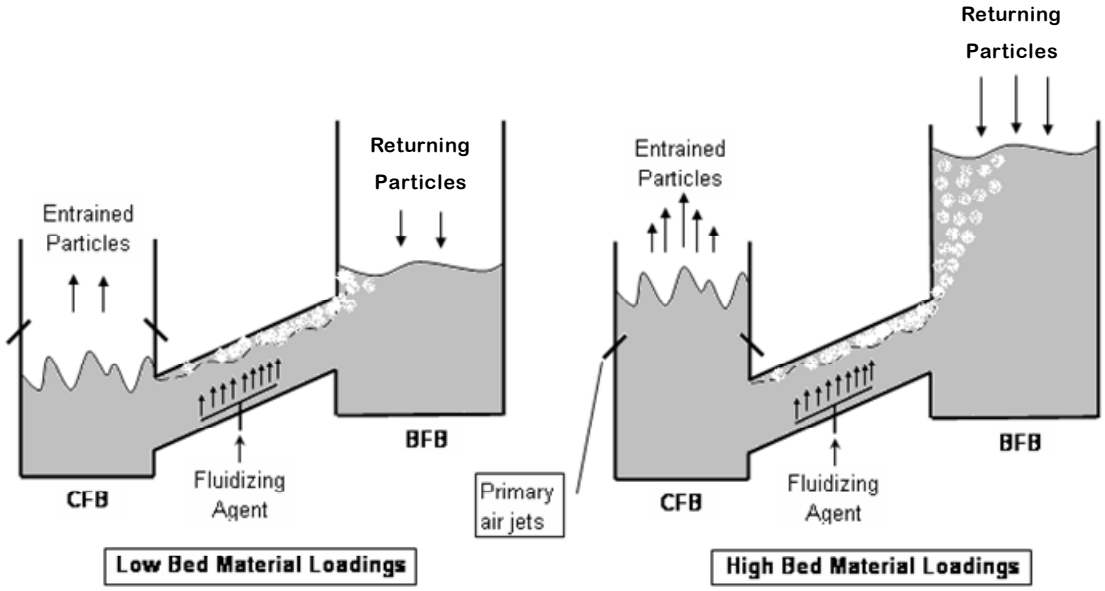

Figure 5.15: Expected characteristics of different bed material loadings in a FICFB gasifier. Higher bed loadings could increase particle residence times in both fluid beds.

As bed heights increased, the fluidizing regime of the BFB changed from a heavily bubbling to a lightly bubbling regime as the mass loading increased. The rest level of the BFB increased by 105 mm during this test and the rest level in the CFB increased by 145 mm. The greater increase in bed height in the CFB was due to the internal diameter of the reactor being smaller and hence any given volume occupies a greater height in the column.

5.1.7 Analysis of Changes in Counter Pressure in the Flue Gas and Producer Gas Lines

Changing the Flue Gas Line Restriction

A visual observation was performed to assess the effect of increasing the counter pressure at the exit of the flue gas line. This is relevant because in the future if a larger scale plant is constructed, the flue gas may have to pass through emission control apparatus which could raise back pressure in the flue gas line.

Increasing the counter pressure by restricting the exit of the flue gas line caused an immediate lowering of the sand level in the standpipe. This occurred because more flue gas tried to push its way through the siphon to exit via the producer gas line. This is unfavourable as it is likely

to deteriorate the quality of the producer gas by introducing non combustible gases into the producer gas mix. It is also likely to encourage more gas to track along the chute into the gasification column.

Changing the Producer Gas Line Restriction

A visual observation was performed to determine the effect of increasing the counter pressure at the exit of the producer gas line. The flow of gas out this passage was so small during the cold tests that no obvious changes occurred. Under hot testing conditions, producer gas would be generated in the gasification column so this flow rate would be substantially larger.

5.2 Investigation into the influx of Air into the Gasification Column

A set of tests was performed under cold testing conditions to study the ways air enters the gasification reactor, especially focusing on determining the amount of air that tracks up the chute from the combustion column. Any influx of air into the gasification column is unfavourable under hot operating conditions because it introduces nitrogen which lowers the calorific value of the producer gas. Before this testing regime was performed, it was unclear how much air passed from the combustion column and into the gasification column through the chute. The proportion of chute fluidizing gas, and siphon fluidizing gas entering the gasification column was also poorly understood.

This study was accomplished by supplying nitrogen in place of air and steam into different regions of the gasifier under cold testing conditions. Section 4.1.2 explains the experimental set up for this batch of tests. The collected data was used in a mass balance spreadsheet to iteratively derive a solution that fitted three different testing scenarios that were performed on the gasifier. The mass balance was calculated in terms of oxygen, since this could be measured in the gasification column with existing equipment, and any air that entered the gasification column introduced oxygen which the sensor measured. Since nitrogen did not introduce any oxygen, it allowed the three different scenarios presented in Appendix E to be analysed.

The only assumption that had to be made was that the entire chute fluidizing gas stream tracked up the inclined chute and entered the gasification reactor. The results from the spreadsheet proved that there is a net flow of air from the combustion column, through the

chute and into the gasification column. The magnitude of this flow rate depends on the relative pressure differential across the chute, but successively higher levels of primary air and fluidizing air in the combustion column appeared to encourage more air to enter the gasification reactor. Under the cold test conditions studied, 10-11 L/min of air originating from the combustion column entered the gasification column through the chute, exiting out the producer gas line. This corresponded to 0.5 % of the total air flow entering the combustion column (when 1890 L/min is introduced), or between 5-10 % of the (180 L/min of) fluidizing air used in the combustion column.

As is explained in the background literature section, other researchers have found that undesirable quantities of air track up the chute of FICFB gasifiers originating from within the combustion reactor. This is one of the reasons why the primary air jets are situated higher up in the combustion column, to limit the amount of air that is pushed downwards, along the chute into the gasification reactor.

This investigation confirmed that 100 % of the chute fluidizing gas, and approximately 60-70 % of the siphon fluidizing gas, flows into the gasification column and out the producer gas line. It was found that even if all the siphon and chute fluidizing gases entered the gasification reactor, that oxygen levels in the gasification column were never high enough to match the measured oxygen readings in the gasification reactor. This proved that some air must track from the combustion column, up the chute and into the gasification column. Hence our initial assumption that 100 % of the chute fluidizing gas enters the gasification reactor is valid, since a pressure differential between the columns would not create counter flowing gases between the reactors. Learning that all chute fluidizing gas entered the gasification column, prompted the modification to fluidize the chute with steam instead of air as discussed in Section 3.1.6.

The amount of leakage between the fluidizing air in the combustion column through to the gasification column was also investigated in the FICFB gasifier at Vienna University in Austria. It was discovered that increasing the angle of the chute caused more air to pass into the gasification column. Having a steeper chute incline also means less fluidizing gas is required to pass the bed material through and circulation rates are higher for any given level of chute fluidization (Bolhar-Nordenkampf *et al.*, n.d.).

5.3 Particle Circulation Time and Entrainment Capacity Assessment

This test was done to better understand the entrainment capabilities in the combustion reactor and to measure the circulation time for material to pass from the BFB inclined feed port and circulate around to the standpipe. These times would represent complete circuit times if the time for material to pass through the siphon was included, but because the circulated material could not be viewed clearly entering the gasification column; the time to reach the clear standpipe section was measured during cold testing. Under normal circulation rates it is estimated a particle would take two to eight seconds to pass through the siphon.

It was found that whole wood pellets could not be entrained out of the combustion column during cold testing at all, for all ranges of primary air able to be supplied. Under hot conditions this is likely to be the same since higher than usual primary air flow rates were introduced during this cold test. However, whole charcoal pellets, which are generated only under hot operating conditions, are likely to get entrained since their density is much lower than whole wood pellets. This phenomenon is to our advantage since longer residence times are needed in the CFB to generate more heat for the gasification reactor.

An assessment was carried out by introducing coarse vermiculite particles into the original feed port situated halfway up the gasification column. The vermiculite was used to simulate char since it had a comparably low density and consisted of similar sized particles. This test was to provide operators of the gasifier with a basic understanding of circulation times to convey char-like material around the plant. The vermiculite took 50 seconds on average to travel from the existing inclined feed port situated half way up the gasification column, to the clear standpipe section installed before the siphon. This circuit time included passing through the BFB, chute, CFB, getting entrained up the combustion column and being separated out by the flue gas cyclone before dropping into the standpipe. The amount of fluidizing air introduced into the BFB appeared to influence circuit times, possibly because the vermiculite was so light that it may have been buoyant in the upper region of the BFB and not passed down into the chute entrance. If char behaves in a similar manner this would influence the char residence time during gasification.

A third assessment indicated that it only took about five seconds for vermiculite to travel from the combustion column view port located just above the primary air jets to the clear

standpipe section. This proves that the first stage of particles passing through the BFB, chute and up through the CFB to the level of the primary air jets takes the majority of the circulation time (about 45 seconds). These particle entrainment and circulation assessments had the additional benefit of confirming that the chute was performing adequately by consistently passing material through itself.

5.4 Consideration to Install a Louvers to Reduce Pellet Entrainment

The installation of louvers was considered in the combustion column to knock-out large wood pellets and char particles from being entrained out of the combustion column, before they combusted to a smaller size. This was considered because it was identified from early hot tests that the gasifier did not generate enough heat in the combustion column relative to the heat input requirements for the endothermic gasification reactions.

The risk of a louvers creating blockages or causing excessive back pressure against the entraining air flow was too severe to ever adopt this idea. It was later realised from hot testing with the plant, that the circulation of hot glowing char pellets is favourable. The circulation of fuel particles in a FICFB gasifier can not be thought of as a once through process. Char can circulate four to five times or more before it has been gasified and combusted to ash. The circulation of the hot char appears to be a highly effective way of ensuring the wood pellets are at high temperature when they enter the gasification reactor. By circulating hot glowing char particles, the efficiency of the bed material contacting to transfer heat to the char particles becomes less important. It is possible that the char alone can transfer the required heat between the reactors; however the bed material has a higher heat capacity necessitating lower circulation rates. Additionally the smaller particle size of the bed material acts as a better barrier between the reactors to the exchange of gases through the chute and the siphon. The bed material also flows more readily than the char which often causes blockages in the siphon if not enough bed material is mixed with it.

6.0 Results and Discussion of Hot Testing on the 100kW FICFB Gasifier

6.1 Aims of the Hot Testing Trials

The aims of the hot testing trials performed at the University of Canterbury was to begin establishing the most favourable operating conditions for the FICFB gasifier, so that a medium calorific value producer gas could be generated (for CHP applications) with low levels of tars. This research focused on observing trends in the producer gas composition, producer gas yield, total tar levels and the cold gas efficiency, as certain parameters were varied. It is hoped that these test results will provide a base of information for continued experimentation on the 100 kW gasifier at the University of Canterbury and other plants developed in the future.

6.2 Preliminary Hot Testing with the 100kW FICFB Gasifier

The preliminary hot testing of the gasifier presented in this thesis has spanned 5-6 months. Preliminary hot tests are defined as the periods when the gasifier was operated under hot conditions to understand more about its operational characteristics and to assess the performance of the plant modifications made. These preliminary hot runs were intended to be the start of the hot runs to see how the gas compositions could be influenced, but instead they continued to identify necessary equipment and operational changes, plus measurement limitations on the gasifier. The important characteristics of the gasifiers operation have been discussed in detail for following operators of the gasifier.

6.2.1 Operational Characteristics Learned about the 100kW Gasifier

The preliminary hot testing period yielded much information on the operation of the 100 kW gasifier. Firstly it was verified that it takes on average five hours for the gasifier to heat up to 750 °C with a 12 kg loading of greywacke bed material. This is because of the high thermal mass of the system, especially the refractory lined reactor columns. Both reactor columns are heated by combusting LPG in their bases, before the LPG on the gasification column is turned off, and significantly reduced on the combustion column (some supplementary firing is maintained).

After the heat up phase is complete, wood pellet fuel and then steam are supplied to the gasification reactor. This is when the actual gasification process begins. Some supplementary LPG firing is necessary in the combustion column during gasification to hold plant temperatures at whichever temperature plateau is selected. This is in addition to the heat generated from combusting char.

Due to the departmental requirement for operators to be always present with the gasifier when it is running, it is usually only operated for a period of 10-11 hours at one time. So for each experimental test the plant goes through a heat up, gasification and cool down cycle. The cool down cycle usually takes 1-2 hours before the plant is considered safe to leave over night, so a narrow window of only 3-4 hours to perform all the gasification tests for the day exists. For the hot tests discussed in this thesis, many gas and tar samples are taken under varying conditions to investigate trends in producer gas composition and total tar levels. Because of the requirement to obtain many gas and tar samples within a 3-4 hour period, the gas and tar sampling needs to be very rapid, reliable and easy to perform.

During the heat up phase, the LPG has to be successively reduced to the combustion column to prevent the flame front propagating in pulses out of the combustion reactor and into the flue gas cyclone. As the plant heats up, this occurrence becomes more frequent and is apparent by a distinct popping noise occurring. This causes a pressure surge into the flue gas cyclone and often a small amount of bed material passes out with the pulses of flue gas. The tendency for this to occur is predictable from observing the live temperature plots on the monitoring computer, and the combustion reactor oxygen sensor readings always drop below 5 % before this problem occurs. The flue gas cyclone temperature then begins to rise and deviate from the other temperatures being plotted, indicating that operator intervention is required to reduce the LPG input.

During the gasification stage when char is circulating around the plant, the siphon tends to have the highest temperatures measured by thermocouples to be as high as 840-850°C. This is undesirable in case it causes clinker to form resulting in blockages and necessitating shutdown of the plant. It has been discovered that when more fluidizing air is introduced into the siphon, that the siphon temperatures increase as the char amongst the bed material combusts. This is one of the reasons why it is desirable to convert the siphon over to steam fluidization during gasification conditions as discussed in Section 3.1.3. When a blockage

does occur in the siphon due to the ratio of char to bed material being too high, the flow of material through the siphon is grossly hindered and often the char needs to be burned out before material can continue circulating.

Preliminary hot test runs on the gasifier have revealed that the energy balance in the gasifier needs improvement. More heat generation is required in the combustion column relative to the thermal energy requirements of the gasification column. The gasifier was intended to be self sufficient with its energy requirements, where the combustion of charcoal from the gasification column was expected to generate enough heat to support the gasification reactions. However, 13-19 L/min of additional LPG firing is required in the combustion column usually to maintain steady gasification temperatures under a range of operating conditions. About 4-8 % excess oxygen is present in the flue gas, because of the high quantities of primary air introduced to entrain bed material, which also ensures complete combustion occurs. The large heat losses from the gasifier and poor waste heat recovery from the flue gas means that higher levels of fuel need to be combusted for heat generation than would otherwise be necessary in this plant.

A limitation with FICFB gasifiers is that the thermal energy generation in the combustion column relative to the thermal energy requirements in the gasification column are rather constrained. Changing the feed rate into the gasifier does not change this, as higher fuel feed rates mean that more heat is required for the endothermic pyrolysis-gasification reactions in proportion to the increased heat generation from the exothermic combustion process. Hence the energy balance in this FICFB gasifier is highly coupled, and only factors such as additional firing of fuel into the combustion column, or changing the residence times of the combustion stage relative to the residence time of the gasification stage, can change this situation. The lack of additional firing in the combustion column significantly constrains the flexibility of any FICFB gasifier's performance!

In a larger scale gasifier aiming to only consume renewable fuels, a method to decouple the thermal energy balance between the reactors would be required without continuous firing of fossil gases such as LPG. A method to achieve this might be to have an independent auger to feed biomass directly into the combustion column. Experience on the 100 kW lab scale plant at the University of Canterbury has revealed that fuel particles such as wood pellets are not conveyed out of the combustion column until they have combusted to a small enough size to

be entrained. This means they remain in the combustion column generating heat for the process. Alternatively a slip stream of producer gas can be introduced and combusted, but this has the disadvantage of reducing the final producer gas yield from the gasifier.

Designing a FICFB gasifier so that the fuel particles obtain the correct residence times during the gasification and the combustion processes is highly important. The relative heights of the fluidized beds and the fluidizing regimes are likely to influence the residence times of fuel particles in the different stages. A practical way to increase the residence time of the fuel particles in the combustion column of FICFB gasifiers may be to operate the gasifier with different bed depths in the combustion column. This is further discussed in Section 3.2.4 based on the principle that on average fuel particles should spend longer in a deeper fluidized bed before rising above the level of the primary air jets and being entrained back to the gasification reactor. This should change the thermal energy balance between the processes in the two reactors.

6.2.2 Bed Material Particle Size Distribution and Entrainment Analysis

Greywacke sand was initially used as the gasifier bed material because it is a readily available aggregate in New Zealand. It was discovered that the size distribution of the bed material is very important. Most fines below 200 μm need to be removed because the flue gas cyclone does not effectively separate and return the finer particles into the circulation loop, and instead they are lost with the flue gas. This also causes larger sized bed material particles to be drawn out of the gasifier system with the fines and overall excessive bed material losses occur. All particles over 1 mm in diameter are removed before use in the gasifier because of the excessively high velocities required to entrain them up the combustion column. The common particle distribution of the greywacke bed material used in the FICFB gasifier is shown in Figure 6.1.

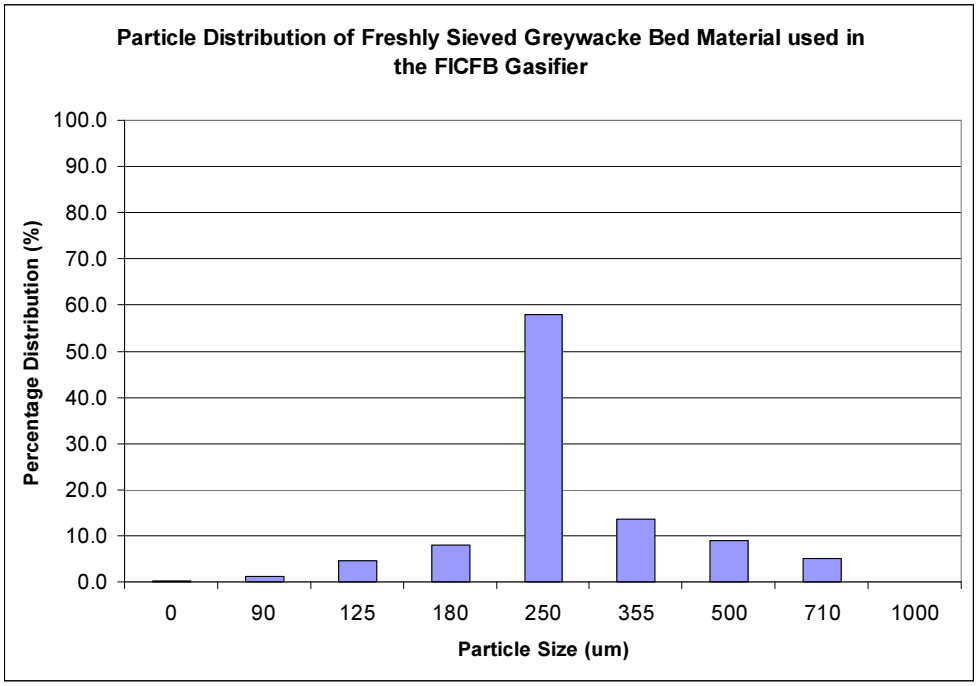

Figure 6.1: The usual particle distribution of the bed material used in the FICFB gasifier. (58 % of the particles are in the size range from 250 to 355 μm).

It was found that introducing higher levels of primary air of around 860 L/min (12.5 on the primary air rotameter), increased the heating up rate of the gasifier by supplying more oxygen with the LPG for combustion. However, when the primary air is set at this level, it can cause undesirable bed material loss. Bed material can pass out the flue gas line because the cyclone does not efficiently separate out the sand particles from the exiting flue gas stream at high primary air flow rates. Since most fines below 200 μm are now removed, this problem has been substantially reduced. It still appears to be a balance between having high levels of primary air to minimise the heating up period of the reactors and maintaining the bed material loss rates at an acceptable level.

In early gasifier trials, bed material loss rates from the reactors was as high as 38 % with 12 kg of bed material being used in a 10-11 hour test run. This has now been substantially reduced to 7-9 % by better controlling the intensity of the combustion regime in the gasification reactor during the heating-up phase, and removing the particles below 200 μm. It has been found that most of the bed material loss taking place at the time of writing this thesis occurs out of the gasification reactor during the heating-up stage of a test run. The erupting LPG bubbles in the BFB, project particles into the upper freeboard region of the gasifier and

they get entrained out the producer gas line. This is clearly visible when looking into the gasification column through a view port.

A set of calculations was performed to compare the superficial velocity in the gasification reactor, to the terminal velocity of the different particle size groups in the greywacke bed material at 25 °C and 700 °C. These two temperatures represent conditions at the beginning and near the end of the heat-up phase of the gasifier's operation. This assessment was performed to see what particle sizes are likely to be entrained out under normal superficial flow rates. The effects of combustion in the BFB were initially ignored, yielding an average superficial velocity of 0.16 m/s. The calculations can be found in Appendix D.

After completing the calculations, all terminal velocities for particle size groups larger than 90 microns were found to be above the superficial velocity of 0.16 m/s. Therefore entrainment of particles in the size ranges analysed should not be occurring unless the superficial velocity of 0.16m/s is sometimes exceeded. From visual observations into the gasification column, it can be clearly seen that the sporadically combusting bubbles of LPG and air send a spray of particles up in the gasification column, often nearing the entry port of the producer gas line leaving the reactor. So the violently combusting bubbles of LPG during the heat-up phase are responsible for the majority of the bed material loss. To reduce this problem, the quantity of LPG and amount of fluidizing air introduced into the gasification reactor was reduced. The BFB fluidizing air must be kept below 67 L/min (corresponding to eight on the rotameter scale) with the greywacke bed material used, and the LPG flow rate was adjusted to maintain about 6 % excess oxygen during heating up.

By keeping the fluidizing air below this threshold, the combustion regime in the BFB is more sedate and fewer particles are projected into the upper freeboard region of the reactor and drawn out. This does not adversely affect the heating up rate of the reactors; as the circulation of hot sand from the combustion column transfers enough heat to bring all regions of the plant satisfactorily up to operating temperature. Bed material loss rates have now been reduced to 7-10 % of the 12 kg of bed material used in the gasifier under hot testing periods of 9-11 hours. This loss rate could be further reduced if the freeboard height in the reactor was larger and/or a larger internal diameter was designed in the freeboard region of the reactor to reduce the velocities up the column.

6.2.3 Agglomeration Problems with the Bed Material

Repeatedly during the preliminary hot testing phase of the gasifier, the bed material in the gasifier stopped circulating between the reactors. This occurred either in the final stages of heat up just before actual gasification occurred, or when the transition to gasification of wood pellets first begun. The cause of the problem was the fusing of bed material often into a large chunk immediately above the fluidizing nozzles on the combustion column distributor. However, sometimes clinker also formed in the chute and in the gasification reactor. Because the chute passes bed material into the base of the combustion column immediately above the CFB distributor, clinker in the CFB prevents bed material being circulated between the reactors. Figure 6.2 shows the base of the combustion column with the distributor removed, and Figure 6.3 shows a chunk of agglomerated bed material in the base of the combustion column.

The agglomeration problems were caused by softening and fusion of the inert components in the bed material. The composition of the greywacke and olivine bed materials can be seen in Appendix G, Table G1 and G2 respectively. The role of any ash introduced from the wood pellets forming a eutectic is unknown, but it appeared to be largely a function of temperature and bed material composition. This conclusion was drawn because the same clinker problems occurred irrespective of whether wood feed had begun or not.

Figure 6.2: View looking from the underside of the combustion column up the inclined chute when it is empty. The combustion column distributor has been removed and the two perforated tubes of the fluidizing sparger can be seen in the chute.

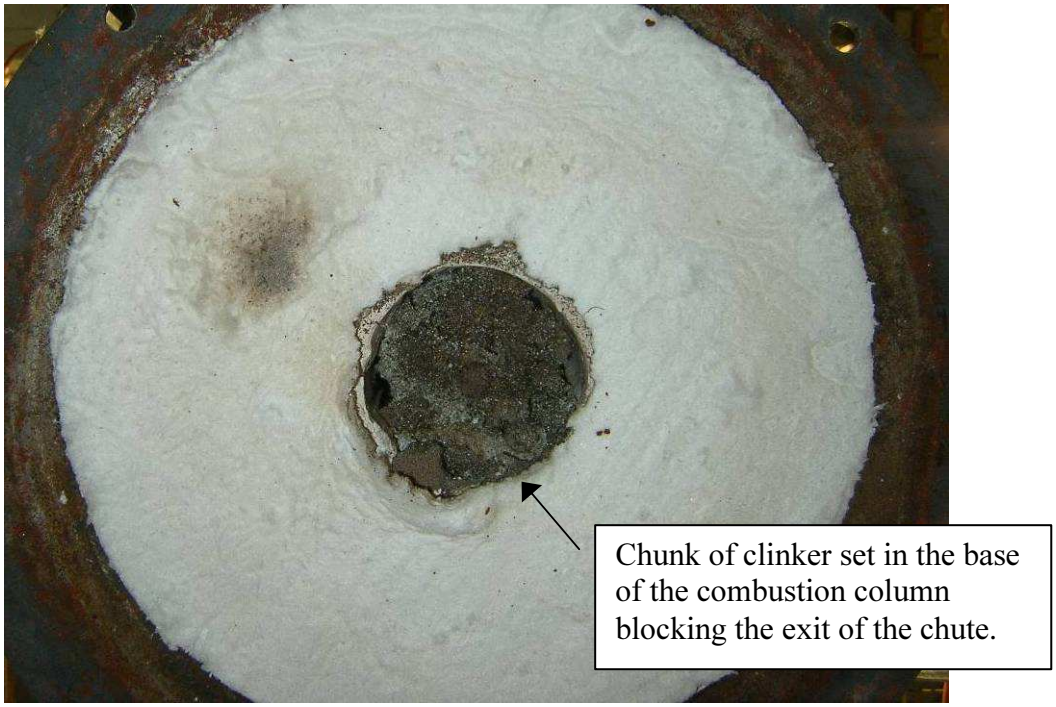

Figure 6.3: A view from below looking up at agglomerated bed material (clinker), blocking the base of the combustion column. This chunk was 100 mm in diameter and approximately 80 mm high. It caused all circulation to cease in the gasifier since it blocked the base of the CFB and chute.

A set of regression formulas shown in Appendix H was applied to the greywacke bed material and the wood pellets to estimate their fusion temperatures. These formulas's used the ultimate analysis data for the wood and greywacke bed materials shown in Appendix A and G respectively. The fusion temperatures were defined as the 'softening temperature' for the inert components in the materials. This was considered to represent the on set of particle agglomeration.

The fusion temperature of the greywacke sand was indicated as being around 835 °C, which reflected the operating temperatures that circulation often ceased at (commonly around 840 °C and above). The fusion temperature of the wood pellets was calculated as being significantly higher, estimated from the regression formulas to be about 1300 °C. This temperature was higher than expected and has not been clarified for accuracy, but experience with the 100 kW gasifier suggests that the wood pellets have no significant influence on the fusion problems which were encountered. Some hot tests were performed with olivine bed material (forsterite). One of these tests will be discussed later, but from the regression formula's, olivine bed material was expected to have a fusion temperature of around 1295 °C.

Operational experience with olivine does not align with this high fusion temperature as clinker formed on each of the olivine test runs performed with peak operating temperatures of 740 °C and 845 °C (measured in the siphon).

To rectify the agglomeration problems, a number of methods were applied. Firstly, the gasification process was operated at a lower overall temperature. Instead of heating the gasification column up to 800 °C or above, and then beginning gasification of wood, gasification was instead initiated at 750 °C and all plant temperatures were prevented from exceeding about 820 °C. Combustion temperatures are always higher than the gasification temperatures since heat is transferred by the circulating bed material between the reactors, and heat losses occur as the sand moves around the plant. Additionally, the endothermic gasification reactions consume thermal energy. So for any given temperature in the gasification column, the temperatures in the combustion column are always greater.

Secondly, it was noted that almost always, the clinker formed immediately above the nozzles of the distributors. This is where premixed LPG and air pass into the reactors amongst the bed material during the heat-up stage. It was realised that the combusting LPG creates high localised flame temperatures in the region directly above the fluidizing nozzles. To avoid peak flame temperatures being reached that occur during stoichiometric combustion of a fuel (Kehlhofer *et al.*, 1999), the fuel to air ratio for the LPG is now kept rich. Lastly, it became apparent that keeping the beds fluidized at all stages during heat-up was essential to maintain adequate heat distribution and prevent hot-spots forming in the bed immediately above the distributor nozzles.

By maintaining a rich flame, keeping the beds fluidized and preventing reactor temperatures exceeding 820 °C, all fusion problems with the greywacke bed material were alleviated. It is hoped that other types of bed material testing will follow; comparing their producer gas and tar data with the base results obtained using the greywacke bed material discussed throughout Section 6.3.

6.2.4 **Ash Removal Effectiveness and Analysis**

The hot testing performed with the 100 kW FICFB gasifier has confirmed that ash removal is very effective in this design of plant. Traditionally this is a challenging area for engineers, but no ash has ever accumulated in the reactors during operation of the FICFB gasifier. This is believed to be due to the design of this gasifier, where superficial gas velocities in both reactor columns are significantly higher than in most other gasifier types. The high superficial gas velocities efficiently entrain the light ash components out of the gasifier where they are collected in the particle traps in the producer gas and flue gas lines. Of more concern with the current plant design is the constant loss of bed material from the reactors which also removes the ash.

A proximate and an ultimate analysis were performed on material collected in the producer gas cyclone particle trap. The location of this particle trap can be seen in Figure D1 of Appendix D and the proximate and ultimate analysis results are presented in Appendix I. The proximate analysis revealed the sample contained about 48 % inert matter (ash plus sand), 42 % fixed carbon, 7 % moisture and 3 % volatile matter on an as-received basis. The low volatile content indicates that the sample contained little tar (Murray, 2008) and the pyrolysis reactions well approach completion. The gross calorific value of the sample was 14.8 MJ/kg (as-received basis). This was higher than expected but is a result of the high carbon content in the sample.

Of the 48 % inert matter, the majority was the bed material which had been entrained out of the gasification reactor. The ultimate analysis measured 39 % carbon from the char and tar amongst the sample, of which the majority was fine char particles smaller than 250 μm. Although this seems like an unfavourable level of fine char is being lost out with the producer gas unreacted, normally only 0.44 kg/h of total matter is collected in the producer gas particle trap with a wood pellet feed rate of 18.4 kg_{dry}/h. More char is probably lost out of the flue gas line with its higher velocities but fine char is not effectively collected in the flue gas particle trap because it gets entrained back out of the unit. In a larger scale plant it could be feasible to tolerate these loss rates and collect and screen the material so that it can be reintroduced back into the gasification reactor.

6.3 Description of Investigative Hot Tests Performed on the 100kW Gasifier

After the extended constriction phase on the gasifier, and completion of the cold testing and the preliminary hot testing phase, the 'investigative' hot testing regime to improve the producer gas composition and study plant performance began. All these tests were performed with New Zealand radiata pine wood pellets. The investigative hot tests performed up until 17 March 2008 included varying the following parameters:

1. Varying the wood pellet feed rate (using 12 kg of greywacke bed material and the original over-bed auger).
2. Varying the amount of steam into the gasification reactor (using 12 kg of greywacke bed material and the original over-bed auger).
3. Operating with a higher than usual bed material loading (using 20 kg of greywacke bed material instead of 12 kg) and varying the wood feed rate. (Using original over-bed auger).
4. Varying the gasification temperatures throughout a range between 640-760 °C. (Using 12 kg of greywacke bed material and the original over-bed auger).
5. A steady state run where the gasifier was operated without varying settings. (Using 12 kg of greywacke bed material and the original over-bed auger).
6. Using olivine bed material with varying fuel feed rates (using 12 kg of olivine bed material and the original over-bed auger).

During these investigative hot tests, tar samples were collected in SPE columns, but these had to be stored as the method of analysis for the tar samples was still being developed at the University of Canterbury. A commercial laboratory was contracted to analyse ten tar samples, six of which were obtained from the 'gasification temperature' test of Section 6.3.4 and four which were obtained from the 'gasification steam variation' test of Section 6.3.2. This was done to verify that the quality of the tar samples was sufficient before this method of collection and analysis was further pursued at the University of Canterbury. Unfortunately this was not established in time for the writing of this thesis, so tar quantities generated during the other investigative hot tests cannot be reported upon.

All the gasifier tests were performed with the original over-bed auger feed system. The intention is for following researchers to test the new in-bed auger feed system (described in Section 3.1.11), and compare the gas composition and performance results against the results presented in this thesis. All investigative hot tests have the test date clearly stated so that following researchers on the gasifier project can easily revisit the original test data. The measured producer gas compositions are tabulated in Appendix J and the method used to calculate the LHV's of the producer gas is shown in Appendix K. All producer gas yields are expressed on a dry, tar-free basis in Nm^3/h. Hence, they represent only the volume of producer gas being generated per hour, excluding the volume occupied by moisture or tar in the producer gas. Moisture and tars are measured and reported separately.

The cold gas efficiency is regularly discussed in the following sections and is calculated on a LHV dry gas basis as shown in Appendix L. The supplementary firing of LPG (100 % propane) in the combustion reactor with the char is included, plus the energy required to externally generate the different quantities of steam introduced at a temperature of 200 °C. Note the amount of supplementary LPG was occasionally varied during a test run to try to maintain constant gasification temperatures with the testing conditions changing. The small amount of heat contributed from the pilot burner in the combustion column is considered negligible and not included in the cold gas efficiency calculation.

6.3.1 Assessment of varying Fuel Feed Rate

The first investigative hot test to be performed on the 100 kW FICFB gasifier was studying what effect fuel feed rate had on the producer gas composition and the overall gasifier's performance. This was chosen as the first testing parameter because it was the easiest process variable to adjust. The feed rate of wood pellets was varied over a range from 11.2-24.8 kg_{dry}/h (59 kW fuel input to 131 kW fuel input). This test was performed on 7 February 2008. The experimental procedure followed can be found in Section 4.2. The results from the microGC of the change in the producer gas composition with varying fuel feed rate can be seen in Figure 6.4. The overall plant performance is displayed in Table 6.1.

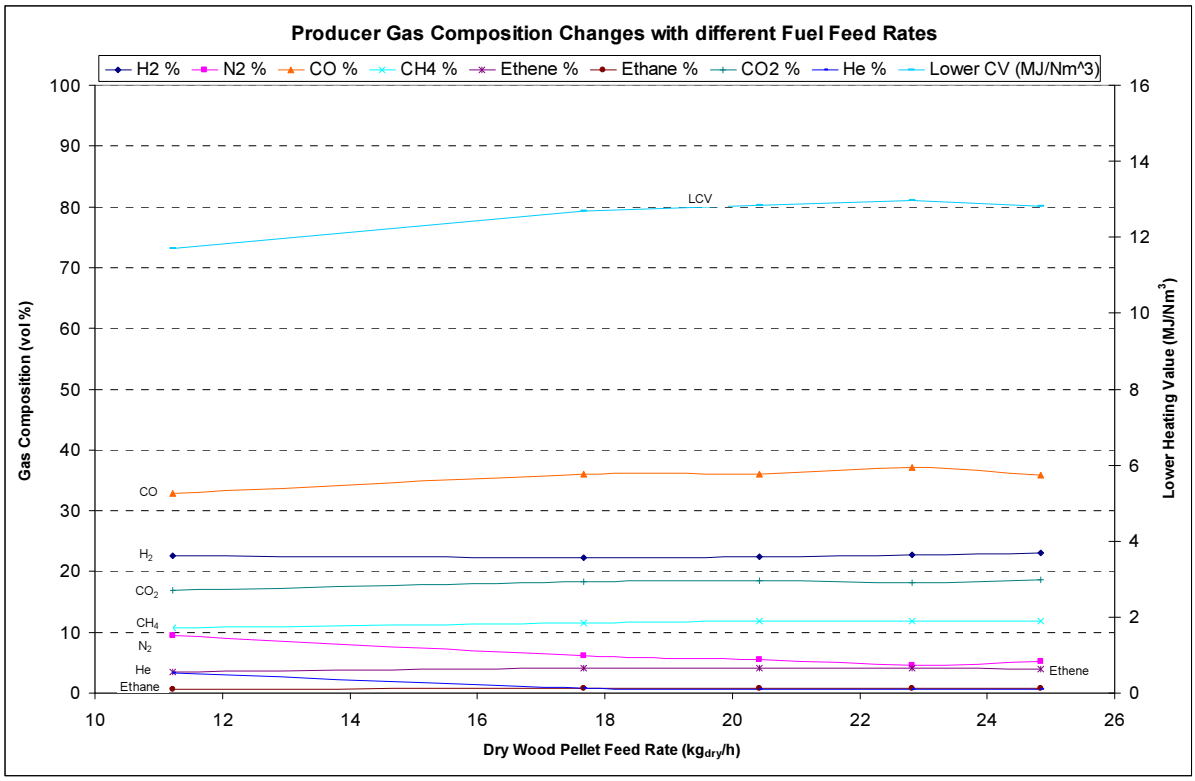

Figure 6.4: Plot of the producer gas composition as the feed rate of wood pellets into the gasifier is changed from 11.2-24.8 kg_{dry}/h. (Note: the helium tracer gas was set at a lower flow rate after the 11.2 kg_{dry}/h data set).

Table 6.1: Gasifier performance parameters when fuel feed rate is varied. (Small fluctuations in the tracer gas flow rate caused the producer gas yield not to be sequential).

Dry Wood Feed Rate (kg_{dry}/h)	LCV (MJ/Nm^3)	Producer Gas Yield (Nm^3/h)	Combustion Energy of Producer Gas (kW)	Cold Gas Efficiency (%)
11.2	11.7	7.0	22.9	26
17.7	12.7	9.3	32.7	27
20.4	12.8	9.9	35.4	26
22.8	13.0	12.2	43.9	29
24.8	12.8	11.4	40.6	27

The conditions of the test were: a gasification temperature maintained between 704-723 °C, a total steam input rate between 9.8-10.4 kg/h and a primary air flow rate of 835 L/min. This was the first time the helium tracer gas injection method was set up to measure the producer gas flow rate and it was found that a helium flow rate of 1.29 L/min was sufficient to provide a tracer gas concentration of less than 1 % in the final gas mix.

The most noticeable effect of increasing the feed rate of wood pellets from 11.2-24.8 kg_{dry}/h was the quantity of producer gas generated. As the feed rate increased by 121 % the quantity of producer gas generated increased by 63 %, from 7.0-11.4 Nm^3/h. Correspondingly combustion temperatures also increased from 793 °C to 816 °C in the upper part of the combustion column as a greater amount of char was circulated through.

The main reason for the higher producer gas yield was the increase in the amount of pyrolysis gases being evolved as more wood was supplied. Correspondingly gasification temperatures progressively decreased as the endothermic gasification reactions drew more thermal energy from the circulating bed material.

The lower calorific value of the producer gas increased as the wood pellet feed rate increased. This began at 11.7 MJ/Nm^3 and reached 12.8 MJ/Nm^3 when the feed rate was 24.8 kg_{dry}/h. The two contributing factors to the LHV increase were: resetting the helium tracer gas to a lower flow rate, and the decrease in the relative proportion of nitrogen as more producer gas was generated. The proportion of nitrogen in the producer gas decreased because the bulk of the nitrogen is not introduced from the fuel. Most of the nitrogen enters the gasification reactor from air leaking up the chute (from the combustion column) and the purge gas from the fuel auger. This quantity of introduced nitrogen is static so any increase in the total producer gas yield reduces the volume percentage of nitrogen in the final gas composition.

Due to the larger producer gas yield with higher wood feed rates, the total combustion energy output from the gasifier increased from 23-41 kW. However the cold gas efficiency remained about the same at approximately 27 %. This is because both the total energy of the producer gas and the feedstock input to the plant both increased by similar proportions (see the cold gas efficiency formula in Section 2.1.6).

Since the steam input rate into the gasification reactor was kept constant and the fuel feed rate was varied, this caused the steam to biomass ratio to also change during the test. The steam to biomass ratio varied from 0.93 $kg/kg_{pellets}$ at a feed rate of 11.2 kg_{dry}/h, to 0.39 $kg/kg_{pellets}$ at a feed rate of 24.8 kg_{dry}/h. Despite this change, the gas composition did not change very much. From the point of view of maximising the LHV of the producer gas, running the gasifier with higher feed rates is most favourable to dilute any non-fuel gases such as nitrogen.

6.3.2 Assessment of varying the amount of Gasification Steam

The second investigative hot test to be performed on the gasifier was changing the amount of steam supplied to the gasification reactor. This test was performed on 15 February 2008. Only the fluidizing steam introduced through the distributor at the base of the gasification reactor was varied. The chute fluidizing gas is believed to enter the gasification column and contribute to the total steam input into the gasification reactor. The amount of steam supplied to the chute was kept constant at 4 kg/h so that minimal secondary changes occurred in the plants operating conditions such as inconsistency in the circulation rate of bed material.

The amount of total steam supplied to the gasification reactor was varied from 7.1-15.4 kg/h in nine incremental steps. This meant the steam to biomass ratio varied from 0.39-0.84 $kg/kg_{pellets}$ respectively. Readers should be aware that the steam to biomass ratio is calculated on the amount of steam introduced into the gasifier, and does not take into account the degree of water/steam conversion in the gasification reactions. A minimum steam flow rate of 3 kg/h was passed through the gasification column distributor to keep the BFB fluidized. Figure 6.5 shows the producer gas composition plot and Table 6.2 the overall plant performance results.

The conditions of this test were: a wood pellet feed rate of 18.4 kg_{dry}/h with a constant helium (tracer gas) injection flow rate of 1.29 L/min. A gasification temperature of around 725 °C, a chute steam flow rate of 4.0-4.2 kg/h and a primary air flow rate maintained close to 850 L/min. The experimental procedure followed can be found in Section 4.2.

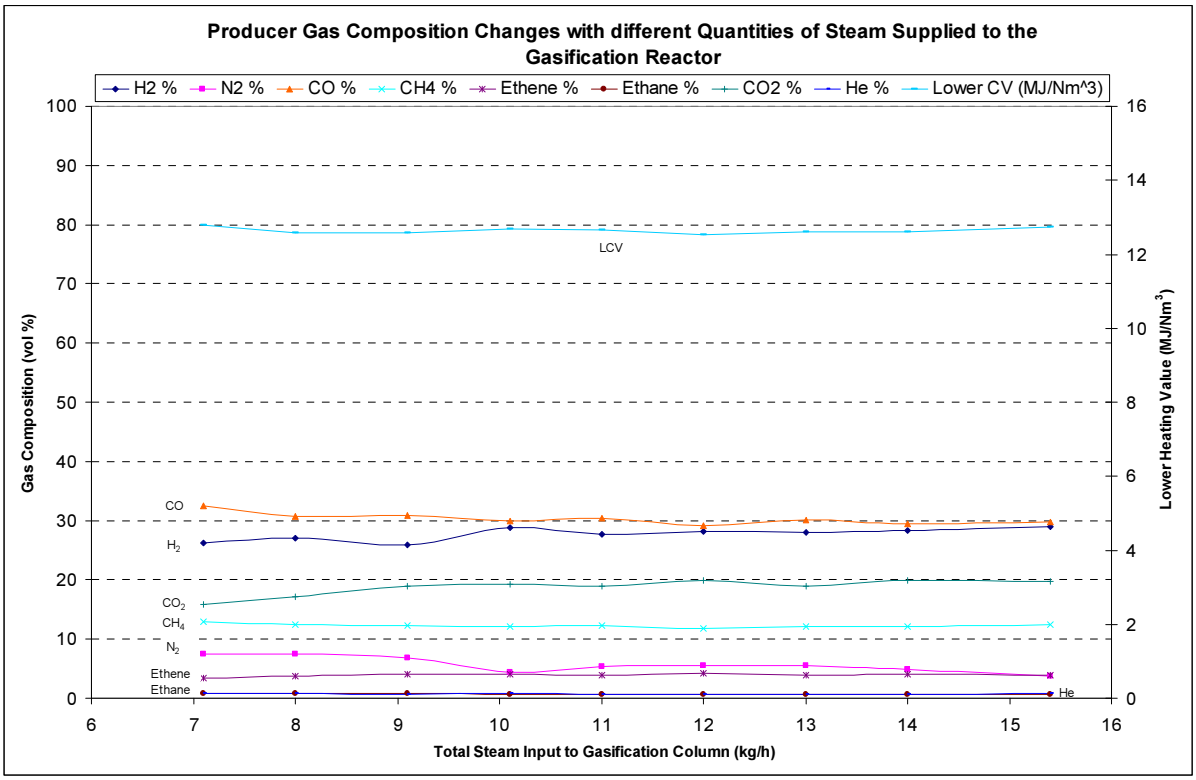

Figure 6.5: Changes in the producer gas composition as the amount of steam supplied to the gasification reactor is varied.

Table 6.2: The overall performance values for the gasifier when steam rates are varied. (Small deviations in the tracer gas flow rate caused the producer gas yields to waver).

Total Steam into Gasification Reactor (kg/h)	Steam to biomass ratio	LCV (MJ/Nm^3)	Producer Gas Yield (Nm^3/h)	Combustion Energy of Producer Gas (kW)	Cold Gas Efficiency (%)
7.1	0.38	12.8	8.6	30.4	24
8	0.43	12.6	9.0	31.4	24
9.1	0.49	12.6	10.8	37.8	30
10.1	0.55	12.7	9.6	34.0	27
11	0.60	12.7	10.6	37.2	29
12	0.65	12.5	10.6	36.9	29
13	0.71	12.6	10.8	37.8	30
14	0.76	12.6	10.3	36.2	29
15.4	0.84	12.7	9.2	32.7	26

Changing the amount of total steam introduced into the gasification reactor had little effect on changing any of the overall performance parameters that were measured on the plant. The total producer gas flow rate did appear to generally increase in approximate proportion to the greater amount of steam being introduced, but wavered noticeably and remained in the range of 8.6-10.8 Nm^3/h. Unfortunately the gasifier was not equipped with a method to regularly monitor the change in the humidity of the producer gas, so it has to be assumed that humidity increased with increasing amounts of steam being supplied to the gasification reactions. This is the trend found from other researchers with the FICFB gasifier at Vienna University of Technology, as discussed in Section 2.2.3.

In steam blown gasification, literature suggests that the majority of the hydrogen found in the producer gas is supplied from the introduction of steam to the reactor and not from the feedstock (see Section 2.1.5). Surprisingly the concentration of hydrogen in the producer gas did not change much as the amount of steam supplied to the gasification reactions increased by 117 %. The hydrogen concentration stayed between 25-29 vol% as plotted in Figure 6.5. However, the proportion of carbon monoxide decreased slightly from 33-30 vol%, with the shift mainly occurring at the lower steam injection rates. Carbon dioxide showed the opposite trend where its concentrations increased slightly from 16-20 vol%, again mainly at the lower steam injection rates tested. This is likely to be due to the water-gas shift reaction being influenced where the presence of more steam causes more carbon monoxide to be consumed and yields larger quantities of carbon dioxide and hydrogen. The water gas shift reaction is:

$$CO + H_2O_{(g)} \Leftrightarrow CO_2 + H_2$$

As seen in Table 6.2, the lower calorific value of the gaseous mix changed very little about 12.7 MJ/Nm^3. The total combustion energy output and cold gas efficiency of the gasifier ranged from 30-38 kW and 24-30 % respectively. These values were consistent with the previous test and upon analysis of the results displayed in Table 6.2, it appears that running the gasifier with a steam to biomass ratio in the vicinity of 0.45-0.7 kg/kg_{dry} is most favourable when a medium LHV gas is desired while limiting the amount of steam that needs to be generated. The 8 MW FICFB gasifier in Güssing, Austria operates within this range (see Section 2.2.3).

Four tar samples obtained during this test were sent to a commercial laboratory for analysis. Figure 6.6 shows the graphed results where 16 polycyclic aromatic hydrocarbons (PAH's) from the SPE columns were analysed. Sixteen individual tar components were summed to obtain a total quantity of tars for each of the four samples. Too few samples were analysed to conclude a trend, however researchers at Vienna University have found that tar levels in producer gas generally decrease as a greater ratio of steam to biomass is introduced into the gasification reactor (see Figure 2.15). The tar levels in the producer gas ranged between 2.5-3.5 g/Nm^3. Table 6.3 shows the quantities of the 16 individual tar components and their abundances. Since 100ml of dry producer gas was drawn through the SPE columns, the units of µg/sample can be converted into g/Nm^3 by multiplying by 1000 L/m^3 x 303K/273 K. (Since the 100ml of producer gas is cooled to approximately 30 °C in the sampling syringe).

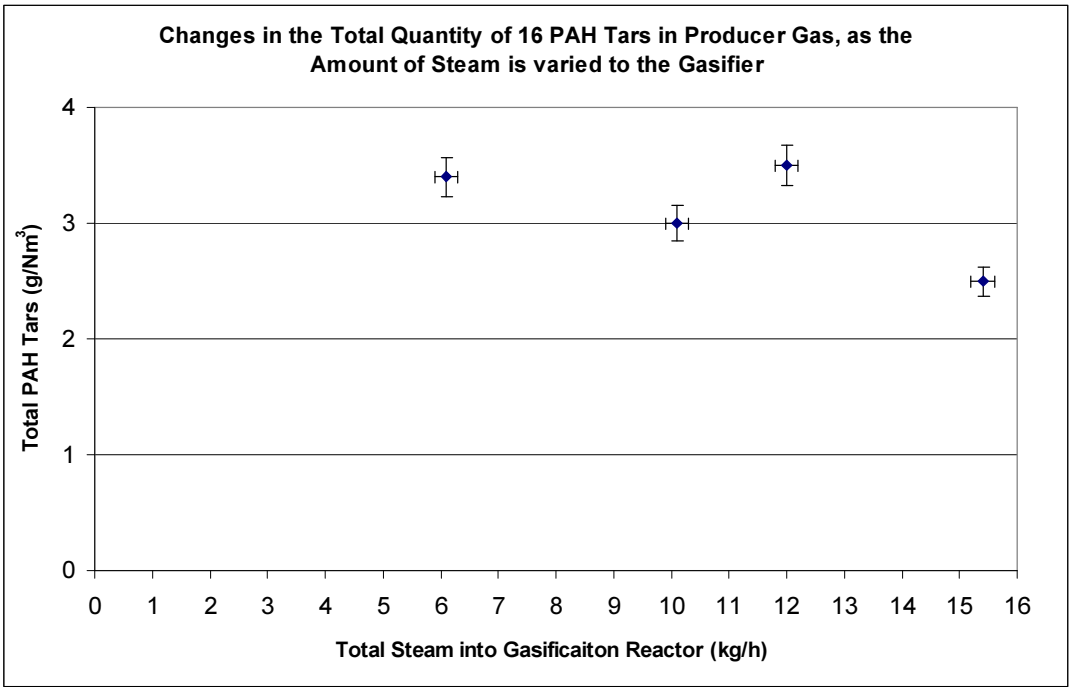

Figure 6.6: Summation of 16 PAH tars from the producer gas as measured by GC-MS at four different steam injection rates into the gasification reactor. (Experimental errors could only be determined for the accuracy of drawing a 100ml gas sample in the y-direction, since the method of tar extraction and analysis by the commercial laboratory was not revealed).

Table 6.3: Data from GC-MS analysis of 16 PAH tar components in the producer gas.

Steam to gasification reactor: Units:	**6.1kg/h** µg/sample	**10.1kg/h** µg/sample	**12kg/h** µg/sample	**15.4kg/h** µg/sample	Percentage (%)
Acenaphthene	9.2	7.9	8.5	7.6	3.0
Acenaphthylene	83.4	78.7	89.7	68.7	28.8
Anthracene	14.7	12.7	15	13.1	5.0
Benzo[a]anthracene	4.7	3.6	3.9	3	1.4
Benzo[b]fluoranthene	4.4	3.4	4.1	2.8	1.3
Benzo[a]pyrene (BAP)	4.3	3	3.5	2.4	1.2
Benzo[g,h,i]perylene	1.8	1.1	1.2	0.9	0.5
Benzo[k]fluoranthene	1.9	1.3	1.6	1.1	0.5
Chrysene	4.2	3.2	3.6	2.7	1.2
Dibenzo[a,h]anthracene	1.2	0.7	0.7	0.5	0.3
Fluoranthene	11.4	9.4	10.8	9.6	3.7
Fluorene	31.1	29.3	34.3	28.3	11.1
Indeno(1,2,3-c,d)pyrene	2.3	1.3	1.6	1	0.6
Naphthalene	72.2	64.6	77.5	37.5	22.7
Phenanthrene	42.8	37.2	44	39.8	14.7
Pyrene	12.7	10.2	11.5	9.8	4.0
Total of 16 PAH (µg/sample)	*302*	*268*	*312*	*229*	Total 99.3%
Total PAH Tars in g/Nm^3	**3.4**	**3.0**	**3.5**	**2.5**	

The data in Table 6.3 indicates that acenaphthylene at 28.8 %, is the most abundant tar component followed by naphthalene at 22.7 %. The next four most abundant tars were phenanthrene at 14.7 %, fluorine at 11.1 %, anthracene at 5 % and pyrene at 4 %. The most abundant tar components displayed in Table 6.3 are similar to the most abundant tar components found by the researchers at Vienna University with their 100 kW FICFB gasifier fuelled with wood pellets. The reader must be aware that the quantity of total tars could be understated as it was not known if other tar components were present and if some tar components evaporated during storage before the analysis occurred.

6.3.3 Assessment of Gasifier Performance with a High Bed Material Loading

This gasifier test was somewhat different to the others as it was performed to observe how the gasifiers operation was influenced when using a greater loading of greywacke bed material (20 kg instead of the usual 12 kg). The reason for this test was that other FICFB gasifiers such as the one situated at Vienna University of Technology in Austria, use a much greater bed material loading than the gasifier at the University of the Canterbury does for a similar sized plant. The gasifier at Canterbury University does not have a way to increase the quantity of bed material during operation so this parameter could not be varied during

operation. To obtain more than one set of data points the wood pellet feed rate was instead varied between 10.5-25.6 kg_{dry}/h with a 20 kg loading of bed material.

This test was performed on 19 February 2008. The experimental procedure followed is outlined in Section 4.2. Figure 6.7 shows the producer gas composition plot and Table 6.4 shows the overall plant performance results. The conditions of the test were: 20 kg of greywacke bed material used rather than the usual 12 kg, and a gasification temperature between 712-727 °C. The chute steam input rate was around 4 kg/h and the BFB steam input rate was kept between 6-6.5 kg/h. The primary air flow rate remained between 835-855 L/min.

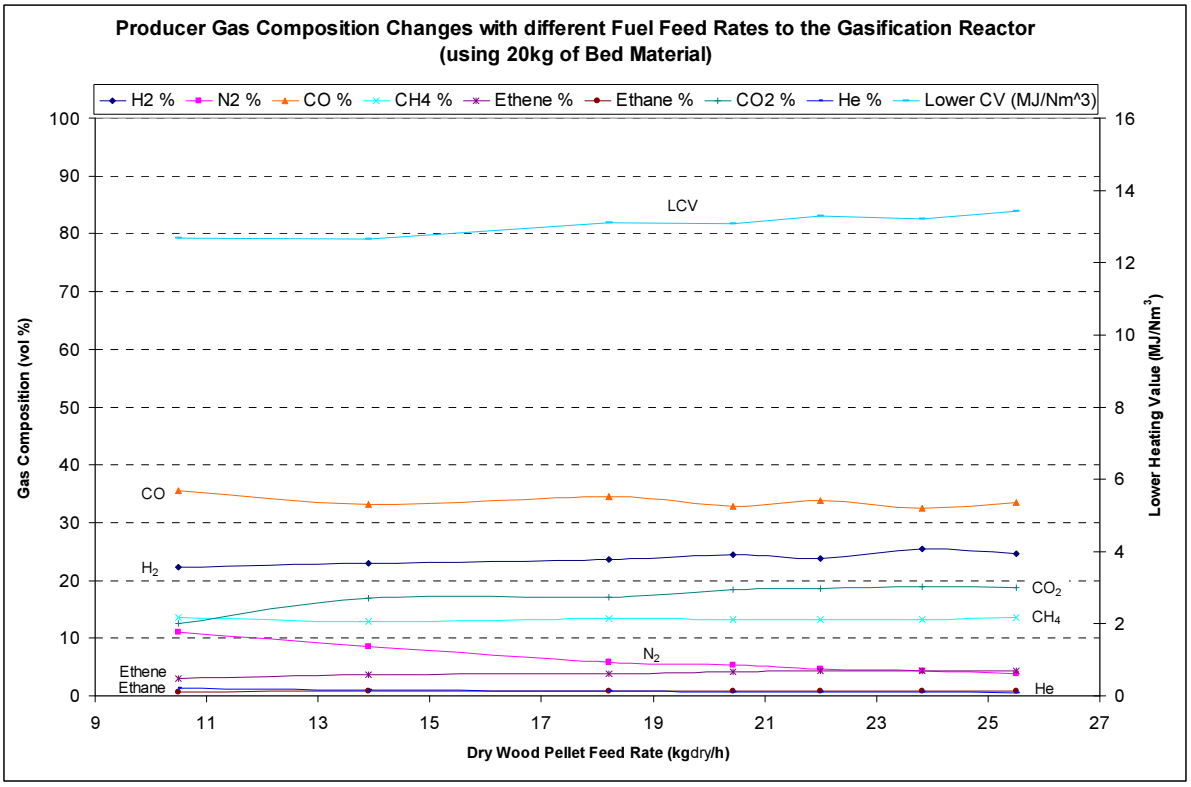

Figure 6.7: Plot of the producer gas composition and LHV of the gas as wood feed rate is varied using 20 kg of bed material instead of the usual 12 kg. (Note a small air leak occurred when obtaining the first producer gas sample).

Table 6.4: Overall plant performance parameters while using 20 kg of greywacke bed material.

Dry Wood Feed Rate (kg_{dry}/h)	LCV (MJ/Nm^3)	Producer Gas Yield (Nm^3/h)	Combustion Energy of Producer Gas (kW)	Cold Gas Efficiency (%)
10.5	12.7	5.1	17.8	21
13.9	12.6	6.5	22.9	23
18.2	13.1	8.5	31.0	24
20.4	13.1	10.3	37.4	27
22.0	13.3	11.6	42.6	30
23.8	13.2	10.6	39.0	25
25.6	13.4	12.8	47.9	29

Using 20 kg of bed material caused exceptional running problems and required a significantly extended heat-up period of 8.5 hours instead of the usual 5 hours. This was due to the increased thermal mass of the plant (from the extra bed material), and from the pilot burners frequently cutting out. The height of the sand inside the reactor columns was so high that it partly submerged the pilot burners, (especially in the combustion column). For safety reasons, when a pilot burner (for ignition purposes) cuts out, the LPG supplied through the distributor at the base of that reactor is automatically shut off. This meant regular operator intervention was required to restart the burners, slowing the heat-up period.

A high loss rate of bed material occurred during this test run (40 % instead of the usual 7-9 %), partly due to the extended heating-up phase and the fact that the freeboard heights in the reactors were reduced. It was also noted that as the amount of bed material used in the gasifier increases, the amount of primary air required to achieve normal levels of circulation decreases. This is thought to be because a greater quantity of bed material is available above the elevation of the primary air jets which entrain sand and char around the gasifier circuit.

The most significant result from increasing the wood pellet feed rate from 10.5-25.6 kg_{dry}/h, was the notable increase in the volume of producer gas generated. This increased from 5.1-12.8 Nm^3/h, an increase of 151 % as wood feed rate increased by 144 %. This is believed to be mainly due to the increased quantity of pyrolysis gas evolved from the volatile component of the wood, as discussed in Section 6.3.1. When comparing the first feed rate test (Section 6.3.1) to this test, the producer gas yields were about 5 % lower. This is likely to reflect small

differences in test conditions such as gasification temperature and the amount of supplementary LPG firing.

The total combustion energy output of the producer gas increased by 167 % from 18 kW at a fuel feed rate of 10.5 kg_{dry}/h, to 48 kW at a fuel feed rate of 25.6 kg_{dry}/h. This was due to the greater quantity of producer gas generated. The LHV of the producer gas increased slightly but remained within the range of 12.6-13.4 MJ/Nm^3. The cold gas efficiency of the gasifier increased from 21 % to around 30 % as the LHV of the producer gas and the gas volumes generated changed. (Note the amount of supplementary LPG in the combustion column sometimes needed changing in order to maintain a constant gasification temperature).

The most noticeable variation in the producer gas composition was the reduction in the proportion of nitrogen. This was due to the increased volume of producer gas diluting the consistent amount of nitrogen which enters the gasification reactor from air leaking through the chute and from the purge gas in the fuel auger. The same trends were noticed in other gaseous components as occurred during the first investigative hot test (of Section 6.3.1), where fuel feed rate was varied using 12 kg of greywacke bed material.

Due to the extended heat-up period and operational problems with the pilot burners, it is recommended that bed material loadings greater than 14-15 kg are avoided in the FICFB gasifier at the University of Canterbury. This constraint is not characteristic of all FICFB gasifiers; it is purely a function of the plant design, especially the height at which the pilot burners are located above the dense phase of the fluidized beds. Additionally, the freeboard height of any FICFB gasifier must be sufficient for the intended bed material loadings, so that entrainment of sand out of the gasification reactor is minimised.

6.3.4 Assessment of varying Gasification Temperature

This hot test was performed on 21 February 2008, to investigated the effect of varying gasification temperature to analyse changes in the producer gas composition, plant performance and the total quantity of tars. Gasification temperatures were varied over a range from 642 °C to 758 °C. Six sets of data were obtained within this range and the producer gas composition is plotted in Figure 6.8 with the overall plant performance results displayed in

Table 6.5. The experimental procedure followed for this test is explained in Section 4.2. The conditions of this test were as follows: the feed rate was held constant at 18.4 kg_{dry}/h. The BFB and chute steam rates were held at 6 kg/h and 4 kg/h respectively. The primary air flow rate was kept between 820-835 L/min to maintain a fixed circulation rate of bed material.

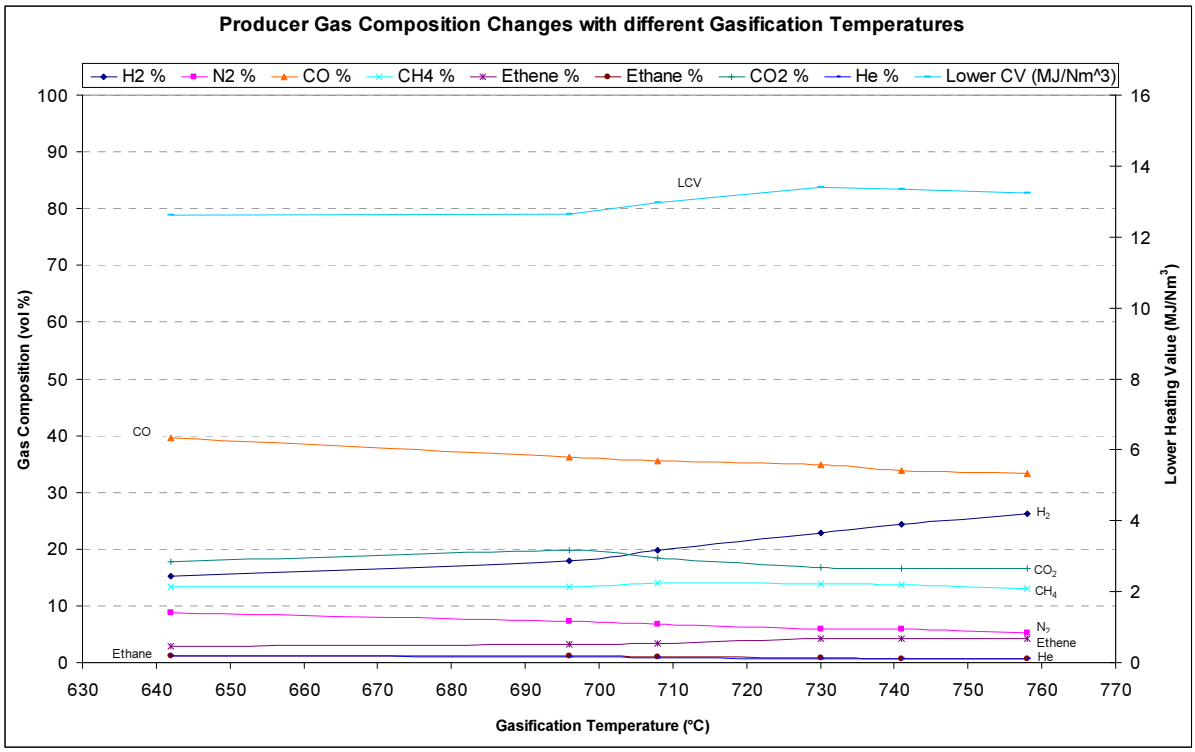

Figure 6.8: The producer gas composition plot for wood pellets at different gasification temperatures between 642-758 °C.

Table 6.5: Overall changes in the gasifiers performance at different gasification temperatures.

Gasification Temperature (°C)	LCV (MJ/Nm^3)	Producer Gas Yield (Nm^3/h)	Combustion Energy of Producer Gas (kW)	Cold Gas Efficiency (%)
642	12.6	6.0	21.1	16
696	12.6	6.8	23.9	19
708	13.0	7.7	27.8	22
730	13.4	10.2	38.0	29
741	13.4	9.4	34.8	26
758	13.2	10.8	39.7	30

The most noticeable effect with changing the gasification temperature was the change in the producer gas yield. This increased by 80 % from 6.0-10.8 Nm^3/h as gasification temperature was varied from 642 °C to 758 °C. The increase in the gas yield is believed to be due to the following factors: Char conversion to gaseous products is likely to be higher at elevated reaction temperatures and the pyrolysis reactions should be more rapid as the heating rate and final temperature of the fuel particles are greater. This might mean that the char is fully devolatilised in the BFB before it passes out of the gasification reactor. It is unclear what residence time is required for the pyrolysis reactions to be completed in the BFB and how long the wood/char remains in there. The water conversion into producer gas products is expected to be higher at elevated temperatures (see Section 2.2.3) and some cracking of higher hydrocarbons and tars could occur at the higher gasification temperatures.

As higher gasification temperatures liberated more producer gas, it became necessary to increase the quantity of additional LPG firing in the combustion column to hold the endothermic gasification reaction temperatures constant. This is partly due to the greater heat loss rates at higher temperature, but it may also be a result of higher char conversion into producer gas components, with less char being available to fuel the combustion process. The cold gas efficiency increased from 16-30 % as gasification temperature increased from 642-758 °C. This is because the higher producer gas yields increased the total combustion energy output (in kW) of the gasifier for the same wood input rate.

The LHV of the producer gas increased from 12.6-13.4 MJ/Nm^3 as gasification temperature increased. This is because a greater proportion of fuel gas evolved from the gasification reactor relative to the amount of non-fuel gases (N_2 and He). This was confirmed by the volume percentage of nitrogen decreasing from 8.7-5.3 vol%. Some leakage of air through the chute and siphon always occur introducing nitrogen into the gasification reactor, but this quantity remains static. Instead, higher gasification temperatures promoted a greater producer gas yield which makes the volume percentage of nitrogen decrease. The same trend was observed with the helium tracer gas which also decreased by a similar amount, as total gas yield increased.

The most noticeable change in the producer gas composition was the distinct increase in the hydrogen content from 15-26 vol% as gasification temperature increased from 642 °C to 758 °C. Four reactions listed in Section 2.1.4 encourage the production of hydrogen as

reaction temperatures are increased. These are the primary and secondary carbon-water reactions, the steam methane reforming reaction and the hydrogenation reaction. The individual contribution of each of these reactions to the increase in hydrogen content is unknown, but in the future measuring the change in humidity of the producer gas should help clarify this, as water is a component in three of the four reactions.

Over the same temperature range, the carbon monoxide volume percentage decreased from 40-33 vol%. The methane and carbon dioxide levels only varied by 0.8 percentage points and 4 percentage points respectively, about common values of 13.5 vol% and 17 vol%. The ethene content increased with increasing gasification temperature from 2.9-4.2 vol%. This small change has a more prominent effect on the LHV of the producer gas, since ethene has a higher heat of combustion than most of the other gaseous components (at 49.8 MJ/Nm^3). Ethane also has a high heating value (58.4 MJ/Nm^3) compared to most of the other gaseous components measured, but ethane decreased from 1.2-0.6 vol% as gasification temperature increased.

During sampling of the producer gas, there was a distinct visual reduction in the smokiness of the producer gas when gasification temperatures exceeded about 700 °C. It was thought that this was due to the reduction in tars amongst the producer gas but this does not align with the tar data shown in Figure 6.9. Six tar samples were taken during this test simultaneously with the six producer gas samples. The SPE columns containing the tar samples were analysed for 16 polycyclic aromatic hydrocarbon (PAH) components which are listed in Table 6.6. The 16 individual component quantities were summed to determine the total quantity of tar in g/Nm^3 for each sample. As seen in Figure 6.9, the total quantity of tars was between 0.9-4.7 g/Nm^3 and appears to have increased as higher gasification temperatures were used. This trend is unexpected and contradicts with the conclusions of other researchers performing gasification of wood. The reason for this uncommon trend is thought to be a result of evaporation of previously condensed tars on the internal surfaces within the gasifier as the plant was successively brought up in temperature.

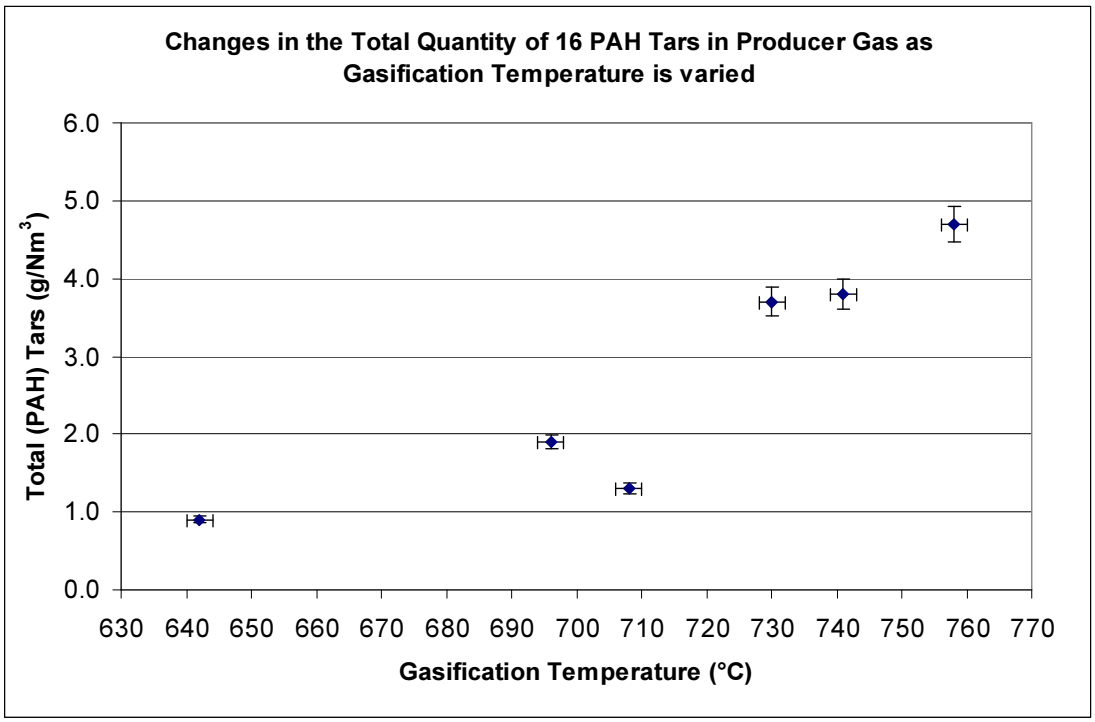

Figure 6.9: Summation of 16 PAH tars in the producer gas as measured by GC-MS at six different gasification temperatures. (Experimental errors could only be determined for the accuracy of drawing a 100ml gas sample for the y-direction, since the method of tar extraction and analysis by the commercial laboratory was undisclosed).

Table 6.6: Data from GC-MS analysis of 16 PAH tar components in the producer gas.

Gasification Temperature: Units:	**642°C** µg/sample	**696°C** µg/sample	**708°C** µg/sample	**730°C** µg/sample	**741°C** µg/sample	**758°C** µg/sample	Percentage (%)
Acenaphthene	4.5	7.2	6	9.2	8	8.4	3.0
Acenaphthylene	16	40	27.7	84.4	87.7	111	25.0
Anthracene	4.9	8.1	6.2	13.8	13.9	16.5	4.3
Benzo[a]anthracene	1.4	2.7	1.9	4.5	4.7	5.1	1.4
Benzo[b]fluoranthene	1.2	2.4	1.6	4.1	4.4	5.2	1.3
Benzo[a]pyrene (BAP)	1	2.1	1.5	3.8	4.3	4.7	1.2
Benzo[g,h,i]perylene	0.6	0.9	0.6	1.2	1.2	1.3	0.4
Benzo[k]fluoranthene	0.5	0.9	0.6	1.6	1.7	1.9	0.5
Chrysene	1.3	2.5	1.8	4	4.2	4.7	1.3
Dibenzo[a,h]anthracene	0.4	0.5	0.4	0.7	0.8	0.8	0.2
Fluoranthene	3.2	6	4.4	10.1	11.2	13	3.3
Fluorene	10	16.3	12.1	28.7	29.1	37	9.1
Indeno(1,2,3-c,d)pyrene	0.6	1.1	0.7	1.5	1.7	1.9	0.5
Naphthalene	16.9	44.7	29.8	114	118	145	32.0
Phenanthrene	14.3	23.8	18	41.2	40.8	48.1	12.7
Pyrene	4.4	7.5	5.7	12.1	13	14.3	3.9
Total of 16 PAH (µg/sample)	*81*	*167*	*119*	*335*	*345*	*419*	Total 100%
Total PAH Tars in g/Nm^3	**0.9**	**1.9**	**1.3**	**3.7**	**3.8**	**4.7**	

As seen in Table 6.6, the most abundant tar component was naphthalene at 32 %, followed by acenaphthylene at 25 %. The four next most abundant tar components were phenanthrene at 12.7 %, fluorine at 9.1 %, anthracene at 4.3 % and pyrene at 3.9 %. These tar composition

results are similar to what other researchers at the Vienna University of Technology found with their FICFB gasifier also fuelled with wood pellets (see Section 2.3.1).

A new batch of greywacke bed material was used in the gasifier for this test run, with the same particle size distribution as for the other tests. However, the bed material appeared different in colour and was found to be more resistant to agglomeration than the other batches of greywacke bed material used in the past. The combustion column temperature reached 875 °C during this test, which would have traditionally caused clinker to form. This did not happen, and it can be confirmed that the bed material fusion temperature is highly important in controlling what gasifier operating temperatures can be used. An X-Ray Diffraction (XRD) analysis revealed that this greywacke bed material consisted of 90 % quartz with 10 % albite. This was slightly different to the greywacke bed material used in many of the other tests which was analysed as 100 % quartz.

The trends noticed in the producer gas composition, changes in the LHV of the producer gas and the gas yields were all in agreement with other researchers findings as discussed in Section 2.2.1. However the apparent increase in the tar levels with increasing temperature did not agree, although the total quantity of tars measured for each sample was in the vicinity reported by other researchers (see Section 2.4.1). In summary, gasification temperatures above 750 °C appear to be most favourable in FICFB gasifiers fuelled with wood, because higher cold gas efficiencies are achieved with the greater producer gas yields. The LHV of the producer gas was not adversely affected at a gasification temperature of 758 °C and despite these experimental results, tar levels are usually lower at higher reaction temperatures.

6.3.5 Steady State Assessment of the Gasifier

This test was performed to observe how steady the gasifier operated when consistent settings were maintained. The plant was operated under normal gasification conditions for over two and a half hours while data were collected. Towards the end of the day a second operating condition was investigated where the supplementary LPG firing in the combustion column was turned off to see what effect this had on plant operation. These tests were performed on 3 March 2008. The experimental procedure followed is outlined in Section 4.2.

Figure 6.10 shows the producer gas composition plot with the different stages of the gasifiers operation indicated, and Table 6.7 contains the overall plant performance data. Gas samples were intentionally taken during the transition stage from heat-up to steam-gasification to learn more about the conditions in this region. Moisture samples were also taken during this test by drawing producer gas through silica gel and using gravimetric techniques to determine the moisture content. This is further explained in Appendix M.

The conditions of this test were: a wood pellet feed rate of 18.9 kg_{dry}/h, a gasification temperature of 724-741 °C, a total steam input maintained between 9.8-10.2 kg/h and a primary air flow rate of 835 L/min.

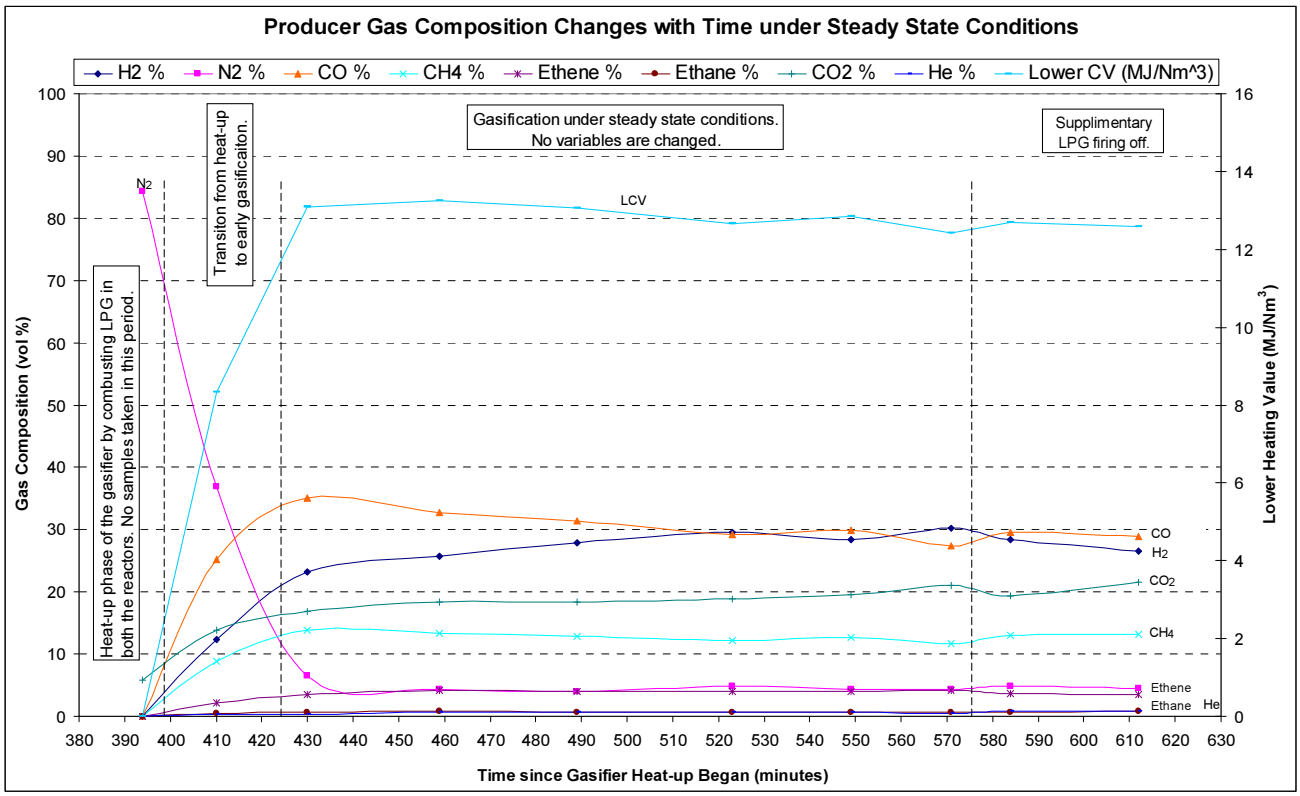

Figure 6.10: Gas composition measured from the gasifier over time, showing the different stages of plant operation. (Note: the lines drawn between the points plotted in the transition region may not accurately represent the true gas composition paths).

Table 6.7: Overall performance results of the gasifier during the steady state test run.

Time since Heat-up Began (Minutes after start-up)	LCV (MJ/Nm^3)	Producer Gas Yield (Nm^3/h)	Combustion Energy of Producer Gas (kW)	Cold Gas Efficiency (%)
394 (End of heat-up stage)	-	-	-	-
410 (Air gasification of wood pellets)	*8.3*	*19.8*	*45.9*	*33*
430 (Start of steam gasification)	13.1	23.5	85.3	62
459 (Normal gasification)	13.3	12.5	46.2	36
479 (Normal gasification)	13.1	12.4	45.1	36
523 (Normal gasification)	12.7	12.9	45.3	36
549 (Normal gasification)	12.8	13.6	48.4	38
571 (Normal gasification)	12.4	14.6	50.3	40
584 (Supplementary LPG off)	12.7	10.2	35.9	33
612 (Supplementary LPG off)	12.6	10.0	34.9	33

The first thing to clarify is the second and third lines of the results displayed in Table 6.7 after 410-430 minutes of gasifier operation. Both these results have occurred under transient conditions and they are not representative of steady state conditions. The producer gas yield during the transition period appears unusually high which has caused the combustion energy of the producer gas and the cold gas efficiency results to be over expressed. The LHV's of the producer gas in the transition region are thought to be correct however.

The reasons for the larger than expected producer gas yields at 410 minutes and 430 minutes since start-up of the gasifier are unknown. However the microGC did analyse the producer gas compositions as having lower than usual helium (tracer gas) concentrations at these two times, suggesting that there was a large volume of other gaseous products present in proportion to the amount of helium. So identifying the reason for the low concentration of helium in the producer gas should identify the cause of these high values. This is not obvious and it is unknown whether higher than usual flow rates out of the gasification reactor were actually present or whether the low helium concentrations are due to other factors such as uneven flow rates of gas from the gasification reactor.

Other reasons for the low helium concentration could be that the flow rate of helium injection into the producer gas line was set too low initially; however the experimental data suggest

that the flow rate was correctly set. Accumulation of wood and char could have temporarily occurred in the BFB during the transition from air to steam fluidization in the chute causing higher than usual producer gas yields. However, the producer gas results for 430 minutes from start up, occur approximately five minutes after the chute was converted over to steam fluidization, which should be enough time for fuel loadings to even out. The total volume flow rates of fluidizing gas entering the gasification reactor were lower during the air gasification stage than when steam was used in place of air, so the helium was not simply being diluted because greater quantities of air were being used in place of steam.

The LHV of the producer gas of 8.3 MJ/Nm^3, being generated under air gasification conditions was higher than expected for this mode of operation. Commonly air-blown gasifiers yield a producer gas with a LHV in the range of 4-6 MJ/Nm^3, not 8.3 MJ/Nm^3. However this value appears correct because 37 vol% nitrogen was measured in the producer gas and under air gasification conditions, the nitrogen content is expected to be much higher than for steam gasification where it is commonly 3-6 vol%. To further understand why this value was higher than expected, the equivalence ratio was calculated. An equivalence ratio of slightly greater than 0.06 was determined, estimated to be in the range from 0.06 to 0.12. Too little information was available to determine this more accurately, as the quantity of char which is combusted as it circulates through the combustion column and back to the gasification reactor is unknown. However the equivalence ratio indicates that the gasifier was operating mainly in the pyrolysis region as discussed in Section 2.1.1. This explains the higher than expected LHV of the gas since pyrolysis conditions generate higher calorific value producer gas than is found under normal air-blown gasification conditions.

To the surprise of the plant operators, the gas composition was not as steady as expected. In fact some of the largest swings in gas composition throughout the plants history occurred during this test. This was highly unexpected and these steady state test results need to be treated with caution as some operational problems were experienced. Ideally this experiment needs to be repeated for verification of its accuracy.

Despite the unexpected plant performance, the following trends were observed in the producer gas results over the two and a half hours of unvaried settings. Carbon monoxide composition decreased from 35-27 vol% and hydrogen concentration increased from 23-30 vol%. Carbon dioxide concentration also increased from 17-21 vol% and methane levels

decreased slightly from 14-12 vol%. Nitrogen levels remained generally consistent at 4-4.9 vol% and the producer gas generation rate also stayed in the range between 12.4-14.6 Nm^3/h. Ethene, ethane and helium stayed relatively consistent around 4 vol%, 0.7 vol% and 0.6 vol% respectively.

After about 570 minutes from start-up, the supplementary LPG firing was turned off. This meant the only fuel entering the combustion column was char through the chute from the BFB, plus the small amount of LPG (<1 L/min) delivered by the combustion column pilot burner. This burner is always left on during plant operation to ensure any supplementary LPG or other flammable gases are ignited in a controlled manner, preventing the chance of their accumulation creating an explosion risk.

With the supplementary LPG fuelling turned off, the gasifier temperatures began to cycle sinusoidally downwards on the monitoring computer on regular intervals of about 1-2 minutes (this pattern is not shown in Figure 6.10 with the producer gas composition). When the supplementary firing is used, the temperatures plot in a linear manner on the monitoring computer and there is no evidence of this sinusoidal pattern. This temperature fluctuation phenomenon has occurred in the past when the gasifier was first being test fired without supplementary LPG. Supplementary LPG firing was adopted to allow greater control of combustion temperatures, as this is the only independent method available to influence the energy generation relative to the energy consumption between the reactors. As discussed in Section 3.2.4 and Section 6.2.1, the heat generated by the char burning in the combustion column, is not great enough to sustain the endothermic gasification reactions above about 700 °C, so supplementary firing has to be used. This phenomenon is due to the design of this FICFB gasifier and not characteristic of all FICFB gasifiers. However provision for supplementary firing is advisable.

The cold gas efficiency of the gasifier ranged from 36-40 % during the period of unvaried settings. This was noticeably higher than during other tests because of the higher than usual producer gas yields. When the supplementary firing was turned off, the cold gas efficiency dropped to around 33 % and is likely to have further decreased as gasification temperatures fell away.

After two sets of data had been obtained without supplementary LPG firing being used, only char began being circulated around through the siphon. Seconds later the siphon blocked because no bed material was amongst the char to carry it through the siphon and the plant had to be shut down. This is the most common form of blockage, because the char does not flow as readily as the bed material does through the siphon. There appears to be a maximum allowable ratio for the amount of char that can be amongst the bed material before its ability to flow readily is impaired. Upon inspection, clinker had formed in the base of the gasification column and had prevented any bed material and char passing through the chute into the combustion column. This caused the remaining bed material in the CFB, followed by the char once it had combusted to a small enough size, to be entrained out, emptying the combustion column. It is believed that this clinker had been formed throughout the duration of the test run, since it often begins forming if the beds are not adequately fluidized during the early heat-up phase. Both the formation of the clinker and the release of thermal energy from the refractory (having a high thermal mass) after the heat-up stage is believed to be responsible for the changing test conditions.

A temporary method to measure the water content in the producer gas was set up for this test run. Multiple moisture measurements were taken of the producer gas, since operators were not as busy changing plant settings as occurred in the other investigative hot tests. The moisture content during the air-gasification stage was measured at 0.42 $g/g_{dry\ gas}$ but steady state conditions may not have been established. With steam gasification the moisture content of the producer gas was higher in the range of 0.94-1.15 $g/g_{dry\ gas}$. After turning the supplementary firing off in the combustion reactor, the moisture content was measured as being slightly higher at 1.22-1.36 $g/g_{dry\ gas}$. This same trend occurred in subsequent test runs and is thought to be because plant temperatures decrease, lowering the water conversion (see definition in Section 2.1.6). The producer gas moisture measurements are shown in Figure 6.11, and the method of calculation is explained in Appendix M.

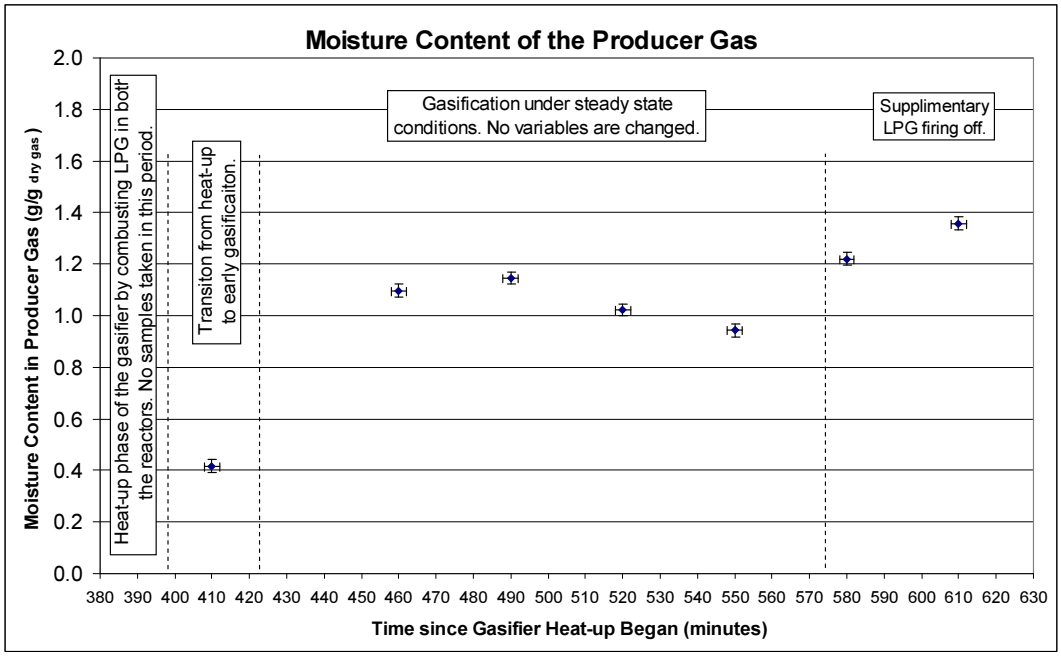

Figure 6.11: Measurements of the moisture content of the producer gas at the different stages of plant operation.

During this gasifier test run and others in the past, it has been observed that when steam is rapidly passed into the gasification reactor in place of air from the heat-up stage, that a rush of gas is sent along the producer gas line to the afterburner. This occurs when wood feed into the gasifier has already begun. A distinct roaring noise can be heard from the afterburner as it receives an increased fuel loading. This rush of gas usually continues for about 5-20 seconds.

It is suspected that this sudden increase in gas output during the transition stage occurs because the equilibrium gasification reactions are suddenly driven in a direction to consume the introduced steam. The following gasification reactions are likely to be influenced and driven in their forward directions as steam is suddenly passed into the reactor:

The primary and secondary carbon-water reactions:

Primary: $C_{(s)} + H_2O_{(g)} \Leftrightarrow CO + H_2$

Secondary: $C_{(s)} + 2H_2O_{(g)} \Leftrightarrow CO_2 + 2H_2$

The steam-methane reforming reaction:

$CH_4 + H_2O_{(g)} \Leftrightarrow CO + 3H_2$

And the water-gas shift reaction:

$CO + H_2O_{(g)} \Leftrightarrow CO_2 + H_2$

All of these reactions liberate gaseous products when shifting to consume water, and often during the gasifier's transition from air fluidization in the chute and BFB, to steam fluidization, some wood/char may temporarily accumulate in the BFB as wood feed into the gasification reactor continues. Additionally, this is likely to cause the evolution of the producer gas to be higher than usual as the wood and char loading in the BFB is temporarily higher. This could have been a factor responsible for the low helium concentration measurements after 430 minutes of operation as discussed earlier in this section, but it is not thought to continue for longer than approximately 20 seconds.

This steady state test was difficult to draw conclusions from because of the unexpected behaviour of the plant; however it appears that it takes longer for the producer gas composition being generated to reach steady state conditions, than it takes for the plant temperatures to stabilise on the digital displays in the laboratory. This may mean that steady state conditions were not entirely achieved during the other hot tests, but this possibility can not be confirmed from this test run due to the operational problems experienced.

6.3.6 Olivine Bed Material Test at Different Fuel Feed Rates

This test was performed to assess the influence of olivine (forsterite olivine) bed material and its influence on the producer gas composition and tar levels. Olivine was chosen because it has been found to have catalytic properties as discussed in Section 2.2.7 and Section 2.4.2. The feed rate of wood pellets was the variable being changed in this test so that olivine could be assessed under more than one operating condition. The range of feed rates tested was from 7.7-15.8 kg_{dry}/h. A greater range of feed rates was intended on being used but clinker formed in the gasifier causing sand circulation to stop during the latter stages of the test. It is unknown to the plant operators what effect clinker has on the producer gas composition. The experimental procedure followed for this olivine test on 17 April 2008 is presented in Section 4.2. Figure 6.12 shows trends in the producer gas data and Table 6.8 contains the plant's overall performance results.

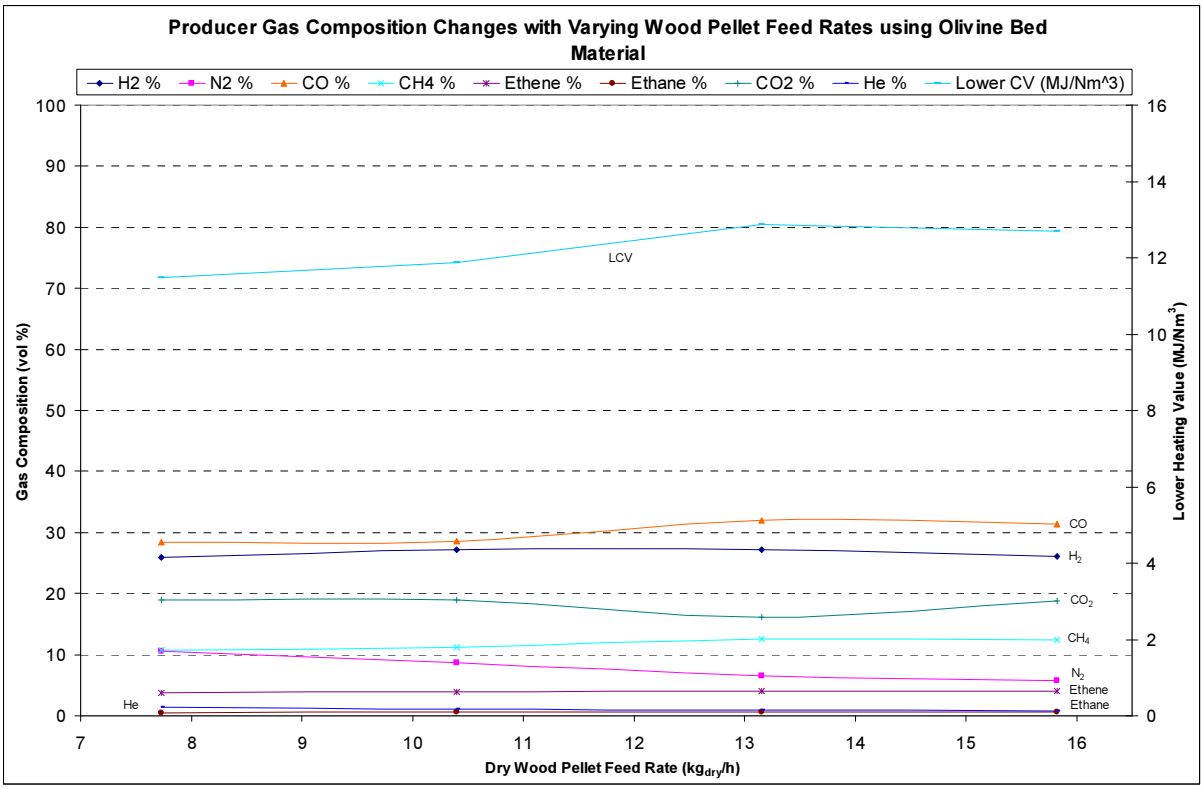

Figure 6.12: Producer gas composition as feed rate of wood pellets into the gasifier is varied using olivine bed material.

Table 6.8: Overall performance results with varying fuel feed rate using olivine bed material.

Dry Wood Feed Rate (kg_{dry}/h)	LCV (MJ/Nm^3)	Producer Gas Yield (Nm^3/h)	Combustion Energy of Producer Gas (kW)	Cold Gas Efficiency (%)
7.7	11.5	6.1	19.5	25
10.4	11.9	7.4	24.3	26
13.2	12.9	8.8	31.4	30
15.8	12.7	10.6	37.6	31

The conditions of the test were: 12 kg of olivine bed material with a size distribution as shown in Figure 4.2. A gasification temperature of 738-768 °C and a total steam input of 10 kg/h with a primary air flow rate of 835 L/min. During this test it was difficult to maintain constant gasification temperatures, possibly because the bulk density of the olivine ($1730 kg/m^3$) was slightly greater than the bulk density of the greywacke ($1614 kg/m^3$) requiring higher fluidizing and entraining gas flow rates to circulate the same amounts of

heat-carrying particles. Additionally, the heat capacity of the olivine may have been different to the greywacke influencing the quantity of heat transferred.

As wood feed rate increased from 7.7-15.8 kg_{dry}/h (41-83 kW of fuel input), the producer gas yield increased from 6.1-10.6 Nm^3/h. This caused the combustion energy of the producer gas to increase from 20-38 kW. When this data is compared to the feed rate tests discussed in Section 6.3.1 and Section 6.3.3, it reveals that the producer gas yield is higher when olivine bed material is used compared to greywacke bed material for similar fuel feed rates. For example, Table 6.1 shows that for a feed rate of 11.2 kg_{dry}/h using greywacke bed material, a producer gas yield of 7.0 Nm^3/h results. However when using olivine bed material and just 10.4 kg_{dry}/h of wood pellets, a producer gas yield of 7.4 Nm^3/h occurs. When comparing the gas yields in Tables 6.4 and 6.6, its shown that 5.1 Nm^3/h of producer gas was generated from 10.5 kg_{dry}/h of wood pellets, when 20 kg of greywacke bed material was used. When using olivine 6.1 Nm^3/h of producer gas was generated from a lower wood feed rate of 7.7 kg_{dry}/h. Hence, when using olivine compared to greywacke bed material, the producer gas yields appear on average to be around 20% higher. However the olivine test was performed over a slightly higher temperature range, so this difference is expected to be less than 20%.

The higher producer gas yields when using olivine improved the cold gas efficiencies of the gasifier for similar wood feed rates when compared to tests using greywacke sand. The cold gas efficiencies in Table 6.8 ranged from 25-31 % but are difficult to directly compare since the feed rate ranges between the tests do not correspond well.

The LHV of the producer gas when using olivine compared to greywacke was similar for the same fuel feed rates. However the olivine test had to be terminated early due to clinker formation, so no data is available at higher wood feed rate settings. The lower heating value of the producer gas in this test ranged between 11.5-12.9 MJ/Nm^3. During the other feed rate tests with greywacke bed material, the LHV of the producer gas was also lower at the slower fuel feed rates, because nitrogen in the producer gas was not diluted to the same extent.

The carbon monoxide concentrations in the producer gas when using olivine were similar to those shown in Figure 6.7 when using 20 kg of greywacke at similar fuel feed rates. In this test carbon monoxide levels were measured as being between 28-32 vol%. Hydrogen levels were similar to other tests using greywacke, measured as being between 26-27 vol%. Carbon

dioxide levels were also similar between Figure 6.4 and Figure 6.12 where the concentration remained between 16-19 vol%. Methane concentrations were again similar when olivine and greywacke bed materials were used. Methane levels ranged between 11-13 vol% as the feed rate was varied. Nitrogen levels were slightly less for the same feed rate values, supporting the finding that more producer gas is generated to dilute the normal quantity of nitrogen that enters the gasification reactor. Ethene and ethane concentrations were measured in the vicinity of 4 vol% and 0.6 vol% respectively, similar to the producer gas composition of the other feed rate tests.

The results obtained from this experiment agree with the findings of other researchers as discussed in Section 2.2.7. It can be summarised that olivine bed material appears to allow a higher liberation of producer gas under similar gasification conditions, without affecting the producer gas composition. This leads to higher cold gas efficiencies being achieved for a given feed rate of wood. In a commercial FICFB gasifier, this means that a lower capital cost could be realised by building a smaller scale gasifier for the same producer gas output requirement. However, other factors also need to be considered, such as the fusion temperature limits, attrition resistance of the bed material, its relative cost and availability.

6.4 Recommendations of Future Hot Tests to Perform on the 100kW Gasifier

6.4.1 Changing the Fuel Entry Point on the Gasification Reactor

One of the first hot tests that should be performed following submission of this thesis is to trial the in-bed auger feeding into the base of the gasification reactor. Researchers should try to establish if any improvements in producer gas composition, efficiency and total tar levels are achieved. It is hoped that a faster particle heating rate will occur so that the pyrolysis and gasification reactions occur more simultaneously reducing the generation of hydrocarbon tars (as discussed in Sections 2.1.3 and 3.1.11).

The auger and intermediate hopper have been constructed and the instrumentation is in place. The only outstanding tasks for this trial to be performed are to install the unit and connect it into the electrical control system. After successful operation is achieved, researchers could trial the auger with no, or very little cooling water passing through the water jacket to see if

pyrolysis is initiated in the auger and what effect this has on producer gas composition and total tar levels. This is discussed more in Section 6.4.2 as a possible method to increase residence times for the thermochemical reactions.

6.4.2 Gasification of Charcoal to Assess the Merits of Separate Pyrolysis before Steam Gasification

This experiment should be performed to see if pyrolysed feedstocks with low levels of volatile matter such as charcoal produce fewer tars than raw wood. This study is based on the idea that the majority of hydrocarbon tars are generated during the devolatilisation stage of the overall gasification process and not during the char-gas and gas phase reactions as shown in Figure 2.4. Quantifying this could mean that an initial pyrolysis process could be beneficial to increase reaction residence times, helping to reduce tar levels. Hence, it may be better to develop a process where a feedstock is first pyrolysed before being steam gasified. This should not reduce the producer gas yield as the char and the pyrolysis gases evolved can be passed into the gasification reactor. Heat to sustain the pyrolysis and gasification processes could be generated from combusting a slip-stream of the tar laden pyrolysis gas in place of char and/or supplementary fuel. It may be best to wholly use char in the gasification reactor to yield a high quality (low tar) producer gas. This is favourable because lower quality pyrolysis gas can be used in place of good quality char and producer gas (as supplementary fuel) to generate heat for the process.

Since the presence of tars in producer gas are such a worldwide problem that limits the applications for which producer gas can be directly used. This preventative measure to the formation of tars, may be better than the primary and secondary tar reduction methods discussed in Sections 2.3.1 and 2.4.

6.4.3 Optimisation of the Bed Material Loading in the Gasifier

Future researchers working on the FICFB gasifier at the University of Canterbury are encouraged to perform a hot test run where the bed material mass loading is varied. The reason for performing this test is so that the influence of bed heights and bed material loading can be better understood in this design of gasifier. This testing regime should be performed once a lock hopper for the bed material has been designed and installed as discussed in Section 3.2.8.

It has been learned that increasing the bed material loading substantially increases the heating up period of the gasifier due to the increased thermal mass of the system. Excessive bed material loadings (20 kg plus) can also cause running problems with the pilot burners if they become smothered. A higher dense phase in the BFB decreases the freeboard height in the gasification reactor and encourages particle loss rates. However the merits of using bed material loadings higher than 12 kg but less than 20 kg have not been investigated.

It is recommended that a test is performed where 0.5 kg increments of bed material are added to the gasifier so that a mass loading range of 12 kg to approximately 16 kg can be studied. Above this level appears unfavourable due to extending the heat-up period for no known performance gains. One factor that this test should seek to determine is, if using bed material loadings higher than 12 kg can increase the fuel particle residence times in either of the reactors. This has been discussed in Section 3.2.4 with respect to improving the heat generation in the combustion reactor. However if the primary air is introduced higher up in the combustion column, the bed material loading in the gasifier may need to be increased anyway to maintain normal circulation rates. Circulation rates should decrease as the elevation of the primary air input is raised, as explained in Section 2.8.1.

6.4.4 Use of Other Catalytic Bed Materials

Different bed materials should be tested in the FICFB gasifier at the University of Canterbury to see what improvements can be gained in the gas composition and tar yields. Abundant locally available aggregates should be targeted, preferably ones believed to have catalytic properties. A good place to begin would be to investigate what bed materials are commonly used in fluidized bed combustors in and around New Zealand, as these materials should have known fusion temperatures and could save a lot of experimentation time by reducing the likelihood of agglomeration occurring.

At some stage in the gasifier project at the University of Canterbury, calcium oxide bed material should be tested. This is expected to promote methane production and the removal of carbon dioxide, so a higher calorific value producer gas could be achieved (Probstein & Hicks, 2006). The following reaction with calcium oxide can occur:

$$CaO + CO_2 \quad \Leftrightarrow \quad CaCO_3 \qquad \Delta H^{o}_{298} = -183 \text{ kJ/mol}$$

This reaction is exothermic in the forward direction and can help to transfer heat from the combustion column to the gasification column with lower circulation rates than are used with non reactive bed materials.

6.4.5 Fuel Particle Limitations Assessment

An assessment should be performed to learn what fuel particle sizes the gasifier can run on. A cold test should be performed first by introducing the fuel into the circulating bed material to ensure blockages do not occur, especially in the siphon. Sawdust is especially a feedstock that needs to be considered because it is often abundant at sawmills. This testing should identify the feedstock size ranges that can be used in the 100 kW gasifier and would help the operators to understand the relationship between fuel particle size and gasifier performance. It should also identify an operational lower limit for fuel particle size. The upper limit for fuel particle size is likely to be set by the fuel feeding system and the flow characteristics through restrictions in the gasifier loop such as in the siphon. Additionally, this test may aid in determining how rapid the devolatilisation process is and the minimum residence time necessary in the BFB for complete pyrolysis to occur.

Supplying the gasifier with larger sized fuel particles may improve the plant's energy balance. Not enough heat is generated in the combustion column to sustain a gasification temperature above about 700 °C without supplementary firing. Higher temperature operation could be achieved by feeding larger sized wood particles, because they are not entrained out and remain in the CFB for a longer period of time generating heat. This concept assumes that the fuel residence time in the gasification reactor under endothermic conditions would be proportionately less than when undergoing combustion.

7.0 Conclusions

The 'Fast Internally Circulating Fluidized Bed' (FICFB) gasifier is far more complex than traditional gasifiers and plant design is critical to achieve stable and reliable operation. Many modifications were made to the 100 kW FICFB gasifier following its initial construction. This was primarily accomplished with improvements made to the flow of bed material and char through the siphon. The type of fluidizing agent and the way they are introduced into components such as the siphon and the chute have a significant impact on the gasifier's reliability and gas quality. The nitrogen content in the producer gas was reduced from concentrations of around seventeen volume percent to as low as four volume percent through the modifications made. Steam fluidization is favourable in both the siphon and the chute but only when plant temperatures are high enough to prevent any condensate forming and inducing blockages.

Installing a helium injection system was a breakthrough in allowing the flow rate of the hot producer gas to be measured. This simple technique can be used on future gasifiers where a gas chromatograph is available. The development of the simultaneous producer gas and tar sampling system proved to be very successful and was well suited to the experimental testing regime performed. Accurate and rapid producer gas and tar samples were collected without the traditional difficulties associated with solvent impinger trains.

Bed material circulation rates as high as 300 kg/h were regularly achieved during cold testing. Increasing the amount of fluidization in the chute increased the bed material circulation rate. As the amount of BFB fluidizing air increased, bed material circulation rates initially increased as the gasification bed became fluidized, but then reached a plateau. Increasing the amount of CFB fluidizing air increases bed material circulation rates once above a minimum threshold, set by the height of the primary air jets. As primary air flow rates are increased, bed material circulation rate increases before peaking and beginning to decrease. This is because excessive amounts of primary air track up the chute restricting the flow of bed material passing into the fluidized combustion bed. Higher quantities of bed material in the gasifier generate greater circulation rates between the reactors. Particles took about 55 seconds to complete a full circulation loop around the gasifier under cold testing

conditions, and whole wood pellets could not be entrained out of the combustion column until they were combusted to a significantly smaller size.

This design of gasifier with its separate gasification and combustion zones generated producer gas with a LHV of 11.5-13.4 MJ/Nm^3, which is two to three times greater than traditional air-blown gasification systems accomplish at 4-6 MJ/Nm^3. Producer gas yields of 14.6 Nm^3/h were measured with wood fuel feed rates of 18.9 kg_{dry}/h. Cold gas efficiencies were calculated as being between 16-40 %, but differed markedly with plant operating conditions such as gasification temperature, wood feed rate and the amount of steam injected. This research-based gasifier has poor waste heat recovery and with improved insulation higher cold gas efficiencies could be achieved.

The quantity of PAH tars measured in the producer gas ranged between 0.9-4.7 g/Nm^3 with naphthalene and acenaphthylene being the most abundant, accounting for around 50 % of the PAH components measured. The moisture content of the producer gas was determined to be 0.9-1.2 $g/g_{dry\ gas}$ at normal operating settings.

Running the gasifier at high wood feed rates was desirable because the lowest concentrations of nitrogen are present in the producer gas. This is because a consistent amount of nitrogen enters the gasification reactor (originating from the combustion air and auger purge gas), and larger producer gas yields dilute the nitrogen to a higher degree, improving the LHV of the producer gas. A steam to biomass ratio in the vicinity of 0.45-0.7 kg/kg_{dry} appeared most favourable when a LHV of 12-13.4 MJ/Nm^3 is desired while limiting the amount of steam that needs to be generated. Higher gasification temperatures above 750 °C encourage the generation of greater quantities of producer gas, but the fusion characteristics of the bed materials limited the plant's operating temperatures. Greywacke and olivine (forsterite olivine) bed materials were tested. Olivine was found to increase the producer gas yields by approximately 20 % without noticeably effecting the producer gas composition.

Variations in producer gas composition were smaller than expected when varying plant operating conditions and it appears the gasifier takes longer to reach a steady state gas composition than it does to reach a steady operating temperature. Overall it was learned that design changes to the gasifier can make stepped changes in plant performance which are often more dominant than varying plant operating conditions.

8.0 Design Recommendations for Future FICFB Gasifiers

- When designing a FICFB gasifier, the heat generation in the combustion column must be great enough to handle the worst case heat loss rates from the gasifier, plus the greatest anticipated thermal energy requirements of the gasification reactions.
- Waste heat recovery needs to be maximised from both the flue gas and the producer gas. Combustion air and steam should be preheated/superheated respectively to as close as allowable to the reactor temperatures.
- Minimising the amount of heat loss through extensive use of insulation is important to achieve good plant efficiencies. In research settings, insulation should be built into the reactors where possible with any exterior insulation being one-piece units, so that they can be easily removed and refitted without having to continually replace it during routine disassembly/reassembly between test runs. Glass fibre is a good insulator but falls apart when being routinely taken on and off, and easily frays with people brushing against it when moving around the plant.
- The freeboard height in the gasification reactor should be above the TDH (transport disengaging height) so that particles stay in the bed and are not drawn out under all operating conditions. The gasification reactor internal geometry should taper out to a larger cross sectional area in the lower freeboard region to minimise the superficial gas velocities and bed material loss rates. This means the freeboard height can be shorter (more compact reactor) and the standpipe length can be maximised for any given height of combustion column.
- In FICFB gasifiers, a long standpipe length is important so that the sand in the standpipe has a wide working range to self regulate its level over. This also improves the quality of the sand seal which prevents the exchange of producer gas and flue gas between the upper reactor sections.
- It is important to have both reactors at the right elevation to each other. This influences residence times depending on how deep each bed is and affects the head of sand across the chute. A shorter and steeper angled chute also helps bed material to pass through, minimising the amount of fluidization required.
- FICFB gasifiers should be designed with methods to control residence times, such as the ability to operate at: different bed material loadings and with a wide range of sand

circulation rates between the reactors. It is likely that running a FICFB gasifier at high bed material loadings could achieve high circulation rates and long residence times of the wood in the BFB or char in the CFB. Changing the relative volumes of the fluidized beds (heights and cross-sectional areas) changes their mass loadings. This is something that needs to be considered when trying to obtain the desired residence times for fuel circulating between both reactors.

- Siphons need to have large enough internal diameters to ensure bed material passes through them freely. They should have a very short upward flowing section because sand does not flow readily up and around a bend. Only enough resistance should be created to ensure an adequate gas seal is maintained. Materials with large particle sizes like wood/char do not flow as readily as sand through siphons.
- Ideally in a FICFB gasifier, a short chute with a low ceiling is favourable so that bed material can readily travel through the chute and a minimum region along the ceiling exists for gases to pass between the reactors.
- Feed systems for gasifiers need to be designed as fuel-flexible as possible so that they can tolerate a wide range of fuel morphologies, densities and feed rates.
- Distributors need to be designed so that they are self-clearing, where any back flowing bed material into the distributor can be discharged back into the bed with gas passing though into the reactor.
- The method of introducing fluidizing agents needs to be carefully considered during plant design. Metal spargers tend to deform in the high temperature conditions. In some circumstances it may be best to cast passages in refractory sections for introducing the fluidizing agents.
- In a FICFB gasifier the flue gas cyclone needs to be designed for high particle loadings to effectively separate out bed material and minimise bed material losses out with the flue gas.
- FICFB gasifiers being built for research purposes should be designed with a discharge system in the base of the reactor columns, so that the bed material can be easily emptied after experimental testing. This should help to minimise preparation times between tests.
- A high level of automation is recommended for ease of operation and to minimise the number of operators required.
- Especially on gasifiers where research is being carried out, all plant components must be easily removable as this is a frequently occurring task.

9.0 References

Abrahamson, J. 2007, Univeristy of Canterbury, New Zealand, personal communication 24 July 2007.

Antal, M. J. (1983). The Effects of Residence Time, Temperature and Pressure on the Steam Gasification of Biomass. In D. L. Klass (Ed.), *Biomass as a Nonfossil Fuel Source*: America Chemical Society.

Arena, U., & Mastellone, M. (2005). *Pyrolysis and Gasification of Solid Wastes in Fluidized Bed Reactors.* Paper presented at the Industrial Fluidization South Africa.

Baines, J. T. (Ed.). (1993). *New Zealand Energy Information Handbook*. Christchurch: Taylor Baines and Associates.

Billings, R. E. (2000). *The Hydrogen World View*. Independence: American Academy of Science.

Bolhar-Nordenkampf, M., Bosch, K., Rauch, R., Kaiser, S., Tremmel, H., Aichernig, C., et al. (n.d.). *Scale-up of a 100kW(th) Pilot FICFB gasifier to a 8MW(th) FICFB gasifier demonstration plant in Guessing (Austria)* Getreidemarkt: Institute of Chemical Engineering.

Brandt, P., & Henriksen, U. (2000). *Decomposition of tar in gas from updraft gasifier by thermal cracking.* Paper presented at the 1st World Conference on Biomass for Energy and Industry, Spain.

Breeze, P. (2005). *Power Generation Technologies* (1st ed.): Newnes.

Brown, R. C. (2003). *Biorenewable Resources: Engineering New Products from Agriculture*: Iowa State Press.

Brown, S. 2006, personal communication, 4 December 2006,2006.

Chase, G., G (n.d.). *Fluidization*: Univeristy of Akron. Retrieved 5 June. 2007, from http://www.ecgf.uakron.edu/~chem/fclty/chase/Solids/SolidsNotes5%20Fluidization.pdf

Ciferno, J. P., & Marano, J. J. (2002). *Benchmarking Biomass Gasification Technologies for Fuels, Chemicals and Hydrogen Production*: US Department of Energy, National Energy Technology Laboratory.

Cowie, P., & Dang, H. (2006). *New Zealand Energy in Brief, March 2006* Wellington.

de Diego, L. F., Garcia-Labiano, F., Abad, A., Gayan, P., & Adanez, J. (2001). *Coupled drying and devolatilization of non-spherical wet pine wood particles in fluidised beds*: Department of Energy and Environment, Instituto de Carboquimica.

Devi, L., Ptasinski, K. J., & Janssen, F. J. J. G. (2002). *A Review of the Primary Measures for Tar Elimination in Biomass Gasification Process* Eindhoven: Eindhoven University of Technology.

Devi, L., Ptasinski, K. J., Janssen, F. J. J. G., van Paasen, S. V. B., Bergman, P. C. A., & Kiel, J. H. A. (2004). *Catalytic Decomposition of Biomass Tars: use of dolomite and untreated olivine*: Eindhoven University of Technology.

East Harbour Management Services. (2002). *Drivers of Woody Bioenergy in New Zealand* Wellington: East harbour Management Services.

Energy Information Administration (2006). *International Energy Outlook 2006*: United States Government. Retrieved 24 July. 2007, from http://www.eia.doe.gov/oiaf/ieo/electricity.html

Energy Information Administration (2007). *International Energy Outlook 2007*: United States Government. Retrieved 19 March 2008. 2007, from http://www.eia.doe.gov/oiaf/ieo/electricity.html

Fercher, E., Hofbauer, H., Fleck, T., Rauch, R., & Veronik, G. (1998). *Two Years Experience with the FICFB-Gasification Process*: Institute of Chemical Engineering, Vienna.

Fletcher, S., Lyon, K., & Rayner, M. (2005). *Biomass Energy Systems*. Retrieved 9 June. 2007, from http:/wwwphys.murdoch.edu.au/rise/reslab/resfiles/biomass/text.html

Fordyce, & Ensor. (1982). *Energy from Waste Wood Burning*: Department of Trade and Industry.

Franco, C., Gulyurlu, I., Pinto, F., & Cabrita, I. (2002). *The Study of Reactions Influencing the Biomass Steam Gasification Process*.
Goss, J. R., & Kaupp, A. (1984). *Small Scale Gas Producer-Engine Systems*: GATE.
Grace, J. R. (1997). *Circulating Fluidized Beds*: Blackie Academic and Professional.
Grassi, G., & Bridgewater, A. V. (1991). *Biomass Pyrolysis Liquids Upgrading and Utilisation*: Elsevier Science Publishers Ltd.
Higman, C., & Burgt, M. (2003). *Gasification*: Gulf Professional Publishing.
Hofbauer, H., & Rauch, R. (2000). *Stoichiometric Water Consumption of Steam Gasification by the FICFB-Gasification Process* Vienna: Institute of Chemical Engineering, Fuel and Environmental Technology, Progress in Thermochemical Biomass Conversion, Innsbruck.
Hofbauer, H., Rauch, R., Foscolo, P., & Matera, D. (2000). *Hydrogen Rich Gas from Biomass Steam Gasification*: Institute of Chemical Engineering, Fuel and Environmental Technology, Vienna, 1st World Cnference & Exibition on Biomass for Energy & Industry, Sevilla, June 2000.
Hofbauer, H., Veronik, G., Fleck, T., & Rauch, R. (1997). *The FICFB-Gasification Process*: Vienna University of Technology, Austria, Developments in Thermochemical Biomass Conversion Vol.2 pp 1016-1025, Banff 1997.
Houben, M. P., & Geldrop, G. T. (2004). Analysis of Tar Removal in a Partial Oxidation Burner. In: Eindhoven University.
Hydrogen Now (2001). *Other uses of Hydrogen*. Retrieved 5 April. 2008, from http://www.hydrogennow.org/Facts/OtherUsesOfHydrogen.htm
Isidoro Martínez (2007). *Combined Brayton-Rankine cycle*, from http://imartinez.etsin.upm.es/bk3/c17/Exercise4.htm
Jeffers, S., Mullen, J. F., Chohen, A. J., & Dangtran, K. (n.d.). Control Problem Waste Feeds in Fluid Beds. Energy Transfer/Conversion.
Joesph, S. 2006, Biomass Energy Services and Technology, Australia, personal communication, 2006.
Jones, C. (2006). *GSBP Bioenergy Presentation.* Paper presented at the Bioenergy Australia 2006 Conference, Fremantle.
Kaupp, A., & Goss, J. R. (1981). *State of the art report for small-scale gas producer engine systems*: University of California.
Kehlhofer, R. (1991). *Combined Cycle Gas and Steam Turbine Power Plants* (1st ed.): The Fairmont Press, Inc.
Kehlhofer, R., Bachmann, R., Nielsen, H., & Warner, J. (1999). *Combined Cycle Gas and Steam Turbine Power Plants* (2nd ed.): Penn Well Publishing Company.
Kinoshia, C. M., Wang, Y., & Zhou, J. (1994). Tar formation under different biomass gasification conditions. *Journal of Analytical and Applied Physics, 29*, 169-181.
Klass, D. L. (1998). *Biomass for Renewable Energy, Fuels and Chemicals*: Academic Press.
Knoef, H. (Ed.). (2005). *Handbook Biomass Gasification*: BTG Biomass Technology Group.
Kunii, D., & Levenspiel, O. (1969). *Fluidization Engineering*: John Wiley & Sons.
Leyland, B. (2004). *New Zealand's Load Growth from 1974 and expected demand to 2025*: Centre for Advanced Engineering. Retrieved 7 November. 2006, from http://www.caenz.com/archive/files/DemandReport.pdf
Liu, Y. P., Wu, M. G., & Qian, J. X. (2006). *Predicting Coal Ash Fusion Temperature based on its Chemical Composition using ACO-BP Neutral Network*: Zhejiang University.
Loffler, G., Kaiser, S., Bosch, K., & Hofbauer, H. (2003). *Hydrodynamics of a dual fluidized bed gasifier. Part 2: simulation of solid circulation rate, pressure loop and stability* Vienna: Institute of Chemical Engineering, fuel Technology and Environmental Technology, Vienna University of Technology.
Loffler, G., Kaiser, S., Bosch, K., & Holbauer, H. (2003). *Hydrodynamics of a dual fluidized bed gasifier. Part 1: simulation of a riser with gas injection and diffuser* Vienna: Institute of

Chemical Engineering, fuel Technology and Environmental Technology, Vienna University of Technology.
Logdberg, S. (2007). *Development of Fischer-Tropsch Catalysts for Gasified Biomass.* Thesis. KTH School of Chemical Science and Engineering.
Murray, G. 2008, personal communication,2008.
New Zealand Forest Industry. (2006). *New Zealand Forest Industry Facts and Figures*: New Zealand Forest Owners Association.
Olofsson, I., Nordin, A., & Soderlind, U. (2005). *Initial Review and Evaluation of Process Technologies and Systems Suitable for Cost-Efficient Medium-Scale Gasification for Biomass to Liquid Fuels*: Umea University and Mid Sweden University.
Pfeifer, C., Hofbauer, H., & Rauch, R. (2004). *In-bed Catalytic Tar Reduction in a Dual Fluidized Bed Biomass Steam Gasifier* Vienna: Institute of Chemical Engineering, Vienna University of Technology.
Power Plants around the World (2007). *Biomass Power Plants in California*. Retrieved 12 April. 2008, from http://www.industcards.com/ppworld.htm
Probstein, R. H., & Hicks, E. R. (2006). *Synthetic Fuels*. Cambridge: Dover Publications Inc.
Quaak, P., Knoef, H., & Stassen, H. (1999). *Energy from Biomass: A Review of Combustion and Gasification Technologies*.
Rauch, R. (2004). *Steam Gasification of Biomass at CHP Plant Guessing-Status of the Demonstration Plant* Getreidemarkt: Institute of Chemical Engineering, Vienna.
Rauch, R., Hofbauer, H., Loffler, G., Kaiser, S., Fercher, E., & Tremmel, H. (2002). *Six Years Experience with the FICFB-Gasification Process*: Institute of Chemical Engineering, Vienna, 12th European Conference & Technology Exhibition on Biomass for Energy.
Read, S., Richards, L., & Perrin, N. (n.d.). *Assessment of New Zealand Greywacke Rock Masses with the Hoek-Brown Failure Criterion*.
Reed, T., & Desrosiers, R. (n.d.). *The Equivalence Ratio: The key to understanding pyrolysis, combustion and gasification of fuels*. Retrieved 8 March. 2007, from http://gasifiers.bioenergylists.org/stovesdoc/BEF/Equivalence_Ratio_Diagram.pdf
Robinson, M. (2006). *Forests, Wood and Australia's Carbon Balance.* Paper presented at the Bioenergy Australia 2006, Fremantle.
Rutherford, J. (2006). *Heat and Power Applications of Advanced Biomass Gasifiers in New Zealand's Wood Processing Industry.* Research Based Thesis. University of Canterbury.
Schuck, S. (2007). *Bioenergy from Forestry-Status and Opportunities for Australia*.Melbourne: Bioenergy Australia. Retrieved 13 December. 2006, from http://www.ensisjv.com/Portals/0/StevenSchuckBioenergyPres.pdf
Sims, R. E. H. (2002). *The Brilliance of Bioenergy in Business and in Practice*. London: James & James (Science Publishers),.
Smith, J. M., Van Ness, H. C., & Abbott, M. M. (1996). *Introduction to Chemical Engineering Thermodynamics*: McGraw-Hill.
Sorensen, B. (2004). *Renewable Energy: Its Physics, engineering, environmental impacts, economics and planning*. London: Elsevier Academic Press.
Sparks, R., & Wilson, C. (2007). *Fluidization*. Retrieved 21 November. 2007, from http://www.nsm.buffalo.edu/courses/gly433/Fluidization.pdf
Supp, E. (1990). *How to Produce Methanol from Coal*: Springer-Verlag.
Sutton, D., Kelleher, B., & Ross, J. R. H. (2001). *Review of Literature on Catalysts for Biomass Gasification*: Centre for Environmental Research, University of Limerick.
The Engineering Toolbox (2005). *The Definition of STP and NTP*. Retrieved 19 October. 2007, from www.engineeringtoolbox.com/stp-standard-ntp-normal-air-d_772.html
The Engineering Toolbox (n.d.). *Thermal Conductivity of some common Materials*: The Engineering Toolbox. Retrieved 19 October. 2007, from http://www.engineeringtoolbox.com/thermal-conductivity-d_429.html
Wergelandsveien (2008). *Gasification*: Zero Emission Resource Organisation. Retrieved 27 April. 2008, from http://www.zero.no/transport/bio/gasification

10.0 Glossary

Absorption: The physical or chemical phenomenon/process in which atoms, molecules, or ions enter some bulk phase (gas, liquid or solid material). This is a different process from adsorption, since the molecules are taken up by the volume, not by surface.

Adsorption: The adhesion of the molecules of gases, liquids, or dissolved substances to a solid surface (such as activated carbon).

Angle of Repose: A concentrated stream of falling solids pile up to form a cone shape. The angle of repose is the angle between the horizontal and one side of the cones surface if looking onto the vertical plane.

Annulus: The outer ring of falling solids in a circulating fluidized bed reactor about the core.

Attrition: The breaking of particles caused by collisions or other stresses (e.g.: thermal expansion).

Blast: Another name for gasifying agent or oxidant which contains oxygen in its chemical composition and causes oxidation.

Clinker: Material which becomes agglomerated and fused into a solid chunk due to over heating.

Cogeneration: This is the production of two or more forms of useful energy from an energy plant. Often it involves the production of electricity and process heat.

Combined Cycle: This is where two thermodynamic cycles operate together. A topping cycle (often the Brayton Cycle) rejects its waste exhaust heat and it is used as the input thermal energy into the bottoming cycle (commonly a Rankine Cycle or variation of it).

Core: The inner stream of solids being funnelled upwards within the annulus of a circulating fluidized bed reactor.

Devolatilise: to remove volatile matter from a substance

Elutriation: The process of separating and physically removing the lighter particles of a powder from the heavier particles by means of an upwardly directed stream of fluid (gas or liquid).

Energy Carrier: An energy carrier is any substance that has a useable form of energy but is not a primary energy source itself. e.g.: hydrogen, producer gas, compressed air.

Equivalence ratio: The amount of oxygen used in the thermochemical process relative to the amount required for complete combustion.

Eutectic: The lowest temperature at which a mixture of two materials will melt.

Flighting: The spiral wound metal inside an auger which rotates translating material.

Fluidization: Fluidization is the method by which solid particles are transformed into a fluid-like state through contacting with an upward flowing gas or liquid.

Gasification: the conversion of any carbonaceous fuel to a gaseous product with a useable heating value.

MJ/Nm^3: Mega Joules/Normal meter cubed. This is a gas volume flow rate adjusted to one atmosphere of pressure and 0 °C.

Moderator: This is a substance such as steam which can be injected into gasification reactors to help control the temperatures but often serves the second purpose of raising the hydrogen content.

Oxidising agent: Any material containing oxygen in its chemical structure that can cause oxidation in a thermochemical reaction (the same as blast or gasifying agent).

Producer Gas: The term used to describe the gas generated from gasifiers which consists of many different individual gases mixed together. The gas components are usually: carbon monoxide, hydrogen, carbon dioxide, nitrogen, methane, ethane, ethane, and water vapour.

Riser: Another name for the vertical combustion column.

Sensible Energy: This is the portion of internal energy of a system associated with the amount of thermal energy of matter in the gas, liquid or solid state.

Siphon: The seal loop that passes bed material and char through itself but prevents the exchange of flue gas and producer gas at the top of the gasification reactor.

Slagging: An event which occurs when temperatures in a gasifier is above the melting temperature of the ash so it becomes a liquid phase (which is often drained off).

Sparger: A tube with many small holes drilled into its underside. It is used to fluidize material in siphons and chutes to help the material travel along.

Standpipe: The vertical pipe section of the gasifier that connects the base of the flue gas cyclone to the siphon.

Superficial velocity: is the mean velocity of a fluid flowing through a column. It is defined as the gas flow rate (m^3/s) divided by the cross sectional area (m^2).

Synthesis Gas: Also called syngas or biosyngas (if derived from biomass). Synthesis gas only consists of two gaseous components: CO and H_2. It is not the same as producer gas because of its lack of other gaseous components, and is often the result of purifying producer gas to remove the other gas components.

Appendix A – Compositional Analysis of the Test Fuel: Wood Pellets

CRL Energy Ltd

REPORT OF ANALYSIS

Date Received: 26-Aug-05

Client: Canterbury University

Description: Wood Chip pellets and Husk samples supplied by client.

CRL Energy Ltd Reference:			76/050	76/051	76/052
Customer Reference:			Sample#1 Chips	Sample#2 Pellets	Sample#3 Husks
Analysis - As Received Basis				NZ Radiata pine wood pellets	
Moisture	ISO 5068	%	52.6	8.0	9.9
Ash	ASTM D1102	%	0.2	0.4	2.6
Volatile	ISO 562	%	39.8	77.4	73.8
Fixed Carbon	By Difference	%	7.4	14.2	13.7
Gross Calorific Value	ISO 1928	MJ/kg	9.53	18.63	17.08
Carbon	micro analytical	%	24.3	47.2	43.7
Hydrogen	micro analytical	%	2.87	5.35	5.07
Nitrogen	micro analytical	%	<0.1	<0.2	0.56
Sulphur	ASTM D4239	%	0.01	0.01	0.06
Oxygen	By Difference	%	20.0	38.7	38.1
CHN determined by Chemsearch Otago University					
Analysis - Dry Basis					
Ash	ASTM D 1102	%	0.4	0.4	2.9
Volatile	ISO 562	%	84.0	84.1	81.9
Fixed Carbon	By Difference	%	15.6	15.4	15.2
Gross Calorific Value	ISO 1928	MJ/kg	20.10	20.25	18.95
Carbon	micro analytical	%	51.2	51.3	48.5
Hydrogen	micro analytical	%	6.10	5.81	5.63
Nitrogen	micro analytical	%	<0.2	<0.2	0.62
Sulphur	ASTM D4239	%	0.02	0.01	0.07
Oxygen	By Difference	%	42.3	42.4	42.9
Ash Constituents	(XRF)				
SiO2		%	28.46	20.50	71.72
Al2O3		%	5.43	4.66	0.11
Fe2O3		%	1.78	2.72	0.28
CaO		%	23.07	24.37	4.37
MgO		%	10.38	8.95	2.76
Na2O		%	1.49	1.75	1.04
K2O		%	18.11	21.51	11.00
TiO2		%	0.20	0.27	0.01
Mn3O4		%	2.28	1.90	0.25
SO3		%	2.60	3.50	1.42
P2O5		%	3.05	5.09	5.62

Appendix B – In-bed Fuel Feed System Design Spreadsheet

Auger Design Calculations for Wood Pellets

General Information

	Doug's 1	(Chosen) Doug's 2	Rick's
Wood pellets bulk density (kg/m^3)	505	668	730
Medium wood chips bulk density (kg/m^3)	160	160	160
Course wood chips bulk density (kg/m^3)	113	113	
Average fuel consumption rate (kg/hr)	20.0		
Average fuel consumption rate (m^3/hr)	0.03		

Auger Feed Calcs

Parameters	(mm)	(m)	
Diameter of screw:	52	0.052	
Lead on screw :	45	0.045	Note: For single threads the lead is equal to the pitch (m)
Distance conveyed per revolution (mm):	45		
Total distance mass is conveyed (mm):	45		

	(rev/s)	(rev/min)	(rev/hour)
Rotational speed:	0.13	8.0	480.9

Number of revolutions:	1	
Density of material conveyed (kg/m^3):	668	
Packing factor of material in screw volume.	0.65	*Determined experimentally from the existing auger, must be between 0.0 - 1.0*
Mass conveyed per revolution (kg/rev):	0.041	(Vol*Density)*Packing Factor
Mass conveyed per hour (kg/hr):	**20.0**	The gasifier uses 20kg/hr of wood fuel so adjust motor frequency to maintain 20kg/hr.
Volumetric fuel consumption rate (m^3/hr)	0.03	

Motor-Gearbox Calculations

Parameters	rpm	Hz	Percentage of 50Hz
Motor Speed into gearbox	561		
Gear ratio (x:1)	70		
Variable speed frequency		23.7	47
Gearbox output speed	8.0		

Hopper Size Calculations

Parameters	(mm)	(m)
Hopper Length (relative to auger axis)	180	0.18
Hopper Width	200	0.2
Hopper internal heigth	430	0.43

Density of material conveyed (kg/m^3):	668	
The auger feed rate is (kg/hr):	**20.0**	The gasifier uses 20kg/hr of wood fuel so adjust rotational speed to maintain 20kg/hr.
Storage volume (m^3):	0.015	20kg of wood pellets occupies a volume of 0.55m^3
Storage mass (kg):	10.341	Vol x Density
Storage quanity w.r.t time (min):	31.1	For example: 1kg of wood pellets lasts 3 mins. The gasifier consumes 0.34kg/min of wood pellets.

Note: If the auger is fully packed (packing factor = 1)

Auger Design Calculations for Wood Chips

General Information

	Doug's 1	(Chosen) Doug's 2	Rick's
Wood pellets bulk density (kg/m^3)	505	668	730
Medium wood chips bulk density (kg/m^3)	160	160	160
Course wood chips bulk density (kg/m^3)	113	113	
Average fuel consumption rate (kg/hr)	20.0		
Average fuel consumption rate (m^3/hr)	0.03		

Auger Feed Calcs

Parameters	(mm)	(m)	
Diameter of screw:	52	0.052	
Lead on screw :	45	0.045	Note: For single threads the lead is equal to the pitch (m)
Distance conveyed per revolution (mm):	45		
Total distance mass is conveyed (mm):	45		

	(rev/s)	(rev/min)	(rev/hour)
Rotational speed:	0.13	33.4	2005.7

Number of revolutions:	1	
Density of material conveyed (kg/m^3):	160	
Packing factor of material in screw volume.	0.65	*Determined experimentally from the existing auger, must be between 0.0 - 1.0*
Mass conveyed per revolution (kg/rev):	0.010	(Vol*Density)*Packing Factor
Mass conveyed per hour (kg/hr):	**19.9**	The gasifier uses 20kg/hr of wood fuel so adjust motor frequency to maintain 20kg/hr.
Volumetric fuel consumption rate (m^3/hr)	0.03	

Motor-Gearbox Calculations

Parameters	rpm	Hz	Percentage of 50Hz
Motor Speed into gearbox	2340		
Gear ratio (x:1)	70		
Variable speed frequency		83	47
Gearbox output speed	33.4		

Hopper Size Calculations

Parameters	(mm)	(m)	
Hopper Length (relative to auger axis)	180	0.18	
Hopper Width	200	0.2	
Hopper internal heigth	430	0.43	
Density of material conveyed (kg/m^3):	160		
The auger feed rate is (kg/hr):	**19.9**	The gasifier uses 20kg/hr of wood fuel so adjust rotational speed to maintain 20kg/hr.	
Storage volume (m^3):	0.015	20kg of wood pellets occupies a volume of 0.55m^3	
Storage mass (kg):	2.477	Vol x Density	
Storage quanity w.r.t time (min):	7.5	For example: 1kg of wood pellets lasts 3 mins. The gasifier consumes 0.34kg/min of wood pellets.	

Note: If the auger is fully packed (packing factor = 1)

Appendix C – Producer Gas Flow Rate Determination

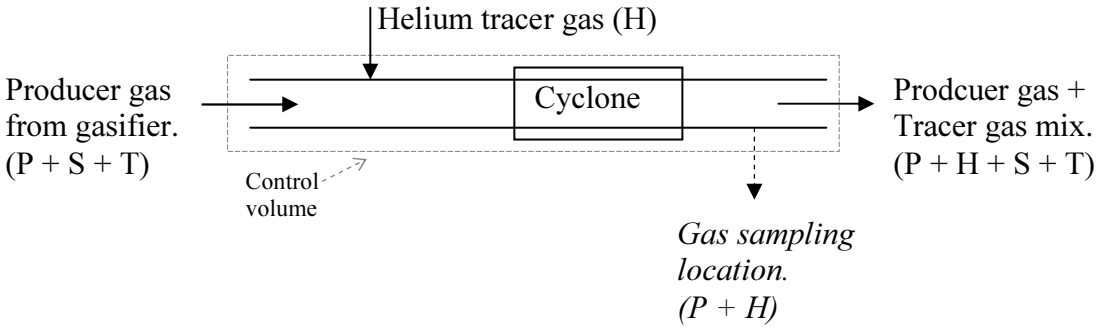

Problem: To measure the flow rate of producer gas from the FICFB gasifier and convert it to a flow rate at STP (0 °C, 1 atm).

Solution: To inject a known flow rate of helium into the producer gas stream and measure the composition of the producer gas + helium mixture in a microGC further down the line after adequate mixing has occurred. From the gas composition, calculate the producer gas flow rate.

Key: Basis for calculations = 1 second.
P = flow rate of dry producer gas (mol)
S = steam flow rate (mol)
H = helium flow rate (mol)
h_{conc} = helium concentration in the producer gas (vol% ≈ mol%)
T = Tar flow rate in producer gas (mol)

When a gas sample is taken, all moisture and tars are removed through an SPE column and a moisture trap, so the measured gas composition in the microGC contains only P + H. Gas sampling is taken at about 650 °C but cools down to room temperature and pressure as the producer gas sample is collected in a syringe before analysis in a microGC.

Assumptions:

1. That all producer gas samples are drawn from a 650 °C environment but cool down to 25 °C during pulling the gas through the sampling apparatus into the syringe for microGC analysis.
2. That the ambient temperature in the lab is 25 °C.
3. Assuming ideal gas laws apply so that vol% ≈ mol%.
4. The collected gas sample is moisture and tar free.

The helium flow rate 'H' is measured by calibrated rotameter. This is at room temperature and pressure (≈25 °C). The helium rotameter is calibrated for a flow rate in L/min.

Helium Balance: **(**Units = mols/min)

$H_{in\ Total} = H_{out\ Total}$

$H_{in\ Total} = h_{conc}\ (P_{out} + H_{out})$

Since: $H_{in} = H_{out} \equiv H$
and, $P_{out} \equiv P$

$H = h_{conc}\ (P + H)$

Measure H and h_{conc} during gasifier operation,

$$P = \frac{H}{h_{conc}} - H$$
$$= H\left(\frac{1}{h_{conc}} - 1\right)$$

Using test data from the hot run on 15/2/08, at sampling time 2.06pm,
The test conditions were: Dry fuel feed rate = 18.4 kg_{dry}/h of wood pellets
Steam injection/generation = 10.1 kg/h of steam at 200 °C, 5 bar.
Gasification temperature = 727 °C (BFB #1 temp)
Producer gas temperature in cyclone = 646 °C
Helium concentration in producer gas = 0.651 vol% (≈mol%)
Helium flow rate = 1.29 L/min at 25 °C (2.5 on rotameter)

Since: 1 mol of ideal gas = 24.45 L (at 25 °C, 1 atm).
1 L of ideal gas = 40.90 x 10^{-3} mol (at 25 °C, 1 atm).

Therefore: Helium flow rate = 1.29 L/min x 40.90 x 10^{-3} mol/L
= 52.76 x 10^{-3} mol/min, (at 25 °C, 1 atm).

$$P = 52.76 \times 10^{-3}\left(\frac{1}{0.00651} - 1\right)$$
= 8.052 mol/min (at 25 °C, 1 atm)
= 8.052 mol/min x 60/1 min/h
= 483.1 mol/h (at 25 °C, 1 atm)

Now convert to m^3/h at 0 °C, 1 atm.

$$PV = nRT$$
$$V = \frac{nRT}{P}$$
$$= \frac{483.1\ \frac{\text{mol}}{\text{h}} \times 8.314\ \frac{Pa \cdot m^3}{mol \cdot K} \times 273\ \text{K}}{101{,}325\ \text{Pa}}$$
$$= 10.8\ Nm^3/h \quad \text{(at 0 °C, 1 atm).}$$

Appendix D – Particle Terminal Velocity and Superficial Velocity Assessment

During hot operation of the gasifier, an unsatisfactory amount of bed material is lost out the producer gas line and is being found in the producer gas cyclone particle trap. These calculations are to compare the superficial velocities present in the gasification reactor, to the terminal velocity of the different particle sizes present in the bed materials. Two sets of calculations have been performed at 25 °C and 700 °C, representing conditions at the beginning and near the end of the heat-up phase of the gasifier.

The total gas flow rate up the gasification column is greatest during the heat-up stage when air and LPG are introduced into the gasification column. Once gasification of wood begins, the fluidizing air is changed over to steam and all LPG supplied to the gasification column is stopped. The release of the pyrolysis gas and fluidizing steam combined creates a lower total gas flow rate than occurs during the heat-up stage with the five components entering the gasification column as listed in Figure D1.

Assumptions:

1. Assume the superficial gas flow up the gasification column is steady.
2. Assume LPG and combustion gases in the gasification reactor can be represented as air.
3. Assume all chute fluidizing gas goes up the chute into the gasification reactor.
4. Assume the flow rate of BFB LPG is 30L/min similar to in the combustion reactor.
5. Assume the bed material particles are all spherical.
6. Assume u (the relative velocity between the particles and the main body of the fluid), is equal to the superficial velocity.

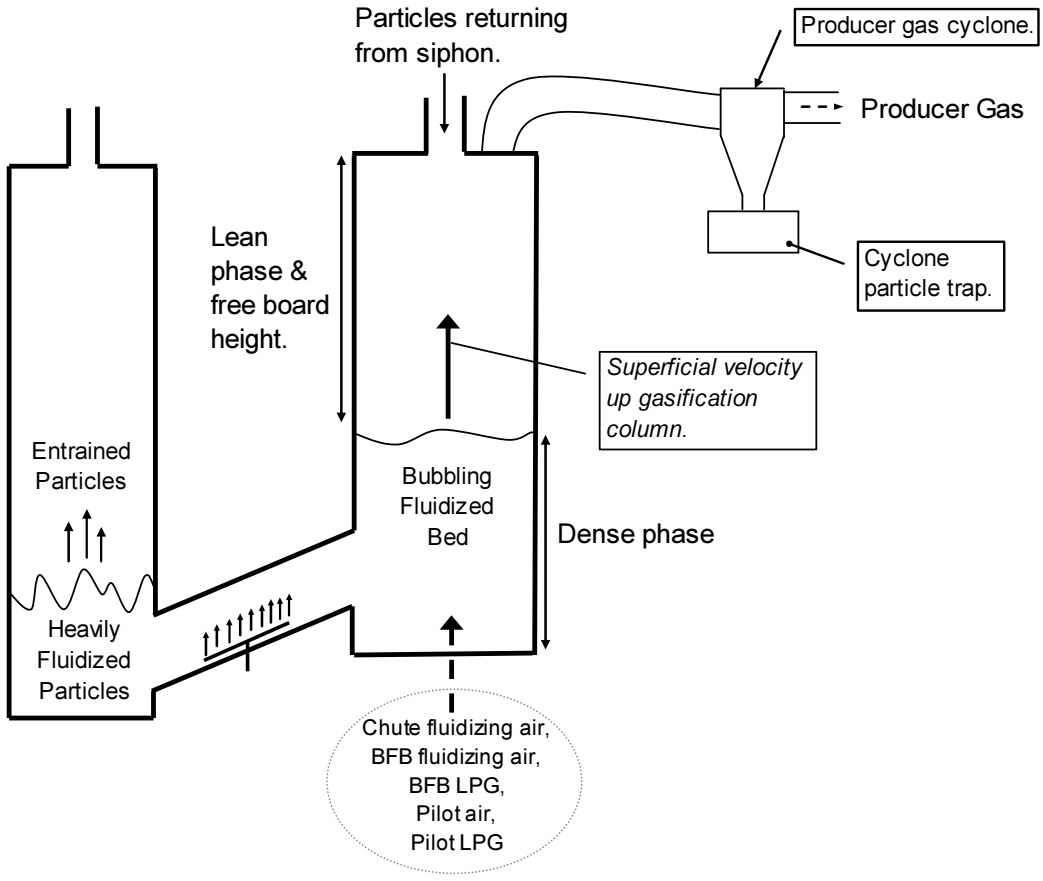

Figure D1: Diagram of part of the FICFB gasifier showing the superficial velocity vector up the gasification reactor and the cyclone and particle trap in the producer gas line.

The superficial gas velocity up the gasification column during the heat-up stage is calculated from the sum of all the individual gas flow rates entering the reactor. The flow rates of gases are measured at ambient temperature, but have been corrected for a 250 °C preheat for the chute and BFB fluidizing air. The effect of combusting gases erupting and projecting particles up the reactor has been intentionally ignored at this stage of the analysis.

Total gas flow rate = Chute fluidizing air + BFB fluidizing air + BFB LPG + Pilot air + Pilot LPG

= 97 L/min + 140 L/min + 30 L/min + 20 L/min + 5 L/min
= 292 L/min
= 292 L/min x 1/1000 m^3/L x 1/60 min/s
= 4.867 x 10^{-3} m^3/s

Cross sectional area of gasification column = $\frac{\pi D^2}{4} = \frac{\pi \times 0.2^2}{4} = 0.03142\ m^2$

Superficial velocity up gasification column = $\frac{\text{Gas flow rate } (m^3/s)}{\text{Cross sectional area } (m^2)} = 0.16\ m/s$

From the assumptions made above, and ignoring the effect of combustion in the gasification column during the heat-up phase, the average velocity up the gasification column is *0.16 m/s*.

Now the terminal velocity of the different particle size ranges in the bed material will be calculated to see if any particles size ranges have a terminal velocity below the superficial velocity up the gasification reactor.

For spherical particles of diameter d_p, the terminal velocity is calculated by:

$$U_{terminal} = \sqrt{\frac{4gd_p(\rho_p - \rho_f)}{3\rho_f C_D}}$$

Equation (1).

Where: $g = 9.81\ m/s^2$
d_p = diameter of particle
ρ_p = density of particle — 2700kg/m^3 for greywacke (Read *et al.*, n.d.).
ρ_f = density of fluid — Assumed to be only air at chosen temperatures.
C_D = Drag coefficient

To obtain the drag coefficient for equation 1, the Reynolds number of each individual particle size needs to be calculated:

$$Re_p = \frac{d_p \rho_f u}{\mu}$$

Where: u = relative velocity between particle and fluid ≈ superficial velocity
μ = fluid viscosity (this value is taken for air at two different temperatures).

For 25 °C: $\rho_f = 1.186$ kg/m^3 for dry air at 1 atm, $\mu = 1.846 \times 10^{-5}$ kg/ms for dry air at 1 atm.

For 700 °C: $\rho_f = 0.3632$ kg/m^3 for dry air at 1 atm, $\mu = 4.026 \times 10^{-5}$ kg/ms for dry air at 1 atm.

The bed material particle size distribution is divided into nine different groups between 0 and 1000+ microns. For particle Reynolds numbers where $Re_p < 0.1$,

$$C_D = \frac{24}{Re_p} \qquad \text{Equation (2).}$$

For particle Reynolds numbers in the range of $0.1 < Re_p < 1000$:

$$C_D = \left(\frac{24}{Re_p}\right)\left(1 + 0.14 \cdot Re_p^{0.7}\right) \qquad \text{Equation (3).}$$

A chart of the particle size distribution of the greywacke bed material is shown in Figure D2. The nine different particle size groups can be seen along the x-axis. For example, the bar corresponding to 250 μm means that 58 % of the bed material particles were collected on a 250 μm sieve and passed through a 355 μm sieve. Hence, there particle size range is 250-355 μm. Any particles that were larger than 1000 μm were removed from the bed material mix. The particle size ranges used in the calculations were equivalent to the nine mesh sizes of Figure D2.

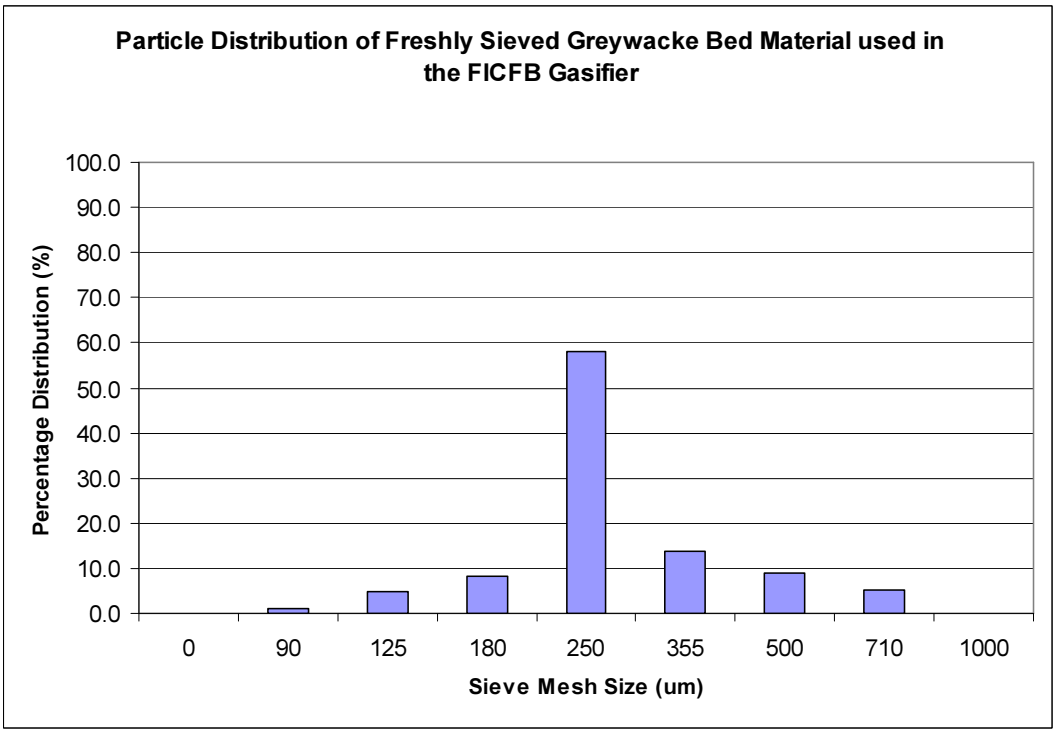

Figure D2: The particle size distribution of the greywacke bed material used in the gasifier.

The results of the calculations performed at 25 °C (298K) are shown in Table D1. These values are representative of the initial heat-up phase of the gasifier.

Table D1: Terminal velocity of the different bed material size range classes at 25 °C.

Particle Size (µm)	$Re_{particle}$ @ 25 °C	C_D @ 25 °C	Terminal Velocity (m/s^2)
0	0.00	-	-
90	0.58	45.1	*0.8*
125	0.81	33.2	*1.2*
180	1.17	23.8	*2.1*
250	1.62	17.7	*3.3*
355	2.30	13.1	*5.5*
500	3.24	9.8	*9.0*
710	4.60	7.3	*14.7*
1000	6.48	5.6	*23.7*

The results of the calculations performed at 700 °C (973K) are shown in Table D2. These values are representative of the final heat-up phase of the gasifier.

Table D2: Terminal velocity of the different bed material size range classes at 700 °C.

Particle Size (µm)	$Re_{particle}$ @ 700 °C	C_D @ 700 °C	Terminal Velocity (m/s^2)
0	0.00	-	-
90	0.08	293.2	*0.5*
125	0.11	217.6	*0.9*
180	0.16	152.4	*1.5*
250	0.23	110.8	*2.4*
355	0.32	79.1	*4.1*
500	0.45	57.0	*6.7*
710	0.65	41.0	*11.3*
1000	0.91	29.8	*18.6*

All terminal velocities for particle sizes larger than 90 microns are above the calculated superficial velocity of 0.16 m/s. Therefore entrainment of particles in the size ranges analysed should not be occurring. However, from visual observations within the gasification column, it can be clearly seen that the combusting bubbles of LPG and air in the BFB send a spray of particles up in the gasification column, often nearing the exit port for the producer gas. So the violently combusting bubbles of LPG during the heat-up phase is responsible for the majority of the bed material loss. To reduce this problem, the fine particles below 200 microns are now removed from the bed material and the quantity of LPG and hence amount of projecting particles during the heat up stage have been significantly reduced. Now bed material loss rates can be maintained around 7-9 % over a 10-11 hour operating period.

Appendix E – Influx of Air Mass Balance Spreadsheet

21/02/2007 **Oxygen Balance:** Senario 1

Nitrogen flowing into chute, siphon and BFB fluidizing distributor

The reason for performing these nitrogen tests was to determine if air did track from the CFB into the BFB through the chute and to basically determine how much flowed into the BFB.

Initally set air coming through the chute to 6 L/min to approximate 0.6% O2 content before running solver.

	Flows in	L/min	L/min
Chute + CFB a	Air from CFB (mostly fluidizing air)		10.2
	Nitrogen from Chute rotameter	49.8	
	Air from Chute rotameter	0	
	Percentage of flow added going to BFB	100	
	Actual N2 going to BFB that was added thru rotameter		49.8
	Actual air going to BFB that was added thru rotameter		0

Total flow going through chute to BFB (CFB air + chute fluidizing gas)	**60.0**	
O2	**2.1**	
N2	**57.9**	
O2	**3.6**	%
N2	**96.4**	%

BFB	Nitrogen from BFB	283.2	
	Air from BFB	0	

Total flow from BFB distributor	**283.2**	
O2	**0**	
N2	**283.2**	
O2	**0**	%
N2	**100**	%

Syphon	Air carryover from CFB		0
	Nitrogen from syphon rotameter	22.2	
	Air from Chute rotameter	0	
	Percentage of flow added going to BFB	67.6	
	Actual N2 going to BFB from siphon		15.0
	Actual air going to BFB from rotameter		0

Total flow	**15.0**	
O2	**0.0**	
N2	**15.0**	
O2	**0**	%
N2	**100**	%

Summary	Total flow to the BFB = total flow out	358.2	
	Total flow O2 to the BFB = total flow out	2.1	
	Total flow N2 to the BFB = total flow out	356.1	
	O2	**0.6**	**%**
	N2	**99.4**	**%**

Target O2	0.6	%
Absolute difference	3.2647E-10	
Total abs diff	0.16865082	

21/02/2007

Oxygen Balance: Senario 2

Air in the siphon only, nitrogen in chute and BFB fluidizing distributor.

Adjusted syphon percentage air into BFB to get correct result of O2 percentage

Flows in

		L/min	L/min
Chute + CFB ai	Air from CFB		10.2
	Nitrogen from Chute rotameter	49.8	
	Air from Chute rotameter	0	
	Percentage of flow added going to BFB	100	
	Actual N2 going to BFB that was added thru rotameter		49.8
	Actual air going to BFB that was added thru rotameter		0

Total flow going through chute to BFB (CFB air + chute fluidizing gas)	**60.0**	
O2	**2.1**	
N2	**57.9**	
O2	**3.6**	%
N2	**96.4**	%

BFB	Nitrogen from BFB	283.2	
	Air from BFB	0	

Total flow from BFB distributor	**283.2**	
O2	**0**	
N2	**283.2**	
O2	**0**	%
N2	**100**	%

Syphon	Air carryover from CFB	0	
	Nitrogen from syphon rotameter		
	Air from Chute rotameter	19.2	
	Percentage of flow added going to BFB	67.6	
	Actual N2 going to BFB from rotameter	0	
	Actual air going to BFB from rotameter	13.0	

Total flow	**13.0**	
O2	**2.7**	
N2	**10.3**	
O2	**21**	%
N2	**79**	%

Summary	Total flow to the BFB = total flow out	356.2	
	Total flow O2 to the BFB = total flow out	4.9	
	Total flow N2 to the BFB = total flow out	351.3	
	O2	**1.4**	**%**
	N2	**98.6**	**%**
	Target O2	1.2	%
	Absolute difference	0.16859	

21/02/2007

Oxygen Balance: Senario 3

N2 in the BFB only with air in the chute and siphon.

Adjusted syphon percentage air into BFB to get correct result of O2 percentage

Flows in

		L/min	L/min
Chute + CFB air	Air from CFB		10.2
	Nitrogen from Chute rotameter	0	
	Air from Chute rotameter	48	
	Percentage of flow added going to BFB	100	
	Actual N2 going to BFB that was added thru rotameter		0
	Actual air going to BFB that was added thru rotameter		48

Total flow going through chute to BFB (CFB air + chute fluidizing gas)	**58.2**	
O2	**12.2**	
N2	**46.0**	
O2	**21**	%
N2	**79**	%

BFB	Nitrogen from BFB	274.8	
	Air from BFB	0	

Total flow from BFB distributor	**274.8**	
O2	**0**	
N2	**274.8**	
O2	**0**	%
N2	**100**	%

Syphon	Air carryover from CFB	0	
	Nitrogen from syphon rotameter		
	Air from Syphon rotameter	21.6	
	Percentage of flow added going to BFB	67.6	
	Actual N2 going to BFB from rotameter	0	
	Actual air going to BFB from rotameter	14.6	

Total flow	**14.6**	
O2	**3.1**	
N2	**11.5**	
O2	**21**	%
N2	**79**	%

Summary	Total flow to the BFB = total flow out	347.6
	Total flow O2 to the BFB = total flow out	15.3
	Total flow N2 to the BFB = total flow out	332.3
	O2	**4.4 %**
	N2	**95.6 %**
	Target O2	4.4 %
	Absolute difference	6.1E-05

Appendix F – Procedures for Operating the FICFB Gasifier

Last updated: 18/4/08

Date

In the Days before Intended Operation

Let fire engineering know we need the lab facilities
Check blower availability
Email we want to run a test (with Shusheng, John A, David Brown)
Check both LPG banks have enough fuel for run
Book use of boiler in workshop logbook
Ensure enough SPA columns are available
Ensure syringe sampling system is set up with dry silica gell
Measure material in flue gas particle trap
Measure material in BFB cyclone particle trap
Measure mass of sand left in beds
Check syphon is clear
Check auger head is clear and no bridging of pellets
Check all viewing ports are clear
Check O2 Sensor lines are clear of char & valve turned onto BFB
Check any bolts that have been undone are tightened
H2, CO and O2 sensors have current calibration
Start all burners & circulate gasifier to check system
Schedule clear, clashes sorted

Pre-run checks

Display sign on combustion lab door
Arc reactor off
Unset alarm and open roller door to particle lab
Wood feeder full
Screw feeder connected, valve closed (V13)
Open black pneumatic value for photocell & control valve air
Extractor duct open for gasifier lab extraction system
"Extractor Fan E1 & E2" on
"Fire Hood Fan" on (should read *65%* or higher)
Safety glasses on

Air start-up

Vent valve in particle lab D175 1/3 open and hole covered
Main red handled blower line valve in lab fully open
Check rotameter valves are closed so floats do not hit stoppers
BFB & Chute pneumatic hose for rotameters connected & turned on
Blower speed 5Hz then set to 20 Hz
Turn main power switchs on too control cabinet (S5 & S6)
Controller in normal mode and faults cleared
Wait 30seconds for control valves to open
When control valves open set rotameter flows as shown below
Check circulation & syphon is clear (syphon pressure drop:40-60)
Check standpipe air is set at ~12 on rotameter
Bed pressure drops correct on meters (CFB ~1.2, BFB ~1.3)
Bed heights reasonable in viewing ports
Turn trace heating switch on
Start computer temperature readings
Flush the gasifier with air for at least 3 minutes to clear gases

Initial Rotameter Settings

CFB dist	Syphon	Prim Air	Chute Air	BFB fluid	A/B Pilot	A/B Main	A/B Dilution
22.5	16.5	11.5	16.5	8	9	6	10

LPG Start-up

Ensure switches (S2, S3 & S4) are all off
LPG on in control room to combustion lab
Yellow LPG valve to A/B solinoid open & LPG supply line
Check LPG pressure gauge reads 15 psig
A/B switch S4 on
A/B controller set to 1, push blue button
Check A/B view port for flame
CFB switch S2 on
Open valve, turn CFB cabinet switch to 1 & push blue button
Check CFB flame visually and temperatures.
Turn on BFB switch S3
Turn yellow LPG valve on for BFB pilot
Turn BFB contoller switch to 1, push blue button
Check BFB fluidizing air rotameter flow at ~8
Check BFB & CFB O2 readings (~10-22)
Check temps and view flames through view ports
All main burner ball & needle valves should be closed
Turn CFB controller to 2
Open yellow CFB valve and needle valve (slowly)
Set the CFB LPG flow to 20L/min for 2 mins
Set the CFB LPG flow to 35L/min for 2 mins
Set the CFB LPG flow to 45-50L/min for heat up
Visual check in CFB and watch O2 reading decrease
Adjust needle until CFB O2 reads about ~6 %
Set BFB controller set to 2
Open yellow BFB LPG valve and needle valve (slowly)
Visual check in BFB view port, watch O2 reading decrease
Adjust needle until BFB O2 reads ~5 %

General Heat up

All readings monitored constantly and recorded every 30 min
Visual inspections every 30 min through view ports
Clear BFB O2 sensor line every 30 minutes
Check for leaks
If temps plateau on computer, increase air & LPG for heat-up
Increase air rates at 680 °C
Increase LPG and check O2
Turn nitrogen purge on low for heat-up (10L/min) once BFB1>500°C
Check wood pellet level in main hopper
Micro GC needs bake out process run before operation

Boiler Start up

Check particle lab steam valve is open in room D113
Get boiler room key from cabinet & return afterwards
Check water level in sight tubes
Turn boiler 'burner' switch on in boiler room
Fill in boiler use book in boiler room (run times, project, initial)

Wood Feeder Start up

Temperature ~770 °C
Operators only in the lab
Turn switch S1 on (interlock will prevent auger operation)
Change O_2 to reading A/B flue gas instead of producer gas
Ensure circulation is adequate and no signs of blockages
Turn nitrogen cylinder flow up to 12
Turn cooling fan on for auger motor
Ensure knife gate valve is shut
Turn up A/B main air to 9 & A/B dilution air to 14.
Main BFB LPG needle off, yellow valve off & controller back to 1
Open main auger circular valve at top of main screw feeder
Check auger switches in Fwd mode (auger will not run unless S1 on)
Start feeding wood on a low setting
Check feed port is not causing pellets to bridge

Steam Start up

Check BFB distributor, syphon and chute temps
Ensure large steam line gate valve is shut
Check steam on at control panel (switch S1)
Empty condensed water into bucket
Turn main steam valve on very slowly to clear water into bucket
Turn BFB pilot burner yellow LPG valve off and controller set to 0
Progressively reduce airflow to BFB & increase steam to 6kg/h
Progressively reduce airflow to chute & increase steam to 4kg/h
Watch BFB #1 probe temp changes
Set syphon air to 6.0 with another operator watching standpipe level
View siphon, check bed material is circulating
Set DP cell threshold to 58
Turn helium tracer gas flow on to 4.5 on helium rotameter

Run hot test experiments!!!!

Set main LPG rotameter to about 20L/min for supplimentary firing
When steady state conditions have been reached, record all plant data in the spreadsheet
Take gas & tar samples & label both samples with sample number & date
Check pellet level in the main hopper regularly.

Standard Instrument Settings during Gasification

Helium	Chute Steam	BFB Steam	CFB fluid.	Syphon	Prim Air	A/B Pilot	A/B Main	A/B Dilution	Standpipe
4.5	4 kg/h	6 kg/h	22.5	6	12	9	6	16	12

Nitrogen	Wood Feed	Bed Material
12	20kg/h	12kg

Stopping Gasification

VSD off at wall and zeroed
Close circular valve at top of main auger
Increase siphon fluidization
Monitor A/B O_2 and adjust air accordingly
Reduce steam flow, increase air to BFB, chute, syphon
Turn off helium tracer gas at bottle
Let char burn out for 30 minutes
Regularly check standpipe view port for char circulation
Turn trace heating switch off located near steam meters

LPG shut down

Check main LPG supply valves are shut off on BFB & CFB
Monitor O2 then shut off pilot burners at main control panel
Leave A/B on for at least 5 min
A/B off at control Panel
LPG off in control room & keys away

Boiler Shut down

Get boiler room key from cabinet and return afterwards
Turn off 'burner' switch
Write down turn-off time in log book

Plant Shut Down

Let the gasifier circulate on air for 20 mins to help cool down
Air flow rates reduced through rotameters
Nitrogen Purge off
Stop Blower
Extraction hood off
Extract fans off
Micro GC computer off
Main power switches on control panel off
Compressed air off on black valve on instrument wall
Shut gasifier lab fire-stop doors
Put all keys away in the cabinet and lock cabin
Cover up warning sign on combustion lab door
Put roller door down to particle lab and reset the alarm switch

Appendix G – Bed Material Composition Analysis

The purpose of this exercise was to understand the composition of the different bed materials used in the FICFB gasifier. Bed materials are exposed to high temperatures possibly up to 900 °C in the combustion reactor, and understanding the composition of the material in relation to the softening temperature of the inorganic components is important to prevent agglomeration. An XRD analysis was performed on two greywacke bed material samples commonly used in the gasifier. One sample was determined as being 90 % quartz with 10 % albite, while the second sample was found to be 100 % quartz. There were noticeably different fusion characteristics of the two samples, and the sample containing 90 % quartz and 10 % albite was found to be more resistant to agglomeration.

XRF results of the major elements present in greywacke from a range of sites in New Zealand are displayed in Table G1. These have not been obtained from the material used in the gasifier, but instead from common sites where greywacke is quarried. They are expressed in terms of percent oxide because the samples are exposed to an oxidising environment during the sample preparation. Total Fe is quoted as Fe_2O_3 because the XRF cannot distinguish between the different oxidation states. LOI (Loss On Ignition) is carried out at 1000 °C and reflects the volatile components such as hydrated water, carbonate and carbon present. Table G2 has the same results for olivine sand which has been identified specifically as being forsterite. Other elements which occur in trace amounts in the olivine sample are displayed in Table G3 (Brown, 2006).

Table G1: XRF quantitative results of the major elements present in greywacke sand sourced from different locations. The greywacke bed materials used in the gasifier came from these regions (Brown, 2006).

Source Location	SiO2 (%)	TiO2 (%)	Al2O3 (%)	Fe2O3T (%)	MnO (%)	MgO (%)	CaO (%)	Na2O (%)	K2O (%)	P2O5 (%)	LOI 1000°C (%)	*Total (%)*
Washdyke	73.8	0.5	11.9	3.3	0.1	1.2	2.8	3.2	1.8	0.1	1.7	*100.1*
Rangitata	69.8	0.5	14.2	3.8	0.1	1.5	2.6	3.7	2.1	0.2	1.6	*100.0*
Wakanui	69.4	0.5	14.4	3.9	0.1	1.5	2.2	3.8	2.3	0.2	1.8	*100.1*
Rakaia	70.2	0.5	14.4	3.6	0.1	1.4	1.9	4.1	2.5	0.2	1.5	*100.3*
Ashburton cliffs	71.3	0.5	13.4	3.4	0.1	1.3	2.6	3.6	2.1	0.1	1.7	*100.1*
Kaitorete barrier	73.8	0.4	12.6	3.0	0.1	1.1	2.5	3.4	1.8	0.1	1.4	*100.2*

Table G2: XRF quantitative results of the major elements present in olivine sand (forsterite) (Brown, 2006).

Sand Sample	SiO2 (%)	TiO2 (%)	Al2O3 (%)	Fe2O3T (%)	MnO (%)	MgO (%)	CaO (%)	Na2O (%)	K2O (%)	P2O5 (%)	LOI 1000°C (%)	*Total (%)*
Olivine	41.1	0.02	0.2	11.0	0.2	46.6	0.3	<0.1	0.0	0.0	0.4	*100.0*

Table G3: Trace element analysis for olivine sand (forsterite) (Brown, 2006).

	V (ppm)	Cr (ppm)	Ni (ppm)	Zn (ppm)	Zr (ppm)	Nb (ppm)	Ba (ppm)	La (ppm)	Ce (ppm)	Nd (ppm)	Ga (ppm)	Pb (ppm)	Rb (ppm)	Sr (ppm)	Th (ppm)	Y (ppm)
Olivine	16	2510	2019	55	7	<2	47	<5	<5	<10	<2	1	5	5	<1	<1

Appendix H – Fusion Temperature Estimations

The ash fusion temperature determination is based on a set of regression formulas from a report titled: 'Predicting Coal Ash Fusion Temperature based on its Chemical Composition using ACO-BP Neutral Network', by Liu, Y. Wu, M. Qian, J of the Institute of Industrial Control Technology. Finding information on fusion predictions for fluidized beds using biomass was difficult, so the regression formulas for coal were applied to Greywacke and olivine bed materials plus, the inert components of the wood pellets in the hope that since they use the ultimate analysis of materials in their calculations, that they could also be applied more widely than just for coal. However, the accuracy of this approach is unknown, especially when applied to biomass and granular bed material. (The ultimate analysis of wood pellets and the bed materials are presented in Appendix A and G respectively).

These calculations are based on the fusion temperatures being represented by the softening temperature of the inert components. Experimental obtaining the fusion temperatures is time consuming and troublesome, so it was hoped that this approach would provide an approximate indication of when the formation of clinker could occur.

Four regression formulas exist for four different compositional groups (Liu *et al.*, 2006):

1. "When the content of SiO_2 is no larger than 60 % and the content of Al_2O_3 is larger than 30 %, the fusion temperature is calculated by:" (Liu *et al.*, 2006).

$T = 69.94 \times SiO_2 + 71.01 \times Al_2O_3 + 65.23 \times Fe_2O_3 + 12.16 \times CaO + 68.31 \times MgO + 67.19 \times A - 5485.7$

Where $A = 100 - (SiO_2 + Al_2O_3 + Fe_2O_3 + CaO + MgO)$

2. "When the content of SiO_2 is no larger than 60%, the content of Al_2O_3 is no larger than 30 %, and the content of Fe_2O_3 is no larger than 15 %, the fusion temperature is calculated by:" (Liu *et al.*, 2006).

$T = 92.55 \times SiO_2 + 97.83 \times Al_2O_3 + 84.52 \times Fe_2O_3 + 83.67 \times CaO + 81.04 \times MgO + 91.92 \times A - 7891$

3. "When the content of the SiO_2 is no larger than 60 %, the content of the Al_2O_3 is no larger than 30 % and the content of Fe_2O_3 is larger than 15 %, the fusion temperature is calculated by:" (Liu *et al.*, 2006).

$T = 1531 - 3.01 \times SiO_2 + 5.08 \times Al_2O_3 - 8.02 \times Fe_2O_3 - 9.69 \times CaO - 5.861 \times MgO - 3.99 \times A$

4. "When the content of the SiO_2 is larger than 60 %, the fusion temperature is calculated by:" (Liu *et al.*, 2006).

$T = 10.75 \times SiO_2 + 13.03 \times Al_2O_3 - 5.28 \times Fe_2O_3 - 5.88 \times CaO - 10.28 \times MgO + 3.75 \times A + 453$

The results obtained from applying these equations are presented in Table H1. The fusion temperature for greywacke bed material appeared to correlate well with operation of the gasifier when clinker formed, but the accuracy of the other fusion temperatures are unverified.

Table H1: The results of the regression formulas applied to different materials.

Material/Substrate	Estimated Fusion Temperature (°C)
Greywacke	830
Olivine (forsterite)	1295
Wood pellets	1298
Wood chips	1298

Appendix I – Gasification Reactor Ash Analysis

CRL Energy Ltd

REPORT OF ANALYSIS

Customer: University of Canterbury **Date Received:** 16-Apr-08

Description: Sample supplied by client

Customer Reference: Coal 16/04/08

CRL Energy Ltd Reference: 83/880

Analysis - As Received Basis

Moisture	%	(ISO 5068)	7.1
Ash Inert matter (ash + sand)	%	(ISO 1171)	47.7
Volatile	%	(ISO 562)	3.3
Fixed Carbon	%	(by difference)	41.8
Calorific Value (Gross)	MJ/kg	(ISO 1928)	14.79
Sulphur	%	(ASTM D4239)	0.04
Carbon	%	(Leco SC DR 144 in house)	39.1
Hydrogen	%	(Otago univ microlab)	0.57
Nitrogen	%	(Otago univ microlab)	0.13
Oxygen	%	(by difference)	5.3

Analysis - Air Dried Basis

Moisture	%	(ISO 5068)	2.7
Ash Inert matter (ash + sand)	%	(ISO 1171)	50.0
Volatile	%	(ISO 562)	3.5
Fixed Carbon	%	(by difference)	43.8
Calorific Value (Gross)	MJ/kg	(ISO 1928)	15.49
Sulphur	%	(ASTM D4239)	0.04
Carbon	%	(Leco SC DR 144 in house)	41.0
Hydrogen	%	(Otago univ microlab)	0.60
Nitrogen	%	(Otago univ microlab)	0.14
Oxygen	%	(by difference)	5.5

Date of Issue: 29-Apr-08

Signature:

Grant Murray

Laboratory Supervisor

THIS REPORT MUST NOT BE QUOTED EXCEPT IN FULL

Distribution:

University of Canterbury, Chemical and Process Engineering,PB 4800, CHCH

CRL Energy Ltd, Laboratory

Appendix J – Producer Gas Data from the Hot Testing Experiments

Table J1: Producer gas data for the fuel feed rate variation test of 7/2/08.

Wood Feed Rate (kg_{dry}/h)	He (vol%)	H_2 (vol%)	N_2 (vol%)	CH_4 (vol%)	CO (vol%)	CO_2 (vol%)	C_2H_4 (vol%)	C_2H_6 (vol%)
11.2	3.31	22.6	9.5	10.7	32.8	16.9	3.55	0.66
17.7	0.71	22.4	6.2	11.6	36.0	18.3	4.12	0.79
20.4	0.67	22.5	5.6	11.8	36.0	18.4	4.17	0.82
22.8	0.58	22.7	4.6	11.9	37.2	18.1	4.06	0.83
24.8	0.60	23.0	5.2	11.9	35.8	18.6	3.99	0.84

Table J2: Producer gas data for the steam rate variation test on 15/2/08.

Total Steam Input (kg/h)	He (vol%)	H_2 (vol%)	N_2 (vol%)	CH_4 (vol%)	CO (vol%)	CO_2 (vol%)	C_2H_4 (vol%)	C_2H_6 (vol%)
7.1	0.82	26.2	7.5	13.0	32.5	15.9	3.40	0.79
8	0.78	27.1	7.5	12.4	30.7	17.1	3.68	0.74
9.1	0.65	25.8	6.7	12.3	30.9	18.9	3.99	0.75
10.1	0.73	28.8	4.4	12.1	30.0	19.2	3.97	0.71
11	0.67	27.6	5.4	12.3	30.5	19.0	3.93	0.70
12	0.66	28.2	5.5	11.9	29.1	20.0	4.14	0.68
13	0.65	28.0	5.5	12.2	30.1	18.9	3.89	0.68
14	0.68	28.3	4.8	12.2	29.5	19.9	4.01	0.68
15.4	0.76	29.0	3.7	12.4	29.7	19.8	3.93	0.68

Table J3: Producer gas data for the wood feed rate variation test using 20kg of bed material in the gasifier on 19/2/08.

Wood Feed Rate (kg_{dry}/h)	He (vol%)	H_2 (vol%)	N_2 (vol%)	CH_4 (vol%)	CO (vol%)	CO_2 (vol%)	C_2H_4 (vol%)	C_2H_6 (vol%)
10.5	1.38	22.3	11.0	13.5	35.5	12.6	2.98	0.73
13.9	1.08	23.0	8.6	12.9	33.1	16.9	3.70	0.78
18.2	0.83	23.7	5.9	13.4	34.5	17.1	3.83	0.80
20.4	0.68	24.5	5.4	13.2	32.8	18.5	4.13	0.79
22.0	0.61	23.7	4.7	13.3	33.8	18.7	4.39	0.79
23.8	0.66	25.4	4.4	13.2	32.5	18.9	4.30	0.77
25.6	0.55	24.6	3.8	13.7	33.6	18.7	4.37	0.78

Table J4: Producer gas data for the gasification temperature test of 21/2/08.

Gasification Temperature (°C)	He (vol%)	H_2 (vol%)	N_2 (vol%)	CH_4 (vol%)	CO (vol%)	CO_2 (vol%)	C_2H_4 (vol%)	C_2H_6 (vol%)
642	1.17	15.2	8.7	13.4	39.6	17.8	2.88	1.19
696	1.03	17.9	7.2	13.3	36.3	19.9	3.28	1.13
708	0.91	19.8	6.8	14.0	35.6	18.5	3.46	0.97
730	0.69	22.9	5.9	13.9	34.9	16.7	4.15	0.79
741	0.75	24.4	5.9	13.7	33.9	16.5	4.20	0.72
758	0.65	26.2	5.3	13.3	34.2	16.6	4.24	0.63

Table J5: Producer gas data for the steady state gasifier test on 3/3/08.

Time since start up (minutes)	He (vol%)	H_2 (vol%)	N_2 (vol%)	CH_4 (vol%)	CO (vol%)	CO_2 (vol%)	C_2H_4 (vol%)	C_2H_6 (vol%)
394	0.00	0.0	84.3	0.0	0.0	5.8	0.01	0.00
410	0.42	12.4	36.8	8.8	25.2	13.8	2.10	0.44
430	0.35	23.2	6.5	13.8	35.0	16.8	3.52	0.75
459	0.66	25.7	4.3	13.4	32.7	18.4	4.17	0.77
479	0.66	27.9	4.0	12.9	31.4	18.4	4.03	0.71
523	0.64	29.6	4.9	12.1	29.3	18.9	3.95	0.66
549	0.61	28.4	4.3	12.6	29.8	19.5	4.09	0.70
571	0.57	30.2	4.4	11.7	27.3	21.1	4.11	0.68
584	0.81	28.3	4.8	13.0	29.5	19.4	3.60	0.73
612	0.82	26.5	4.6	13.2	28.9	21.6	3.54	0.87

Table J6: Producer gas data for the feed rate variation test using olivine bed material on 17/3/08.

Wood Feed Rate (kg_{dry}/h)	He (vol%)	H_2 (vol%)	N_2 (vol%)	CH_4 (vol%)	CO (vol%)	CO_2 (vol%)	C_2H_4 (vol%)	C_2H_6 (vol%)
7.7	2.30	25.4	18.4	9.2	23.8	16.8	2.41	0.35
10.4	1.33	25.9	10.5	10.7	28.4	19.0	3.66	0.51
13.2	1.11	27.2	8.7	11.1	28.6	18.9	3.83	0.55
15.8	0.94	27.1	6.6	12.6	32.0	16.1	3.96	0.63

Appendix K – Calculation of Producer Gas Calorific Value

A typical composition of producer gas generated in the FICFB gasifier is shown in Table K1. The enthalpies of combustion have been derived from literature based on the lower heating values of the gases. Since the producer gas would be cooled to about 50 °C or less before being fed into an engine, any water would be condensed out and removed in practice. So the lower calorific value is on a dry gas basis.

Table K1: Measured composition of producer gas from the FICFB gasifier and the lower enthalpies of combustion of each gaseous component. The gas composition was obtained from the hot test on 15/2/08 at 2.06pm. Enthalpies of formation were derived from (Smith *et al.*, 1996).

Gas Component	**Gas Composition (Vol %)**	**Enthalpy of Formation** at 298K **(J/mol)**	**Enthalpy of Combustion** at 273K **(MJ/Nm^3)**
Methane	12.3	-74,520	32.8
Ethane	0.75	-83,820	58.4
Ethene	4.0	52,510	49.8
Hydrogen	25.8	-241,818	9.9
Carbon monoxide	30.9	-110,525	11.6
Carbon dioxide	18.9	-393,509	0
Oxygen	0		0
Nitrogen	6.7		0
Helium (tracer gas)	0.651		0

The lower calorific value can be calculated by the equation below:

CV_{lower} (MJ/Nm^3) = ∑ (mol fraction of each gas x enthalpy of combustion of each gas or LHV's)
where mol% ≈ vol% assuming ideal gas conditions.

CV_{lower} = (0.123 x 32.8) + (0.0075 x 58.4) + (0.040 x 49.8) + (0.258 x 9.9) + (0.309 x 11.6)
CV_{lower} of the dry gas composition in Table K1 = *12.6 MJ/Nm^3* at 273K/0 °C, 1 atm).

Note: Conditions for Nm^3 are considered to be Standard Temperature and Pressure equal to 0 °C and 1 atm (The Engineering Toolbox, 2005).

Using heat of formation data found from literature (Smith *et al.*, 1996), enthalpies of combustion expressed in kJ/kmol can be determined as follows in units of MJ/Nm^3. This assumes ideal gas conditions and that the enthalpy of combustion at 0 °C, 1 atm is ≈ to the enthalpy of combustion at 25 °C, 1 bar (the error induced is considered negligible):

From ideal gas laws: PV = nRT

V = nRT/P

If: n=1 mol, $R = 8.314 \frac{kPa \cdot m^3}{kmol \cdot K}$, T = 273K and P = 101.325 kPa

Then: 1 mol of ideal gas ≈ 24.45L (at 273K, 1 atm)

And: 1kmol of ideal gas ≈ 24.45 m^3 (at 273K, 1 atm)

For Methane:

$$CH_4 + 2O_2 \rightarrow CO_2 + 2H_2O_{(g)}$$

ΔH_{comb} or LHV $(CH_4) = \sum(\Delta H_{f\ prod}) - \sum(\Delta H_{f\ react})$

$= [1 \times -393509 + 2 \times -241818] - [1 \times -74520 + 2 \times 0]$

$= -802625$ J/mol or kJ/kmol at 298K/25 °C, 1 bar

≈ -802625 kJ/kmol at 273K/0 °C, 1 atm

Since: 1 kmol of ideal gas $\approx 24.45\ m^3$ (at 0 °C, 1 atm)

$$\Delta H_{comb} \text{ or LHV } (CH_4) = \frac{802625\ kJ/kmol}{24.45\ Nm^3/kmol}$$

$= 32.8\ MJ/Nm^3$ at 273K/0 °C, 1 atm

For Ethane:

$$C_2H_6 + 7/2O_2 \rightarrow 2CO_2 + 3H_2O_{(g)}$$

ΔH_{comb} or LHV $(C_2H_6) = \sum(\Delta H_{f\ prod}) - \sum(\Delta H_{f\ react})$

$= [2 \times -393509 + 3 \times -241818] - [1 \times -83820 + 7/2 \times 0]$

$= -1428652$ J/mol or kJ/kmol at 298K/25 °C, 1 bar

≈ -1428652 kJ/kmol at 273K/0 °C, 1 atm

Since: 1 kmol of ideal gas $\approx 24.45\ m^3$ (at 0 °C, 1 atm)

$$\Delta H_{comb} \text{ or LHV } (CH_4) = \frac{1428652\ kJ/kmol}{24.45\ Nm^3/kmol}$$

$= 58.4\ MJ/Nm^3$ at 273K/0 °C, 1 atm

For Ethene:

$$C_2H_4 + 3O_2 \rightarrow 2CO_2 + 2H_2O_{(g)}$$

ΔH_{comb} or LHV $(C_2H_6) = \sum(\Delta H_{f\ prod}) - \sum(\Delta H_{f\ react})$

$= [2 \times -393509 + 2 \times -241818] - [1 \times -52510 + 3 \times 0]$

$= -1218144$ J/mol or kJ/kmol at 298K/25 °C, 1 bar

≈ -1218144 kJ/kmol at 273K/0 °C, 1 atm

Since: 1 kmol of ideal gas $\approx 24.45\ m^3$ (at 0 °C, 1 atm)

$$\Delta H_{comb} \text{ or LHV } (CH_4) = \frac{1218144\ kJ/kmol}{24.45\ Nm^3/kmol}$$

$= 49.8\ MJ/Nm^3$ at 273K/0 °C, 1 atm

For Hydrogen:

$2H_2 + O_2 \rightarrow 2H_2O_{(g)}$ $\Delta H_{f\,298} = -241{,}818$ J/mol (Smith *et al.*, 1996).

H_2O has a heat of formation of 241,818 kJ/kmol at 298K, 1 bar which corresponds to H_2 having a heat of combustion of 241,818 KJ/kmol at 298K, 1 bar.

Since: 1 mol of ideal gas ≈ 24.45L (at 0 °C, 1 atm)

and: 1 kmol of gas $\approx 24.45\ m^3$ (at 0 °C, 1 atm)

ΔH_{comb} or LHV $(H_2) = 241{,}818$ (kJ/k mol) / 24.45 (m^3/kmol)

$= 9.9\ MJ/Nm^3$ (At 273K / 0 °C, 1 atm)

For Carbon Monoxide:

$$CO + 1/2O_2 \rightarrow CO_2$$

ΔH_{comb} or LHV (CO) $= \sum(\Delta H_{f\ prod}) - \sum(\Delta H_{f\ react})$

$= [1 \times -393509] - [1 \times -110525 + 1/2 \times 0]$

$= -282984$ J/mol or kJ/kmol at 298K/25 °C, 1 bar

≈ -282984 kJ/kmol at 273K/0 °C, 1 atm

Since: 1 kmol of ideal gas $\approx 24.45\ m^3$ (at 0 °C, 1 atm)

$$\Delta H_{comb} \text{ or LHV } (CH_4) = \frac{282984\ kJ/kmol}{24.45\ Nm^3/kmol}$$

$= \textit{11.6 MJ/Nm}^3$ at 273K/0 °C, 1 atm

To calculate the calorific values, ideal gas conditions were assumed. This is a reasonable assumption since the gases are at high temperature, well away from any phase changes and are at atmospheric pressure. This assumption allowed the mol % to approximately equal the vol % shown in Table K1.

The lower heating value of the gas composition shown in Table K1 (12.7 MJ/Nm^3) is higher than most traditionally designed gasifiers of 4-6 MJ/Nm^3 since steam is used as the oxidising agent not air. This prevents introducing high proportions of nitrogen which dilute the producer gas. The nitrogen in this producer gas largely comes from the nitrogen purge in the feed augers, and some air which travels along the chute from the base of the combustion column.

The Güssing 100 kW lab scale FICFB gasifier has an average nitrogen content of about 5 %, while their 10 kW test rig of a slightly different design had 2.5 % nitrogen (Hofbauer,Veronik *et al.*, n.d.).

Note: The higher and lower heating values of a gas are the same if they do not involve the formation of water! Hence the lower and higher CV of carbon monoxide is the same, but this is not the case for fuels which contain hydrogen.

Appendix L – Producer Gas Chemical Energy and Gasifier Cold Gas Efficiency

Using the producer gas output rate from Appendix C, the total combustion energy of the producer gas and cold gas efficiency of the gasifier can be calculated. The cold gas efficiency is expressed on a lower heating value basis for the dry producer gas. The data used is from the test run on 15/2/08 at 2.06pm. This data has been used because it represents the gasifier at normal operating conditions.

Test conditions: Fuel feed rate = 20.0 kg/h of wood pellets with 8wt% moisture
Dry fuel feed rate = 20.0 kg/h x 0.92 = 18.4 kg_{dry}/h wood pellets
Steam injection/generation = 10.1 kg/h with steam at 200 °C, 5 bar.
Gasification temperature = 727 °C (BFB #1 temp)
Producer gas sampling temperature = 646 °C
LHV of producer gas = 12.6 MJ/Nm^3 (from Appendix K).
Producer gas output rate = 10.8 Nm^3/h (from Appendix C).
Lower CV of LPG (propane) = 86.5 MJ/Nm^3 (Baines, 1993)

$$\text{Cold gas } \eta = \frac{\text{Chemical energy of the producer gas [LHV dry gas basis]}}{\text{Total Energy to Gasifier (biomass + external energy used) [LHV dry fuel basis]}} \text{ x } 100\%$$

Total combustion energy producer gas = 10.8 Nm^3/h x 12.6 MJ/Nm^3 x 1/3600 h/s x 1000/1 kJ/MJ

= 37.8 kW (LHV dry gas basis).

Gross CV of dry wood pellets = 20.3 MJ/kg_{dry}, (determined by CRL Ltd report in Appendix A). From the dry basis composition of the wood pellets in Appendix A, the chemical formula of the wood pellets was determined as: $CH_{1.36}O_{0.62}$ with a molar mass of 23.28 g/mol.

If one kg of dry wood pellets is combusted, it was calculated that 0.526 kg of water is formed in the products. $\Delta H_{vapourisation\ of\ water}$ = 2.442 MJ/kg,
$HHV_{\text{wood pellets}}$ (MJ/kg) – 0.526 (kg) x 2.442 (MJ/kg) = $LHV_{\text{wood pellets}}$ (MJ/kg)
$LHV_{\text{wood pellets (dry basis)}}$ = 19.0 MJ/kg_{dry}

Energy of the wood to the gasifier = 19.0 MJ/kg_{dry} x 18.4 kg_{dry}/h x 1/3600 h/s x 1000/1 kJ/MJ

= 97.1 kW (LHV dry wood basis)

Supplementary propane to the combustion reactor = 16 L/min x 86.5 MJ/m^3 x 1/60 x 1/1000

= 23.0 kW (LHV dry fuel basis)

Energy consumed for the external steam generation = 2791.6 kJ/kg x 10.1 kg/h x 1/3600 h/s

= 7.8 kW (to generate steam at 200 °C, 5 bar)

The design input of wood pellets to the gasifier was 100 kW. This agrees very closely with the usual operating conditions where approximately 97 kW of wood pellets are consumed.

$$\text{Cold gas efficiency} = \frac{37.8}{97.1 + 23.0 + 7.8} \text{ x } 100\%$$

= *30 %* at the operating conditions chosen.

Appendix M – Humidity Measurement and Calculation for the Producer Gas

An automated method to measure the water content in the producer gas was not in place during the experiments performed for this thesis, so an alternative temporary method was used. This involved drawing a measured quantity of producer gas into a 2 L syringe through a glass wool filter to collect any tars and then through silica gel. The moisture content was determined gravimetrically. Sampling was performed after the cyclone in the producer gas line, the same as for the producer gas and tar samples.

It was assumed that the mass increase from any tars that were not filtered out and collected on the silica gel was negligible. The calculation procedure followed was:

Initial mass of apparatus (g) = x ± 0.0001g
Final mass of apparatus + moisture (g) = x + H ± 0.0001g
Mass of moisture (g) = (x + H) – x
= H ±0.0002g

Dry gas volume drawn through silica gel into syringe (Nm^3) = V ± 3.8 %
(Corrected for Nm^3 at 0 °C).

Moles of dry producer gas drawn through silica gel into syringe (mol) $= \frac{V \text{ at } 0\,°C}{24.45 \times 10^{-3}}$
= n ± 3.8 % (at 0 °C).

(Calculated using ideal gas laws).

Molecular weight of the dry gas composition = Mr
Mass of dry producer gas drawn through silica gel (g) = n x Mr
= m ± 3.8 %

Moisture content in the producer gas $\left(\frac{g_{water}}{g_{dry\ producer\ gas}} \right) = \frac{\text{mass of moisture 'H'}}{\text{mass of dry producer gas 'm'}} \pm 0.02$